TSINGHUA-PRINCETON-COMBUSTION INSTITUTE

2026 SUMMER SCHOOL ON COMBUSTION

Spectroscopic Diagnostics for Combustion Chemistry

Pascale Desgroux

University of Lille-CNRS, France

July 06-07, 2026

TSINGHUA-PRINCETON-COMBUSTION INSTITUTE

2026 SUMMER SCHOOL ON COMBUSTION

Key Activities / 重要活动			
July 5 (Sunday) /7 月 5 日 （周日）	10:00-17:30	Registration 注册	Northeast Gate, Lee Shau Kee Sci. and Tech. Building 李兆基科技大楼东北门
	18:30	Welcome Reception 开班仪式	A-278, Multifunction Room, Lee Shau Kee Sci. and Tech. Building 李兆基科技大楼多功能厅
Class Schedule / 课程安排			
Schedule 时间	Location 地点	Morning 上午 (9:00-9:50/10:00-10:50/11:00-11:50)	Afternoon 下午 (14:00-14:50/15:00-15:50/16:00-16:50)
July 6-10 (Monday-Friday) /7 月 6-10 日 （周一至周五）	Zone A, 6th Teaching Building 第六教学楼 A 区	**Theoretical and Numerical Combustion** **classroom: 6A018 (0th floor)** Thierry Poinsot	**Combustion Chemistry: From Fundamentals to Kinetic Modelling for Low-Carbon Technologies** **classroom: 6A018 (0th floor)** Alison Tomlin
July 6-7 (Monday-Tuesday) /7 月 6-7 日 （周一至周二）	Zone A, 6th Teaching Building 第六教学楼 A 区	**Spectroscopic Diagnostics for Combustion Chemistry** **classroom: 6A203 (2nd floor)** Pascale Desgroux	**Quantum Mechanics, Statistical Mechanics,and Machine Learning for Molecular Simulations** **classroom: 6A203 (2nd floor)** Alexandre Tkatchenko
July 8-10 (Wednesday-Friday) /7 月 8-10 日 （周三至周五）	Zone A, 6th Teaching Building 第六教学楼 A 区	**Introduction to Plasma-assisted Combustion** **classroom: 6A203 (2nd floor)** Deanna Lacoste	**AI for Combustion** **classroom: 6A016 (0th floor)** Matthias Ihme
Special Activities / 特殊活动			
July 5 (Sunday) /7 月 5 日 （周日）	13:30-17:30	Art Museum Visit / 艺术博物馆参观	Tsinghua University Art Museum 清华大学艺术博物馆
July 7 (Tuesday) /7 月 7 日 （周二）	17:00-18:00	Campus Tour / 校园游览	Tsinghua University 清华大学

July 8 (Wednesday) /7 月 8 日 （周三）	17:00-17:30	Group Picture Taking / 暑期学校合影	Mong Man Wai Concert Hall 蒙民伟音乐厅
July 8 (Wednesday) /7 月 8 日 （周三）	18:30-19:30 19:30-21:00	Poster Presentation / 海报展示 Career Panel / 职业发展论坛	B-518, Lee Shau Kee Sci. and Tech. Building 李兆基科技大楼 B-518 会议室
July 9 (Thursday) /7 月 9 日 （周四）	18:00	Farewell Reception / 欢送会	Guan Chou Yuan Restaurant 观畴园餐厅
July 10 (Friday) /7 月 10 日 （周五）	8:00-18:00	Program Certificate Distribution / 学习证书发放	6th Teaching Building 第六教学楼
July 11 (Saturday) /7 月 11 日 （周六）	9:30-11:30	CCE Laboratory Tour / 燃烧能源中心实验室参观	Northeast Gate, Lee Shau Kee Sci. and Tech. Building 李兆基科技大楼东北门

Electronic version of all lecture materials are available at the summer school website

In situ Spectroscopic Diagnostics in the Gas Phase: Fundamentals

Pascale Desgroux

Tsinghua Summer School, 2026

PC2A

Université de Lille

Lille

80 minutes from London

60 minutes from Paris

35 minutes from Brussels

2

LILLE

- The first french university in students number ***100,000 students***

10000
international students

- "**City of art and history**" status since 2004

- *Among the **top 100 most welcoming cities** in the world*

To whom?

- Experimenters
- Modelers and computer scientists
- Applications in turbulent flames not covered, just a few examples

My message:

- You can obtain some very beautiful LIF images, but if you are unable to interpret them, they are useless.

Main objective of the course:

- To provide you with the basics
- “Historical” references
- Warning: impossible to cover all the details, but to draw your attention to the sensitive issues that must not be overlooked, so that you can then make the effort on your own to overcome them

Outline: Spectroscopic Diagnostics in the Gas Phase

I – A little spectroscopy
II - Natural emission
III – What happens in presence of light (no laser)
  III.1 Absorption
  III.2 Rayleigh – Raman
IV – Discovery of the lasr and consequences on combustion research
V - In situ Spectroscopic diagnostics based on interaction laser/matter
  Non resonant spectroscopic methods (Rayleigh – Raman)
VI - In situ Spectroscopic diagnostics based on interaction laser/matter
  Resonant spectroscopic methods
  VI.1 Cavity RingDown Spectroscpy (CRDS)
  VI.2 Intracavity Laser Absorption Spectroscopy (ICLAS)
  VI.3 Laser Induced Fluorescence (LIF)
VII - Other LIF aspects
  VII.1 The calibration methods
  VII.2 Limitations of the two-level model
  VII.3 About reaching the saturation: wings effect
  VII.4 Predissociated LIF
VIII – Two-photon LIF
IX – LIF thermometry
X – Case study : NO (effect of pressure and interferences)
~~Coherent methods (Coherent Antistokes Raman Spectroscopy CARS)~~

References

Eckbreth A. (1996) :*Laser diagnostics for combustion temperature and species*, Combustion Science and Technnology 3, Gordon and Breach, Amsterdam.

Kohse-Hoïnghaus K., *Combustion at the focus: laser diagnostics and control*, Proceedings of the combustion institute 30 (2005) 89-123

« Applied Combustion Diagnostics », Edited by K. Kohse-Höinghaus and J. Jeffries, Taylor and Francis (2002)

Mark Linne « Spectroscopic Measurement: An Introduction to the Fundamentals" , 2nd Edition (2024), Academic press

Daily J., *Laser induced fluorescence spectroscopy in flames*, PECS 23 (1997) 133-199

Herzberg G. *Spectra of diatomic molecules , Krieger (1950), Electronic spectra and electronic structure of polyatomic molecules, Krieger (1966)*

I. A little spectroscopy

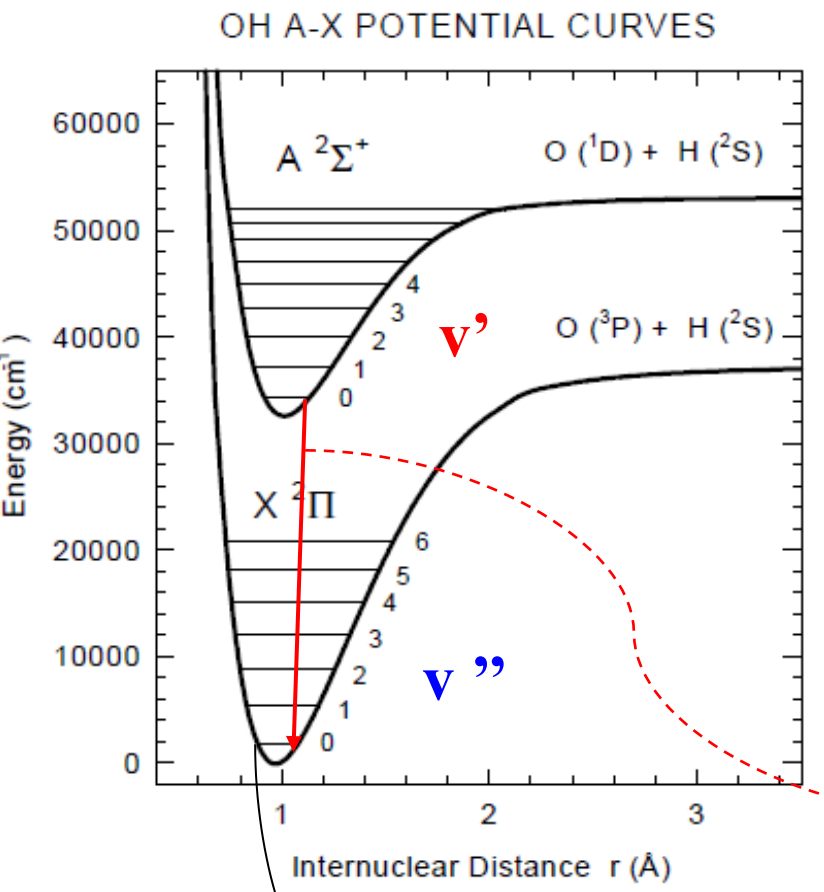

Energy of a molecule

$H\Psi = E\Psi$ **Eq. de Schrödinger**

Quantification of energy

Quantum number

$$E = Ee + Evib + Erot$$

J ou eV → $E = hc\,(Te(n) + G(v) + F(J))$ ← cm^{-1}

Radiative Transition (selection rules)

$$h\nu = hc\sigma = hc/\lambda = E_2 - E_1$$

	1.4	2.05	4.1	12.3	eV
	11111	16667	33330	10^5	cm^{-1}
λ(nm)	900	600	300	100	

Rotational **Vibrational** **Electronic** **Ionisation**

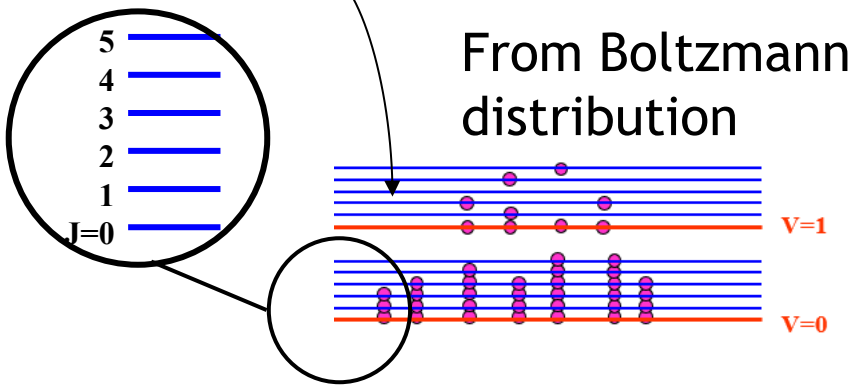

From Boltzmann distribution

Most of our knowledge of molecular spectroscopy was acquired during the first half of the 20th century

The Identification of Molecular Spectra
Pearse and Gaydon (1947)

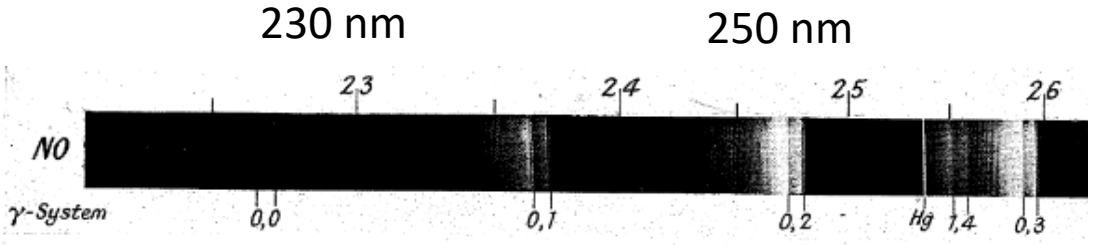

NO in a discharge

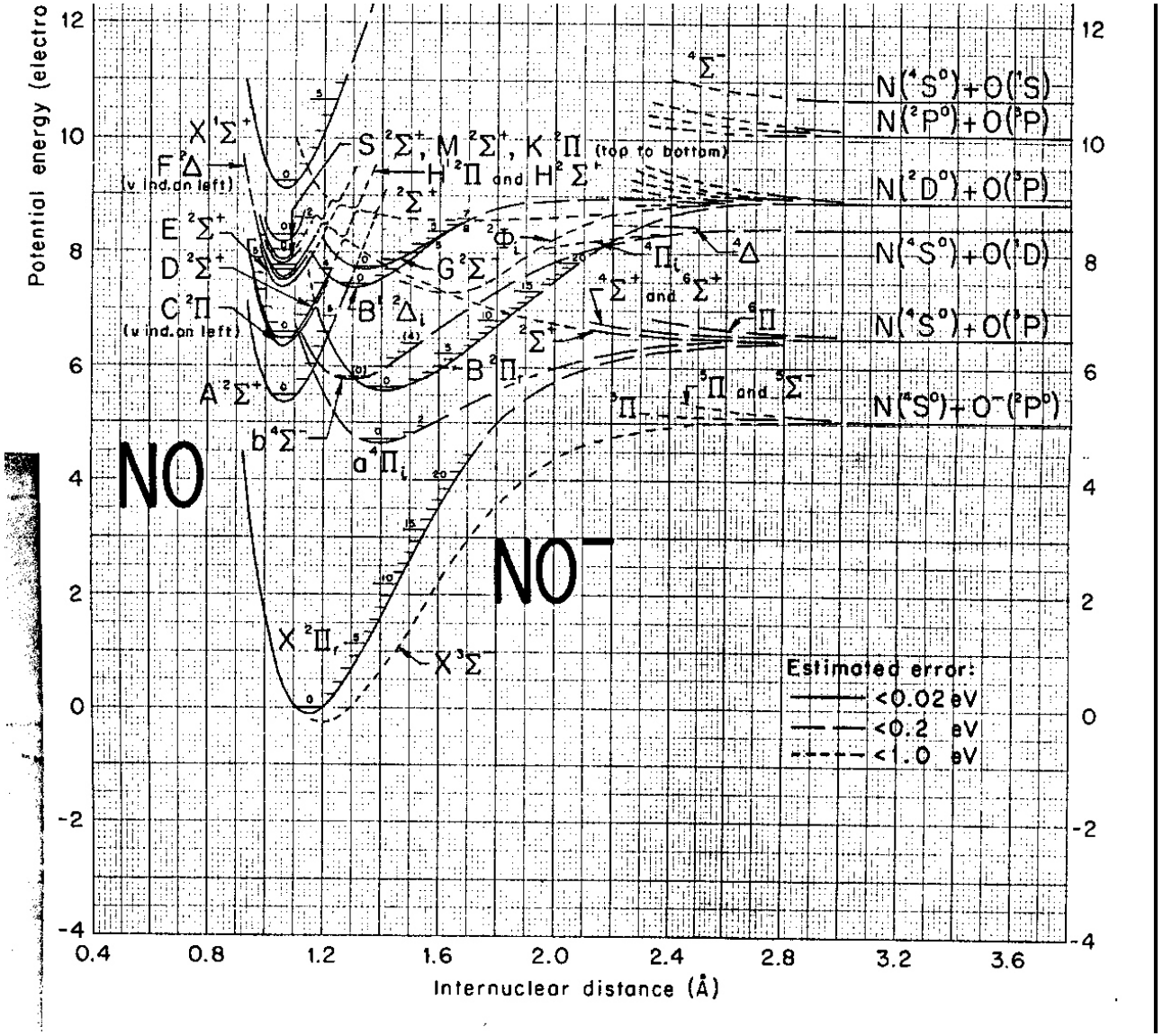

Gilmore JQSRT 5 (1965)

Nomenclature

Electronic state

Spin multiplicity

$^{2S+1}\chi_{\Omega}$

L Component :
State : Σ, Π, Δ…for Λ = 0,1,2…

$\Omega = \Lambda+\Sigma$

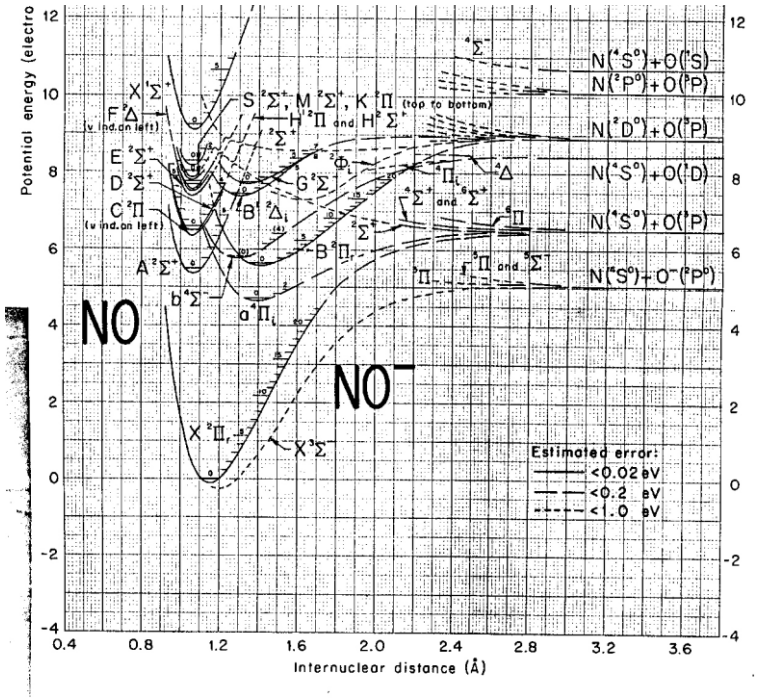

This notation preceded by a letter "X, A, B, C..." for the ground state, the 1st , 2d excited states…

Electronic transition

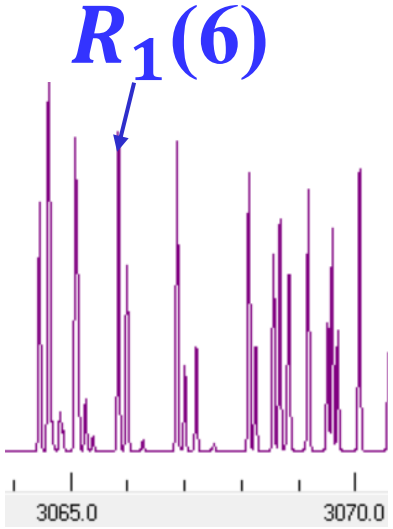

Y = O, P, Q, R, S
ΔN = -2,-1,0,1,2

X = P, Q, R
ΔJ = -1,0,1

$Y_{\alpha\beta}X(N'')$

α = 1, 2,…
J' = N'+S , N'+S-1,…

β = 1, 2,…
J''= N''+S, N''+S-1…

As example, for the OH molecule, there are 12 possible transitions between electronic states:

$^{O}P_{12}$, P_1, P_2, $^{Q}R_{12}$, $^{P}Q_{12}$, Q_1, Q_2, $^{R}Q_{21}$, $^{Q}P_{21}$, R_1, R_2, $^{S}R_{21}$

By convention a transition is always in the following order:

upper state - lower state, for example:

A-X (1-0) means a transition between v’=1 in A state and v ’’=0 in ground state corresponding either to

A-X (1<-0) (absorption)

or

A-X (1->0) (emission)

The quantum numbers in the lower state are noted N’’, J’’, v’’

And in the upper state N’, J’, v’

Distribution of Boltzmann: Boltzmann fraction

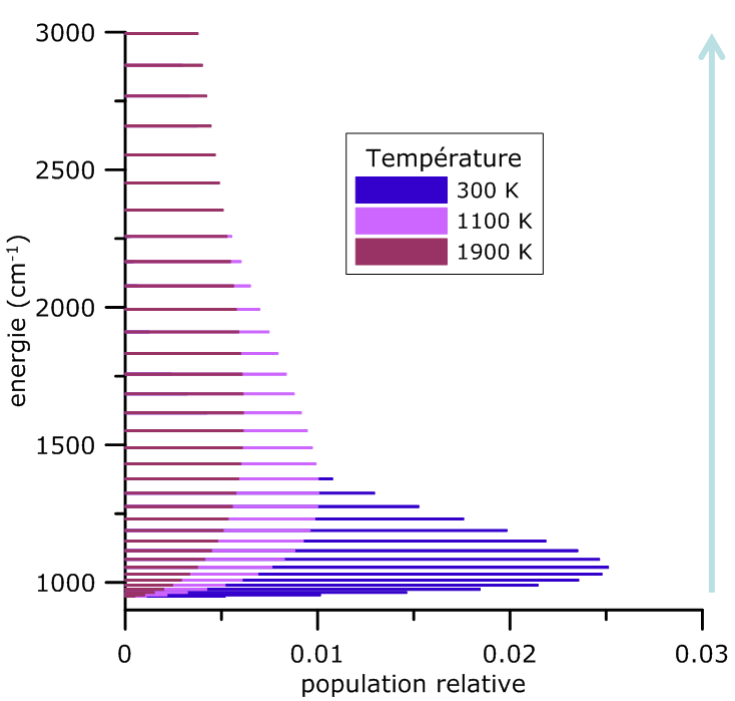

$$N^0_{J''} = f_b(T, J'')N_{tot}$$

$$f_b(T, J'') = \frac{g_{J''}}{Q_e Q_v Q_r} \exp\left(-\frac{E_{elec} + E_{v''} + E_{J''}}{kT}\right)$$

Q_i partition function

$g_{J''}$: 2J''+1 (degeneracy of the level)

Thermodynamic equilibrium (rotational temperature= vibrational temperature= gaz temperature)

Case (a) of Hund

L is electrostatically coupled to the internuclear axis, and S is coupled to L by spin-orbit coupling.

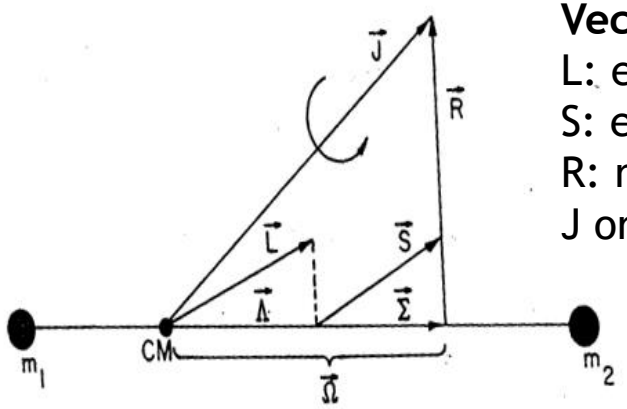

Vector quantities:
L: electronic orbital angular momentum
S: electronic spin angular momentum
R: rotational angular momentum of the nuclei
J or N : total electronic angular momentum

$$Qe = \sum_{\Omega} \sum_{n} (2S+1)(2-\delta_{0,\Lambda}) \exp\left(-\frac{hc}{kT} T_e(n) + A\Omega^2\right)$$

$$\delta_{0,\Lambda} = 1 \quad \text{if } \Lambda = 0$$

$$\delta_{0,\Lambda} = 0 \quad \text{if } \Lambda \neq 0$$

$$Qv = \sum_{v} \exp\left(-\frac{hc}{kT} G(v)\right)$$

$$Qr = \sum_{J} (2J+1) \exp\left(-\frac{hc}{kT} F(J)\right)$$

J=N+S

$R_1(6)$

$Q_2(26.5)$

$$Qr = \frac{kT}{hcB_v} \quad \text{if } T > 300K$$

Case (b) of Hund (OH)

spin-orbit coupling is weak or non-existent

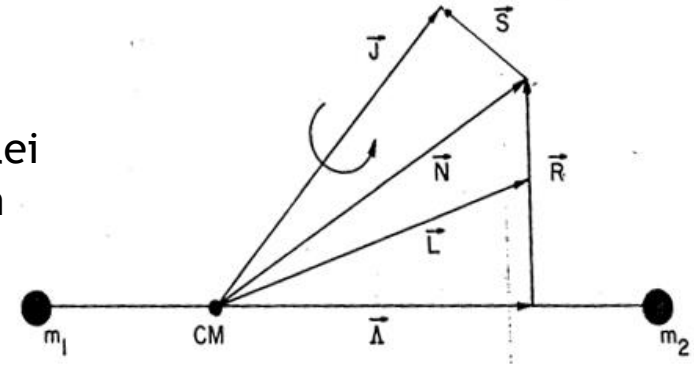

$$Qe = \sum_{n} (2S+1)(2-\delta_{0,\Lambda}) \exp\left(-\frac{hc}{kT} T_e(n)\right)$$

$$\delta_{0,\Lambda} = 1 \quad \text{if } \Lambda = 0$$

$$\delta_{0,\Lambda} = 0 \quad \text{if } \Lambda \neq 0$$

$$Qv = \sum_{v} \exp\left(-\frac{hc}{kT} G(v)\right)$$

$$Qr = \sum_{N} (2N+1) \exp\left(-\frac{hc}{kT} F(N)\right)$$

II. Natural flame emission

The Spectroscopy of Flames

A. G. GAYDON
D.Sc., F.R.S.
Warren Research Fellow
of the Royal Society
and
Emeritus Professor of Molecular Spectroscopy
Imperial College, London

SECOND EDITION

1957

The spectrum of a candle flame was first mapped by **Swan** in **1857** and early observations on spectra of metals in flames were made by **Bunsen** and **Kirchhoff** around 1860.
Later **Wolfhard, Broida**…

Emission

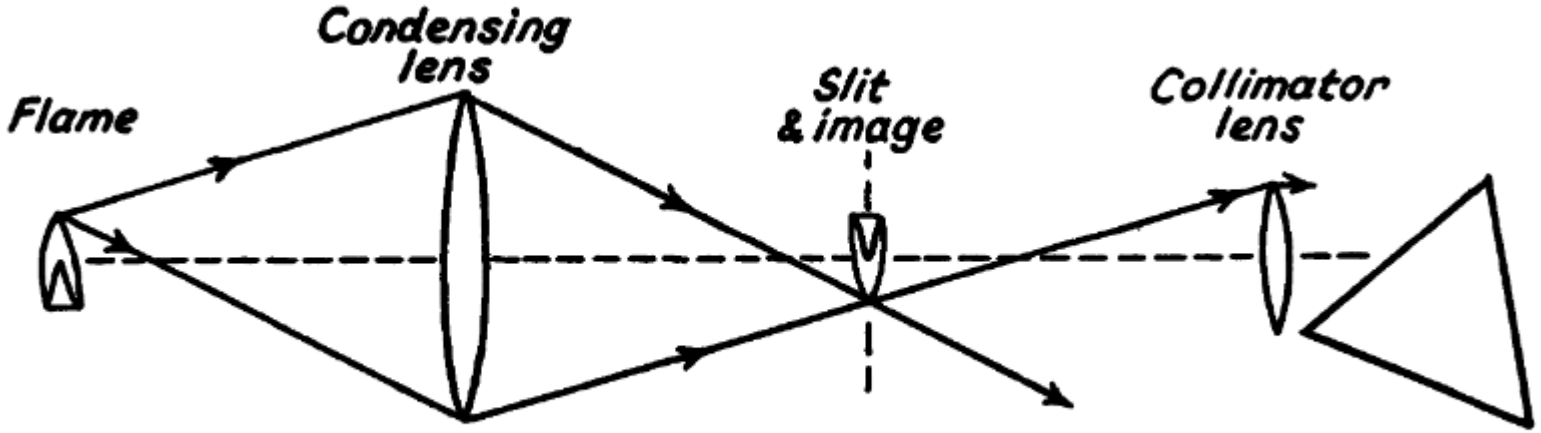

Fig. II.2

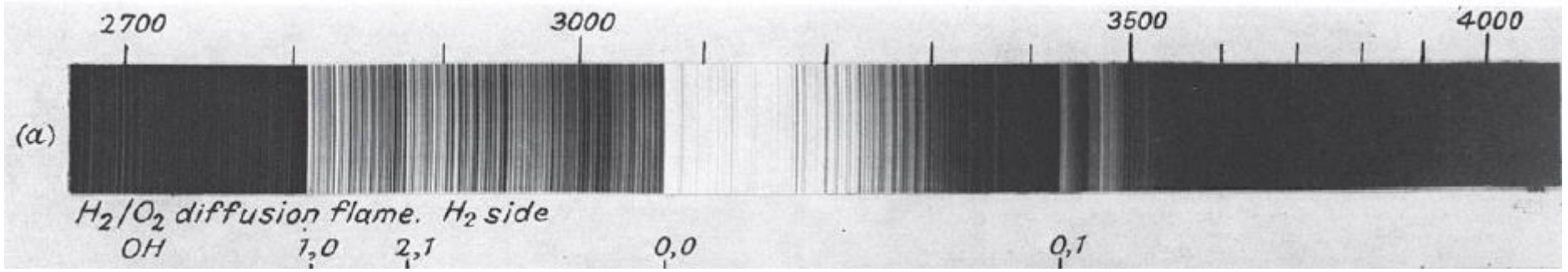

DETECTOR

Gaydon, 1957

Which information from natural (spontaneous) emission?

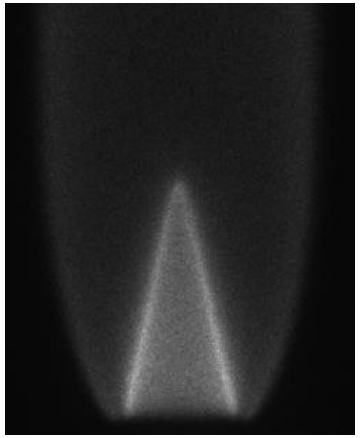

Najm et al., Comb. Flame 113 (1998) 32
Smith et al., Comb. Flame 131 (2002) 59
Kathrotia et al. App Phys B 107 (2012)
Konnov, CnF 253 (2023) 112788+112789
Sharipov et al., CnF 263 (2024) 113407+113417

CH(A-X) 430 nm

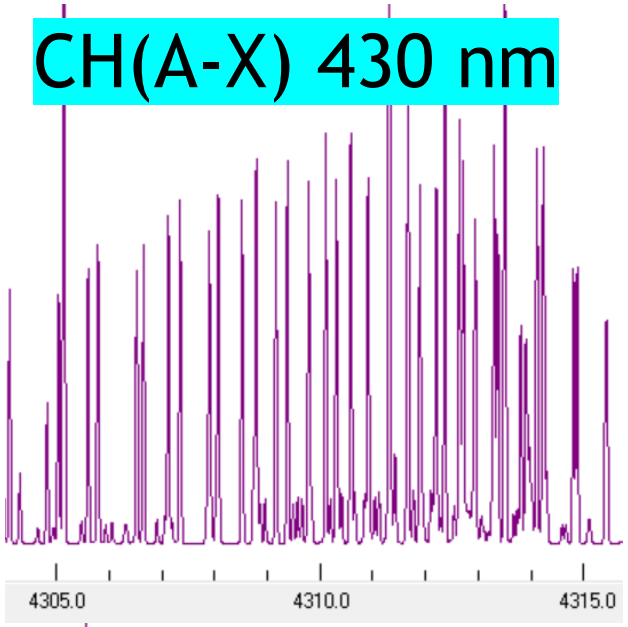

$C_2H + O = CH(A,B) + CO$

Chemiluminescence

OH(A-X) 307 nm

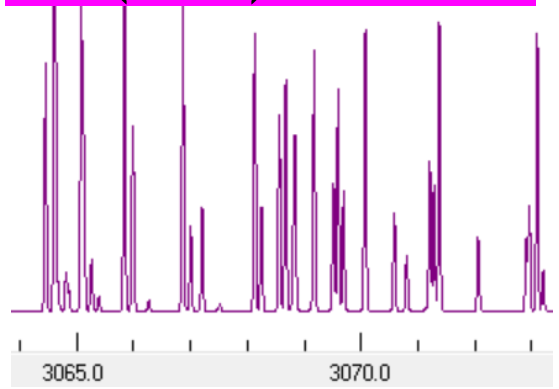

$CH + O_2 = OH(A) + CO$

$H+O+M=OH(A)+M$

LIFBASE spectroscopy tool: *Jorge Luque & David Crosley; SRI*
https://www.sri.com/platform/lifbase-spectroscopy-tool/

What do we measure with spontaneous emission?

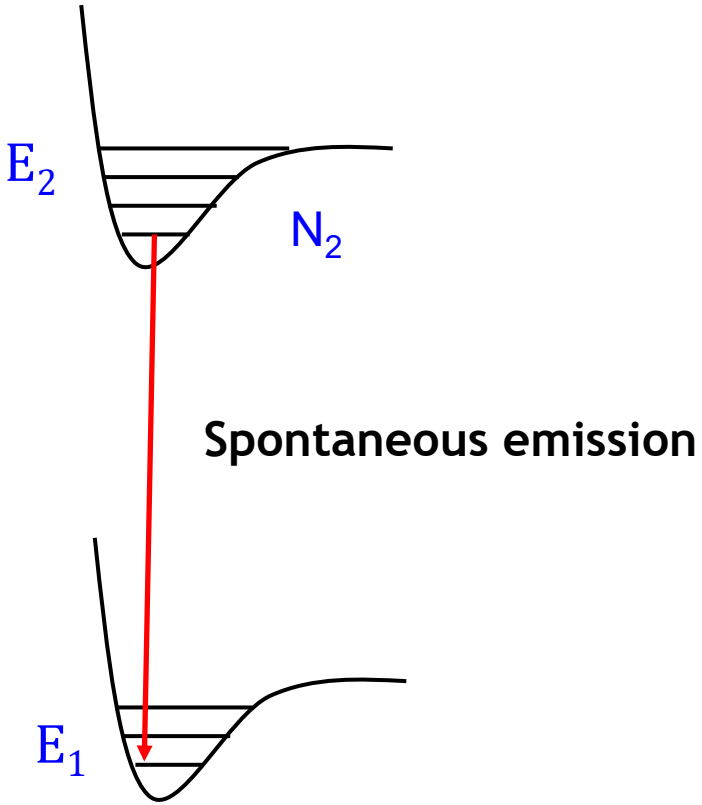

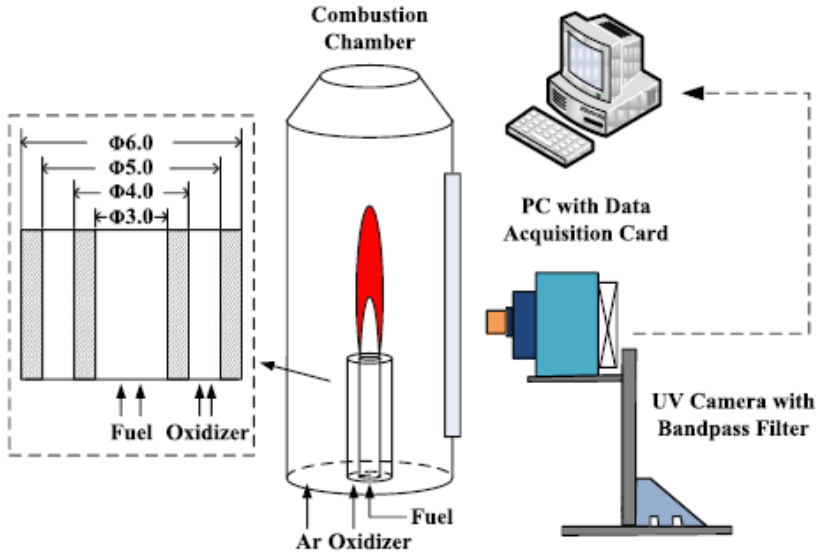

Number of collected emitted photons

$$I_{OH^*} = \mathrm{K}\frac{\Omega}{4\pi}\tau A_{21} F [OH^*] V_{em}$$

A_{21} = 1.45 10^6 s^{-1} (*and not 1.86 10^{-6} s^{-1} , paper's value)*: **Einstein Coefficient for emission.**

F: fraction of signal collected using any optical filter

τ : exposure time

V_{em} : collection volume

$[OH^*]$: Concentration of OH* on the excited state

Lei He et al. CNF 201 (2019) 12

Walsh et al. PROCI 27 (1998) 615

Taking into account the radial distribution through Abel transformation

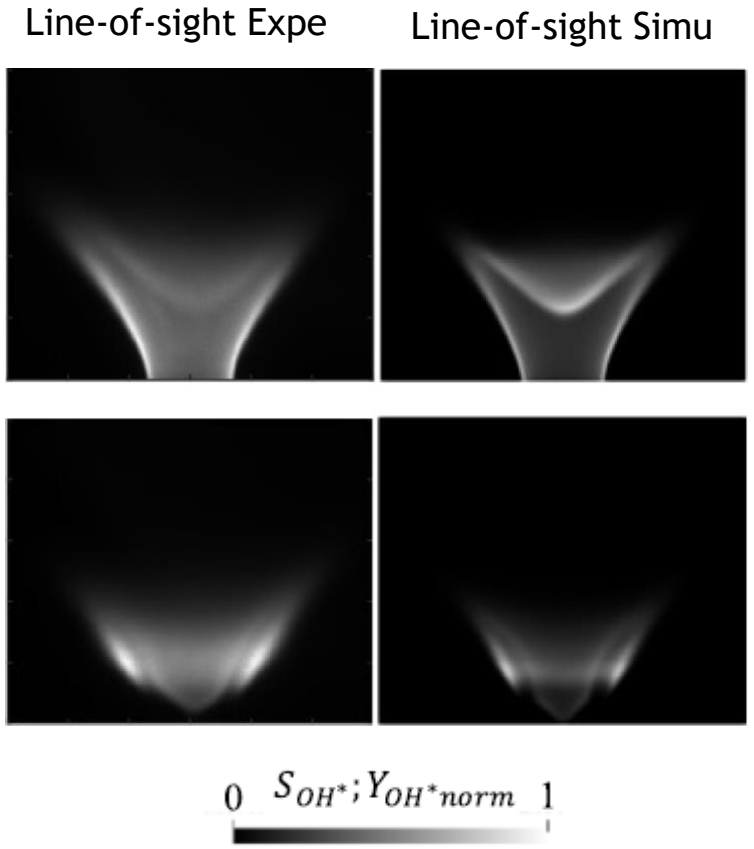

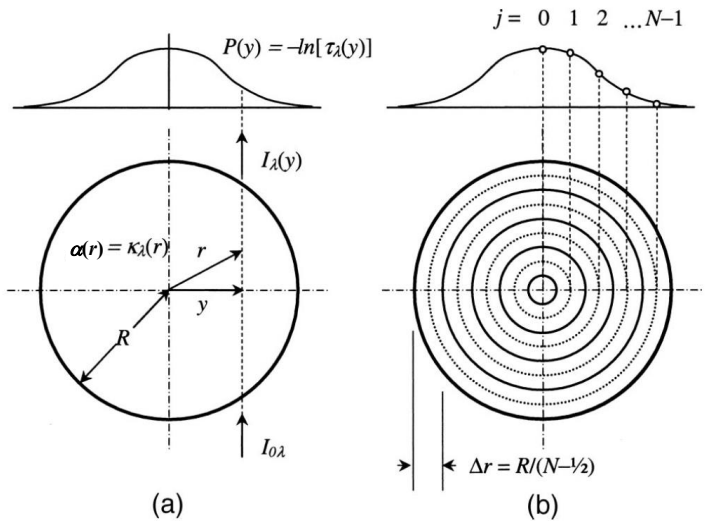

$$P(y) = 2\int_{y}^{R} \frac{\alpha(r) r}{(r^2 - y^2)^{1/2}} dr$$

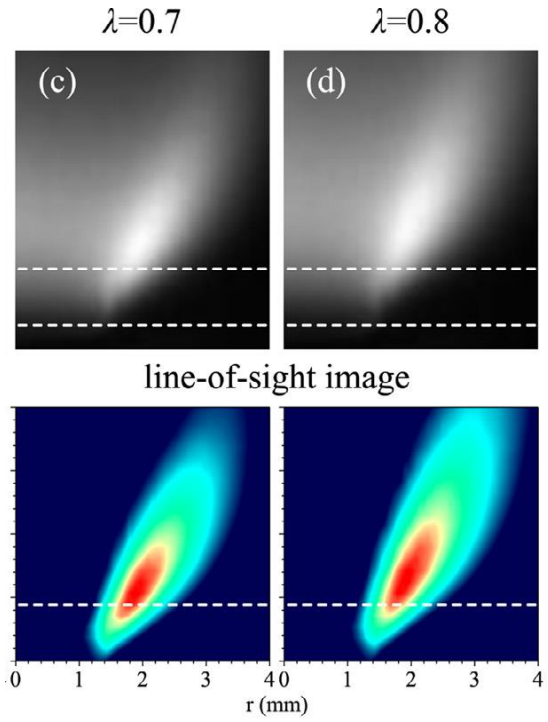

Vilespi et al. Combustion and Flame 283 (2026) 114536

Lei He et al. CNF 201 (2019) 12

Which information from natural (spontaneous) emission?

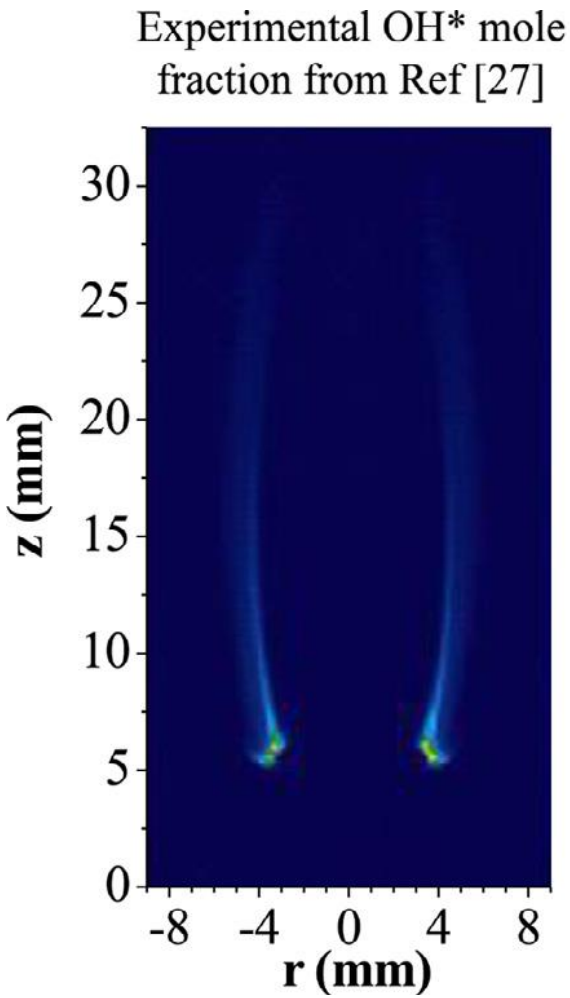

Lei He et al. CNF 201 (2019) 12

[24] Tamura et al., CNF 114 (1998) 502

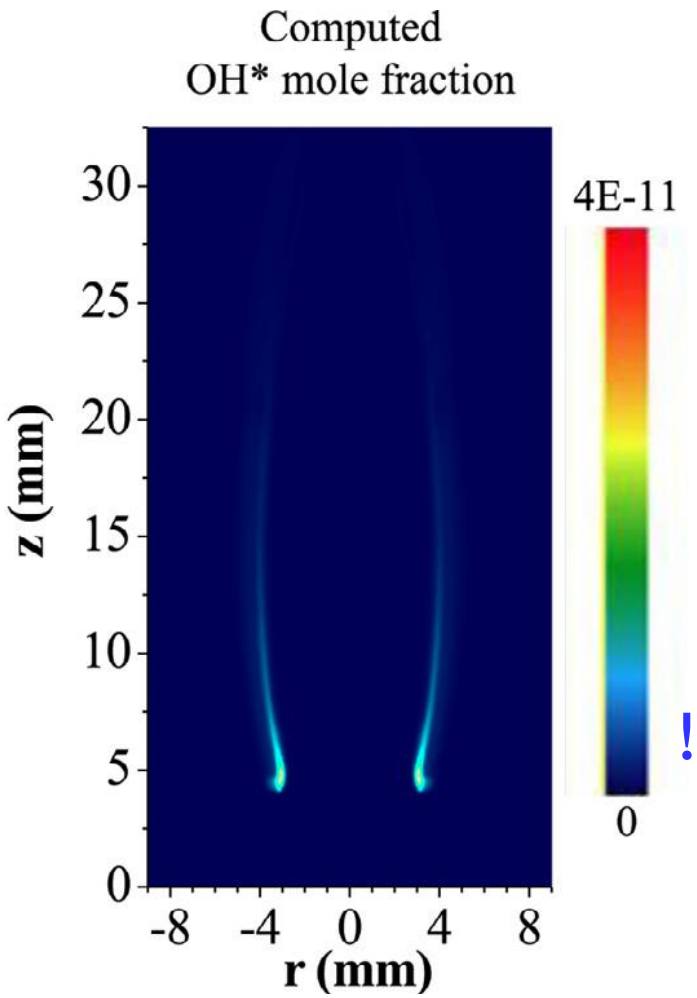

Najm et al., Comb. Flame 113 (1998) 32
Smith et al., Comb. Flame 131 (2002) 59
Kathrotia et al. App Phys B 107 (2012)
Konnov, CnF 253 (2023) 112788+112789
Sharipov et al., CnF 263 (2024) 113407+113417

Chemiluminescence reaction mechanism to model the formation/quenching of OH*[a].

	Reaction	A	B	E_a	Ref.
R1	$H+O+M=OH^*+M$	1.500E+13	0.00	5966	[22]
R2	$CH+O_2=OH^*+CO$	8.000E+10	0.00	0	[23]
R3	$OH^*=OH+h\upsilon$	1.450E+06	0.00	0	[24]
R4	$OH^*+H=OH+H$	1.310E+12	0.50	−167	[24]
R5	$OH^*+OH=OH+OH$	6.010E+12	0.50	−764	[24]
R6	$OH^*+H_2=OH+H_2$	2.950E+12	0.50	−444	[24]
R7	$OH^*+O_2=OH+O_2$	2.100E+12	0.50	−482	[24]
R8	$OH^*+H_2O=OH+H_2O$	5.920E+12	0.50	−861	[24]
R9	$OH^*+CO=OH+CO$	3.230E+12	0.50	−787	[24]
R10	$OH^*+CO_2=OH+CO_2$	2.750E+12	0.50	−968	[24]
R11	$OH^*+CH_4=OH+CH_4$	3.360E+12	0.50	−635	[24]
R12	$OH^*+N_2=OH+N_2$	1.080E+11	0.50	−1238	[24]

[a] Reaction rate coefficient $k=AT^B\exp(-E_a/RT)$, E_a-cal·mol^{-1}, R-cal·mol^{-1}·K^{-1}. h is Planck constant, and υ is the wavelength of chemiluminescent emission.

! Excited species kinetics not well known

- Localisation of the flame front…
- Heat release zone (HRR)
- Active control

Emission spectrum measured in a $NH_3/O_2/N_2$ flame

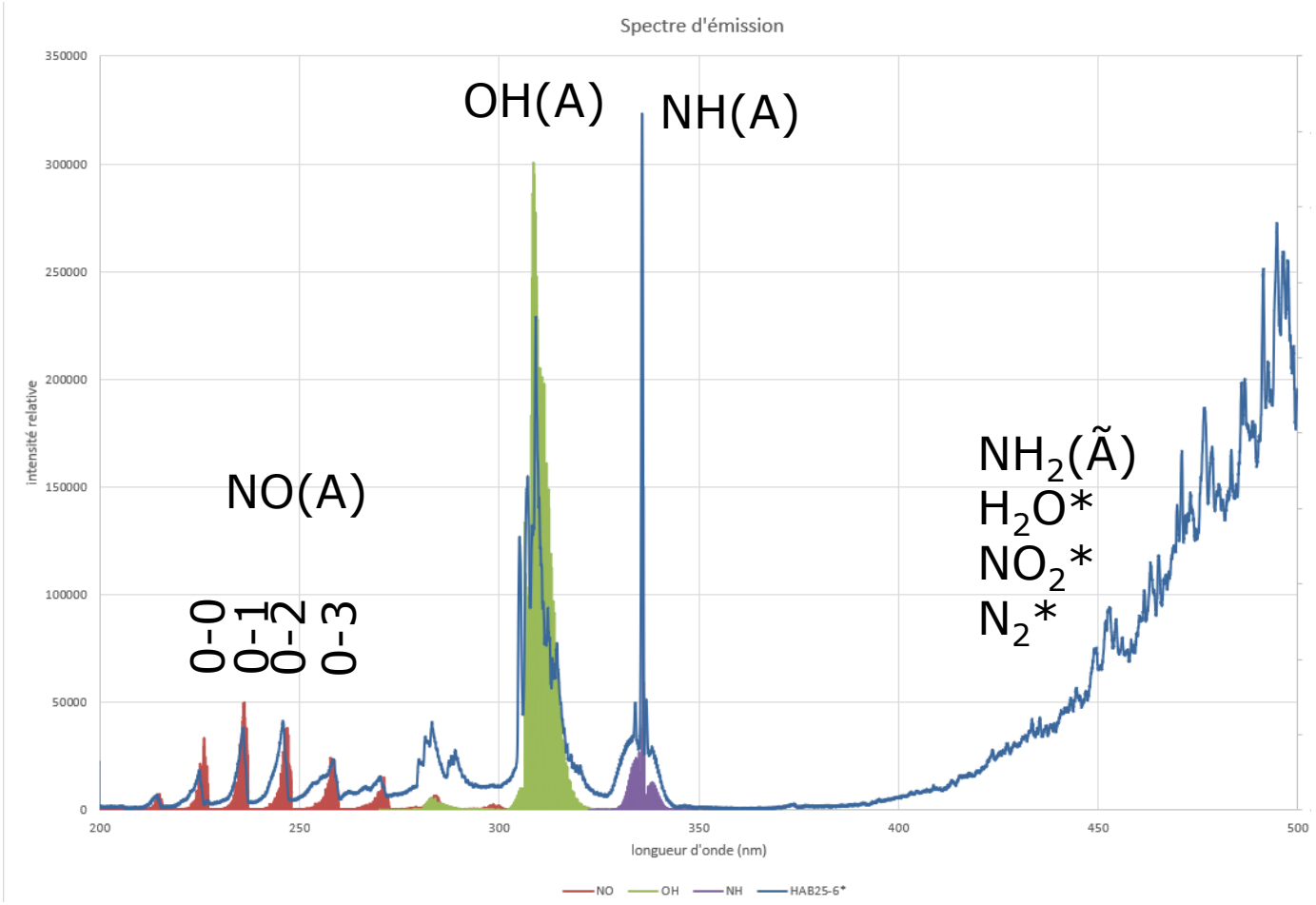

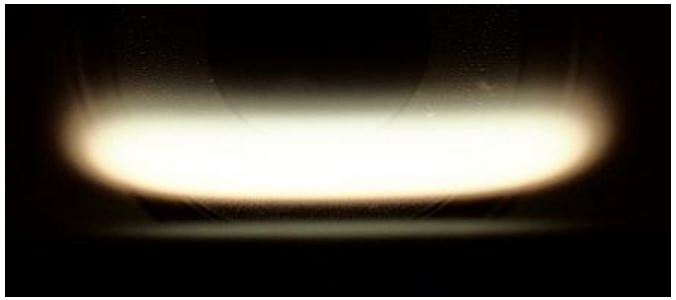

PC2A data

III. What happens in presence of light (no laser)?

III.1 Absorption

From Light lost as it passes through the Earth's atmosphere to the Beer-Lambert-Bouguer's law

Pierre Bouguer (1698-1758)
Essai d'optique sur la gradation de la lumière 1729

Jean-Henri Lambert (1728-1777)
+
August Beer (1825-1863)

Beer-Lambert-Bouguer's law is an empirical relationship linking the attenuation of a light beam to the properties of the medium it passes through and the thickness of that medium : **the absorption law**

Beer-Lambert-Bouguer (1852)

$$I_t = I_0 exp(-\alpha l_s)$$

α (absorption coefficient) proportional to concentration

Interaction lamp light/matter: light absorption

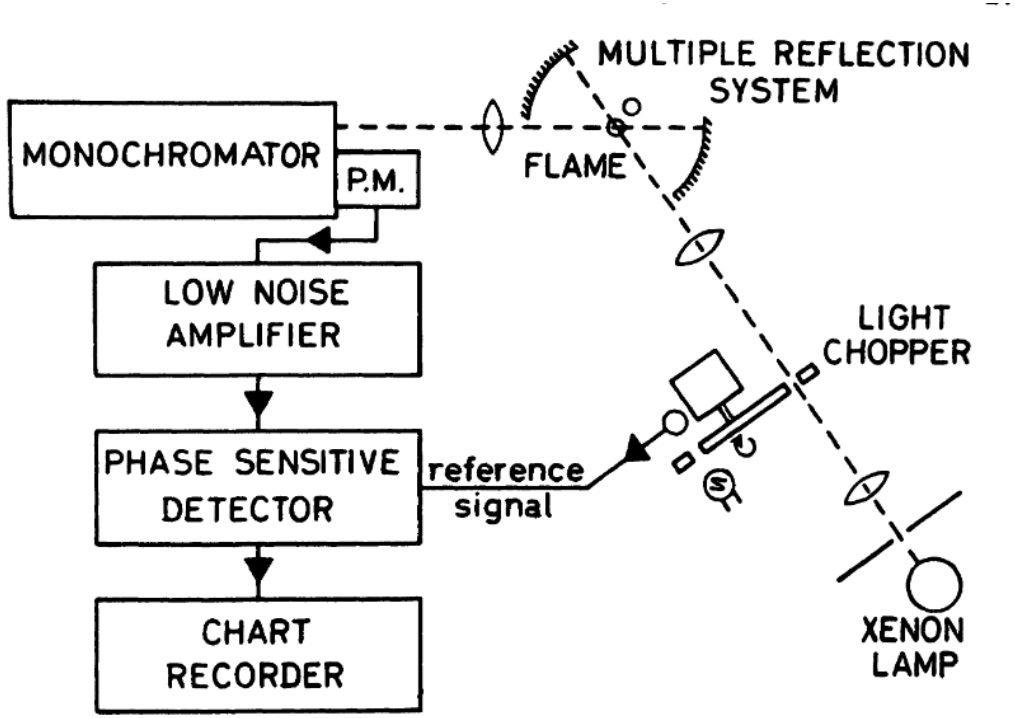

Xenon lamp

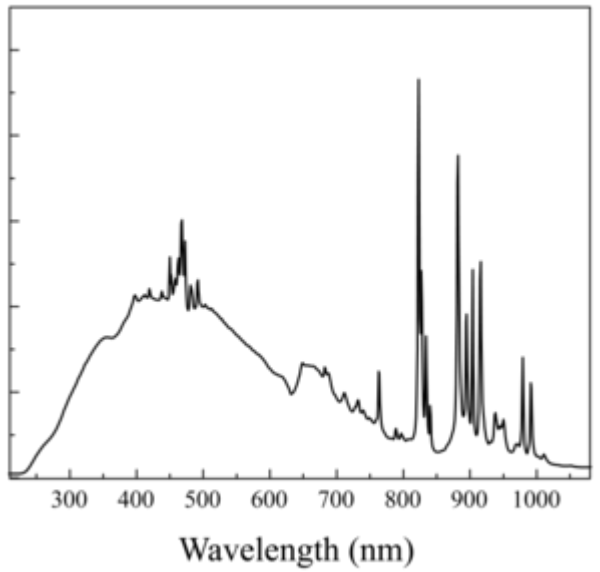

Spectro **1500 mm** focal length, 2nd order
Resolution~0.7 cm^{-1}

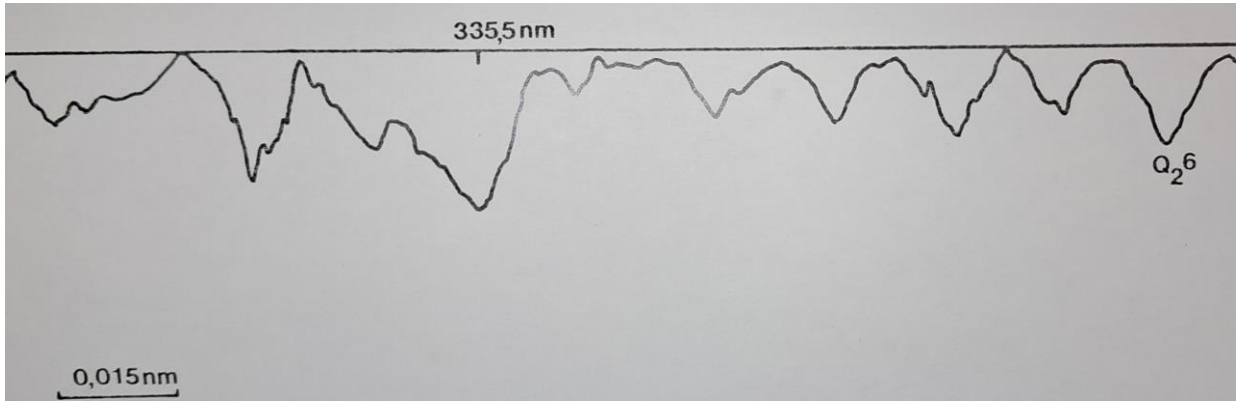

Absorption spectrum of NH ($^3\Pi$-$^3\Sigma$)

Thèse d'Etat Puechberty, CORIA, 1980

From peak absorption to concentration

(*with broadband source i.e. spectral irradiance constant across the spectral absorption width: simplified case*)

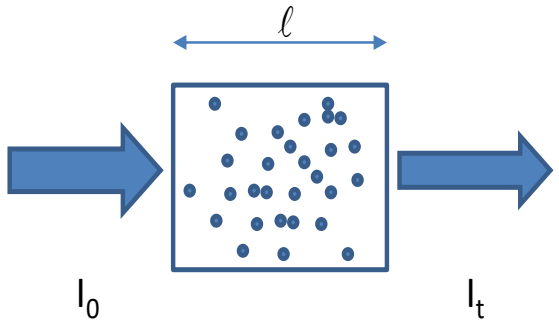

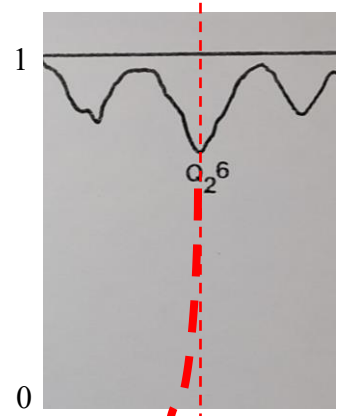

Garo et al. CST 86 (1992)

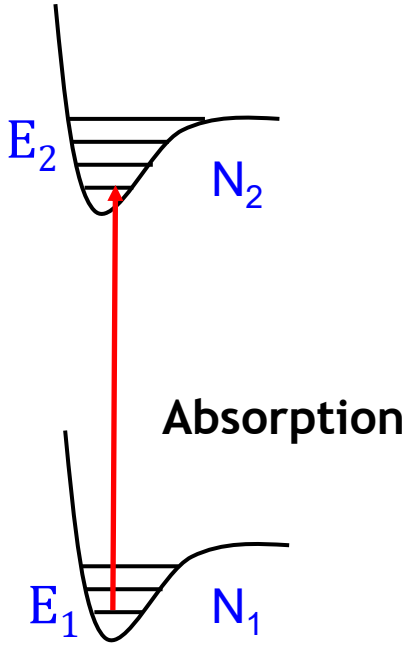

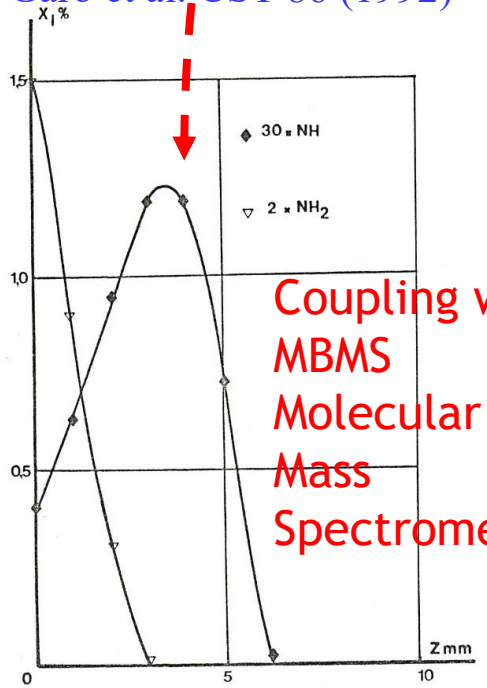

Coupling with MBMS Molecular Beam Mass Spectrometry

$CH_4/NH_3/O_2$ 25 Torr flame

Optical thin limit $\alpha l << 1$

$$\frac{I_{abs}}{I_0} = \alpha_{pk} l = \boldsymbol{\sigma_{pk}(\omega, T) N_T l}$$

with $N_T = N_1 / f_B$.

N_T : total population, N_1 : rotational population in the ground state and f_b : Boltzmann fraction

Several related quantities to determine the absorption

- Peak Absorption cross section ($wavenumber\ \bar{\nu}$)

$$\sigma_{pk}(\bar{\nu}, T) = \sqrt{\frac{4 \ln 2}{\pi}} \cdot \frac{1}{\Delta\bar{\nu}_{1/2}} \cdot \frac{\pi e^2}{m_e c^2} \cdot f_{12} \cdot f_B$$

- Oscillator strength

$$f_{12} = \frac{m_e c}{8\pi^2 e^2} \cdot \frac{g_2}{g_1} \cdot \frac{1}{{\omega_{12}}^2} \cdot A_{21} = \frac{m_e c h}{\pi e^2} \cdot \bar{\nu}_{12} \cdot B_{12}$$

- Einstein coefficient for absorption B_{21}

$$B_{21} = \frac{g_1}{g_2} B_{12} = A_{21} \frac{c^3}{8\pi h \nu^3} = A_{21} \frac{1}{8\pi h \bar{\nu}^3}$$

My message: with broadband sources and suitable highly resolving spectrometers, it has been possible to measure radical concentration in many flames using absorption, thanks to the knowledge of the scientists in spectroscopy. The limitation being the sensitivity…

III.2 Rayleigh-Raman

RAYLEIGH scattering

Rayleigh scattering
known since 1871

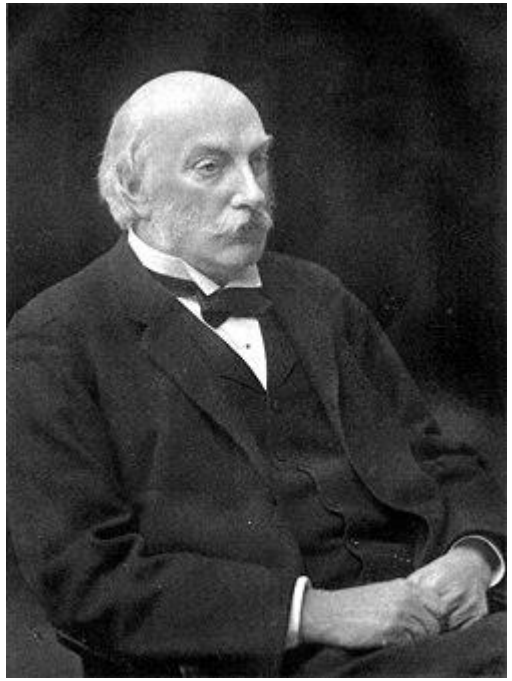

Lord John William Strutt Rayleigh
1842 - 1919

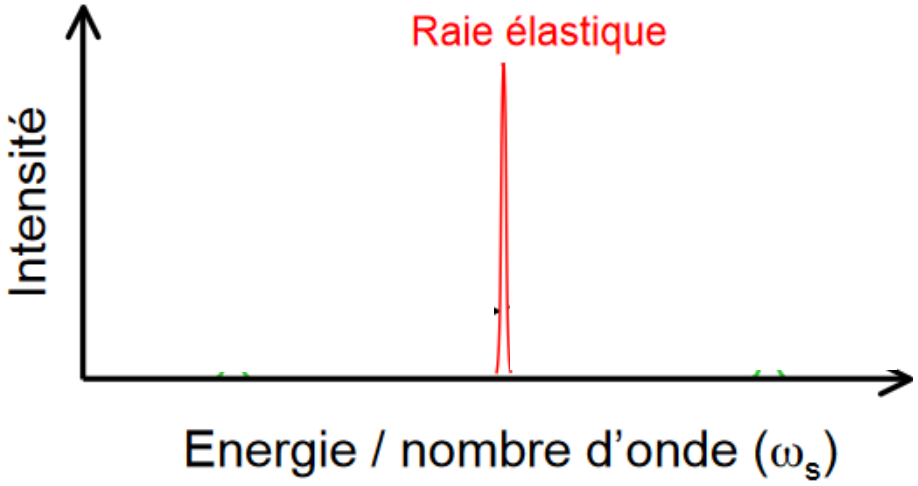

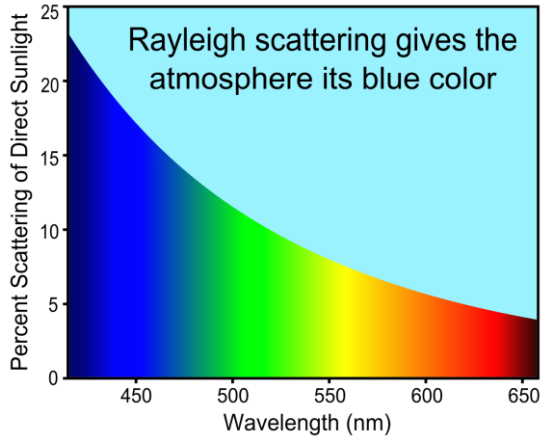

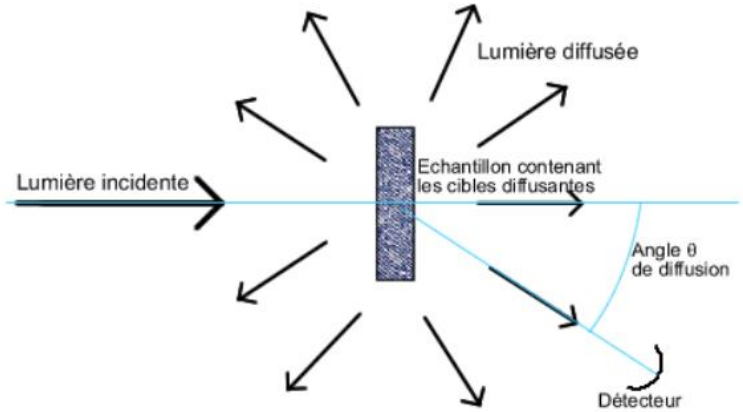

Nobel Prize 1904
for discovering Argon
as a component of air

RAMAN scattering

Chandrashekhara Venkata Râman

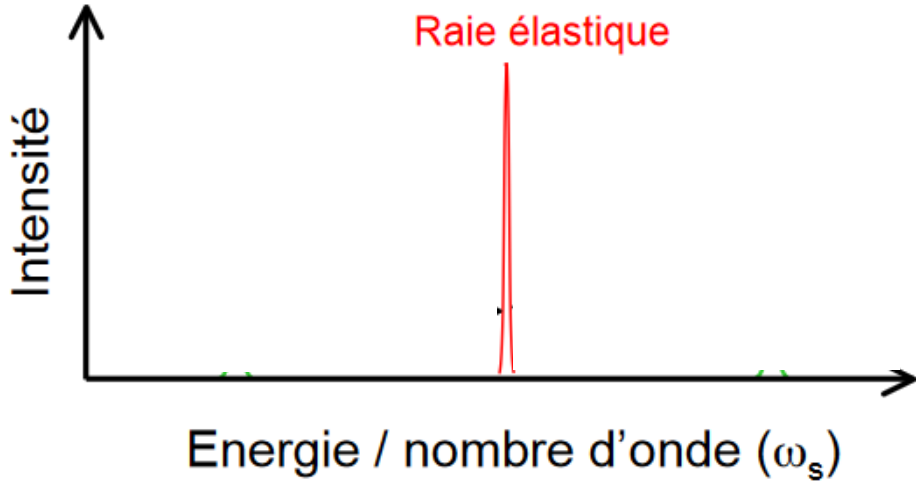

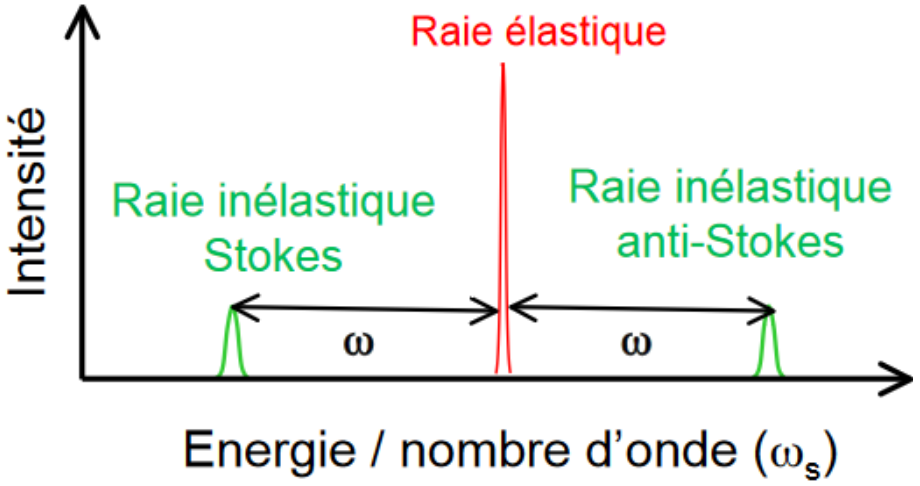

The Raman shift ω is species-specific: spectral signature of a species

Not at scale!

Non resonant spectroscopy: Raman scattering

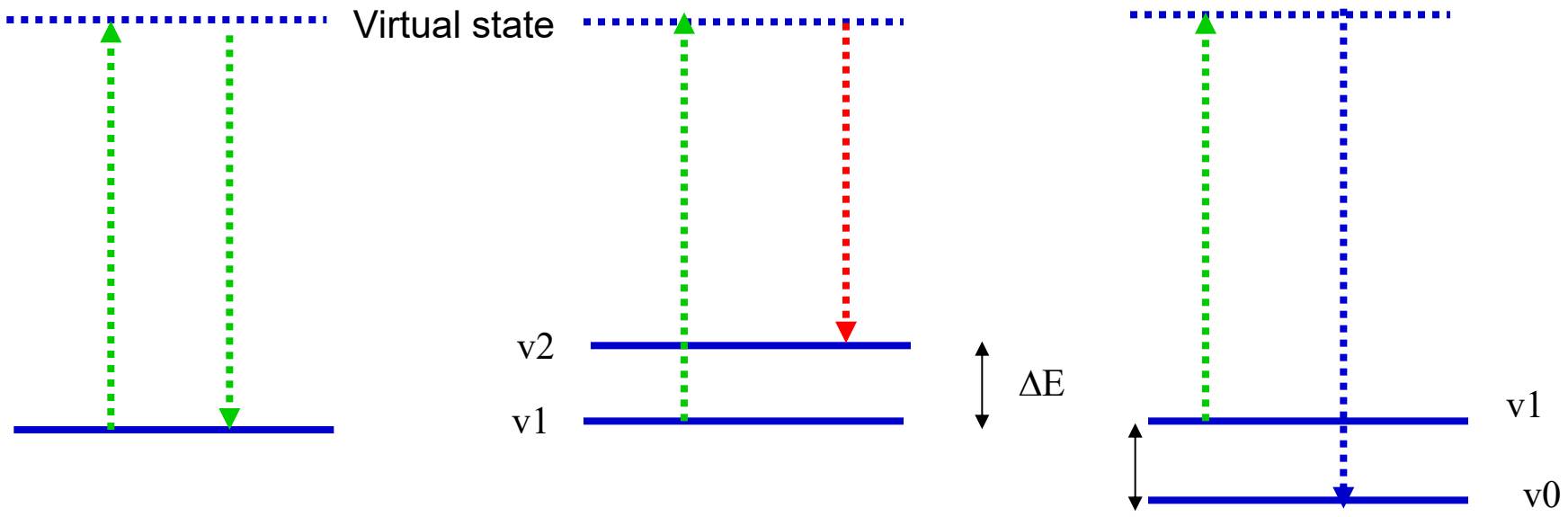

Rayleigh+Raman scattering: occurs whatever the laser wavelength

Raman: $\Delta\nu$ (Raman shift) specific of a major species (selective): N_i

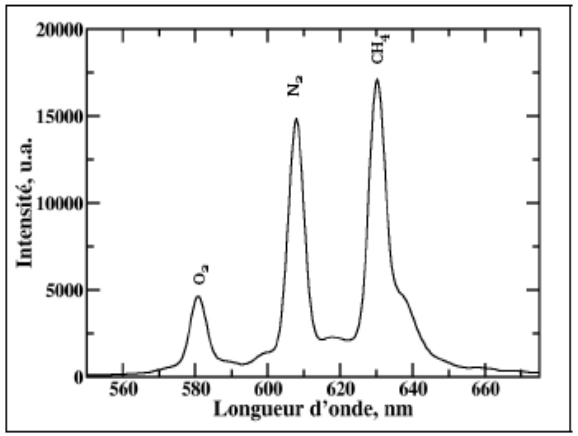

With a laser!

Spectre Raman Stokes. Excitation 532 nm, thèse Guillaume Cléon, Univ. Rouen 2007

Raman & Krishnan, Nature, (1928)

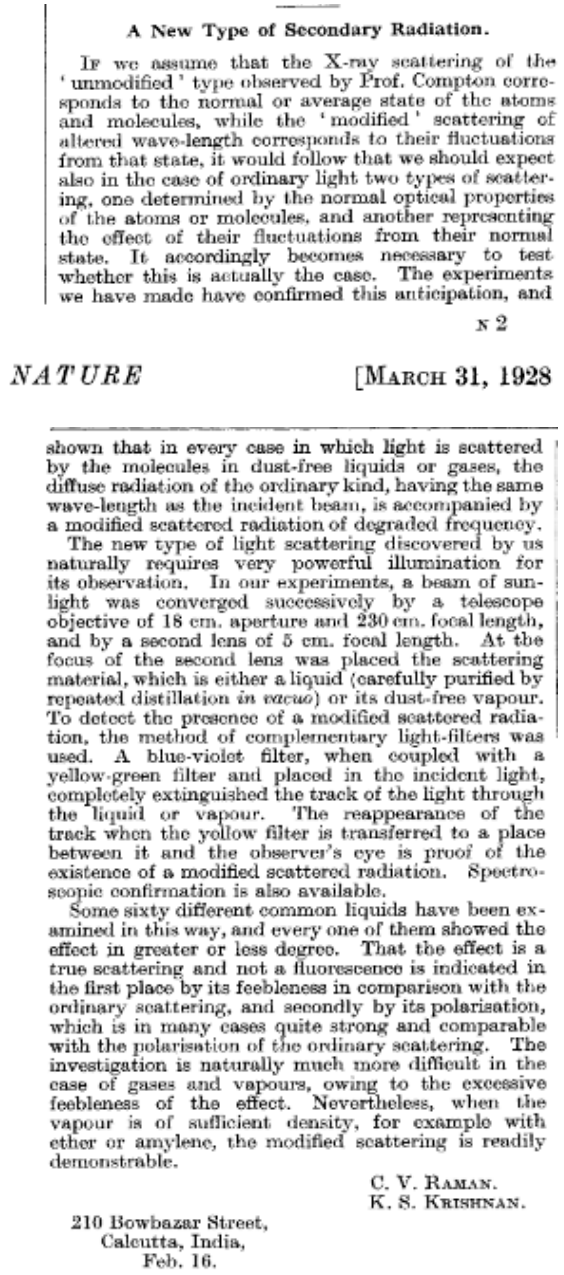

A New Type of Secondary Radiation.

If we assume that the X-ray scattering of the 'unmodified' type observed by Prof. Compton corresponds to the normal or average state of the atoms and molecules, while the 'modified' scattering of altered wave-length corresponds to their fluctuations from that state, it would follow that we should expect also in the case of ordinary light two types of scattering, one determined by the normal optical properties of the atoms or molecules, and another representing the effect of their fluctuations from their normal state. It accordingly becomes necessary to test whether this is actually the case. The experiments we have made have confirmed this anticipation, and

N 2

NATURE [MARCH 31, 1928

shown that in every case in which light is scattered by the molecules in dust-free liquids or gases, the diffuse radiation of the ordinary kind, having the same wave-length as the incident beam, is accompanied by a modified scattered radiation of degraded frequency.

The new type of light scattering discovered by us naturally requires very powerful illumination for its observation. In our experiments, a beam of sunlight was converged successively by a telescope objective of 18 cm. aperture and 230 cm. focal length, and by a second lens of 5 cm. focal length. At the focus of the second lens was placed the scattering material, which is either a liquid (carefully purified by repeated distillation *in vacuo*) or its dust-free vapour. To detect the presence of a modified scattered radiation, the method of complementary light-filters was used. A blue-violet filter, when coupled with a yellow-green filter and placed in the incident light, completely extinguished the track of the light through the liquid or vapour. The reappearance of the track when the yellow filter is transferred to a place between it and the observer's eye is proof of the existence of a modified scattered radiation. Spectroscopic confirmation is also available.

Some sixty different common liquids have been examined in this way, and every one of them showed the effect in greater or less degree. That the effect is a true scattering and not a fluorescence is indicated in the first place by its feebleness in comparison with the ordinary scattering, and secondly by its polarisation, which is in many cases quite strong and comparable with the polarisation of the ordinary scattering. The investigation is naturally much more difficult in the case of gases and vapours, owing to the excessive feebleness of the effect. Nevertheless, when the vapour is of sufficient density, for example with ether or amylene, the modified scattering is readily demonstrable.

C. V. RAMAN.
K. S. KRISHNAN.

210 Bowbazar Street,
Calcutta, India,
Feb. 16.

Nobel prize 1930

« In every case in which light is scattered by the molecules in dust-free liquids or gases, the diffuse radiation of the ordinary kind, having the same wavelength as the incident beam, is accompanied by a modified scattered radiation of degraded frequency »

IV. Discovery of the laser and consequences on combustion research

The invention of the Laser: a global technological revolution, including for combustion research

Theoretical concept (1958): Arthur Schawlow and, above all, Charles Townes (**Nobel Prize, 1964).** A replica of Theodore Maiman's laser, in the center of which one can see the ruby rod that produces the photons (1960)).

Le laser, histoire d'une découverte lumineuse, X. Müller, Journal du CNRS (2015)

The invention of the Laser: a global technological revolution, including for combustion research

1- What to do with a monochromatic coherent light?
In **1966, advent of tunable dye lasers**

High spectral finesse (< 0.1 cm^{-1})
***cw* ring-dye laser < 0.03 cm^{-1}**

High resolution **SPECTROSCOPY!**

2- The advent of the pulsed laser: exceptional available light power enabling instantaneous measurements (during a laser pulse)

Tunable dye laser

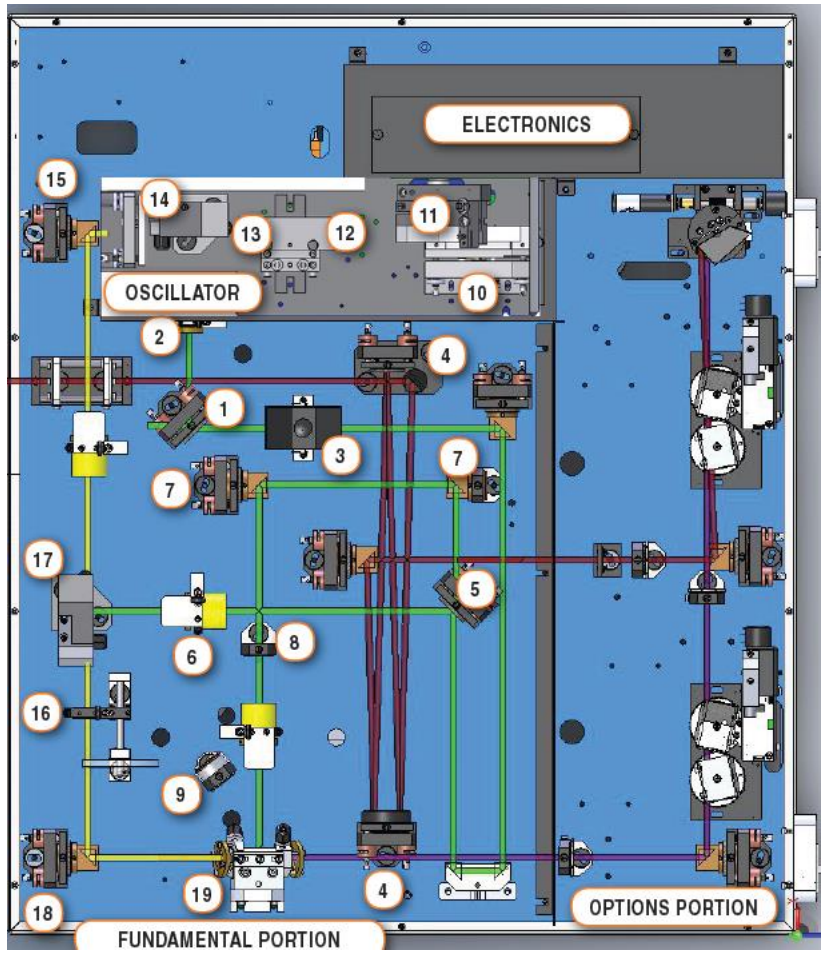

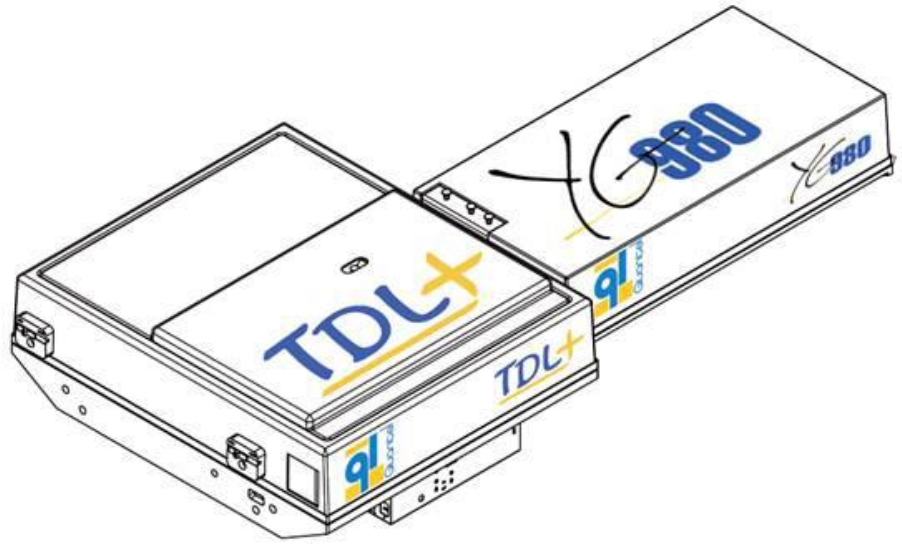

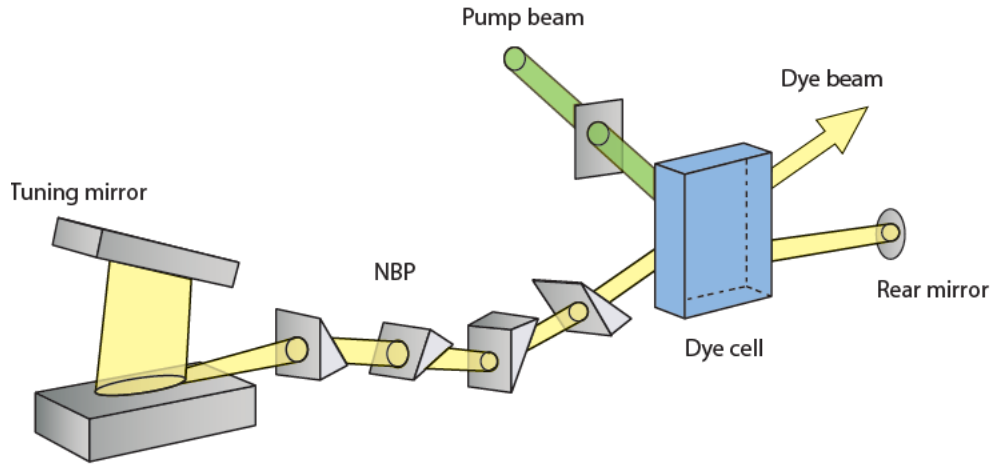

Example of TDL90 Quantel

Power
Pulse duration: ns, ps, fs
Spectral bandwidth
Repetition rate

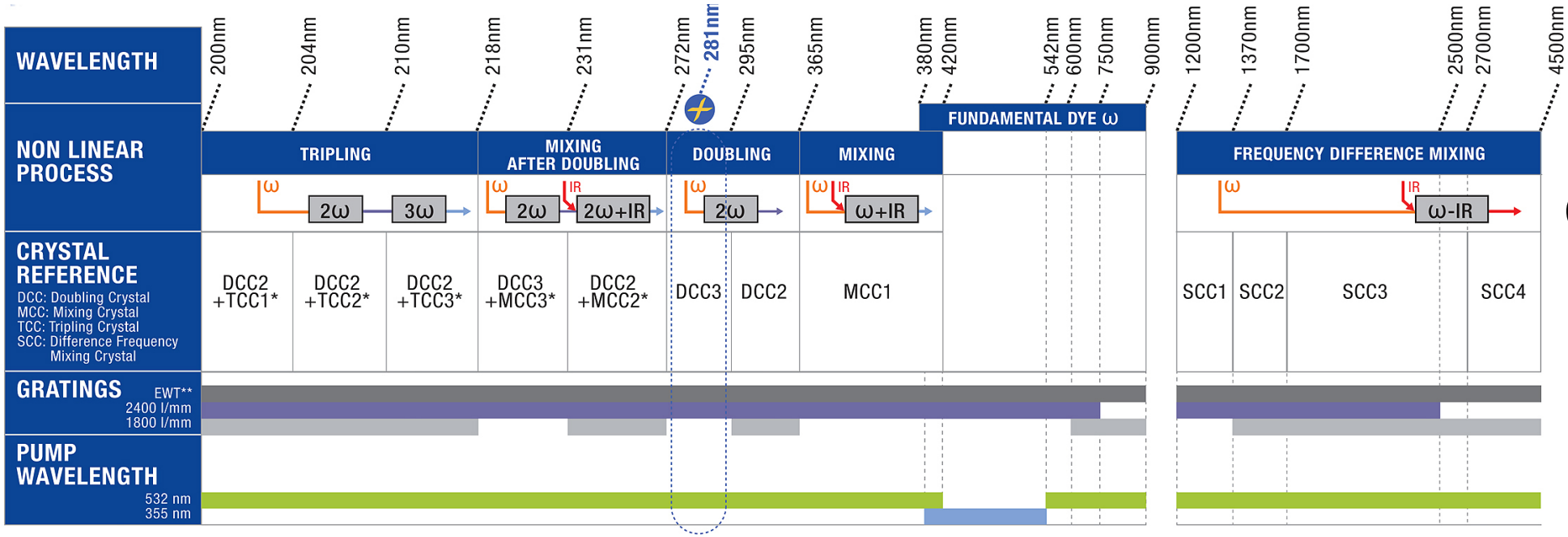

Example of TDL90 Quantel

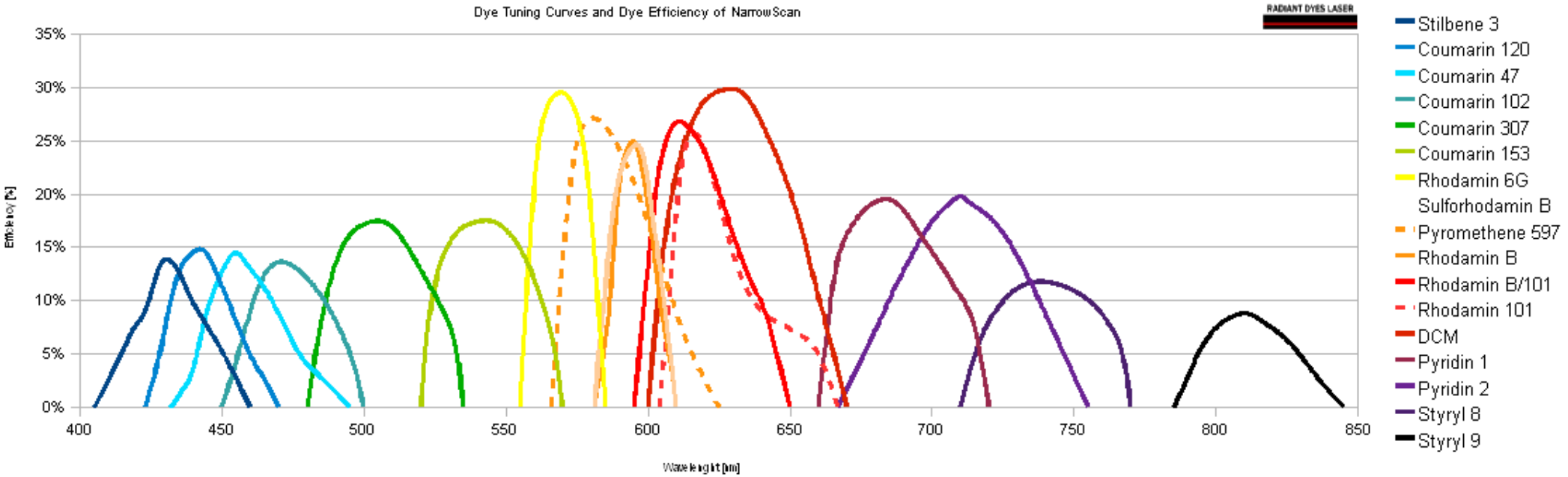

Radiant dye laser chart

Typical laser diagnostic set-up

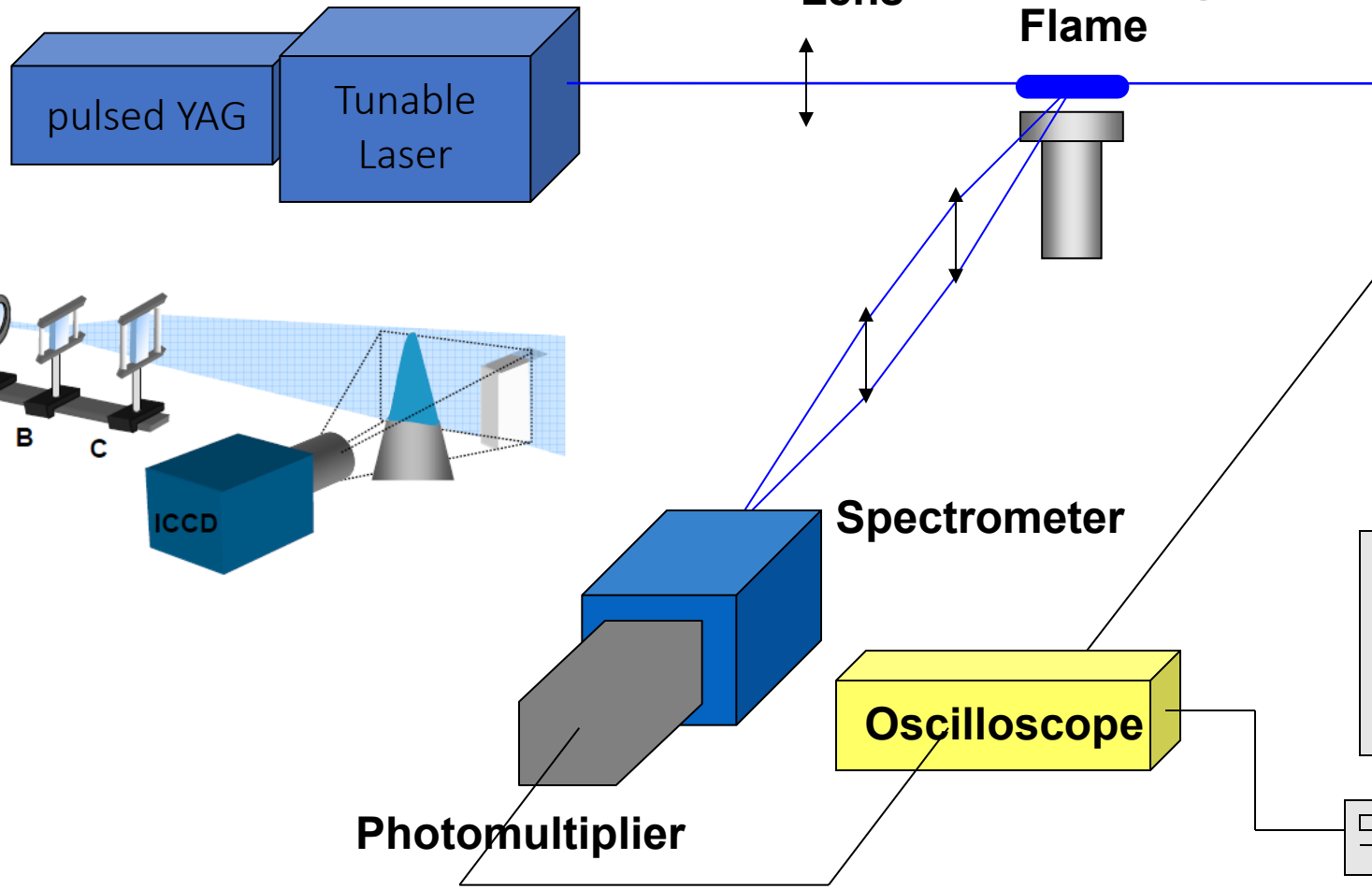

Analysis:

. spectral

. spatial

. temporal

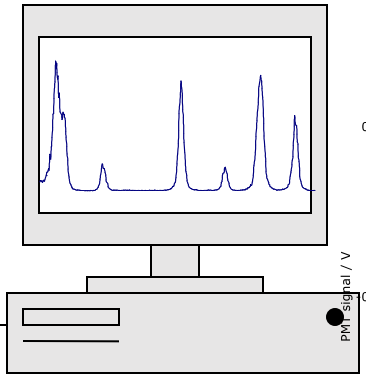

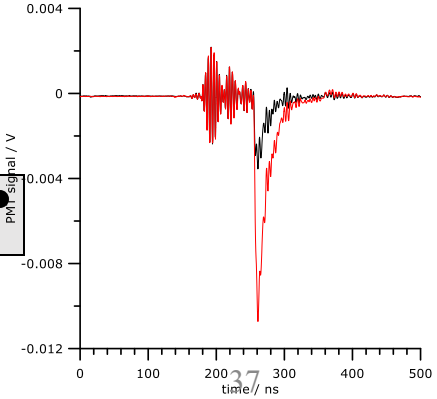

Spectroscopic laser diagnostics for what purpose?

- **Scalar fields (T, P, density, mole fraction (X) of species)**
  - Major species, minor species, **radicals and atoms**
  - Particles (soot, metal)
  - Temperature

- **Main interest**
  - In situ measurements, **spatially resolved**. No flame perturbation
  - local, 2D
  - In stationary or turbulent reactor
  - **Instantaneous** (potential)

ref: « Applied Combustion Diagnostics », Edited by K. Kohse-Höinghaus and J. Jeffries, Taylor and Francis (2002)

Classification of the methods of diagnostic (gas phase)

+CRDS (intermediates)

Non intrusive

+ Raman (major species)
+ Rayleigh

From Kohse-Höinghaus
Prog. Energ. Comb., 20, 203 (1994)

TABLE 1. Techniques for the determination of intermediate concentrations and temperature in combustion systems

Section	Technique*	Characteristic features	Comments; primary applications
2.	Techniques without lasers		
	ESR, MS, thermocouple	Require physical probes, quantitative applications questionable; low spatial and temporal resolution	Have lost their importance in comparison with laser techniques
	Emission, absorption	Low complexity, low spatial resolution	At present, not of primary importance
3.	Laser absorption	Spatial resolution along a line; low complexity of experiment and theory	Well-suited for calibration purposes; useful in spectroscopic or kinetic context; can yield temperature, pressure and velocity
4.	LIF	Very sensitive; two-dimensional applications and multi-species detection possible; sensitive to collisions	Often applied, very versatile technique; suitable for concentration, temperature and velocity measurements; also used with tracers
4.3.	Saturated LIF	High signal intensity, reduced influence of collisions and laser intensity variations; more complicated theory	Rather seldom applied, potential not fully exploited; broadband and high-pressure applications need refined theory
4.5.	LIPF	Excitation of predissociative states; if predissociation is dominant, lower signal than LIF, but less sensitive to quenching	Mainly applied for O_2 and OH; in the case of OH, suitable at moderate pressures and for high number densities
6.2.	PLIF	Spatially resolved instantaneous two-dimensional image of combustion parameters	Indispensable for practical combustion studies, whenever applicable; species and temperature
5.	Multi-photon techniques	Problems with laser-induced dissociation	Primarily used in chemically simple systems
	MPLIF	Enables detection of several atoms including H, C, N, O, Cl	Practical application e.g. in plasma/CVD* systems
	REMPI	Enables detection of non-fluorescing species; requires physical probe; quantitative interpretation difficult	Potential application for monitoring of polyatomic hydrocarbons and halocarbons
6.3.	DFWM	Laser-like signal beam; sensitive; enables detection of non-fluorescing species; two-dimensional imaging and single-pulse 'multiplex' temperature measurement possible	Promising; primarily feasibility studies available; systematic investigations are being performed; complete theory under development
6.4.	ASE	Laser-like signal beam; very sensitive detection of light atoms and some molecules; in general, spatial resolution along a line	Limited to a few species; quantitative interpretation difficult
4.5.	CARS, resonance CARS	CARS in general too insensitive for radical detection in flames, electronic resonance required; laser-like signal beam; complex experimental arrangement and theory	Limited to special applications

*Abbreviations: MS: Mass spectrometry. LIF: Laser-induced fluorescence. PLIF: Planar laser-induced fluorescence. REMPI: Resonance-enhanced multi-photon ionization. DFWM: Degenerate four-wave mixing. CARS: Coherent anti-Stokes Raman scattering. ESR: Electron spin resonance. LIPF: Laser-induced predissociative fluorescence. MPLIF: Multi-photon laser-induced fluorescence. CVD: Chemical vapor deposition. ASE: Amplified spontaneous emission.

Concept of laser diagnostic cross section

For linear processes involving incident intensity, the emitted power P can be expressed as:

$$P = K\, n\, I\, d\sigma/d\Omega\, \Omega\, L$$

where P (W), K is related to the setup, I is the incident power, n is the number of emitters/vol, L is the length sampled by the collection optics along the laser axis, $d\sigma/d\Omega$ is the effective cross-section of the process, and Ω is the solid angle of collection

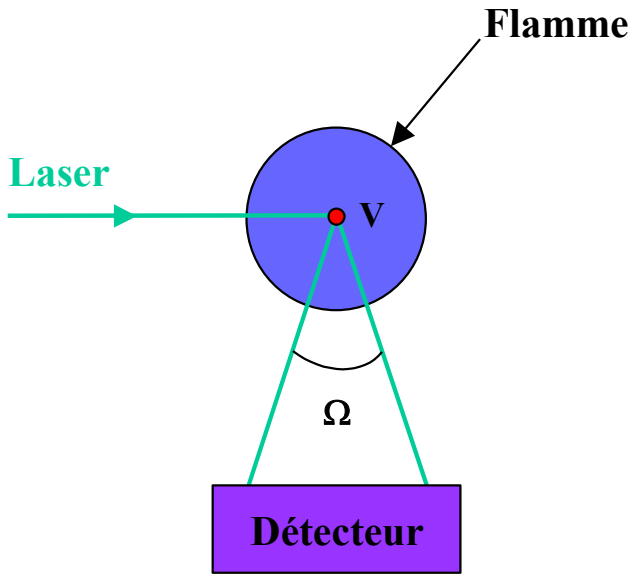

Type d'interaction	Section efficace(cm^2/st)	grandeurs mesurées	Caractéristique
Diffusion de Mie	10^{-15}	taille, suies	Diffusion élastique particule/photon
Diffusion Rayleigh	10^{-27}	T, fraction de mélange	Diffusion élastique molécule/photon
Raman spontané	10^{-30}	majoritaires, T	Diffusion inélastique
LIF	10^{-18}	intermédiaires, radicaux, T	Absorption/émission résonnante

In situ Spectroscopic diagnostics
based on interaction laser/matter

V. Non resonant spectroscopic methods

Introduction

Non resonant spectroscopic methods, whatever λ (no absorption)

- Few words on Rayleigh scattering (Total density of species, Temperature)

- **Raman scattering**
  - Concentration of major species (CH_4, O_2, N_2,H_2O …)
  - Temperature

Used in « clean » flames (without or very few particles responsible of Mie scattering)

Important potential for the study of turbulent flames

Rayleigh

$$I_{ray} = K \cdot I \cdot V \cdot \Omega \cdot N_T \cdot \sigma_{ray,eff}$$

$$\sigma_{ray,eff} = \sum_i x_i \cdot \sigma_{ray,i}$$

$$\sigma_{ray,i} = \frac{4 \cdot \pi^2}{\lambda_0^4} \cdot \left(\frac{n_i - 1}{N_0} \right)^4$$

Raman

$$I_{ram,i} = K.\Omega.V.\ \sigma_{ram,i} . N_i(v).I$$

$$N_i(v) = N_i \cdot e^{\left(\frac{-vh\upsilon}{kT} \right)} \cdot \left(1 - e^{\frac{-h\upsilon}{kT}} \right)$$

caution: σ should be replaced by
$d\sigma/d\Omega$: differential cross section

Rotational Raman scattering

Selection rules :

Vibrational : $\Delta v = \pm 1$

Rotational : $\Delta J = 0, \pm 2$

Q Branch, $\Delta J = 0$

S Branch, $\Delta J = +2$

O Branch, $\Delta J = -2$

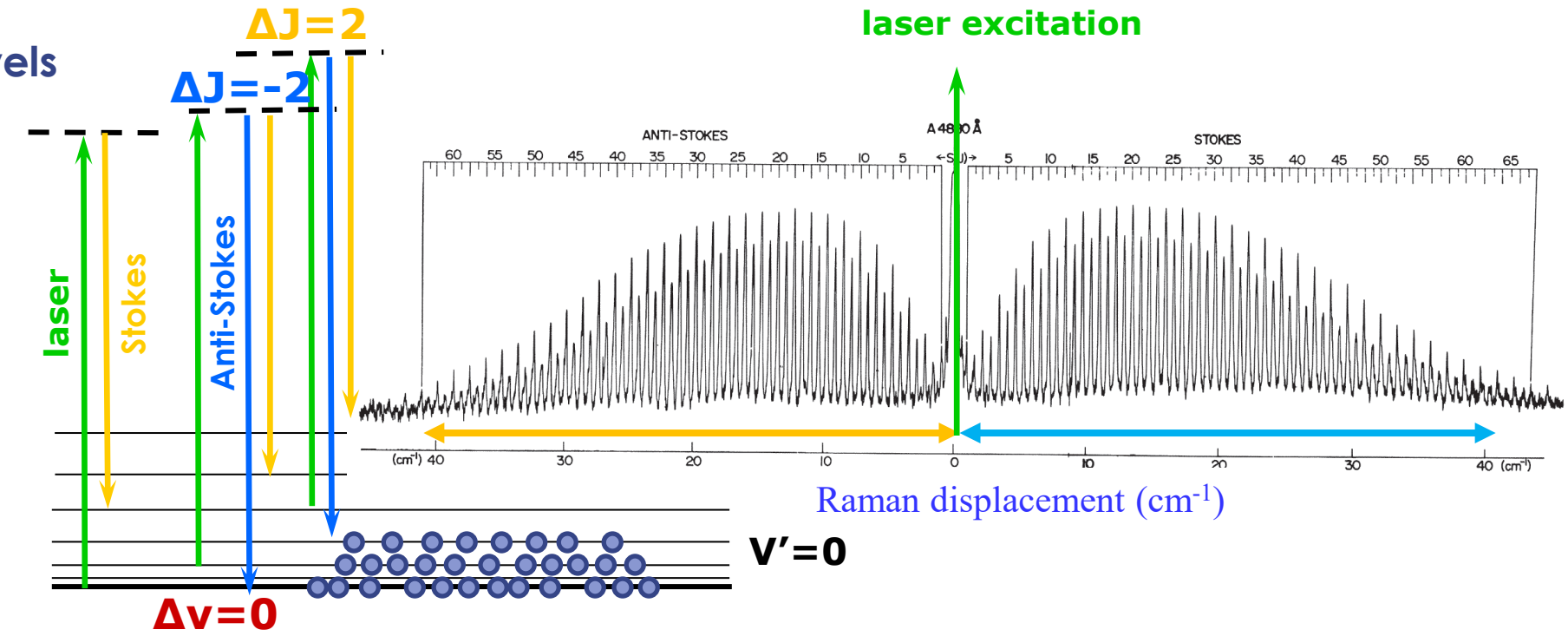

C_2N_2

Courtesy Armelle Cessou, CORIA

Weber, Raman spectroscopy of gases and liquid, 1979

Rotation-vibration Raman scattering at high temperature

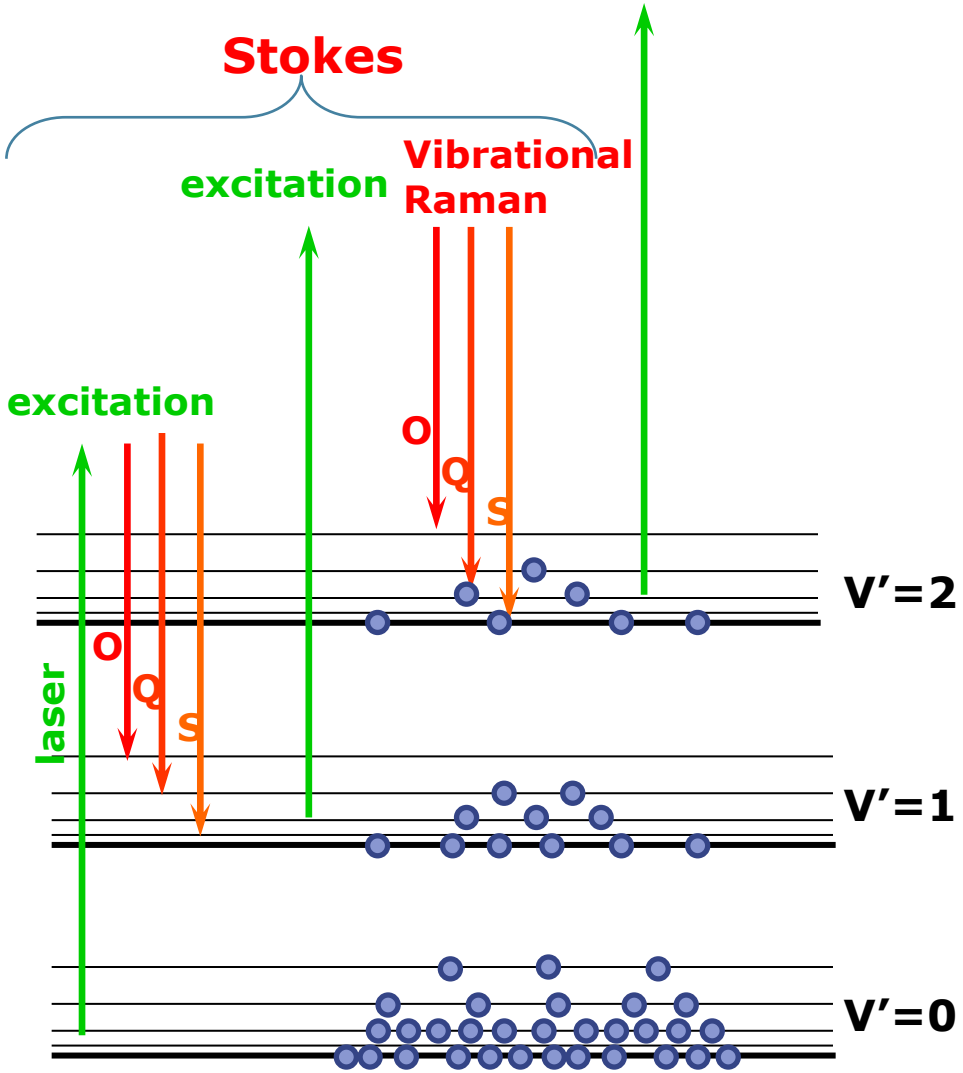

Combustion

burnt gas: 2100 K

N_2

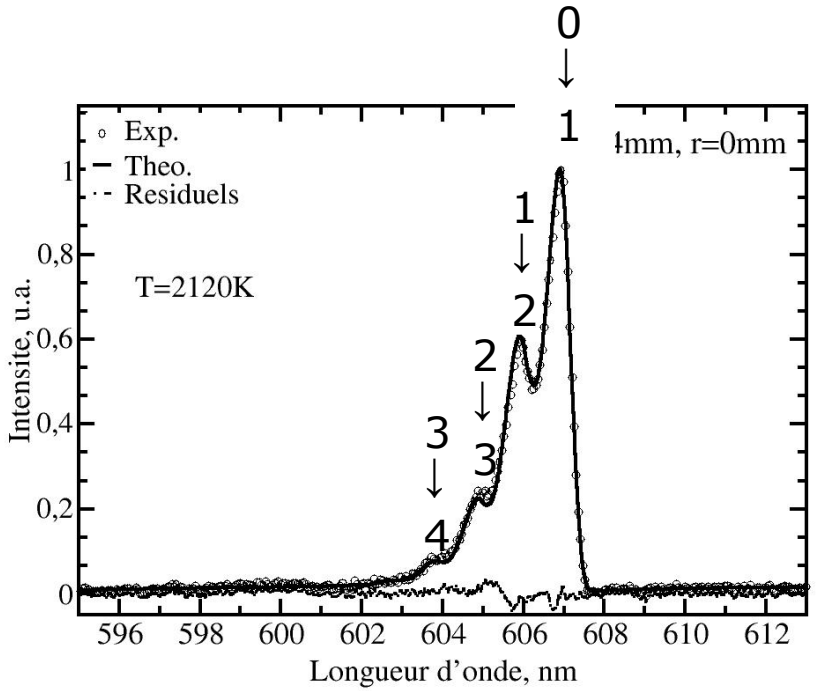

Courtesy Armelle Cessou, CORIA

In a high temperature mixture

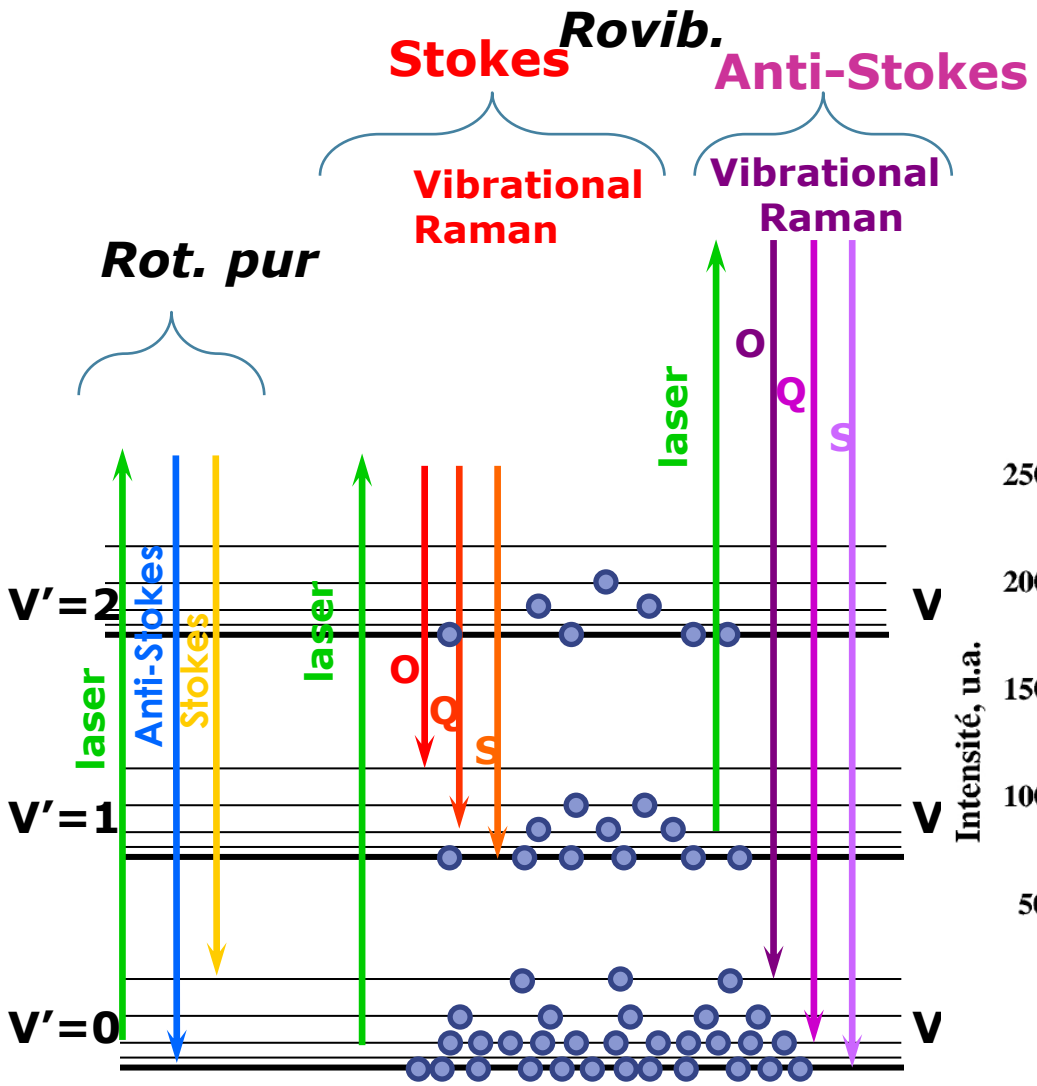

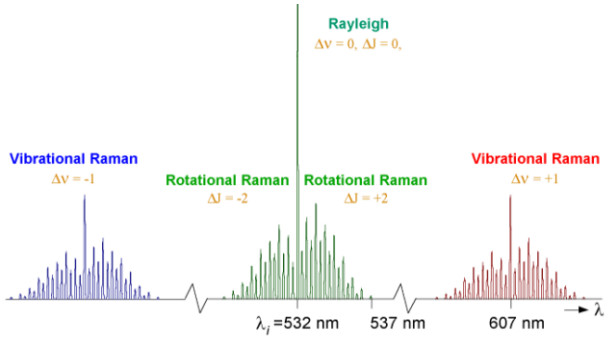

laser excitation @532 nm

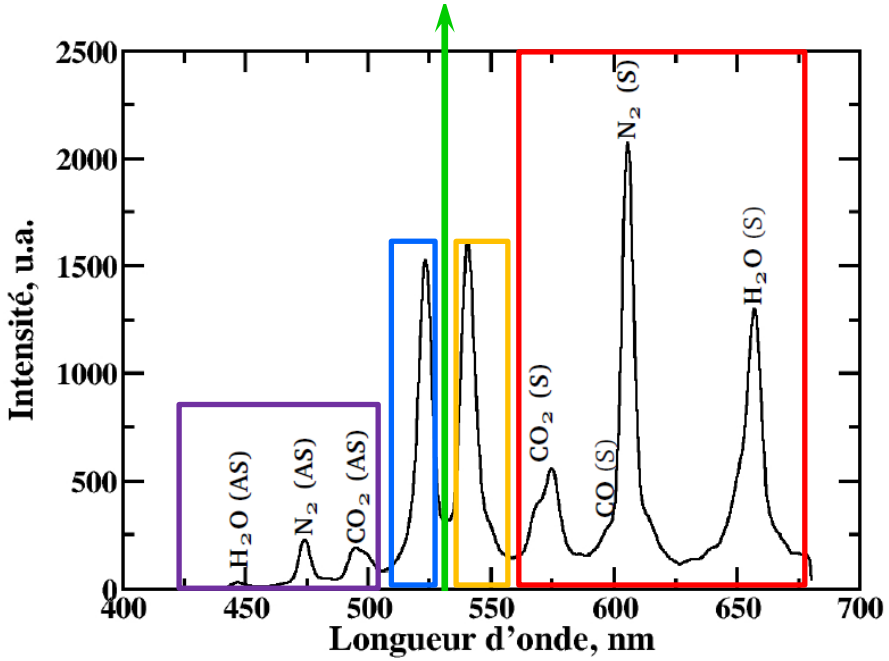

Courtesy Armelle Cessou, CORIA

1D Raman/Rayleigh spectroscopy: iterative post-processing procedure

- **Raman (inelastic) scattering → concentrations $N_i(r)$**

$$S_{ram,i}(\vec{r}) \propto \frac{\partial \sigma_{ram,i}(T(\vec{r}))}{\partial \Omega} I_{Laser} N_i(\vec{r})$$

- **Rayleigh (elastic) scattering → temperature $T(r)$**

$$S_{ray}(\vec{r}) \propto I_{Laser} \sum N_i(\vec{r}) \frac{\partial \sigma_{ray,i}}{\partial \Omega}$$

$$N_T \frac{d\sigma_{ray}}{d\Omega} = \sum_i N_i(\vec{r}) \frac{\partial \sigma_{ray,i}}{\partial \Omega} \longrightarrow T(\vec{r}) \propto \frac{1}{\sum N_i(\vec{r})}$$

Ideal gas law

→ **Determination of N_i, T by iterative procedure:**
Need $\sigma_{ram,i}$ of each species *i*

https://www.cce.tsinghua.edu.cn/__local/0/D5/C1/EAFCAB817075090EEDB9804E9BC_82362CF7_54030F.pdf?e=.pdf
A. Dreizler Technishe Universität Darmstadt

Raman scattering: polarisation effect

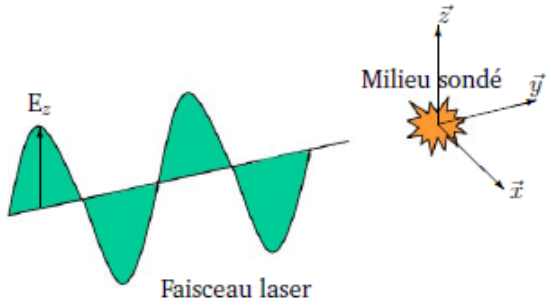

$$\vec{P}=\alpha\,\vec{E}$$

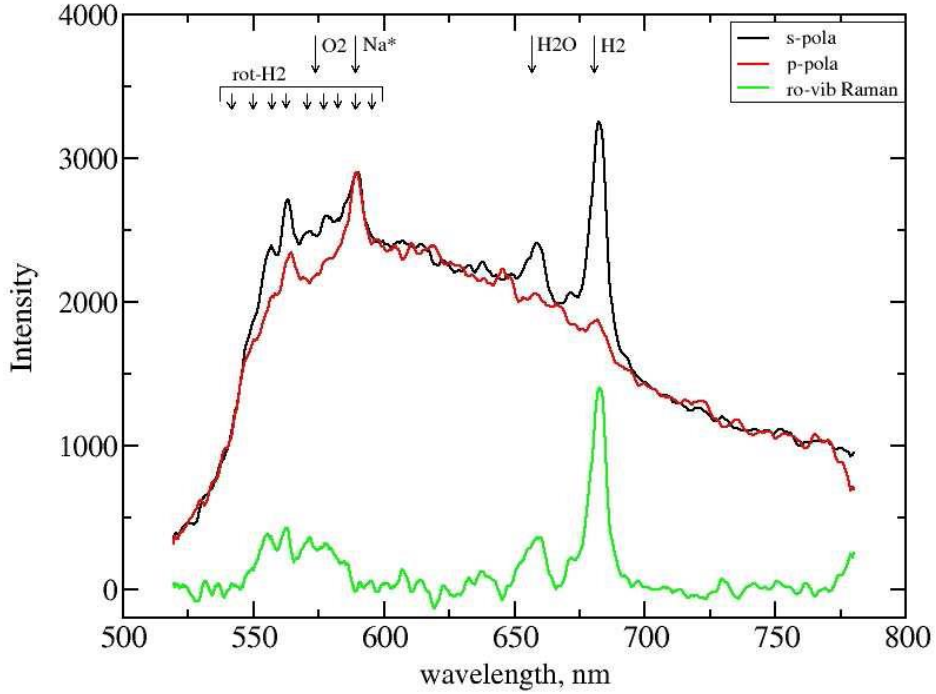

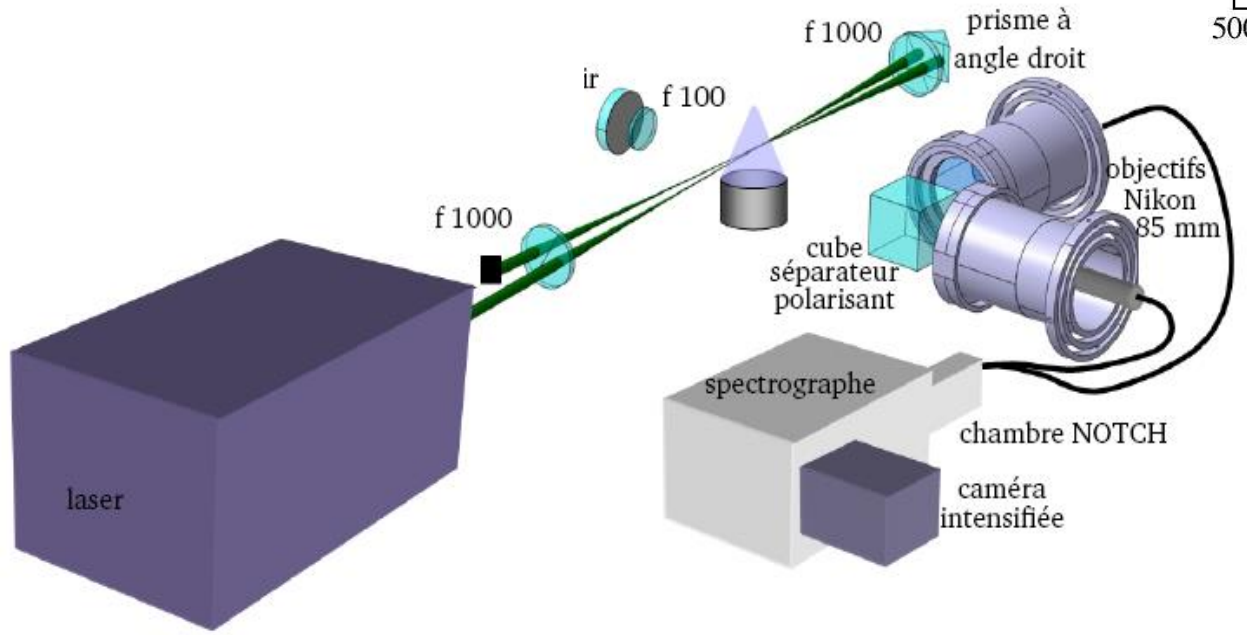

Experimental Raman set-up, High pressure flame (ONERA-MASCOTTE). Excitation at 532 nm, PhD G. Cléon, Univ. Rouen, CORIA 2007

Analysis of a turbulent flame using Raman scattering

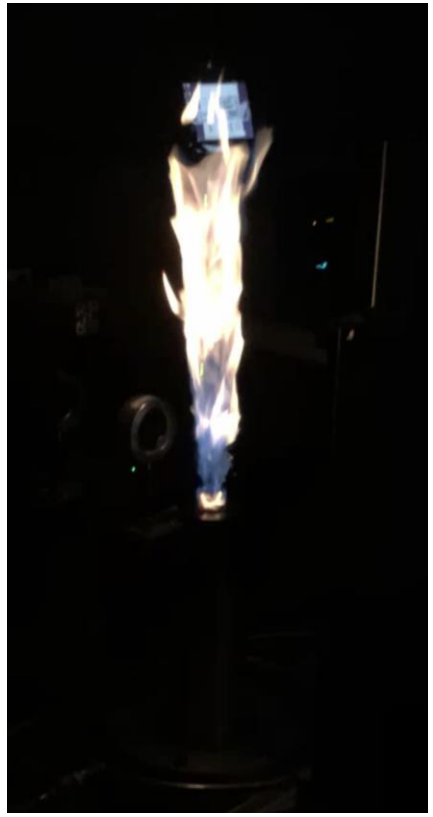

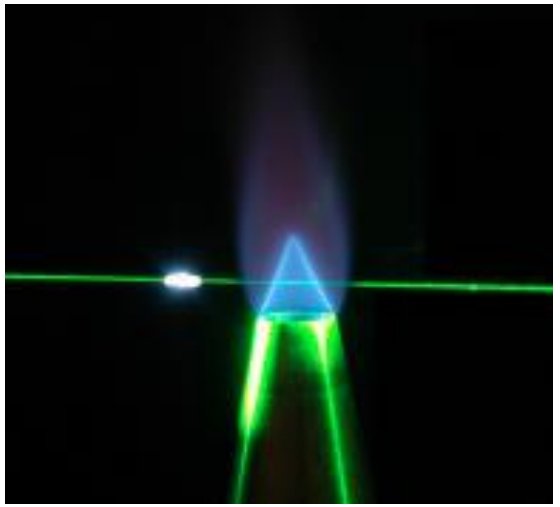

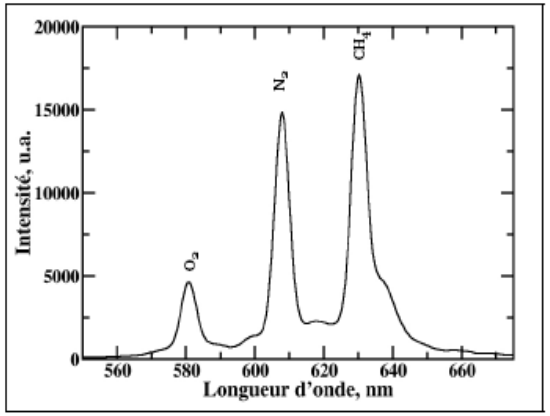

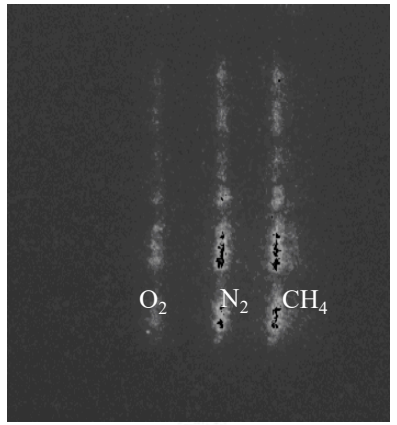

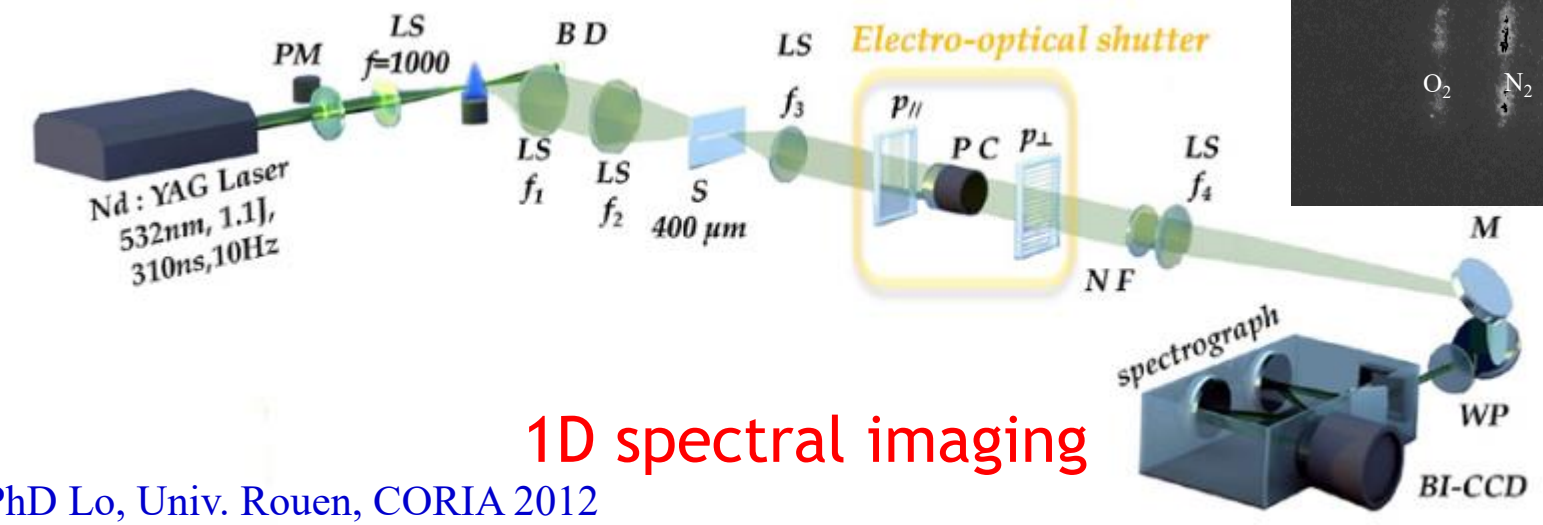

1D spectral imaging

Spectre Raman Stokes. Excitation 532 nm, PhD Lo, Univ. Rouen, CORIA 2012

Determination of instantaneous concentration fields of species and temperature in a turbulent flame

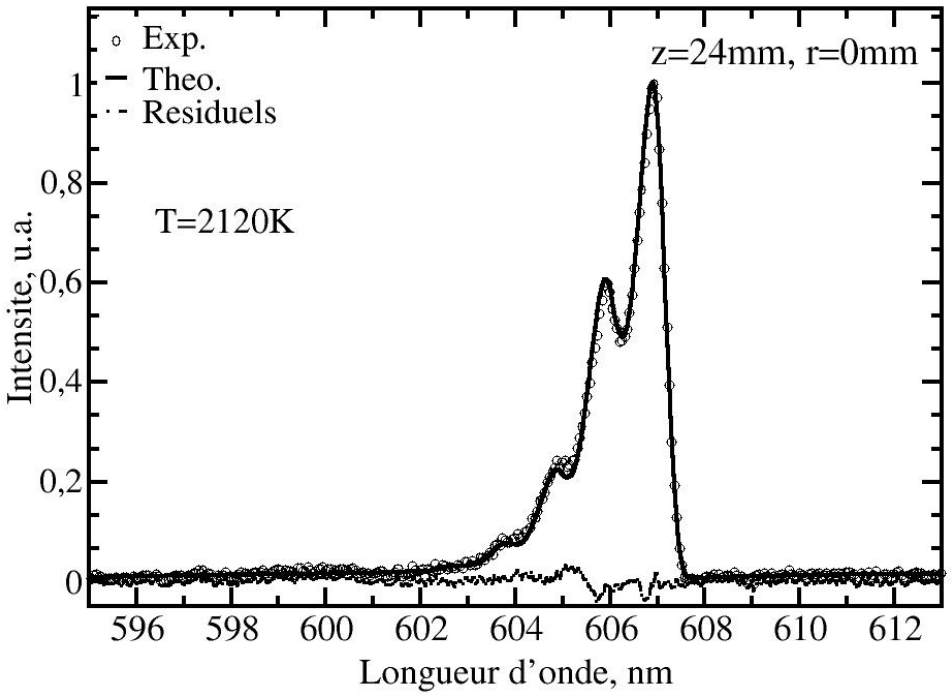

+ instantaneous temperature

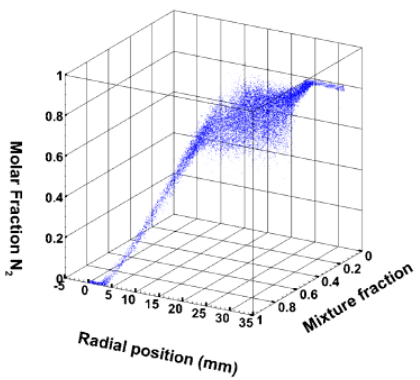

N_2

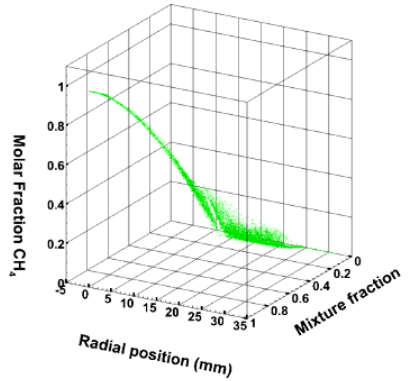

CH_4

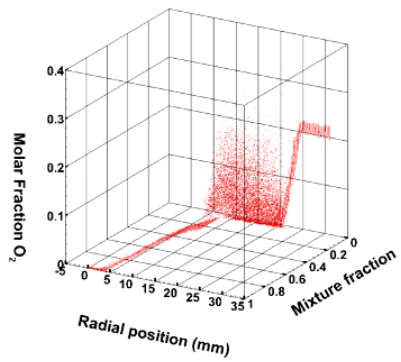

O_2

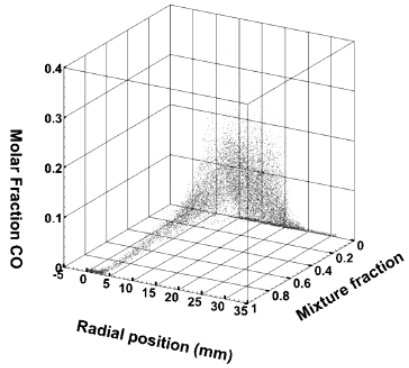

CO

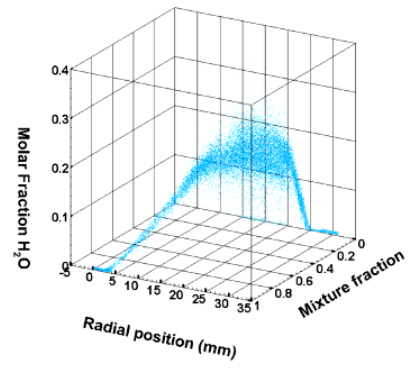

H_2O

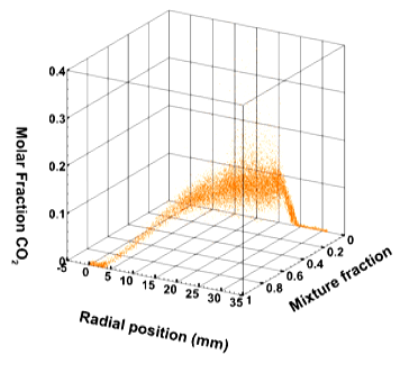

CO_2

PhD A. Lo, CORIA 2012

Polarized Raman light + non-polarized (natural flame emission+LIF)

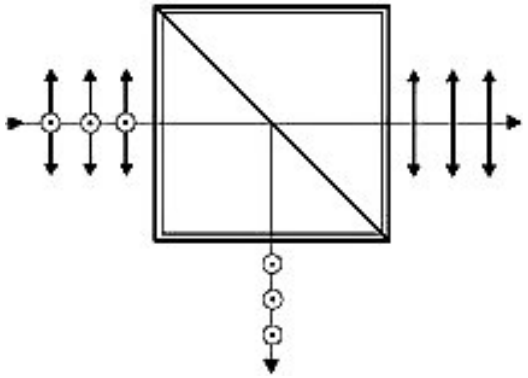

Fast electro-optical shutter
(Pockels cell + 2 crossed polarizers
1µs gate width))

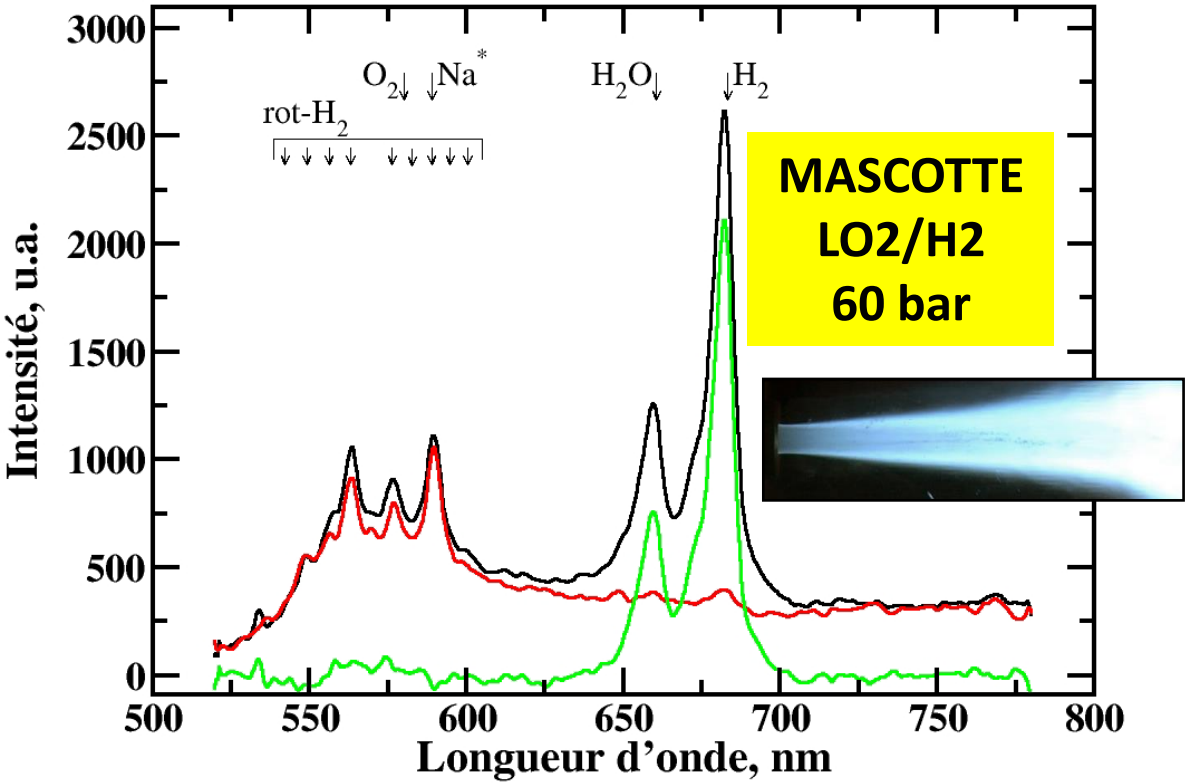

PhD G. Cléon, CORIA 2007

Ajrouche, Lo, Vervisch, Cessou, Meas Sci. Technol. 26 (2015)

In situ Spectroscopic diagnostics
based on interaction laser/matter

VI. Resonant spectroscopic methods

- Absorption, CRDS
- LIF
- Predissociated LIF

Which information ?

- Species concentrations (relative, absolute)
- Temperature, Boltzmann distribution

$$\frac{N_i}{N_{total}} = \frac{g_i e^{-E_i / kT}}{Q_{elec} Q_{vib}(T) Q_{rot}(T)} = f_B(i,T)$$

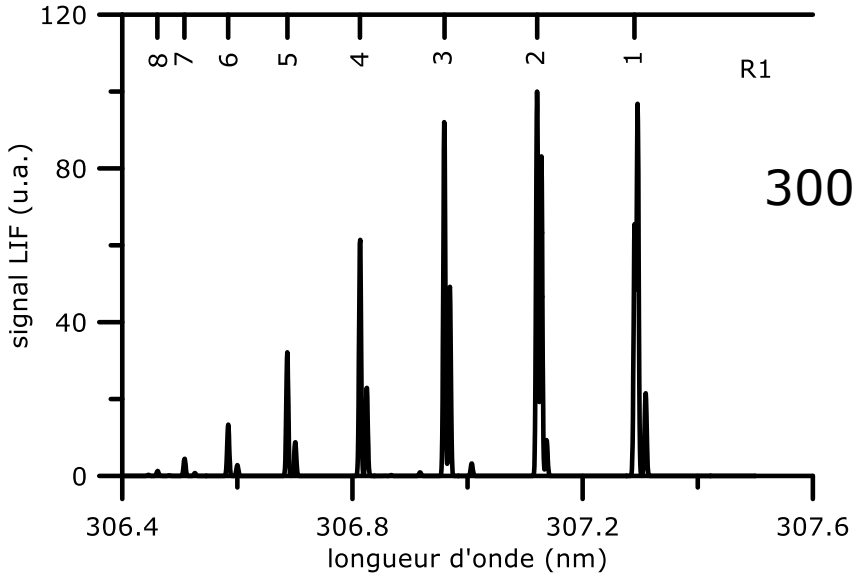

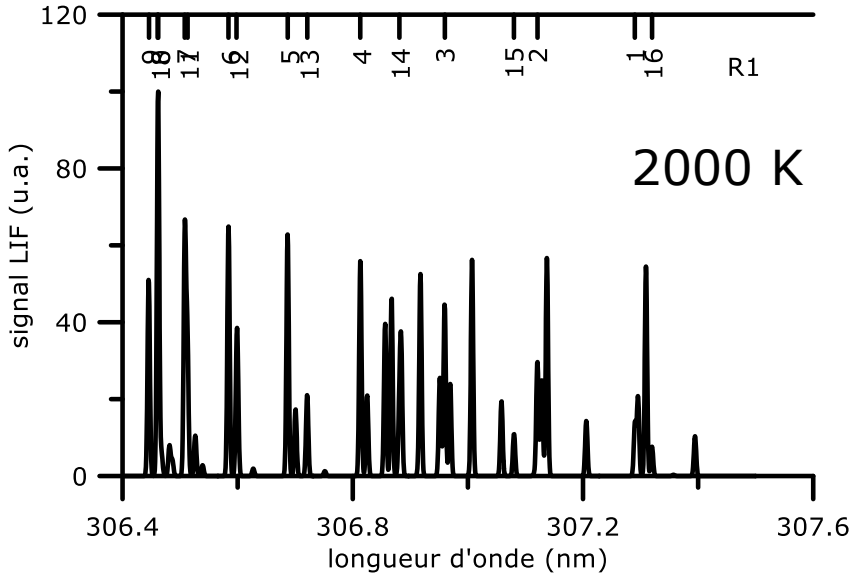

VI.1 Cavity RingDown Spectroscopy (CRDS)

O'Keefe, D.A.G. Deacon, Rev. Sci. Inst. 59. (1988). 2544.
J.J. Scherer et al., Chem. Rev. 97. 1997. 25.
M.D. Wheeler et al., Chem. Soc., Faraday Trans. 94. 1998. 337
D. Romanini, K.K. Lehmann, J. Chem. Phys. 99. 1993. 6287.
P. Zalicki, R.N. Zare, J. Chem. Phys. 102. 1995. 2708.
J.T. Hodges, J.P. Looney, R.D. Van Zee, Appl. Opt. 35. 1996. 4112.
R.T. Jongma, M.G.H. Boogaarts, I. Holleman, G. Meijer, Rev. Sci. Instrum. 66 (1995) 2821.

Single-path absorption

- Absorption method

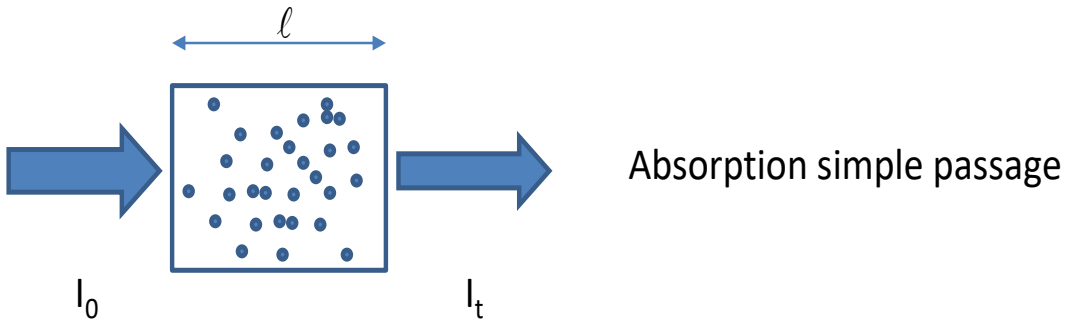

Absorption simple passage

- Beer-Lambert Law
- $I_t = I_0 exp(-\alpha l_s)$, avec αl_s<<1
- Limit of measurable attenuation: a few percent with a pulsed source

CRDS principle

Herbelin et al. App. Opt 19 (1980)

- Cavity Ring-Down Spectroscopy, ringdown time of a resonant optical cavity, constituted of 2 HR mirrors (R)

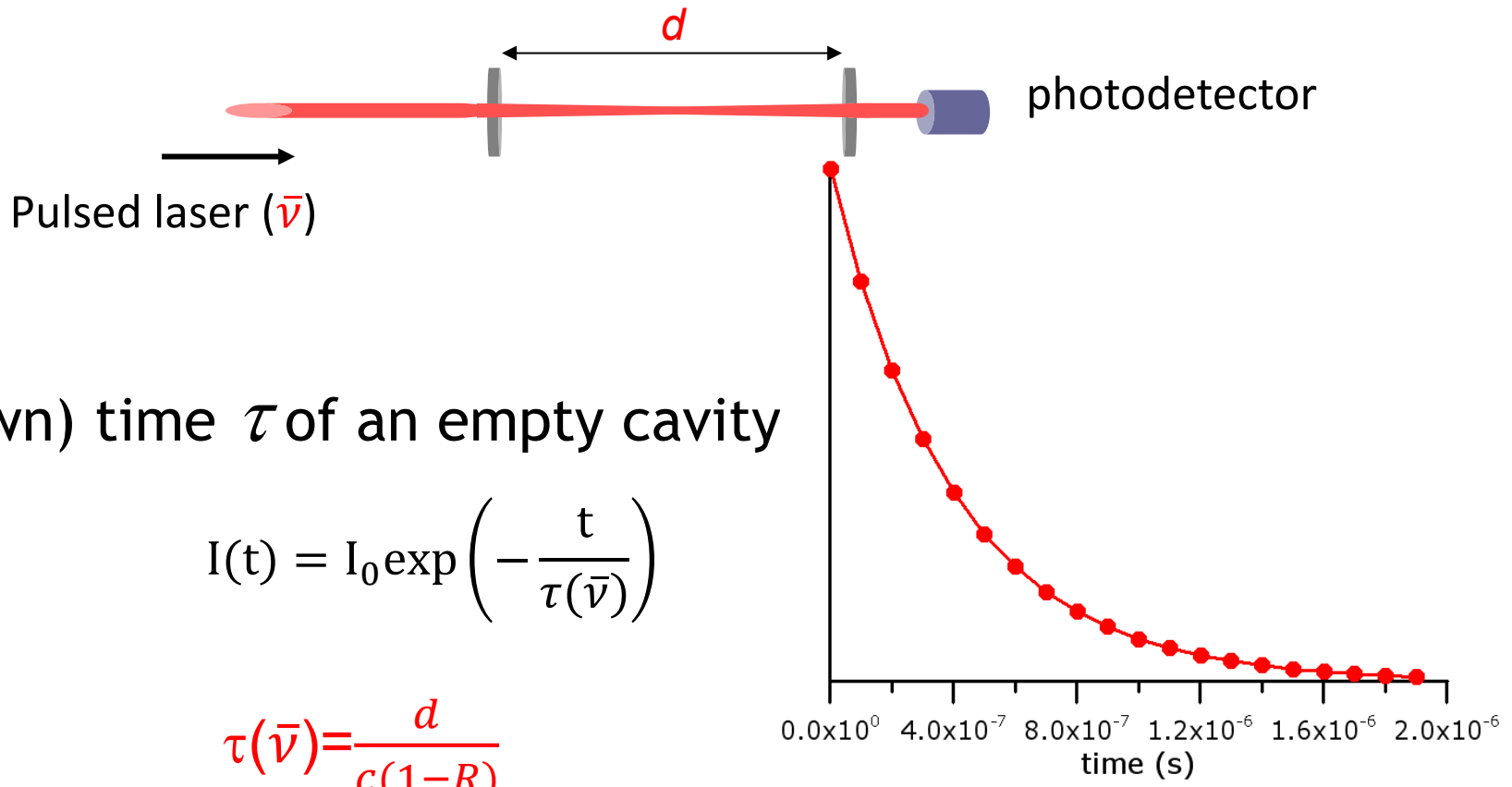

- Decay (ringdown) time τ of an empty cavity

d = 40 cm

τ = 4 10 $^{-7}$ s

R = 99.67%

Light path =120m

Nbr round trips=150

Nbr paths= 300

$$I(t) = I_0 \exp\left(-\frac{t}{\tau(\bar{\nu})}\right)$$

$$\tau(\bar{\nu}) = \frac{d}{c(1-R)}$$

Application of CRDS for measuring species concentration

l_s = 6 cm

τ = 3 10^{-7} s

R = 99.67%

Nbr paths = 225

Flame length=13.5 m

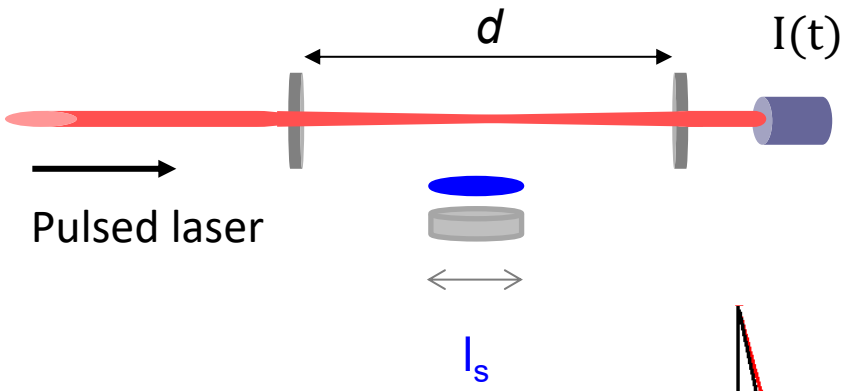

$$I(t) = I_0 \exp\left(-\frac{t}{\tau(\bar{\nu})}\right)$$

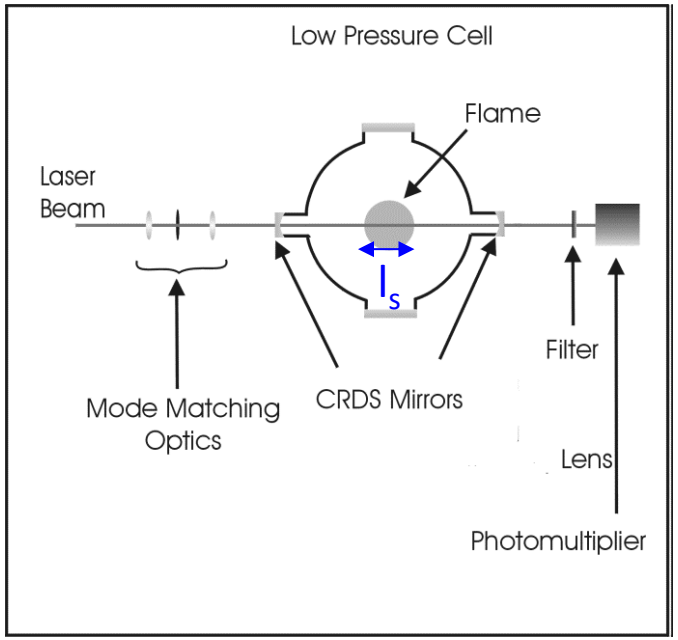

$$S_{CRDS} = \alpha(\bar{\nu}, T) l_s = \frac{d}{c}\left(\frac{1}{\tau(\bar{\nu}_{On})} - \frac{1}{\tau(\bar{\nu}_{Off})}\right)$$

d: cavity size

l_s: (flame) absorption length

$\alpha(\bar{\nu},T)$: absorption coefficient (cm^{-1})

c: light speed

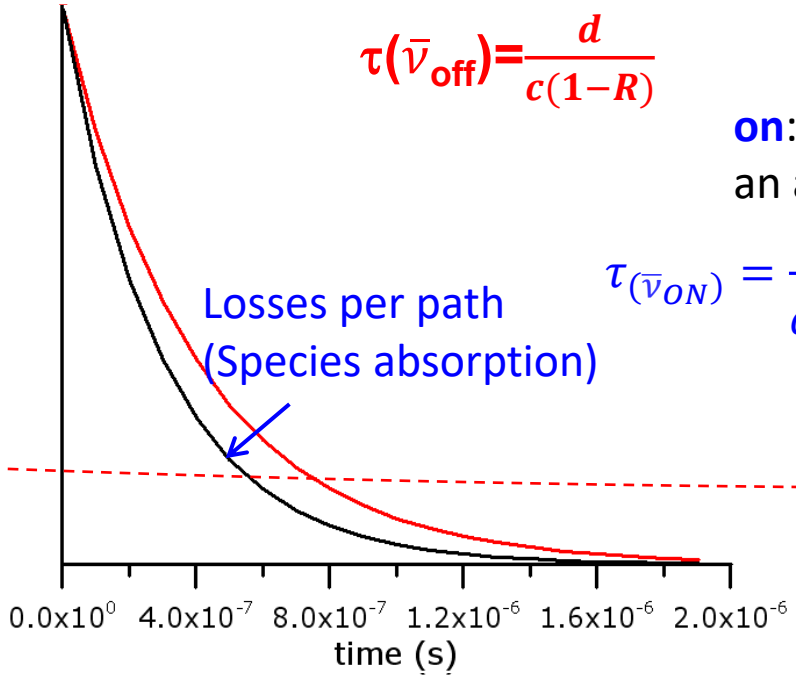

$$\tau(\bar{\nu}_{off}) = \frac{d}{c(1-R)}$$

off: no absorption

on: $\bar{\nu}$ on resonance with an absorbing transition

$$\tau_{(\bar{\nu}_{ON})} = \frac{d}{c\left[(1-R) + \int K_\lambda^{abs} dx\right]}$$

$$\alpha l_s$$

Loss/path

Berden et Engeln, CRDS Techniques and Application, ed. John Wiley

O'Keefe, D.A.G. Deacon, Rev. Sci. Inst. 59 (1988).

Few words on optical cavity and mode coupling

Quasi-concentric cavity well suited for 1D flames

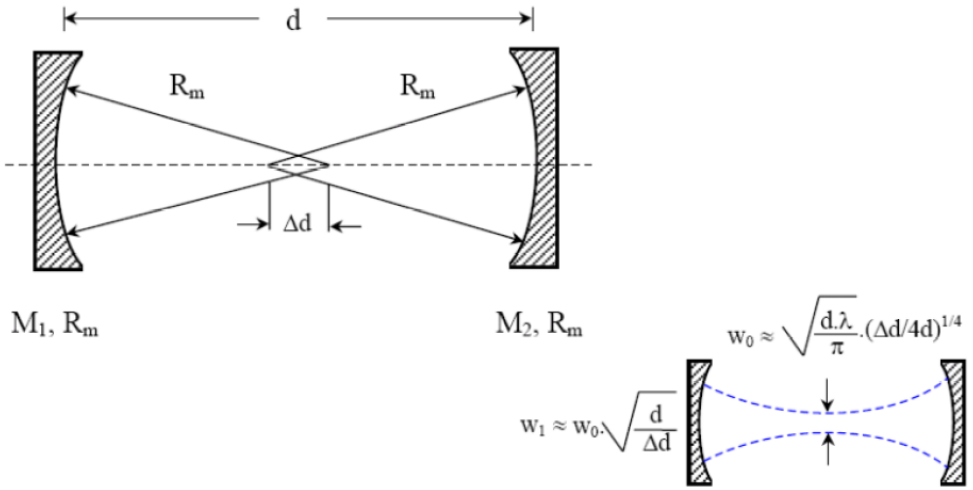

Quasi-plane cavity well suited for shock tube

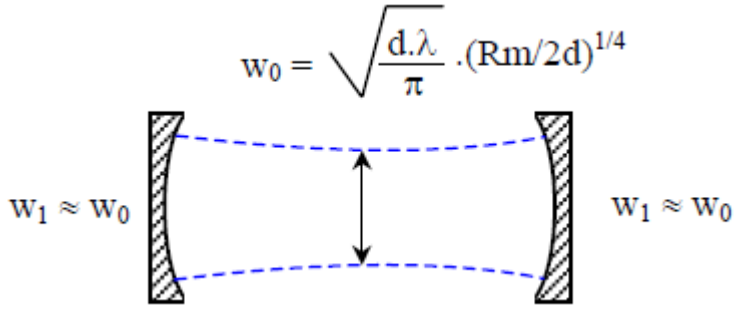

Transmission of modes

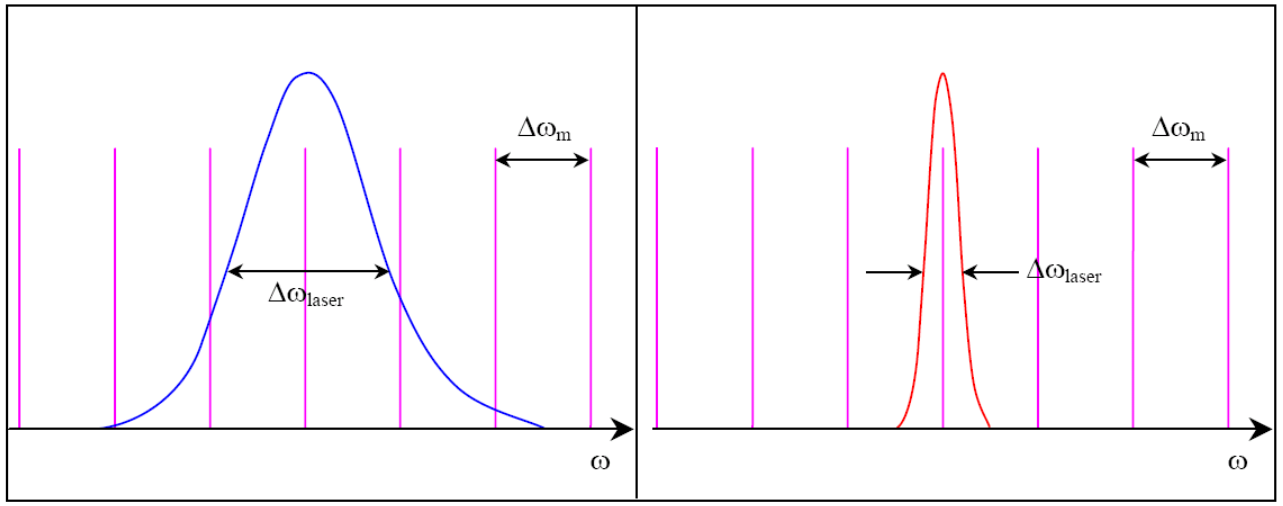

- Multimode pulsed laser **(pulsed - CRDS)**. R > 0.998 (356 nm)
- Several modes of the cavity always in resonance with laser frequency. Better transmission with mode matching.
- 8-12 bit vertical resolution, 735 ns.
- Sensitivity: 10^{-6} cm^{-1}
- Application: flame, plasma, thermal gradient

- Monomode cw laser (**cw-CRDS**). R > 0.99987 (1036 nm)
- Mode matching indispensable for transmission. Piezo-electric transducer (PZT) to modulate cavity length
- 16-bit vertical resolution, 25 µs
- Sensitivity: 10^{-10} cm^{-1}
- Application: sensor, atmospheric chemistry

PhD Xavier Mercier, Lille (2000)

Siegman A. (1986), "Lasers", *University Sciences Books, Mill Valley, CA*

Berden&Engeln, CRDS Techniques and Application, ed. John Wiley

Absorption spectrum (case of NH)

$$S_{CRDS} = \alpha(\omega, T)\mathrm{l}_s = \frac{\mathrm{d}}{c}\left(\frac{1}{\tau(\omega_{\mathrm{On}})} - \frac{1}{\tau(\omega_{\mathrm{Off}})}\right)$$

Lifetime (s)

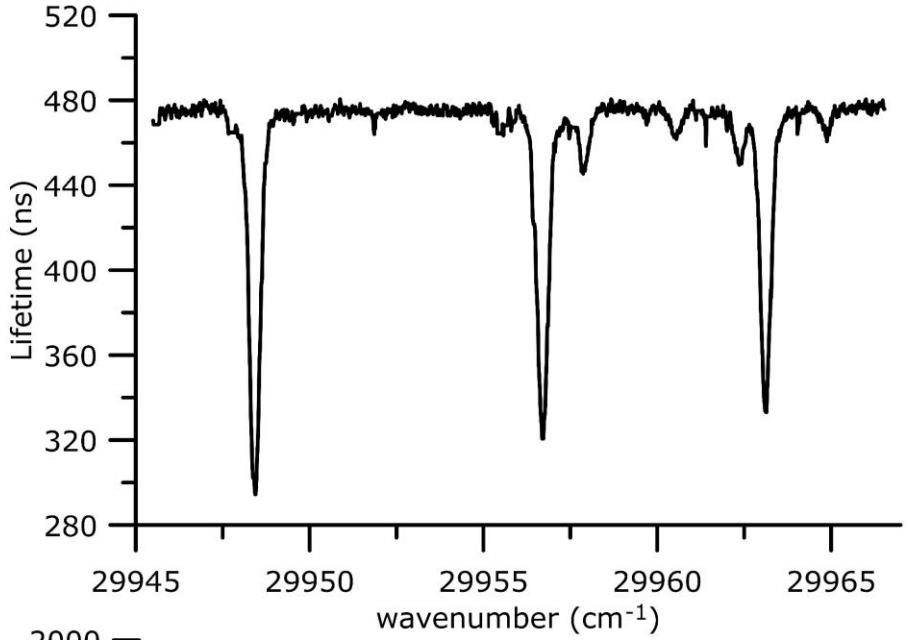

Loss/path

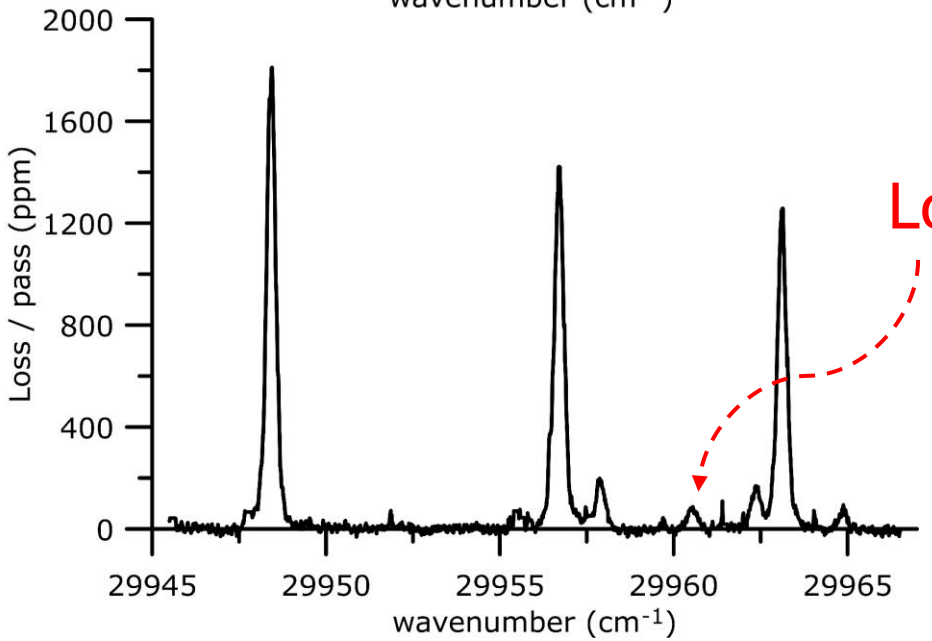

Loss/path=10^{-4}

PC2A data

Illustration of the benefit of CRDS for understanding prompt-NO formation chemistry

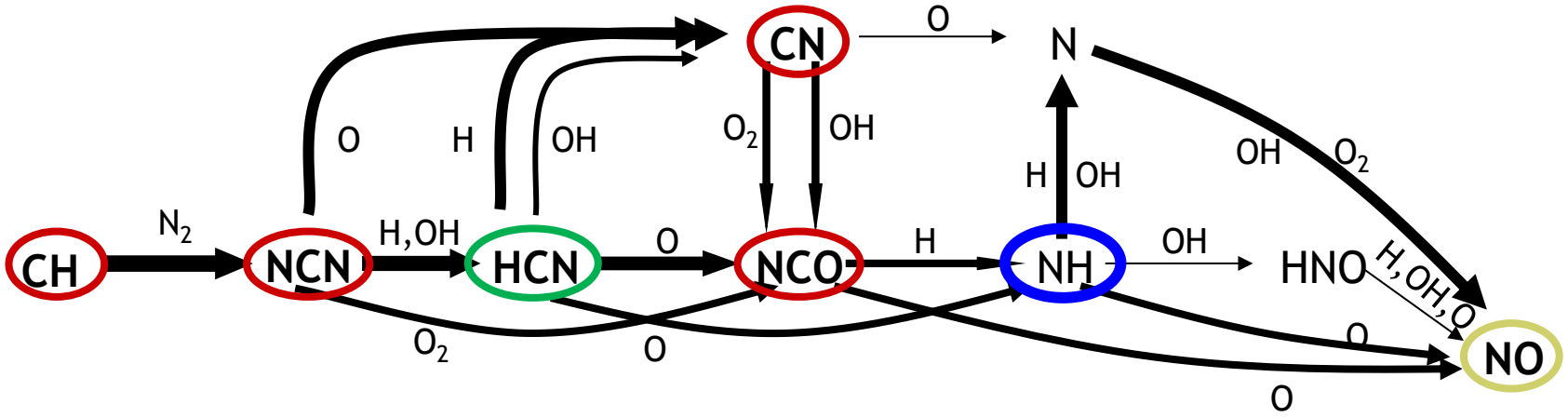

NO-mecha2

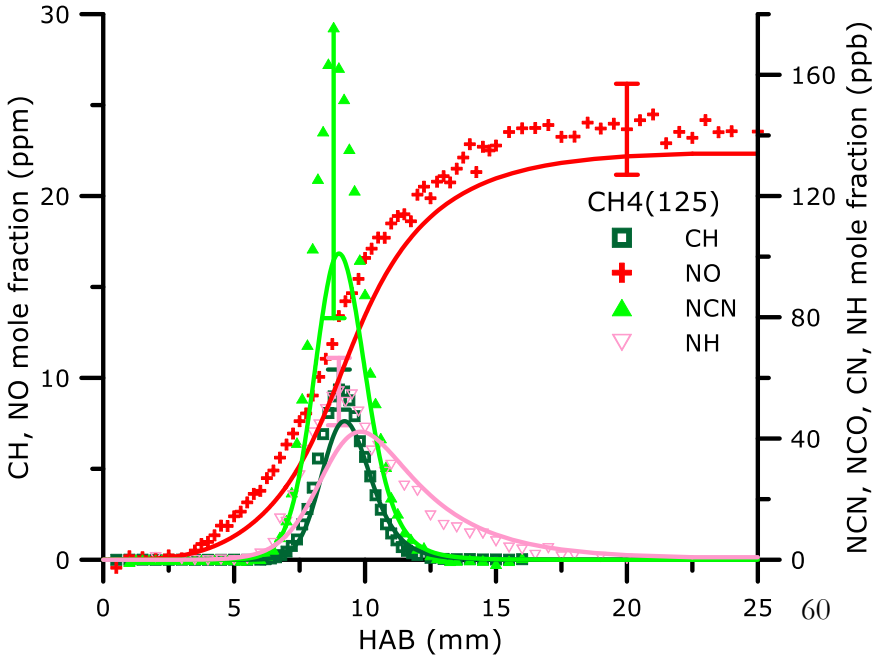

De Persis et al, Fuel 260 (2019) 111331

Lamoureux et al., CF163(2016)

Lamoureux et al. PECS (2021)

VI.2 Another very sensitive absorption technique: Intracavity laser absorption spectroscopy (ICLAS)

ICLAS: principle

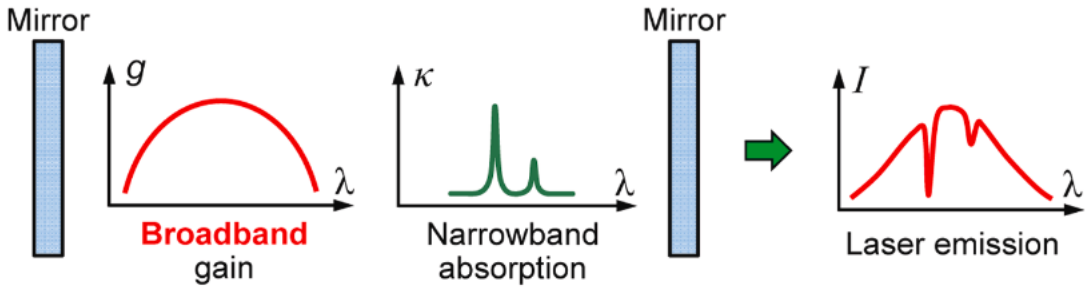

Fig. 1. Schematic of the ICAS process.

If the narrowband absorber is placed inside the cavity of a broadband multimode laser with homogeneous broadening, the time evolution of the laser intensity at a given wavenumber, ν, and generation time, tg, is governed by the following expression:

$$I(\nu, t_g) = I_e(\nu, t_g)\exp\left[-n\sigma(\nu)l_{eq}(t_g)\right]$$

The equivalent optical length, leq, depends on the generation time:

$$l_{eq}(t) = \frac{l}{L}ct_g$$

where l is the optical length of the absorbing compound, L the length of the laser cavity

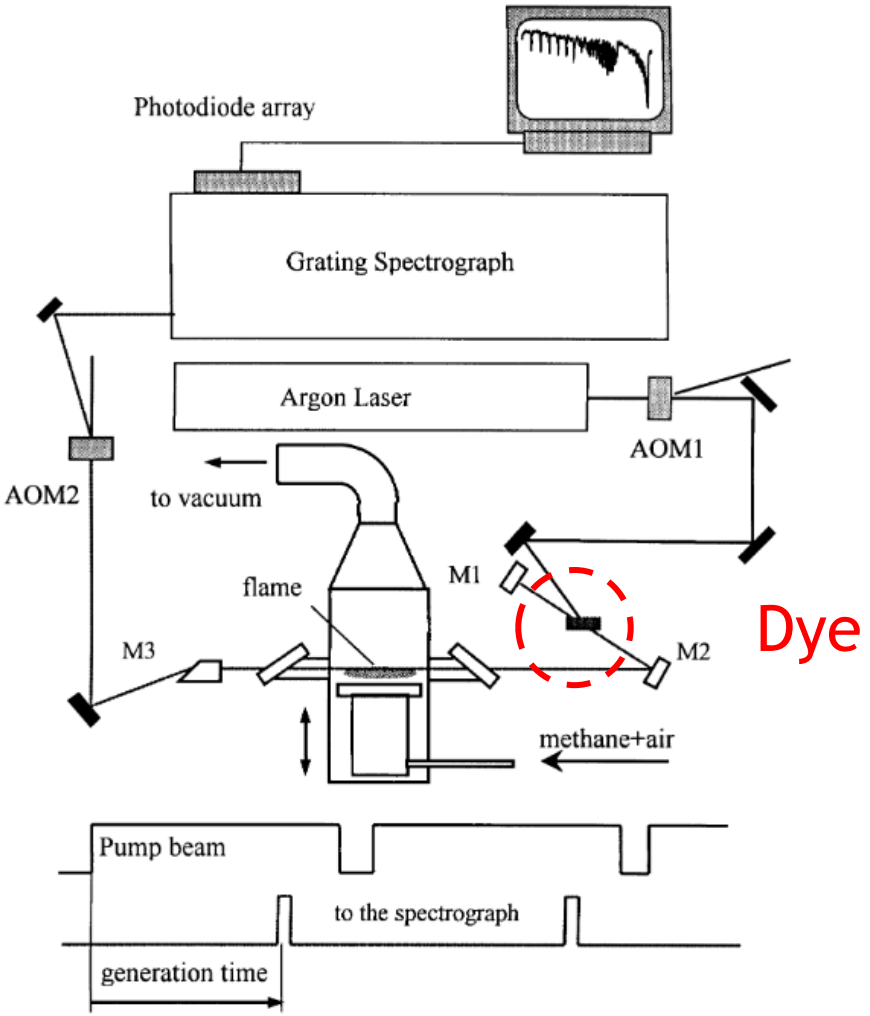

Cheskis, PECS 25 (1999) 233

Zamir, Rahinov et al., Applications in Energy and Combustion Science 17 (2024)100251

ICLAS vs CRDS and LIF

Table 1 (*continued*)

Specie	Ref.	Method	Environment	Laser wavelength	Sensitivity	Temporal resolution	Spatial resolution	Year(s) of publication
C_2	[101]	CRDS	Atmospheric pressure C_2H_2/O_2 flames	near 360.5 nm	~ 2.5×10^6 cm^{-3} at ~2500 K (in the excited $A^1\Pi_u$-state)	Time-averaged in a stationary flame	Path-integrated (followed by Abel inv.), ~ 350 μm in the vertical direction	2002
CN (along with NH_2, HNO and $^1CH_2$ (see Fig. 5)	[91]	ICAS	Flat, low pressure (30 torr) CH_4/air and C_3H_8/air flames doped with NO	near 642 nm	2×10^{10} cm^{-3} at 1700 K	Time-averaged in a stationary flame	Path-integrated, ~ 600 μm in the vertical direction	2002
CN	[97, 103]	CRDS	Flat, low pressure (11.3 and 39.8 torr) $CH_4/O_2/N_2$ flames, undoped and doped with NO	near 387 nm	~ 5×10^6 cm^{-3} at 1800 K	Time-averaged in a stationary flame	Path-integrated, ~ 300 μm in the vertical direction	2001, 2002
CN	[79]	CRDS (with LIF)	Flat, low pressure (40 torr) $CH_4/O_2/N_2$ flames	near 356 nm	~2×10^7 cm^{-3} at 1800 K	Time-averaged in stationary flames	Path-integrated, ~ 300 μm in the vertical direction	2015
CN	[49]	CRDS	Flat, low pressure (30 torr) morpholine/O_2/ Argon flame	near 387 nm	Not reported, S/*N* >100 levels similar to Ref. [97] were observed	Time-averaged in a stationary flame	Path-integrated, ~ 500–700 μm in the vertical direction	2010
CN	[53]	CRDS (with LIF)	Flat, low pressure (25 torr) $CH_4/O_2/N_2$ flame, undoped and doped with NO	near 387 nm	~ 2×10^6 cm^{-3} at 1700 K	Time-averaged in a stationary flame	CRDS-path-integrated, ~700 μm in the vertical direction; LIF- ~ 150 μm	2001
CN	[209]	PLIF	Atmospheric pressure, laminar and turbulent jet, NH_3-doped flames supported on a hybrid McKenna burner with a central (jet-flame) tube	Excitation near 359 nm, with detection at 381.5–392.5 nm range	~7×10^{11} cm^{-3} at 1800 K for single-shot PLIF	Single-shot imaging, sampling rate is limited by the laser repetition rate (up to 30 Hz for long pulse Q-switched model)	~500 μm	2015
NH_2	[48, 66,69, 91, 108, 186]	ICAS	Flat, low pressure (30 torr) $CH_4/O_2/N_2$ flames doped with N_2O, NO and NH_3	near 597 nm and near 642 nm	~ 8×10^{10} cm^{-3} at 1500 K	Time-averaged in stationary flames	Path-integrated (followed by Abel inv [48].), ~ 600 μm in the vertical direction	2000, 2002, 2005, 2006

Part of the table giving the key intermediates detected in flames by ICLAS and other techniques (CRDS, LIF…)

Zamir, Rahinov et al., Applications in Energy and Combustion Science 17 (2024)100251

VI.3 LIF: Laser Induced Fluorescence

Laser induced fluorescence: Principle

Radiative transitions: Einstein coefficients

$h\nu = E_2 - E_1$ (obeys spectroscopic selection rules)

$\Delta J = 0, \pm 1$

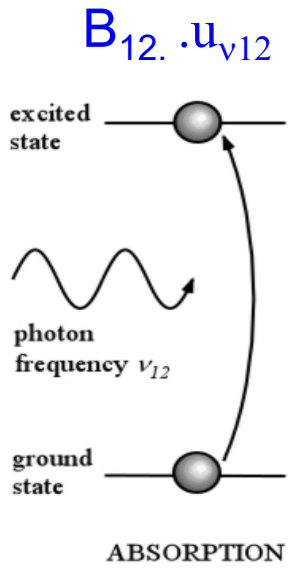

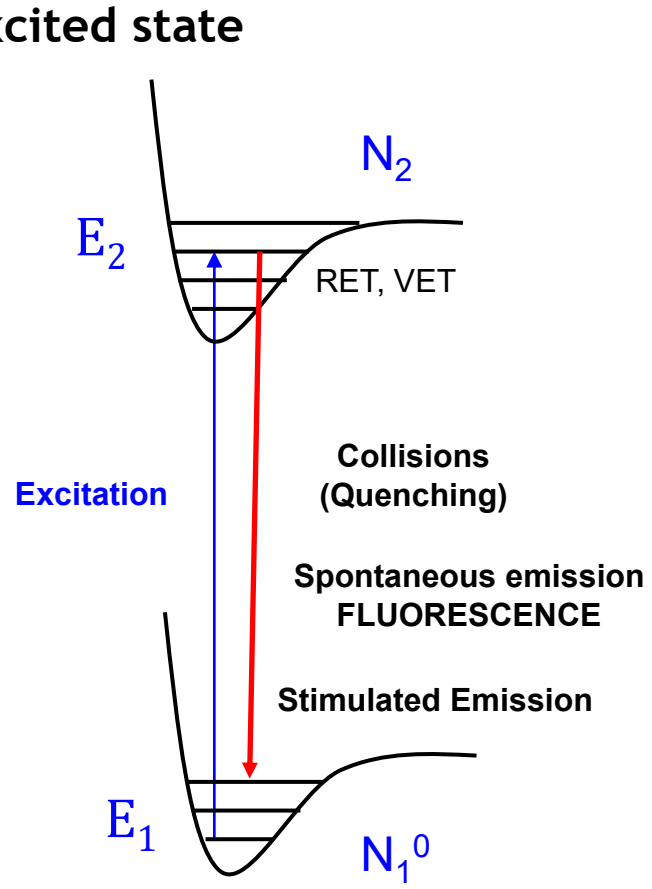

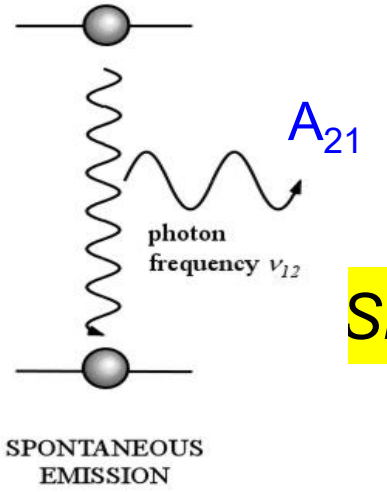

$SF \sim N_2 A_{21}$

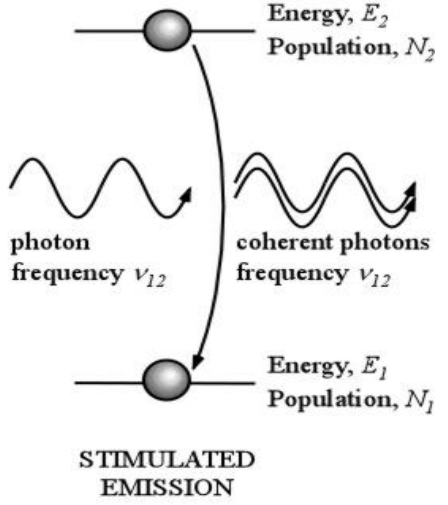

$B_{21}\, u_{\nu 12}$

$u_{\nu 12}$ Spectral energy density of the laser
B_{12} Einstein coefficient for absorption
B_{21} Einstein coefficient for stimulated emission
A_{21} Einstein coefficient for spontaneous emission

Two-level model

Hypothesis :
- Isolated system
- à t=0, N_2=0
- $N_1(t)+N_2(t)=N_1(t=0)=N_1^0$

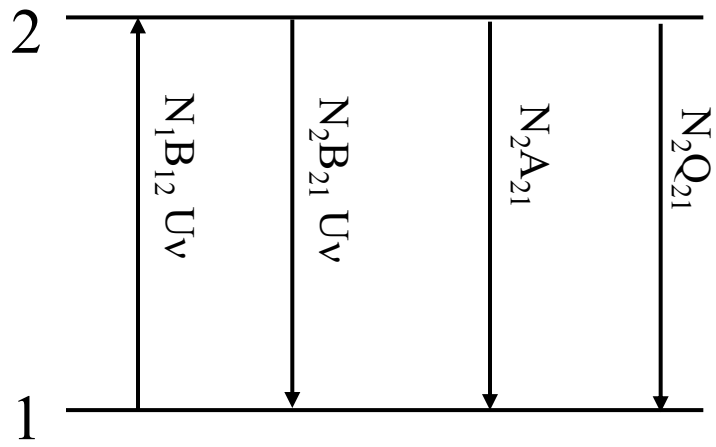

N_i	m^{-3}
A_{21}	s^{-1}
B_{12}	$m^3\ J^{-1}\ s^{-2}$
B_{21}	$m^3\ J^{-1}\ s^{-2}$
U_ν	$J\ m^{-3}\ s$
Q_{21}	s^{-1}

During laser excitation

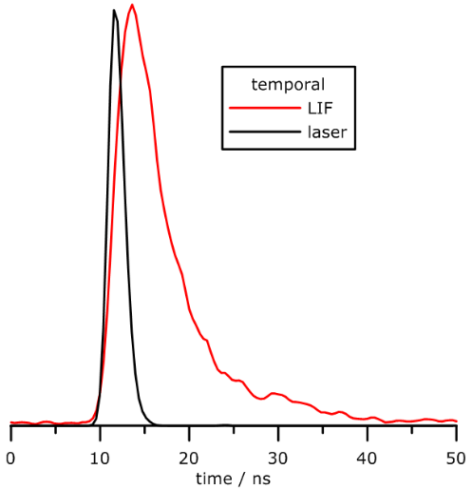

Rate equations

$$\frac{dN_2}{dt} = N_1 B_{12} U_\nu - N_2(B_{21}U_\nu + A_{21} + Q_{21})$$

$$N_2 = N_1^0 \frac{B_{12}U_\nu}{(B_{12}+B_{21})U_\nu + A_{21} + Q_{21}}\left[1 - e^{-t/\tau_P}\right]$$

$$\tau_P = 1/\left((B_{12}+B_{21})U_\nu + A_{21} + Q_{21}\right)$$

τ_p, pumping time

The LIF excitation regimes

$$N_2 = N_1^0 \frac{B_{12}U_\nu}{(B_{12}+B_{21})U_\nu + A_{21} + Q_{21}} \underbrace{\left[1 - e^{-t/\tau_P}\right]}$$

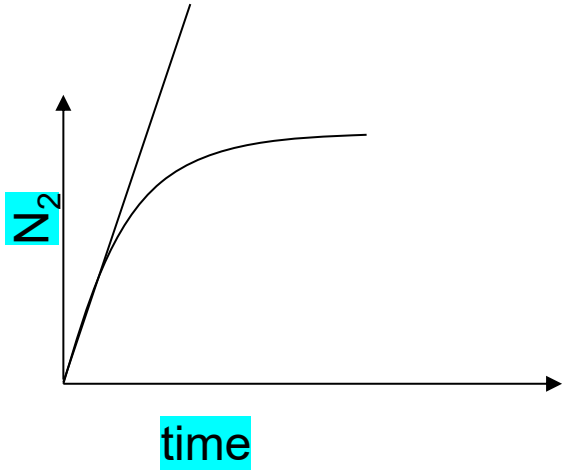

Linear with time

- $t \ll \tau_P$
- Q_{21}, U_ν weak
- $N_2 = N_1^0 B_{12} U_\nu t$

Steady-state t/τ_P

- $t > \tau_P$
- $N_2 = N_1^0 \frac{B_{12}U_\nu}{(B_{12}+B_{21})\,U_\nu + A_{21} + Q_{21}}$
  - $U_\nu^S = \frac{A_{21}+Q_{21}}{B_{12}+B_{21}}$ Saturation energy density
- $N_2 = N_1^0 \frac{B_{12}}{B_{12}+B_{21}} \frac{1}{1+{U_\nu^S}/{U_\nu}}$

$\tau_P = 1/\left((B_{12}+B_{21})U_\nu + A_{21} + Q_{21}\right)$

Limit cases of the fluorescence regimes (theory)

Steady-state regime

$$N_2 = N_1^0 \frac{B_{12}}{B_{12} + B_{21}} \frac{1}{1 + \frac{U_\nu^s}{U_\nu}}$$

$$U_\nu^s = \frac{A_{21} + Q_{21}}{B_{12} + B_{21}}$$

spectral energy density of the laser

Linear in energy ($U_\nu \ll U_\nu^s$)

$$N_2 = N_1^0 \frac{B_{12}}{A_{21} + Q_{21}} U_\nu$$

Saturated Fluorescence (LSF)($U_\nu > U_\nu^s$)

$$N_2 = N_1^0 \frac{B_{12}}{B_{12} + B_{21}}$$

$$g_1 B_{12} = g_2 B_{21}$$

Indpt on quenching

Recommended regime= linear in energy

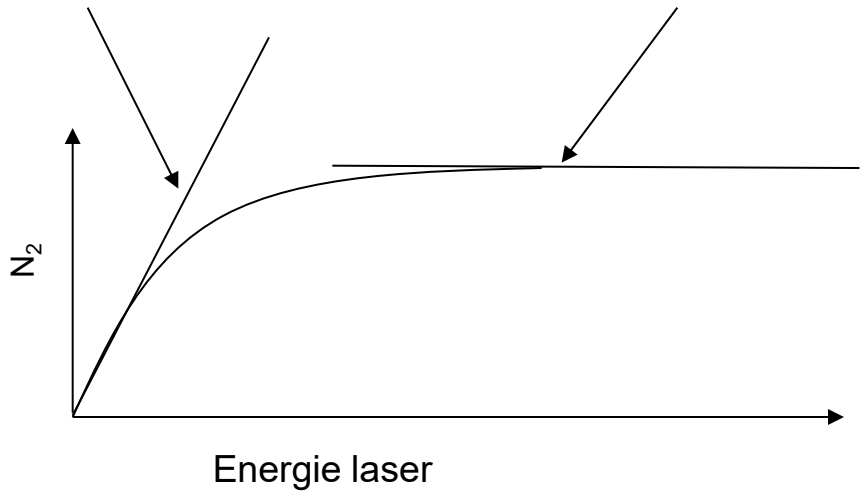

Flux of fluorescence photons

The energy flux of fluorescence (after the laser pulse) issued from a volume V and collected within a solid angle Ω is :

$$\Phi(t) = \iiint_V N_2(t) h\nu \, A_{21} \frac{\Omega}{4\pi} dV$$

If the laser energy density is constant within the volume :

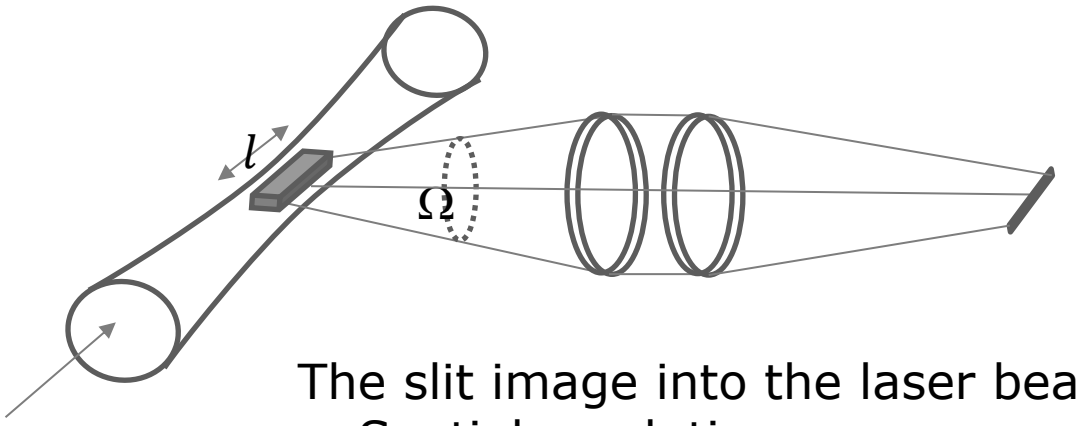

$$\Phi(t) = N_2(t) h\nu \, A_{21} \frac{\Omega V}{4\pi}$$

The slit image into the laser beam defines :

- Spatial resolution
- Measurement volume

Measurement of the concentration, N_{tot}

$$SF = G\frac{\Omega V}{4\pi}N_2 A_{21}$$

In steady-state regime, linear in energy

$$N_2 = N_1^0 \frac{B_{12}}{A_{21}+Q_{21}}U_\nu$$

$$SF = G\frac{\Omega V}{4\pi}N_1^0 B_{12}\frac{A_{21}}{A_{21}+Q_{21}}U_\nu$$

Fluorescence quantum yield, Φ

$$N_{Tot} = \frac{N_1^0}{F_b(J',\nu'',T)}$$

$$\frac{1}{A_{21}+Q_{21}}$$

Fluorescence (effective) lifetime

Kohse-Höinghaus, Prog. Energ. Comb., 20, 203 (1994)

J.W. Daily, Prog. Energ. Comb., 23, 133 (1997)

Determination of the electronic Q_{21}

The number of collisions per time unit between the species measured by LIF and its partners is (the molecule transites from level 2 to level 1):

$$Q_{21} = \sum_q N_q \sigma_{21} V_q$$

N_q : cc of the partner of collision q(m^{-3})
σ_{21} :quenching cross section (m^2)
V_q : velocity between q and the molecule ($m\ s^{-1}$)

Under certain conditions, it is possible to :

- Calculate the quenching; this requires the knowledge of all the collisional cross sections and the cc of the partners (simulation or additional measurements (Raman)).

- Measure the quenching from the temporal LIF decay (after the laser pulse),

$$\frac{dN_2}{dt} = -N_2(A_{21} + Q_{21}) \quad \text{->} \quad \ln(N_2) = -(A_{21} + Q_{21})t + cst$$

If fluo lifetime longer than the laser pulse duration

Fluorescence lifetime, quenching (OH), low-pressure flames

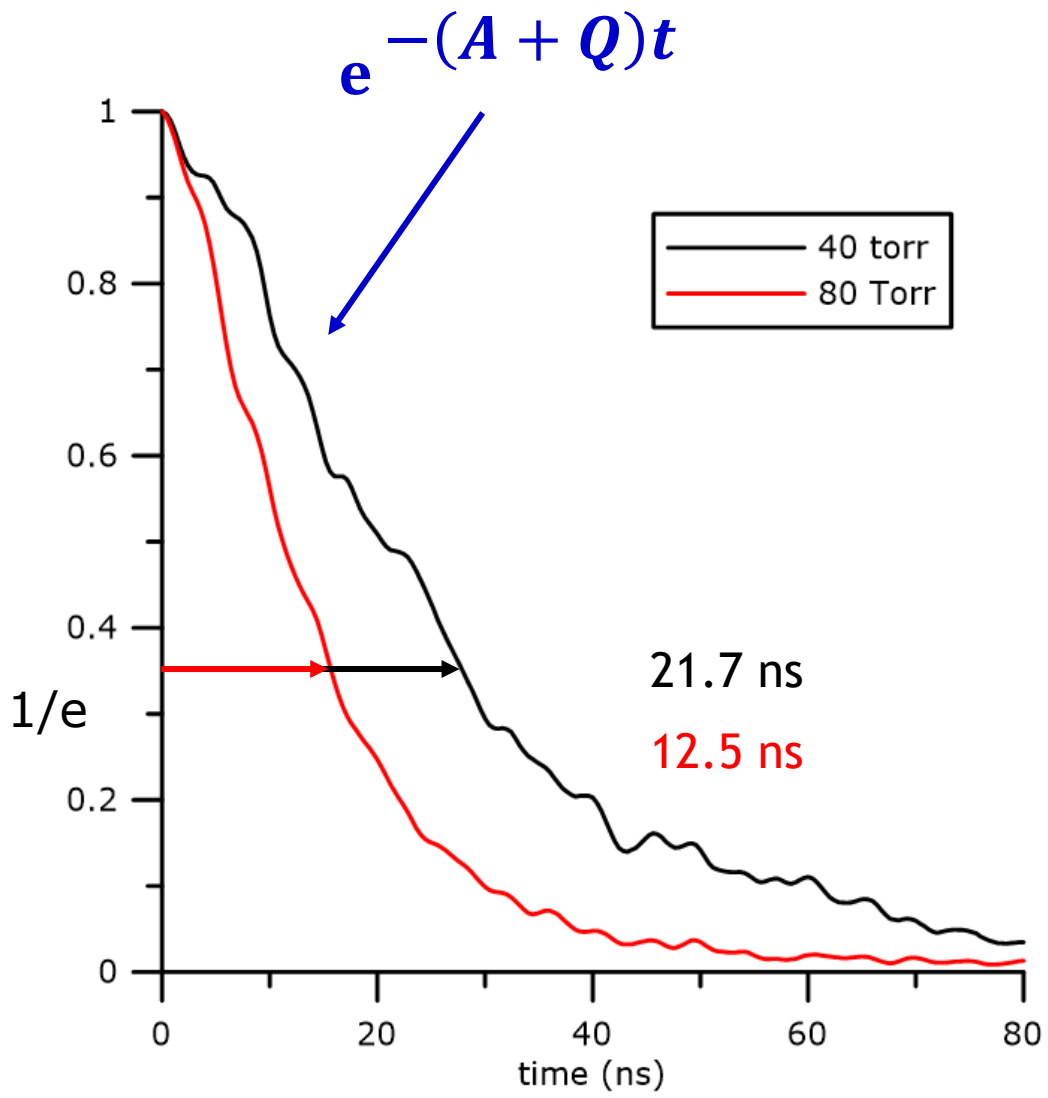

40 torr, A+Q = 4.61×10^7 s^{-1}
80 torr, A+Q = 8.00×10^7 s^{-1}
A = 1.3×10^7 s^{-1}

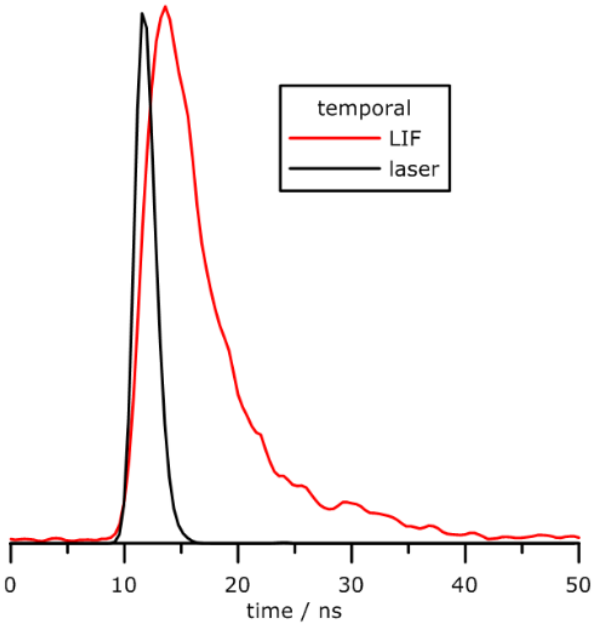

Example of quenching variation along the flame (case of NO)

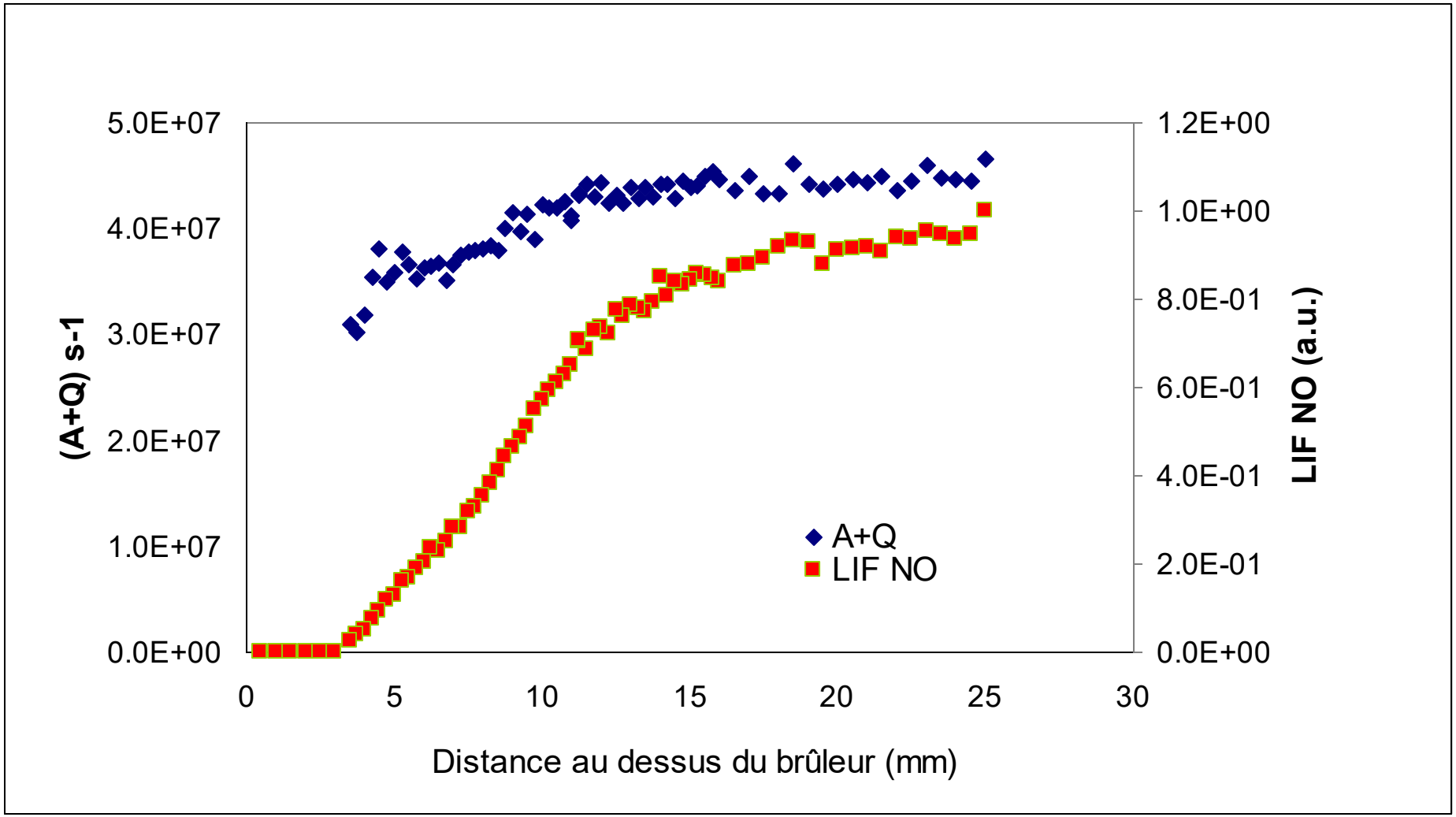

P = 4 kPa

PC2A data

Measurement of collisional cross sections

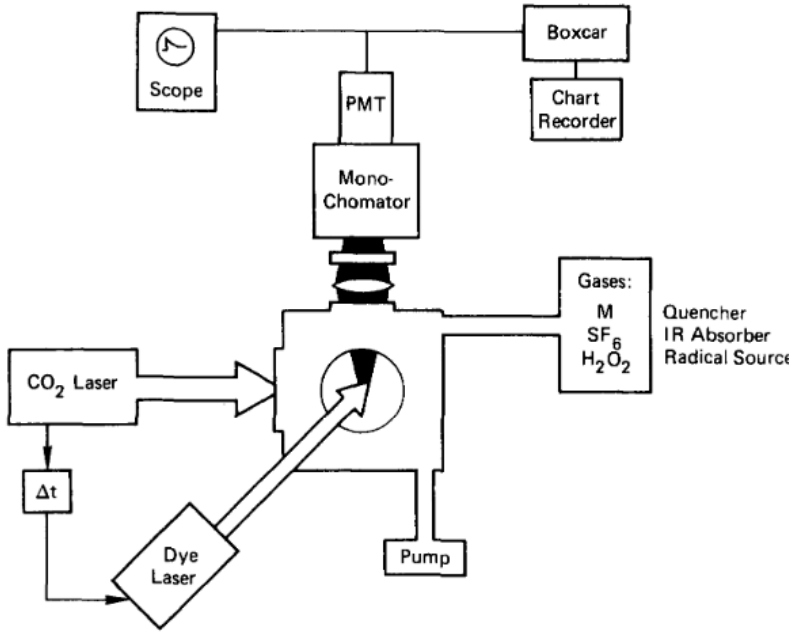

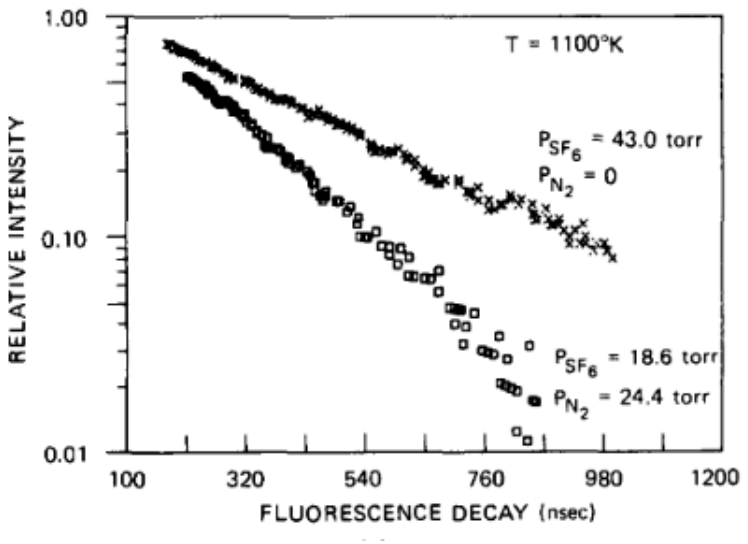

TABLE I. Experimental and calculated cross sections.

Gas	T(K)	k_Q [a]	σ_Q [b]	$\sigma_{Q\,avg}$ [b]	$\sigma_{Q\,calc}$ [b,c]
N_2	1110	1.3	0.89	0.68 ± 0.16	49
	1030	1.0	0.72		
	1200	0.82	0.53		
	1040	0.85	0.59		
SF_6	1130	0.17	0.14	0.14	57
CO	1270	31	20	20	57
CO_2	1200	21	15	13 ± 3	65
	1140	19	14		
	1250	14	9.5		
H_2O	1220	39	23	26 ± 3	89
	1140	47	28		
	1430	44	23		
	1000	47	30		
	(1160)[d]	(75)	(44)		

Laser pyrolysis/LIF set-up
SF_6= Infrared absorber
H_2O_2 = OH precursor
M: quencher

Fairschild et al. J. Chem. Phys 79 (1983) 1795

Measurement of collisional cross sections

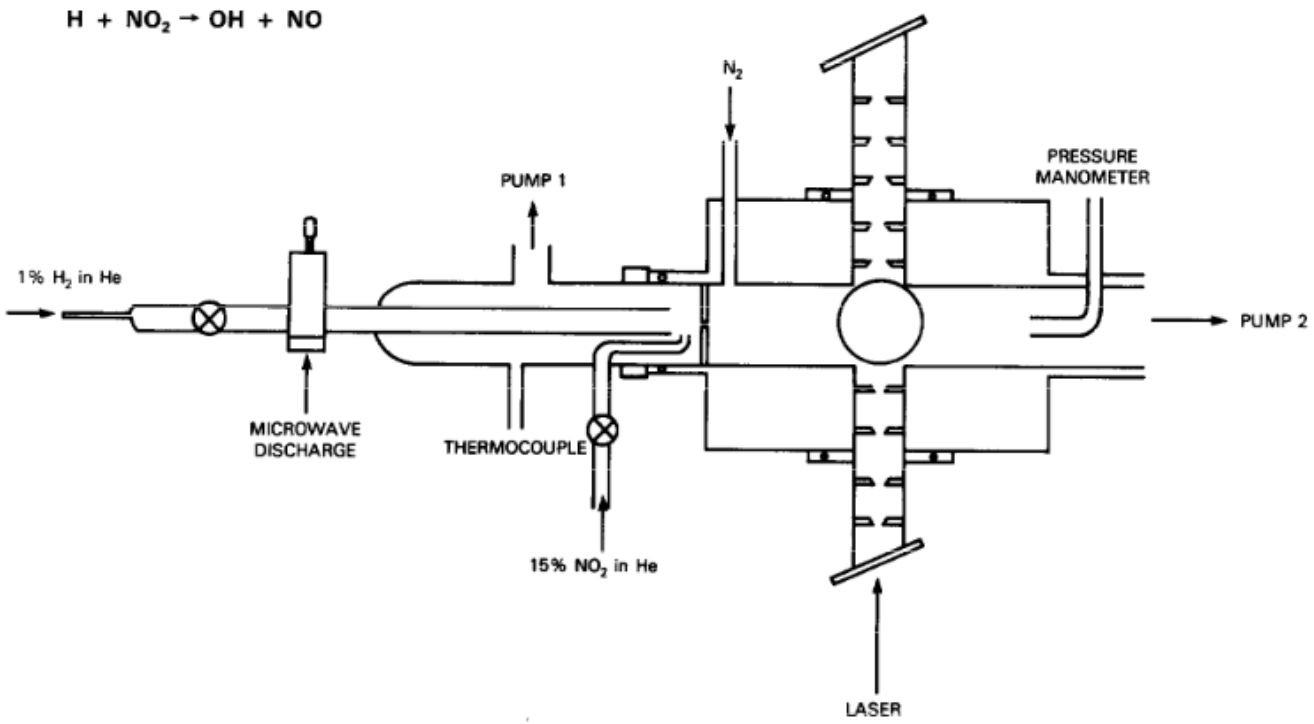

Fig. 1. Diagram of the OH flow cell.

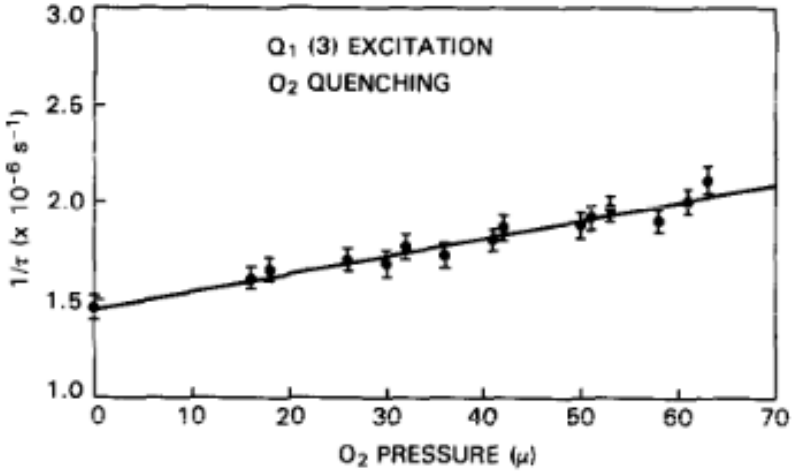

Fig. 5. Stern–Volmer plot of the reciprocal of the OH fluorescence lifetime, $1/\tau$, versus the quenching gas pressure. The data is for $Q_1(3)$ OH fluorescence quenched by oxygen. The solid line are the result of a linear least-squares fit to the data from which the total rate of depletion, k_{tot}, is calculated.

H+ NO_2 -> OH + NO
H produced by a discharge in He + H2
Quenchers: O_2 and N_2
Room T, 1torr

N'	N_2		O_2	
	k_{tot} (10^{-10} cm^3/s)	σ_{tot} (Å^2)	k_{tot} (10^{-10} cm^3/s)	σ_{tot} (Å^2)
0	5.31±0.13	66.4±1.6	3.92±0.12	49.0±1.5
1	5.63±0.21	70.4±2.6	3.85±0.14	48.1±1.8
2	5.19±0.10	64.9±1.3	2.81±0.10	35.1±1.3
3	4.80±0.22	60.0±2.8	2.82±0.11	35.3±1.4
4	4.78±0.21	59.8±2.6	3.20±0.12	40.0±1.5
5			2.65±0.10	33.2±1.3

Burris et al. Chem. Phys. 124 (1988) 251

Model for collisional quenching (OH $A^2\Sigma^+$)

Theoretical calculations (Harponned model) of quenching cross sections and quenching rates are done using mole fractions and temperature obtained from Cantera or Chemkin and empirical relations :

$h_c = C_2 T_r/T$ T_r= 300 K T = Flame temperature

$$\ll \sigma_p(T) \gg = PA\, C_0 \left\{(1+h_c)\exp(-h_c) + C_1 h_c^{2/\alpha}\, \gamma\left(2 - \frac{2}{\alpha}, h_c\right)\right\}$$

Collider P; Species-specific constants from table; Species-specific constants from table; Lower incomplete gamma function

Collider (p)	P_A	C_0	C_1	C_2	α
H_2O	1.12	15.955	2.251	4.302	3.12
O_2	0.537	14.892	1.327	3.866	3.95
NO	1.003	27.157	1.8	1.269	3.9
H	1.038	13.763	1.347	1.399	4
H_2	0.33	12.848	1.36	3.079	3.5

$$< uOH > = \left(\frac{8\, kB\, T}{\pi\, mOH}\right)^{1/2}$$

Molecular masses of OH and collider p

Thermally averaged quenching rate = $Q = \left(\frac{P}{k_B T}\right) < uOH > \sum_p \chi_p \left(1 + \frac{m_{OH}}{m_P}\right)^{1/2} \ll \sigma_P(T) \gg$

Mole fraction of collider p

Paul, JQSRT 51 (1994) 511

Examples of cross section behaviour for OH $A^2\Sigma^+$ (v'=0)

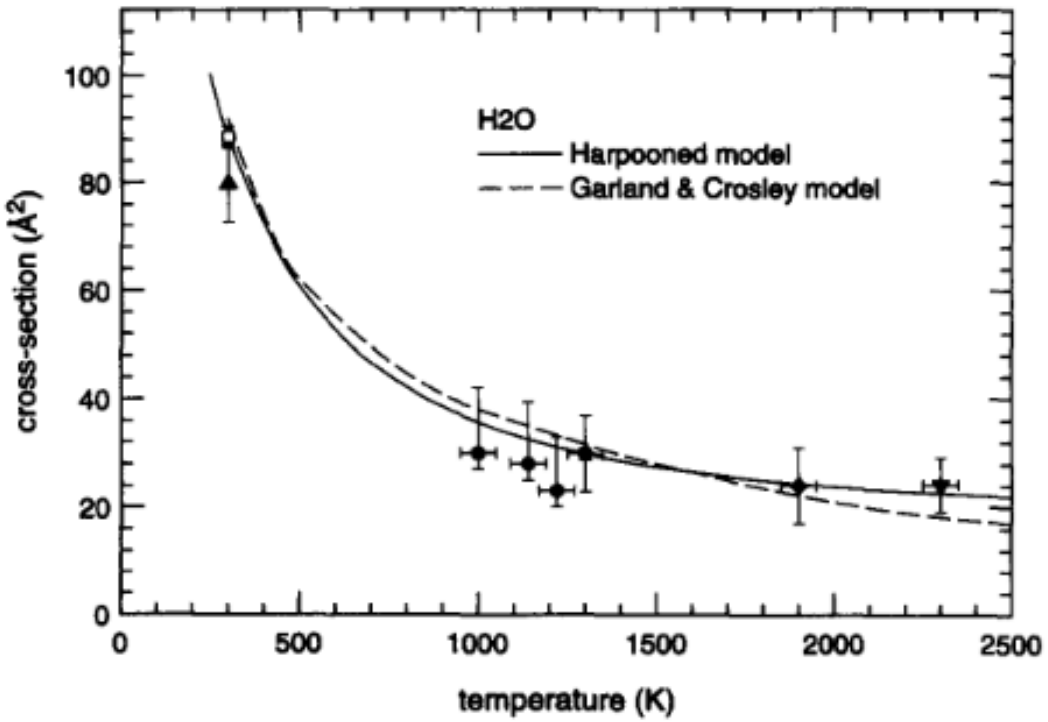

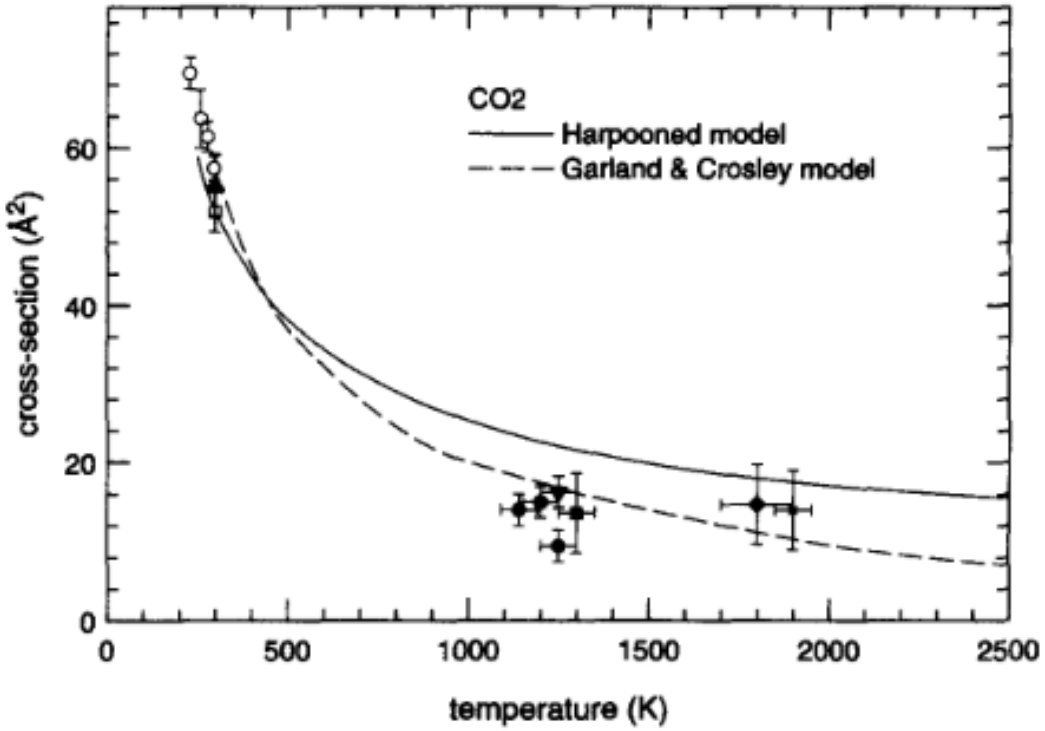

Paul, JQSRT 51 (1994) 511

Examples of cross section behaviour for OH $A^2\Sigma^+$ (v'=1)

+ Paul's empirical relation for OH-H_2O quenching (v'=0)

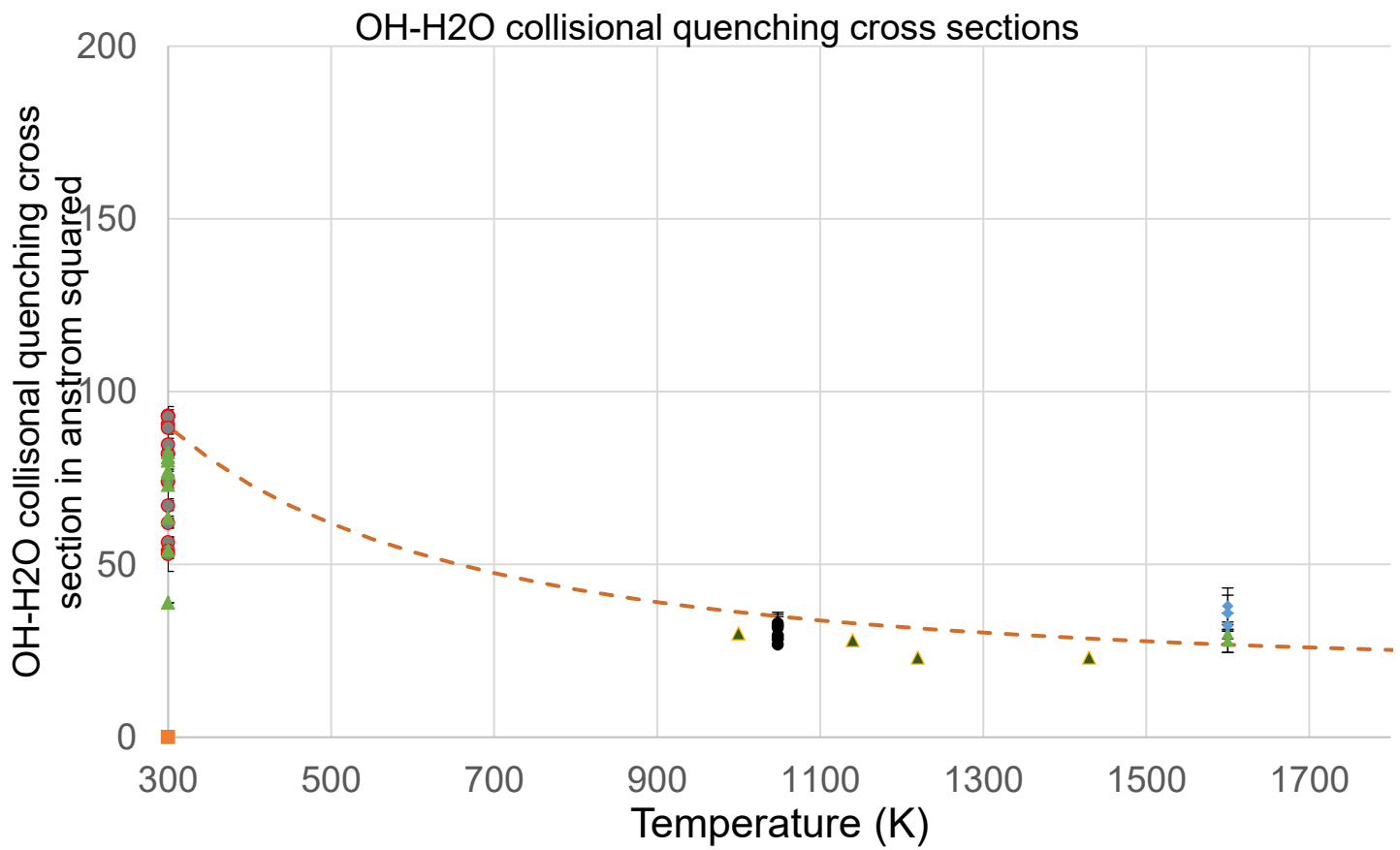

PC2A, Ankit Sahay 2026

Paul, JQSRT 51 (1994) 511

Cattolica and Mataga, Chem. Phys. Lett., Vol. 182, 623 (1991)

Comparison Paul/Tamura ($\sigma_Q = \sigma_{Q\infty}\exp(\epsilon/kT)$) cross sections for OH and NO

Expressions for OH Quenching

Collider	$\sigma_{Q\infty}$ from Paul et al.[29] (Å²)	$\sigma_{Q\infty}$ This Work (Å²)	ϵ/k (K)	Quenching Rate Coefficient (10^{-13} cm³ s⁻¹)	σ_Q 300 K (Å²)
N_2	0.351	0.4	624	$4.47\sigma_Q T^{0.5}$	3.2
O_2	8.00	8	243	$4.37\sigma_Q T^{0.5}$	18.0
H_2O	17.87	20	434	$4.92\sigma_Q T^{0.5}$	85.0
H_2	4.24	4.5	224	$10.88\sigma_Q T^{0.5}$	9.50
CO_2	11.87	11	488	$4.16\sigma_Q T^{0.5}$	56.0
CO	12.30	12	397	$4.47\sigma_Q T^{0.5}$	45.1
CH_4	13.68	11	320	$5.07\sigma_Q T^{0.5}$	32.0
H	14.29	14.5	84	$15.0\ \sigma_Q T^{0.5}$	19.2
OH	14	20	384	$4.99\sigma_Q T^{0.5}$	71.9

Cross Section Expressions for NO Quenching

Collider	Cross Section, σ_Q(Å²)	Quenching Rate Coefficient (10^{-13} cm³ s⁻¹)	σ_Q 300K (Å²)
CO	$5.8 + 5.3\exp(-2100/T) + 22.1\exp(-4200/T)$	$3.82\sigma_Q T^{0.5}$	5.8
N_2	$0.88\exp(-1440/T) + 3.1\exp(-4800/T)$	$3.82\sigma_Q T^{0.5}$	0.007
H_2	$0.001\exp(0.0028/T)$	$10.63\sigma_Q T^{0.5}$	0.001
CH_4	0.1	$4.50\sigma_Q T^{0.5}$	0.1
H_2O	$26\exp(412/T)$	$4.34\sigma_Q T^{0.5}$	102.7
CO_2	$38\exp(157/T)$	$3.45\sigma_Q T^{0.5}$	64.1
O_2	$21\exp(27/T)$	$3.70\sigma_Q T^{0.5}$	23.0
H	13	$14.8\sigma_Q T^{0.5}$	13
OH	72	$4.42\sigma_Q T^{0.5}$	72

Tamura et al. CNF 114 (1998) 502

Calculated OH quenching profiles in H_2 atmospheric flames of various dilution and ϕ

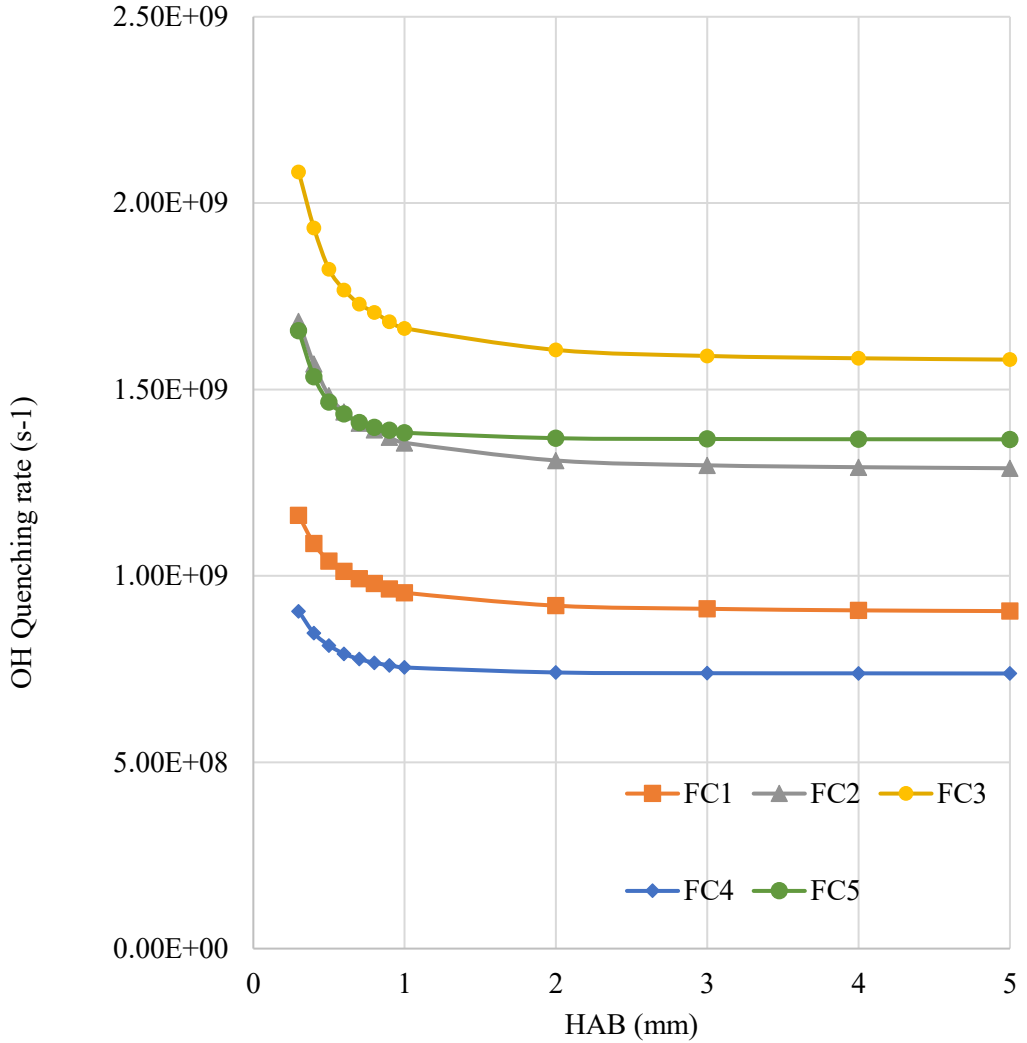

10^9 collisions/second at atmospheric pressure

PC2A data, Ankit Sahay 2026

Paul, P. H., Carter, C. D., Gray, J. A., Sandia National Laboratories Report No. SAND 94-8244, 1994

Quenching: How to overcome it experimentally?

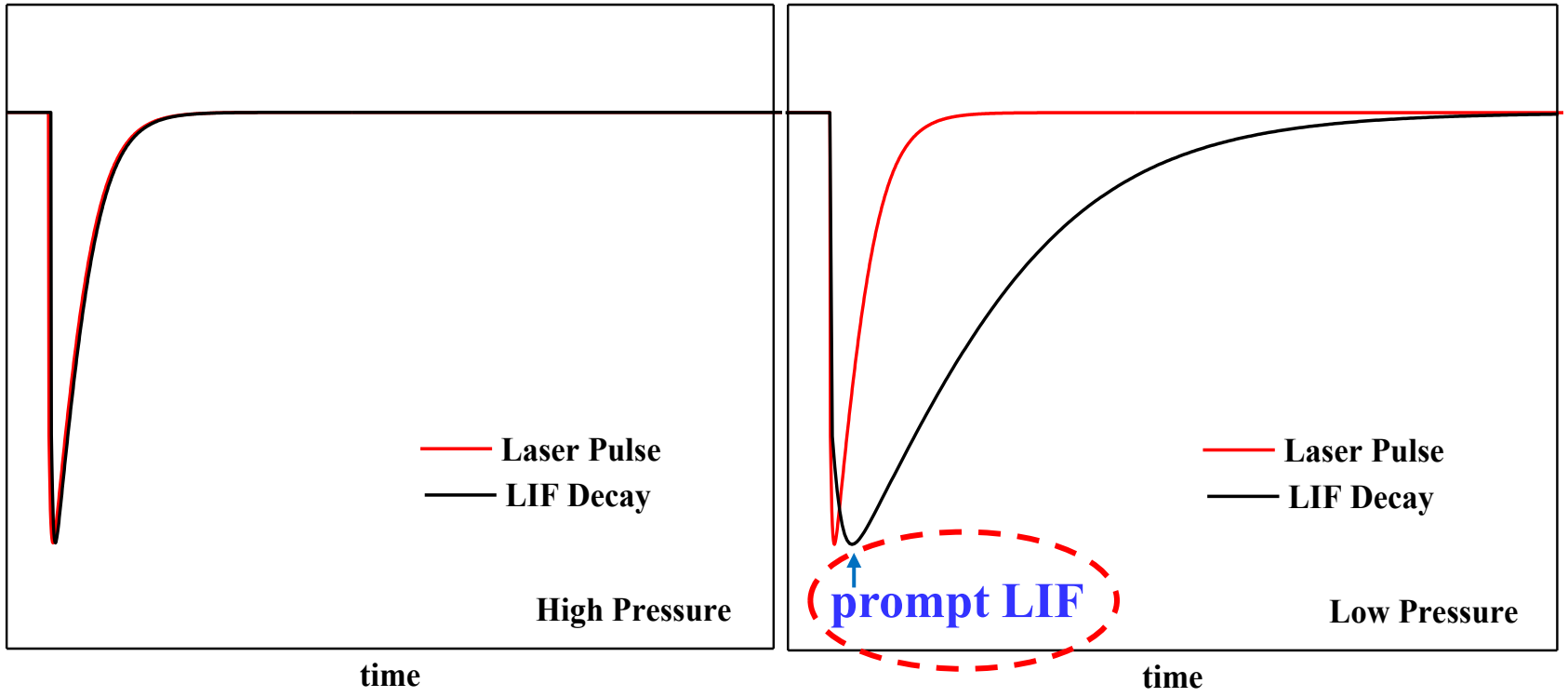

Schwartzwald et al. Chem. Phy. Lett. 142 (1987) 15

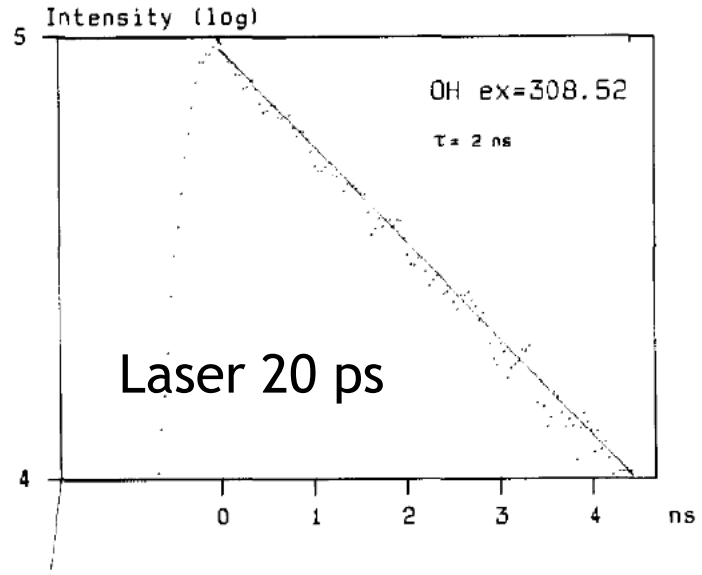

ns-Laser in low pressure flames (Q = a few 10^7/s), A_{21} 10^5-10^6/s
ps-laser (or fs) in atmospheric flames (Q around 10^9/s)

Prompt-LIF not affected by Quenching: Often mentionned in reference literature, never demonstrated

How can this be proven?

1. Experiments performed in 2 similar flames (same composition at 40 and 80 Torr) for OH and NO
2. Measurement of the prompt LIF in the burnt gases of the 2 flames
3. Independent measurement of X_{OH} (absorption) and X_{NO} (standard addition method) in the two flames (it will be explained later). **Independent on Q**
4. Comparison of the ratio of the mole fractions issued from (2) using eq below, with X_{OH40}/X_{OH80} and X_{NO40}/X_{NO80} =**1.33** determined from (3)

$$\frac{X_{NO,1}}{X_{NO,2}} = \frac{\left(S_{LIF}/U_v\right)_1}{\left(S_{LIF}/U_v\right)_2} \times \frac{f_{B,2}}{f_{B,1}} \times \frac{p_2}{p_1} \times \frac{T_1}{T_2} \times \frac{Q_1}{Q_2}$$

or

$$\frac{X_{NO,1}}{X_{NO,2}} = \frac{\left(S_{LIF}/U_v\right)_1}{\left(S_{LIF}/U_v\right)_2} \times \frac{f_{B,2}}{f_{B,1}} \times \frac{p_2}{p_1} \times \frac{T_1}{T_2}$$

X_{NO40}/X_{NO80}= 0.786

X_{NO40}/X_{NO80}= 1.35

El Baba, Desgroux, Lamoureux, CnF264(2024)113424
Mitra, Lamoureux, Desgroux, CnF277(2025)114192

Spectral energy density, U_ν

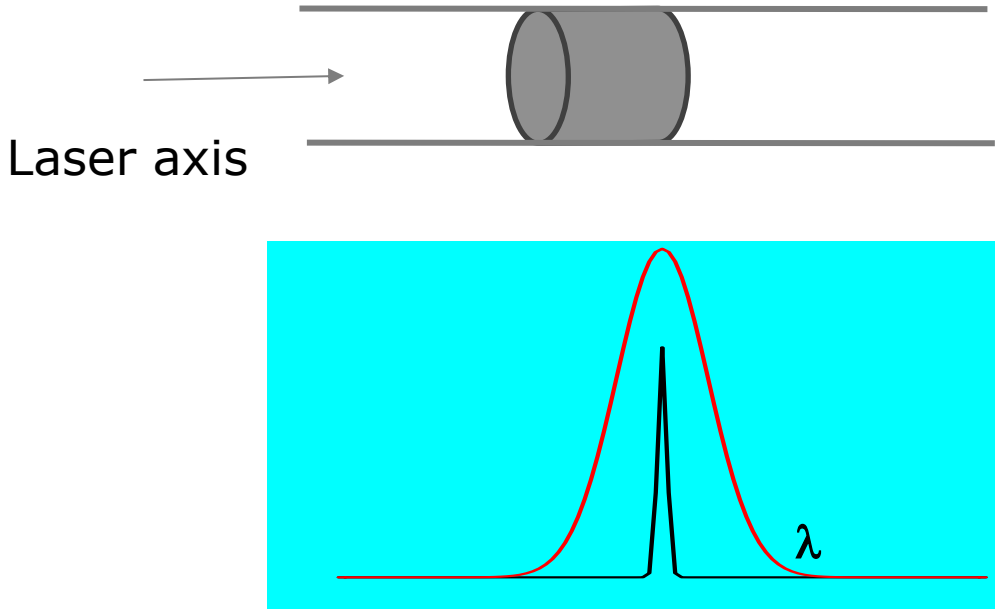

- Unit : J m^{-3} s

$$U_\nu = \frac{n_{ph} h \nu_L}{Ac\Delta t \Delta \nu_L} \Gamma$$

- Measured energy (J)

$$E_L = n_{ph} h \nu_L$$

- Γ: dimensionless spectral overlap between the laser line and the absorption line

h cst Planck (J s)
ν_L fréquence spectrale du laser (Hz)
A section du laser (m^2)
c vitesse de la lumière (m s^{-1})
Δt durée impulsion (s)
$\Delta\nu_L$ largeur spectrale de la raie laser (Hz)

Paul, Dec, Opt. Lett. 19 (1994) 998-1000
Partridge, Laurendeau, Appl. Opt. 34 (1995) 2645-2647
Luque, Crosley, App. Phys. B63 (1996), 91-98

Criteria of transition selection

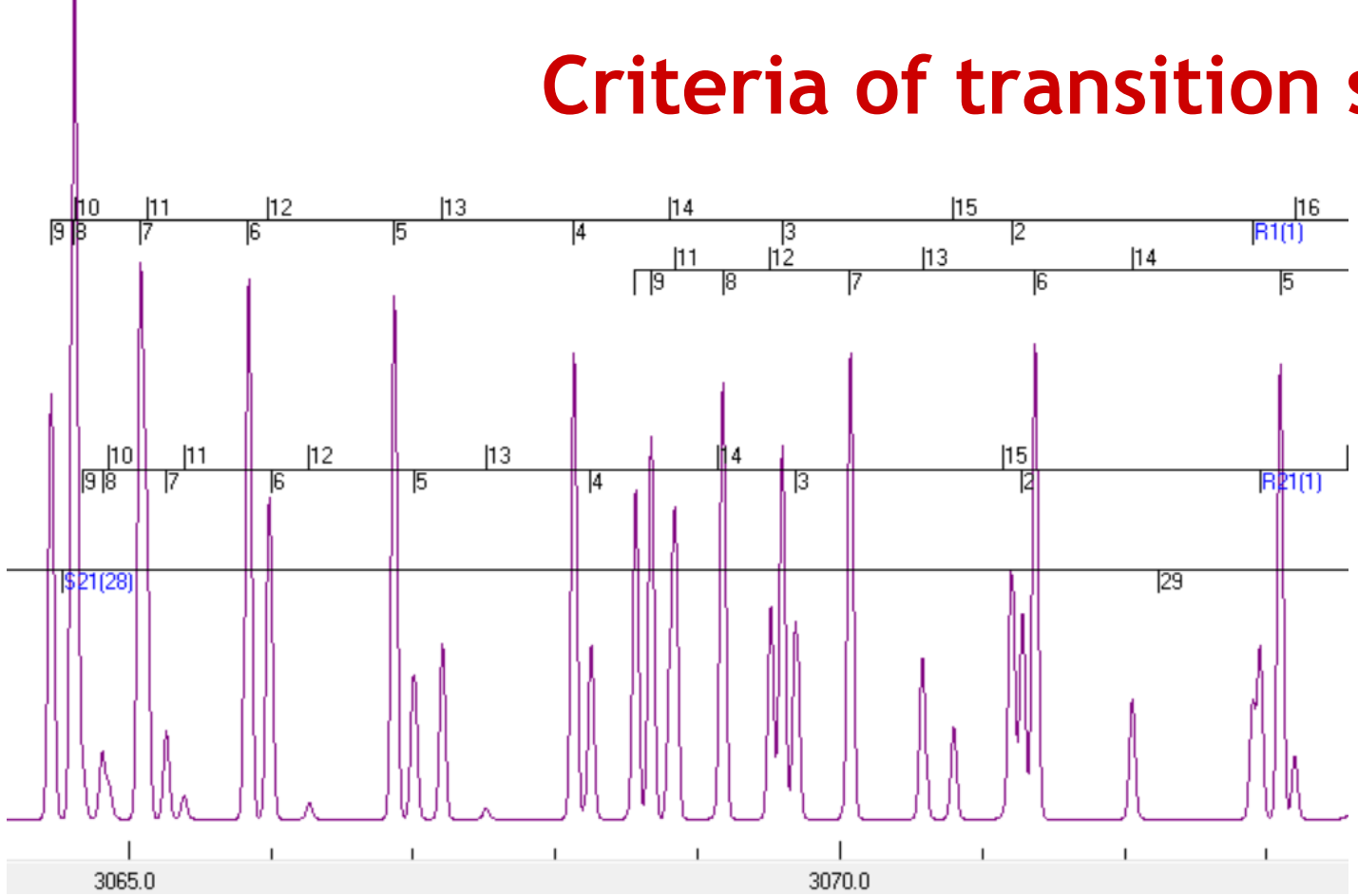

LIFBASE
OH 2000 K
R branch A-X (0-0)

- Isolated line
- With suitable B_{ij} (choice (OH) between $R_{21}(7)$ ($2.8\,10^8$) and $R_1(7)$ ($1.7\,10^9$) as example to be in the linear regime of fluorescence

N''	P1	P2	Q1	Q2	R1	R2	O12	Q12	P12	R21	Q21	S21
1	2.531e09	------	2.412e09	2.861e09	7.069e08	1.425e09	------	1.430e09	2.866e09	1.052e09	1.679e09	1.990e08
2	2.278e09	1.183e09	3.034e09	2.941e09	1.090e09	1.503e09	3.352e08	1.004e09	1.594e09	9.081e08	1.033e09	2.098e08
3	2.208e09	1.535e09	3.365e09	3.228e09	1.332e09	1.603e09	2.989e08	7.348e08	1.125e09	7.166e08	7.095e08	1.818e08

Criteria of transition selection

- With a suitable N'' not too sensitive to the temperature

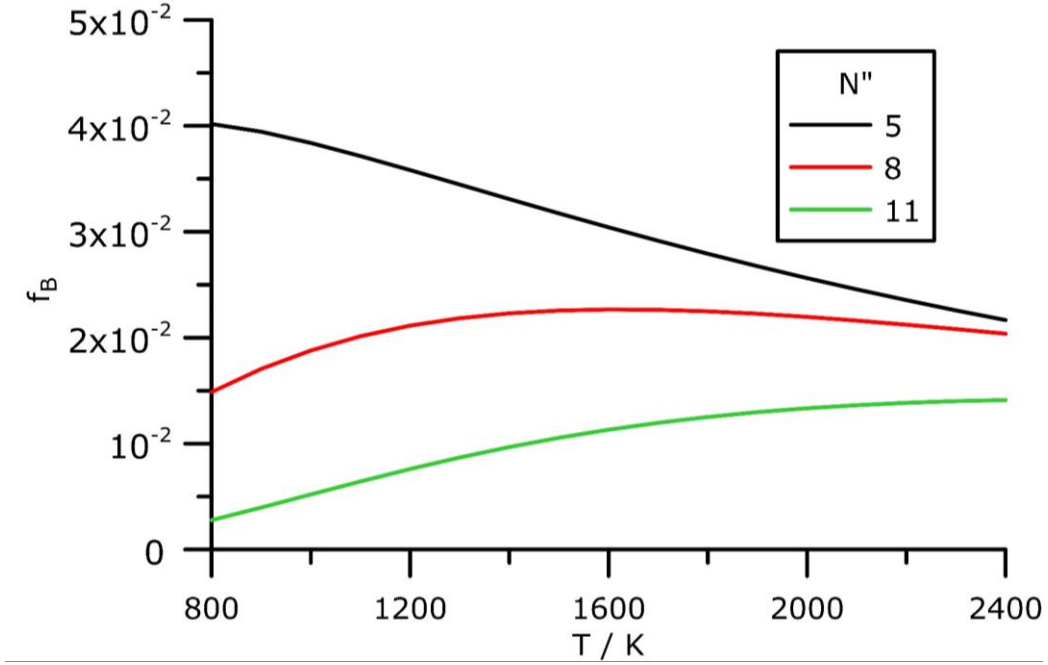

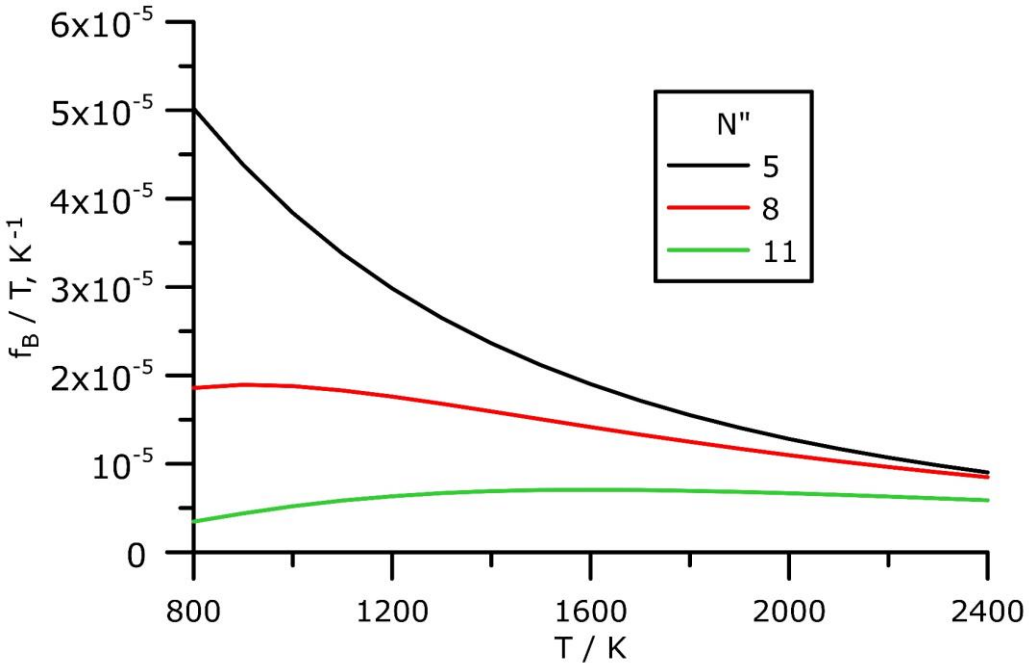

Be carefull on the Boltzmann fraction calculation: depends on the method of normalisation of the Hönl London factor $S_{J',J''}$ (refer to LIFBASE manual for example)

Considering background signal through ON/OFF procedure

- ON/OFF resonance

flame at 5.3 kPa,
MEK + CH4

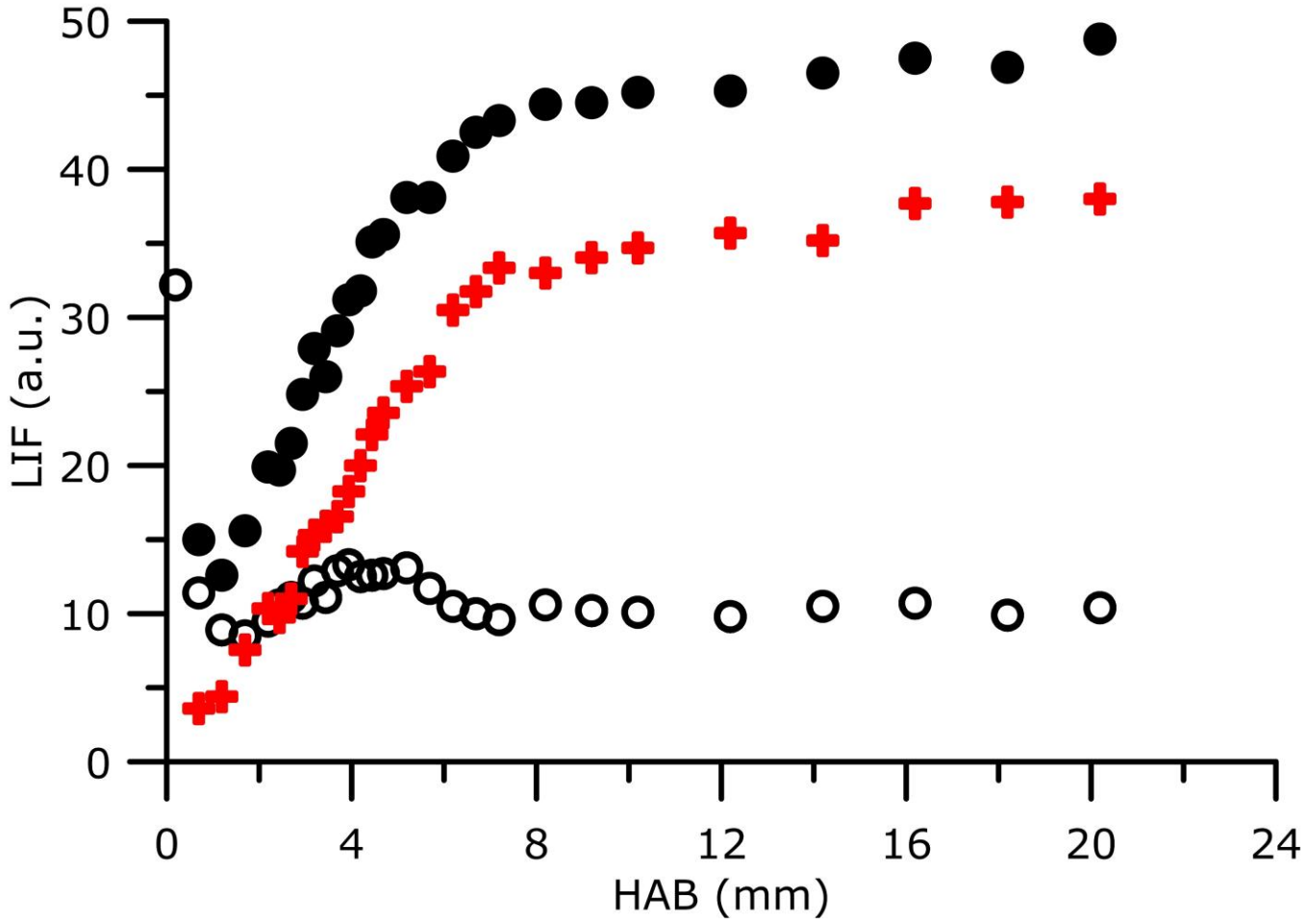

From LIF to the absolute concentration (profile)

Profile of S_{LIF}

$$SF = G\frac{\Omega V}{4\pi}N_1^0 B_{12}\frac{A_{21}}{A_{21}+Q_{21}}U_\nu$$

↓

Profile (relative) of N_1^0

Determination of the fluorescence quantum yield

$$\varphi_{fluo} = \frac{A_{21}}{A_{21}+Q_{21}}$$

$$N_1^0 \propto \frac{SF}{U_\nu \times \varphi_{fluo}}$$

↓

Profile (absolute) of N_1^0 → **Profile of the absolute cc N_{tot}**

Requires T knowledge: $N_1^0 = f_b(T)N_{tot}$

Advantage of low pressure flames: independence from Q if LIF signal measured at its temporal peak

Required calibration

- Rayleigh
- Absorption
- Standard addition method

VII. Resonant spectroscopic methods
Other LIF aspects

VII.1 The calibration methods
VII.2 Limitations of the two-level model
VII.3 About reaching the saturation: wings effect
VII.4 Predissociated LIF

VII.1 The calibration methods (depending on radicals or stable species)

- Rayleigh
- Standard addition
- Kinetics simulation
- absorption + CRDS

Calibration by Rayleigh (linear regime of fluorescence)

$$SF = G\frac{\Omega V}{4\pi}N_1^0 B_{12}\frac{A_{21}}{A_{21}+Q_{21}}U_\nu$$

$$S_{LIF} = \frac{1}{4\pi}\, b_{12}\, \frac{E_{LIF}}{A_{LIF}\Delta\nu}\, n_{CH} f_B \Gamma$$

$$SF = \frac{B_{12}}{c}\frac{E_L}{A_{Las}\Delta\nu_L}N_T\, f_B\Gamma\frac{A_{21}}{A_{21}+Q_{21}}G\frac{\Omega V}{4\pi}$$

$$b_{12} = \frac{B_{12}}{c} \times \underbrace{\frac{A_{21}}{A_{21}+Q_{21}}}_{\Phi} V_{LIF}\Omega\varepsilon\eta$$

$$S_R = \frac{NE_R V_R\left(\frac{\partial\sigma}{\partial\Omega}\right)}{A_R h\nu}\Omega\varepsilon\eta$$

$$n_{CH} = \frac{4\pi S_{LIF}\Delta\nu N E_R\left(\frac{\partial\sigma}{\partial\Omega}\right)}{b_{12}E_{LIF}\Gamma f_B \Phi h\nu S_R}$$

Applied to CH radical quantification

Luque and Crosley, App. Phys.B 63 (1996) 91
Walsh et al. PROCI 27 (1998) 615

Different methods of calibration for stable species: case of NO

Absorption in situ	Calibration at one HAB by using kinetic simulation	Standard addition method	After probe sampling and use of analysers (FTIR or chemiluminescence)

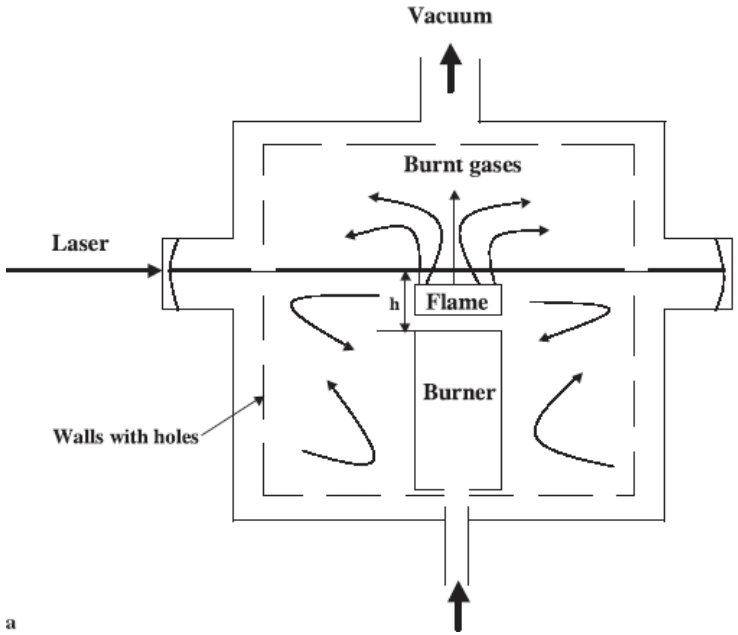

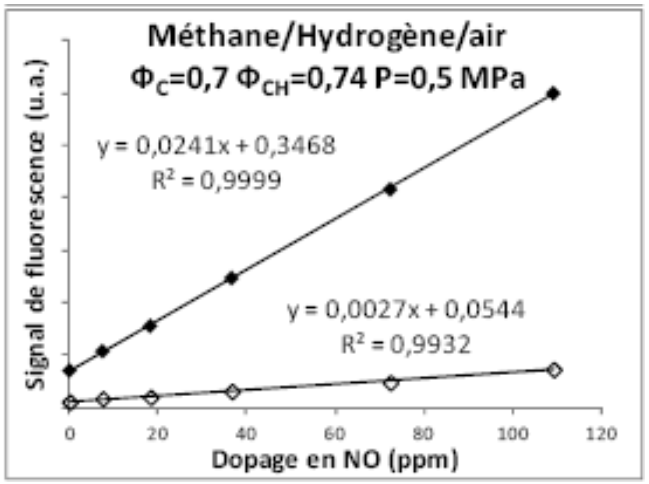

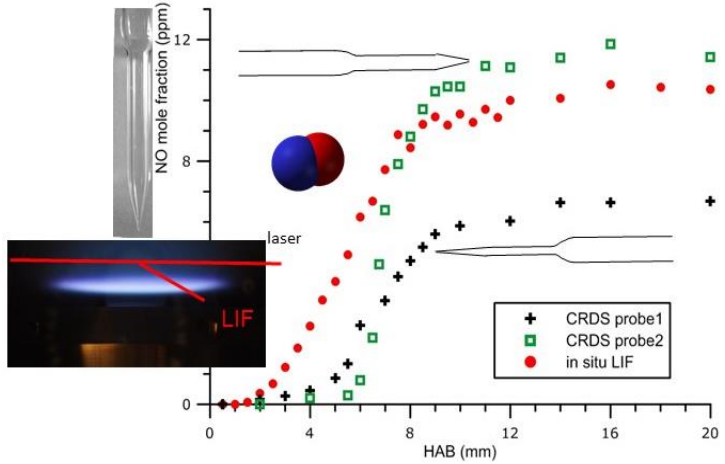

Lamoureux et al. Energy and Fuels 35 (2021), 7107

The standard addition method: case of NO

$$S_{LIF} = \frac{GV\Omega}{4\pi} N_{J"}^{0} B_{J"J'} U_{\nu} \frac{A}{A+Q}$$

$$S_{LIF,0} \propto \chi_{NO,natif}$$

$$S_{LIF} \propto \chi_{NO,added} + \chi_{NO,native}$$

$$\frac{S_{LIF} - S_{LIF,0}}{S_{LIF,0}} = \frac{\chi_{NO,added}}{\chi_{NO,native}}$$

Recommendation:

- Add at most one order of magnitude to the native value
- Check the absence of reburning
- Caution : the seeding is provided by a standard NO-diluted in N_2 (or Ar)

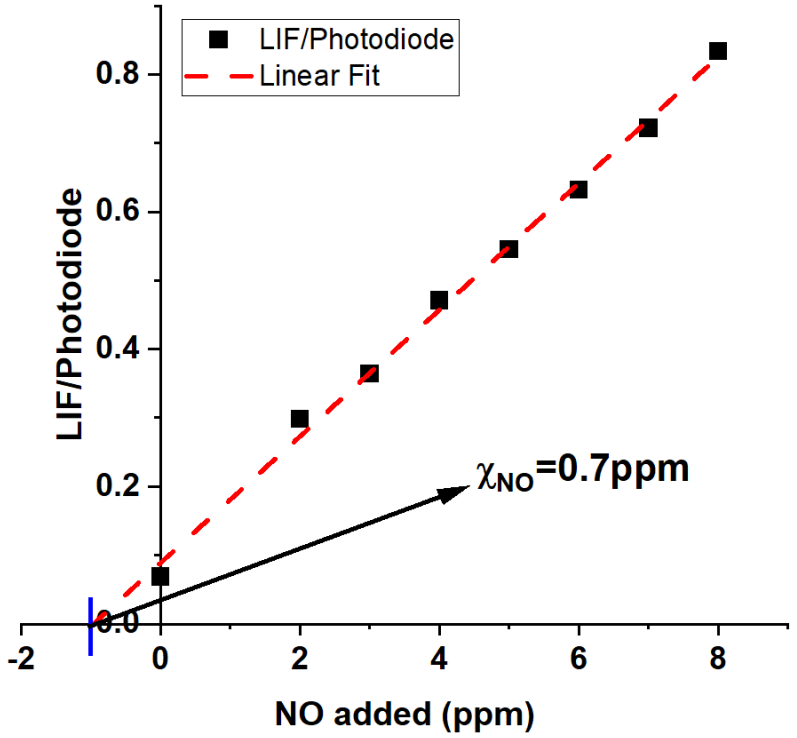

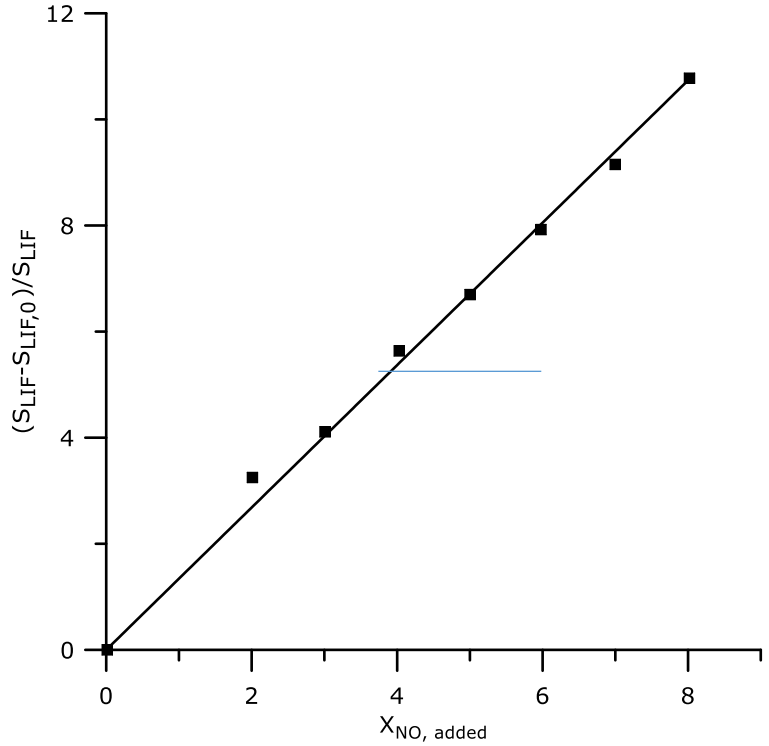

On the interest of standard addition method

Premixed
counterflow
high-pressure flame

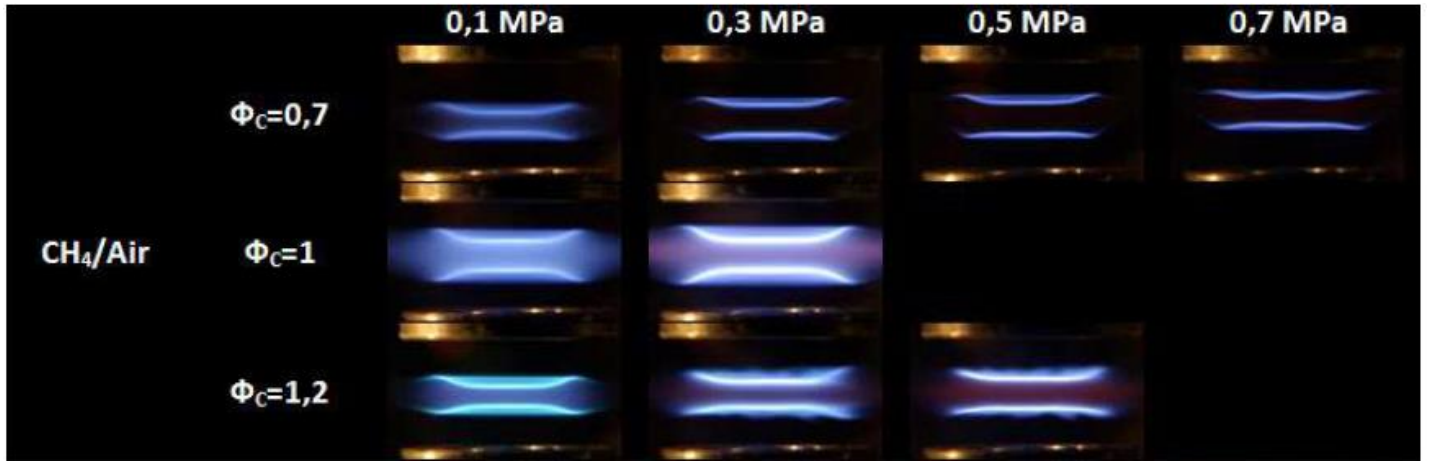

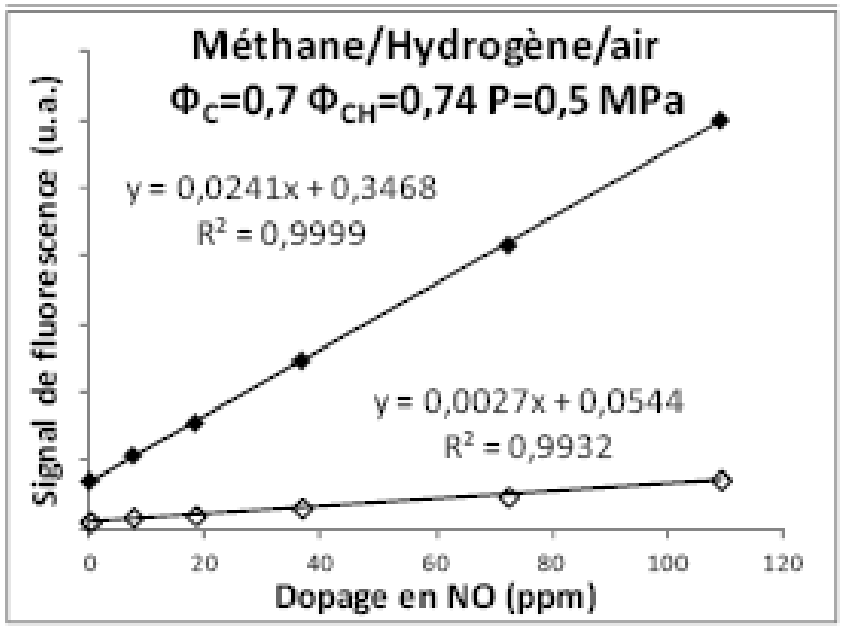

PhD A. Matynia et J. Molet ICARE

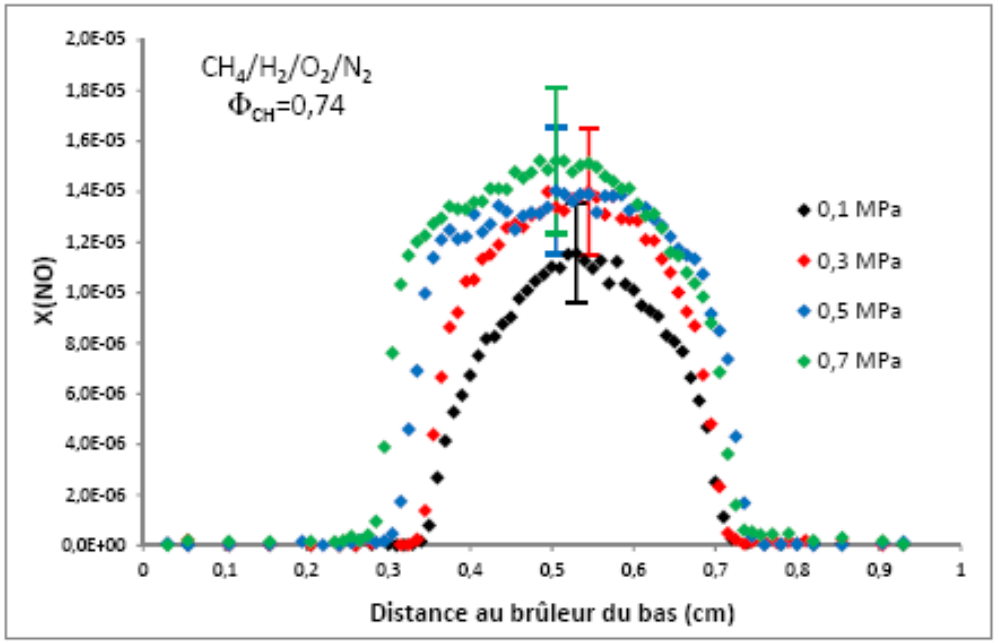

Pillier et al., Fuel 150 (2015) 394

Advantage of combining LIF/CRDS (or absorption)

LIF $S_{LIF} \propto \sigma(\lambda,T)\chi_i \frac{p}{kT}\phi(\lambda,T)$

- Local measurement, point-wise
- Excellent spatial resolution
- Highly sensitive
- **Dependence on Q**. No problem at low pressure
- Relative cc

CRDS $S_{CDR} = \sigma(\lambda,T)\chi_i \frac{p}{kT} l_s$

- Line-of-sight
- Spatial resolution ~ 300 μm
- Very sensitive
- Quantitative

Methodology

- LIF : measurement of relative profiles of $N_{J''}$ in various flame conditions
- CRDS : calibration of $N_{J''}$ in the most suitable condition (where $N_{J''}$ is max).

Advantage of combining LIF/CRDS (or absorption)

Case of NH radical:
a molecule with well isolated lines

LIF experimental set-up

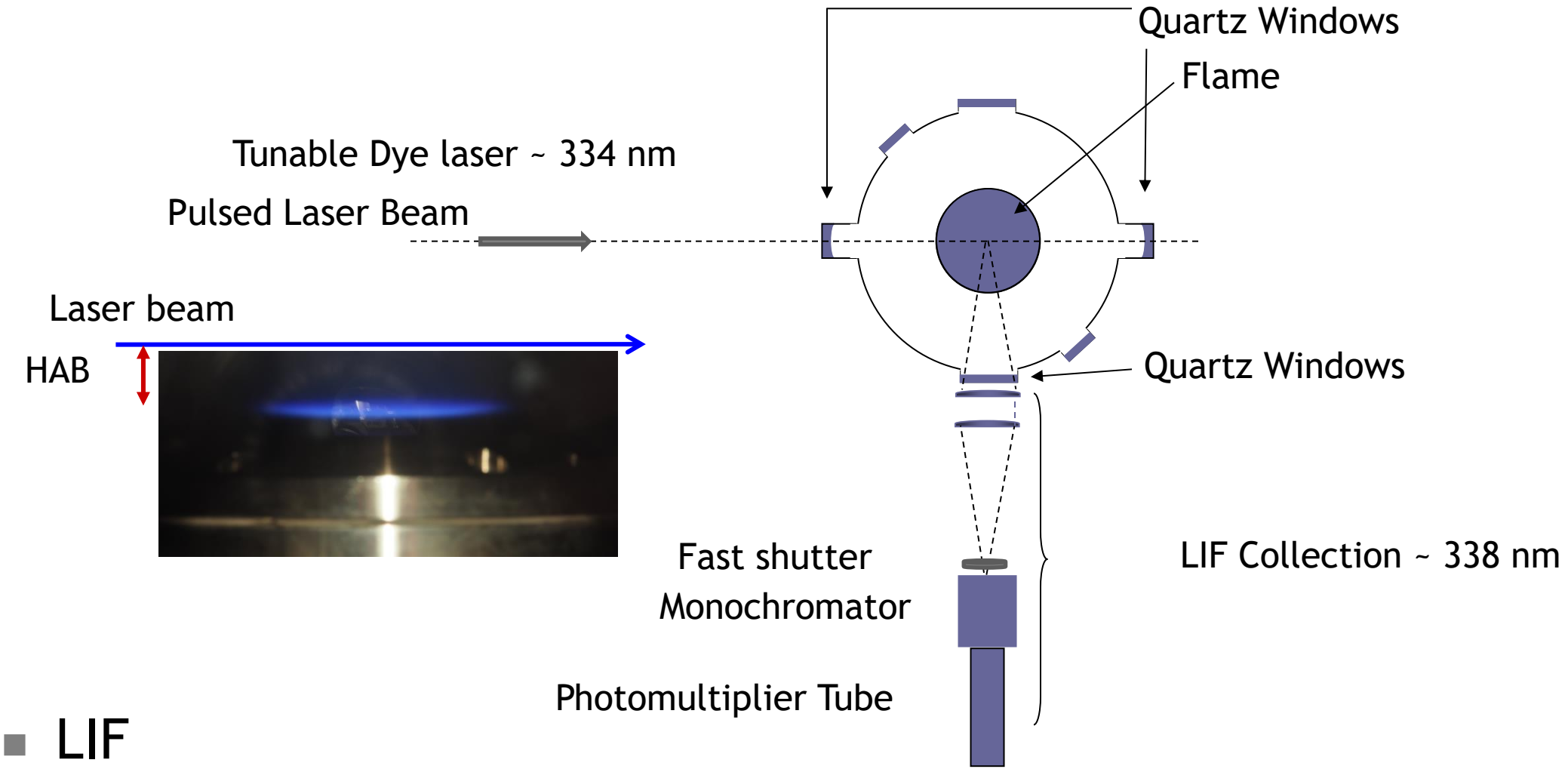

- LIF
  - Local measurement with high sensitivity and spatial resolution, selectivity
  - Relative concentration of NH radicals

Spectroscopy of NH, $A^3\Pi$-$X^3\Sigma^-$(0-0)

- CRDS absorption spectrum at 1790K

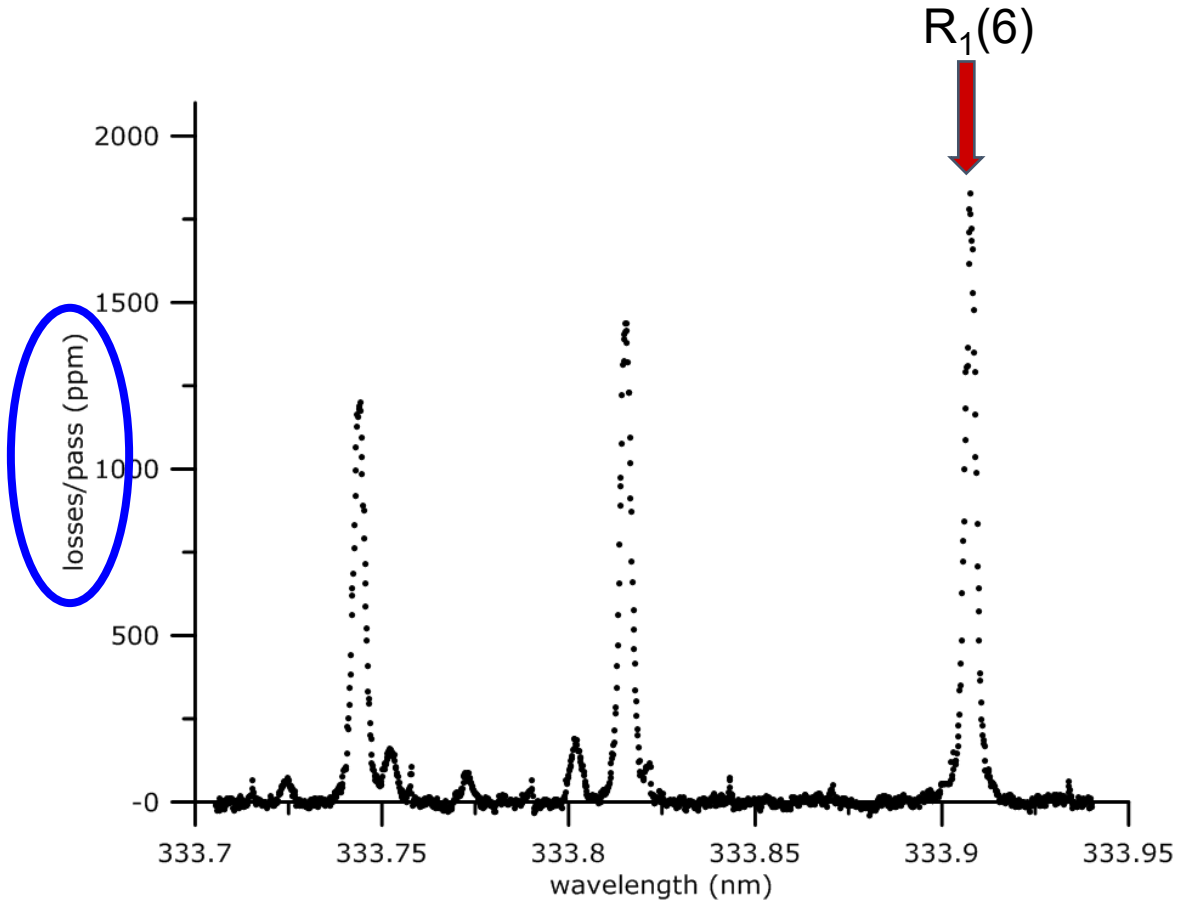

- How to obtain the value of the absorption cross section at 1790 K?

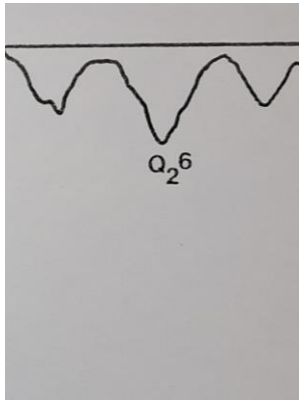

Lamoureux et al., ProCI2018

PGOPHER: An open source program for simulating rotational, vibrational and electronic spectra, *Colin Western, Univ. Bristol, JQSRT 85 (2017)*

- Linear molecules, symmetric tops and asymmetric tops
- Allowed and forbidden transitions, including multiphoton and Raman spectra
- Fitting of experimental data can be to line positions, intensities or band contours

Input data: spectroscopic data like energy terms, radiative lifetime

Spectroscopic Constants (in cm^{-1}) for the $X^3\Sigma^-$ State of NH

	v = 0	v = 1	v = 2
T_v	0.0	3125.57292(25)	6094.87617(57)
B_v	16.3432784(45)	15.6964414(81)	15.050334(26)
$10^3 \times D_v$	1.702786(35)	1.679548(64)	1.65803(30)
$10^7 \times H_{Lv}$	1.23442(115)	1.17513(185)	0.9575(88)
$10^{11} \times L_v$	-1.3974(162)	-1.4396(173)	0.0
$10^{16} \times M_v$	4.18(80)	0.0	0.0
λ_v	0.920063(148)	0.921239(172)	0.91916(31)
$10^6 \times \lambda_{Dv}$	-9.09(142)	-14.67(82)	0.0
$10^2 \times \gamma_v$	-5.4844(22)	- 5.1945(31)	-4.9104(69)
$10^5 \times \gamma_{Dv}$	1.5098(75)	1.4731(117)	1.795(58)
$10^9 \times \gamma_{Hv}$	-1.366(89)	0.0	0.0

Brazier et al. J. Mol. Spectro 120 (1986)

Output: Absorption spectra, Einstein coefficient per line, absorption cross section $\sigma(\overline{\nu},T)$

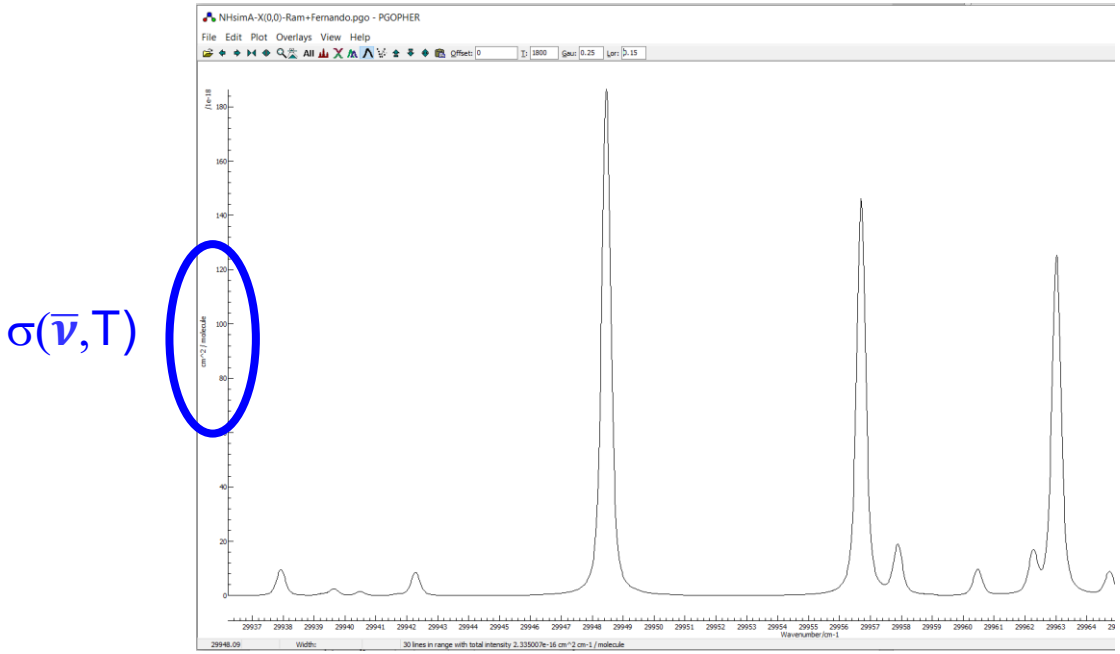

Absorption cross section σ/line/molecule cm^{-2}

Case of NH

http://pgopher.chm.bris.ac.uk/

Loss/path spectrum of NH ($A^3\Pi$-$X^3\Sigma^-$(0-0))

- Absorption spectrum à 1790K
- LIF excitation spectrum

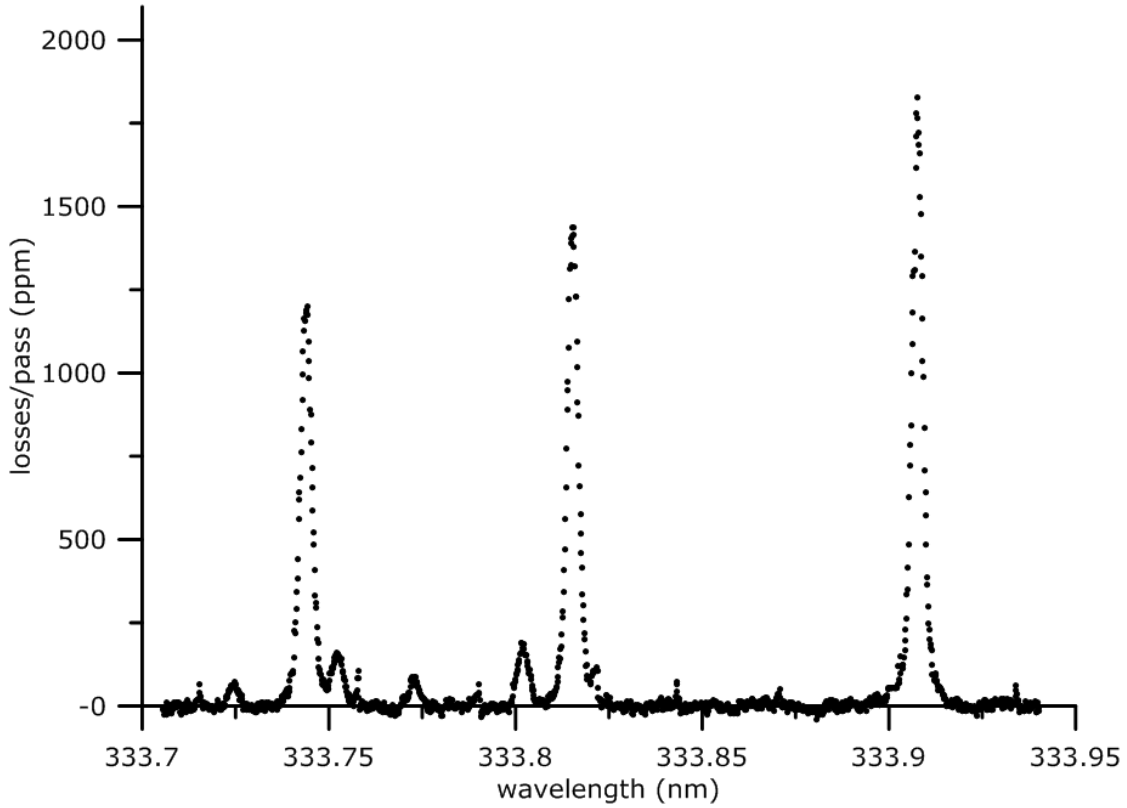

- CRDS
- PGOPHER program $R_1(6)$
  - $A_{J'J''} = 1.375 \times 10^6\ s^{-1}$
  - $\sigma(\lambda, T)$

http://pgopher.chm.bris.ac.uk/

Lamoureux et al., ProCI2018

In practice, in the case of a large or similar laser bandwidth relative to the absorption width (as for pulsed-CRDS), one measures the **integrated absorptivity A_I**.

PGOPHER returns A_{ij}, B_{ij}, f_{ij}, $\sigma(\bar{\nu},T)$

A_I is used to determine the total species concentration N_T (cm^{-3})

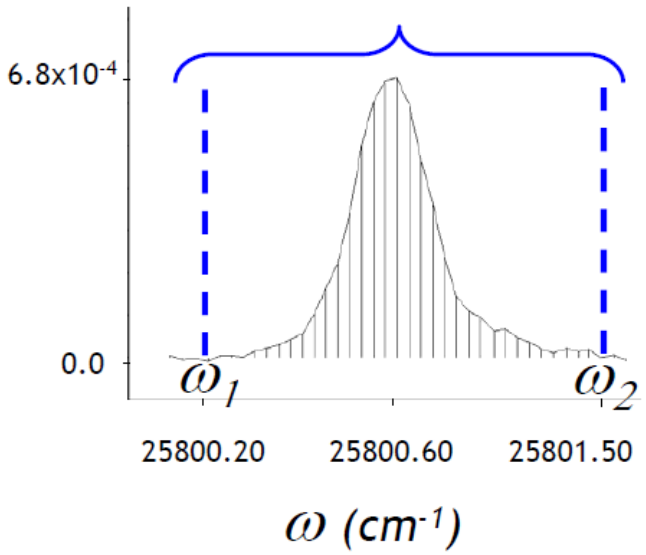

$$A_I = \int_{\omega_1}^{\omega_2} \sigma(\omega,T) N_T l_s d\omega = h\bar{\nu} f_B B_{12} N_T l_s \qquad cm^{-1}$$

$$\sigma(\bar{\nu},T) = \frac{h}{c}\bar{\nu}\ B_{J''J'} f_B(T,J'') g(\bar{\nu})$$

$$\int g(\bar{\nu}) d\bar{\nu} = 1$$

(by definition)

Advantage: the determination of N_T does not require the knowledge of the laser bandwidth

LIF/CRDS NH profiles in N_2O-doped flame at p = 5.3 kPa

- N_2O doped flame to increase the NH density

$$S_{LIF} \propto \phi(T, J'')f_{J''J}, N_{J''}$$

$$L(\bar{\nu}) = \frac{L_{cav}}{c}\left(\frac{1}{\tau(\bar{\nu})} - \frac{1}{\tau(\bar{\nu}_{off})}\right)$$

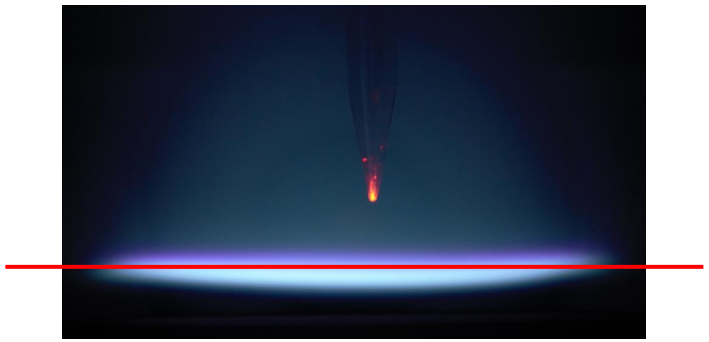

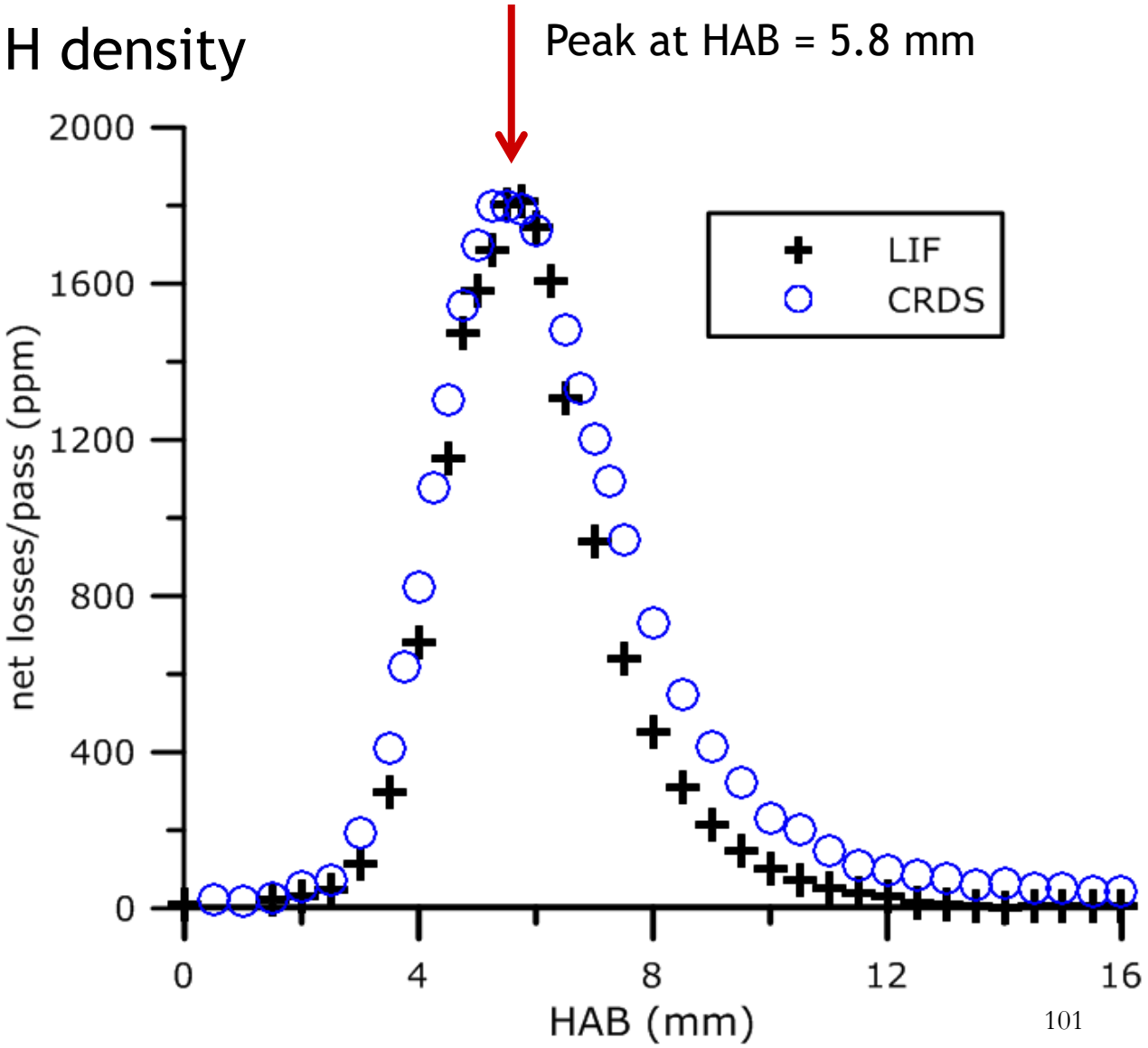

Results at the NH peak location

Flame	$N_{J''}$ LIF (relative)	$N_{J''}$ CRDS (cm^{-3})
CH4-N2O	100	4.70×10^{10}
C2H2(125)	3.66	1.72×10^{9}
C2H2(100)	1.43	6.73×10^{8}
CH4(125)	0.94	4.44×10^{8}
CH4(100)	0.29	1.39×10^{8}

× 27.3

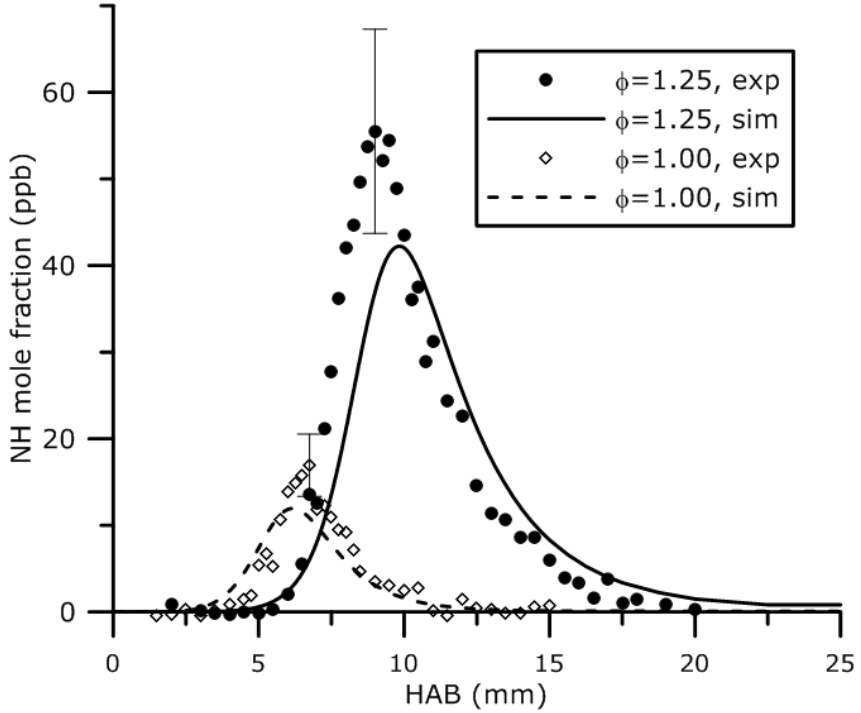

- LIF: wide dynamic range (> 2 orders of magnitude)
- Excellent agreement between LIF and CRDS ratios
- Conversion of $N_{J''}$ into NH absolute concentration and mole fraction
- Temperature profiles: NO-LIF thermometry

VII.2 Limitations of the two-level model

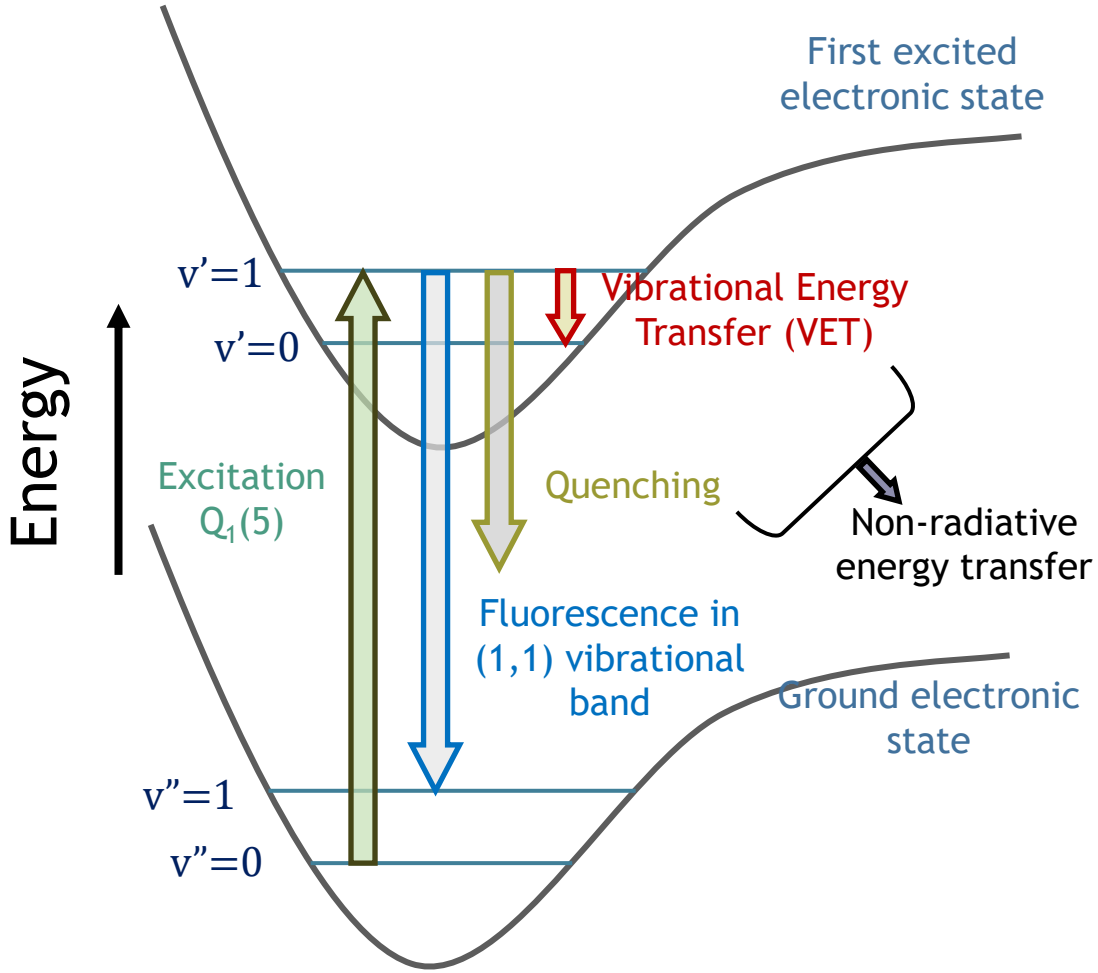

Rotational Energy Transfer (RET)
Vibrational Energy Transfer (VET)

Laser induced Fluorescence : the different spectra

Excitation spectrum:
R branch of OH (0-0)

LIFBASE, T=1800K,
instrumental resolution=
0.003 nm

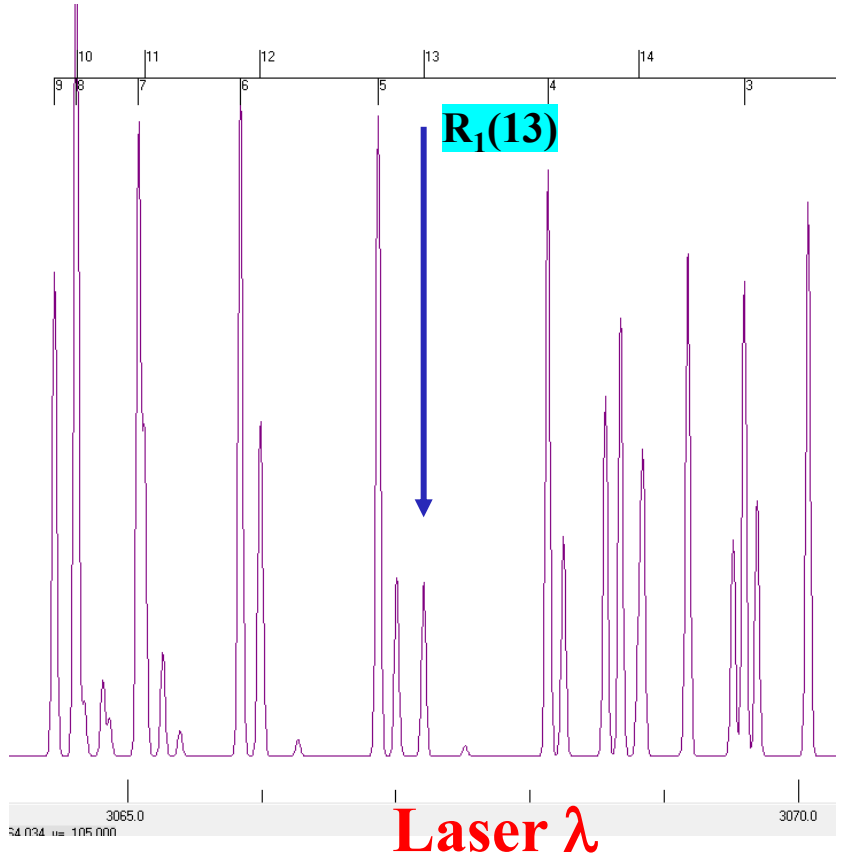

Spectroscopic selection rules $\Delta J=0, \pm 1$

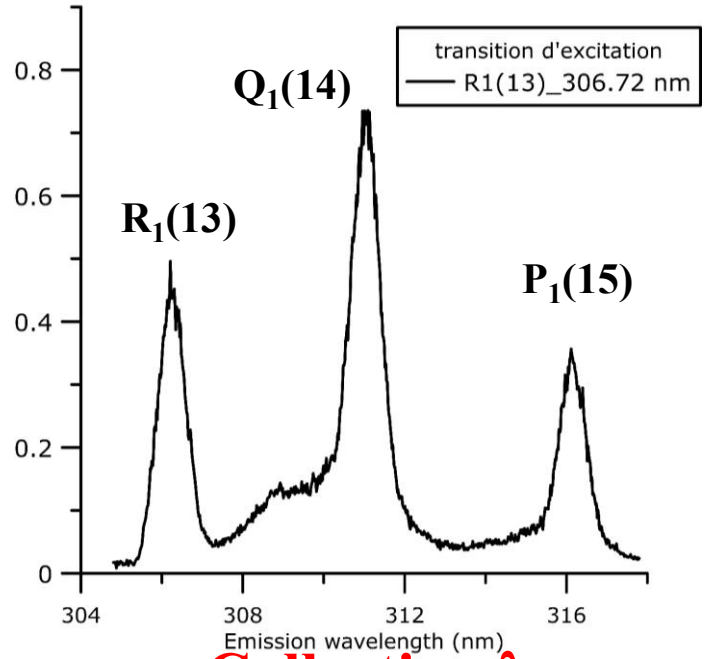

dispersed LIF spectrum

Rotational energy transfers (RET)

Excitation of line $Q_1(7)$ de OH $A^2\Sigma^+$-$X^2\Pi(0\text{-}0)$ at p=20 torr
Collection of the fluorescence spectrum at different times afer the laser pulse

$\Delta J = J' - J'' = 0, +/- 1$ RET

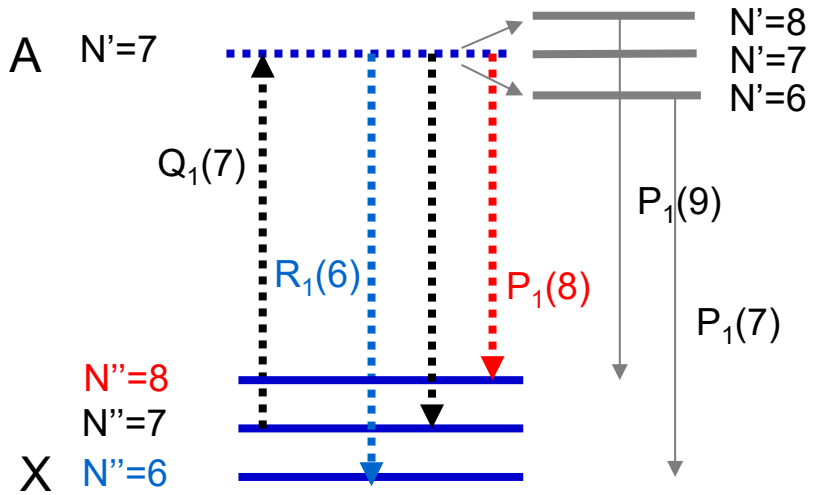

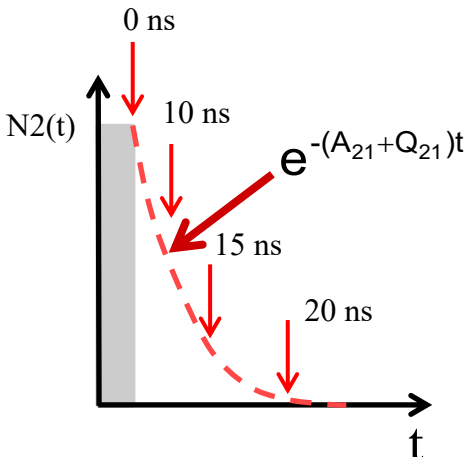

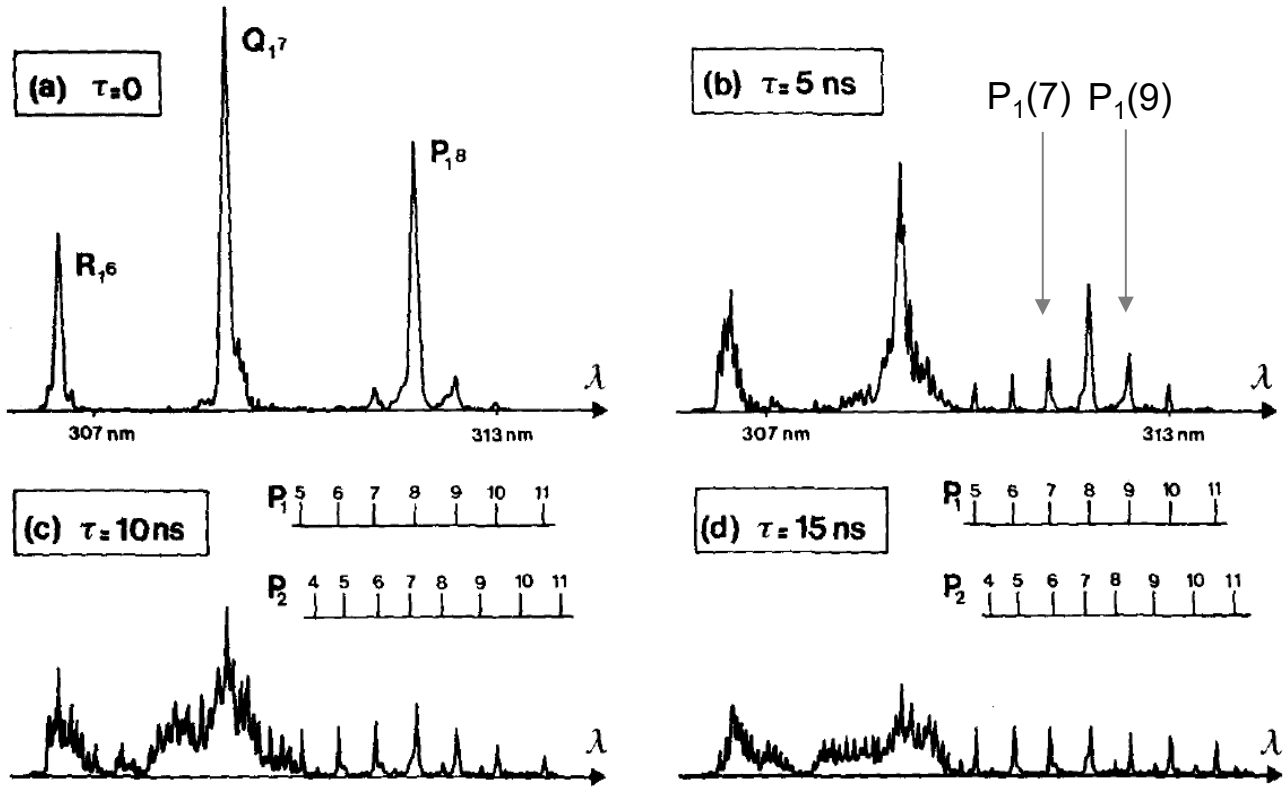

Rq : Two-level approx adequate in prompt detection (temporal peak LIF)!

Stepowski et Cottereau, J. Chem. Phys. 74 (1981) 6674

Evolution of the dispersed LIF spectrum as function of P

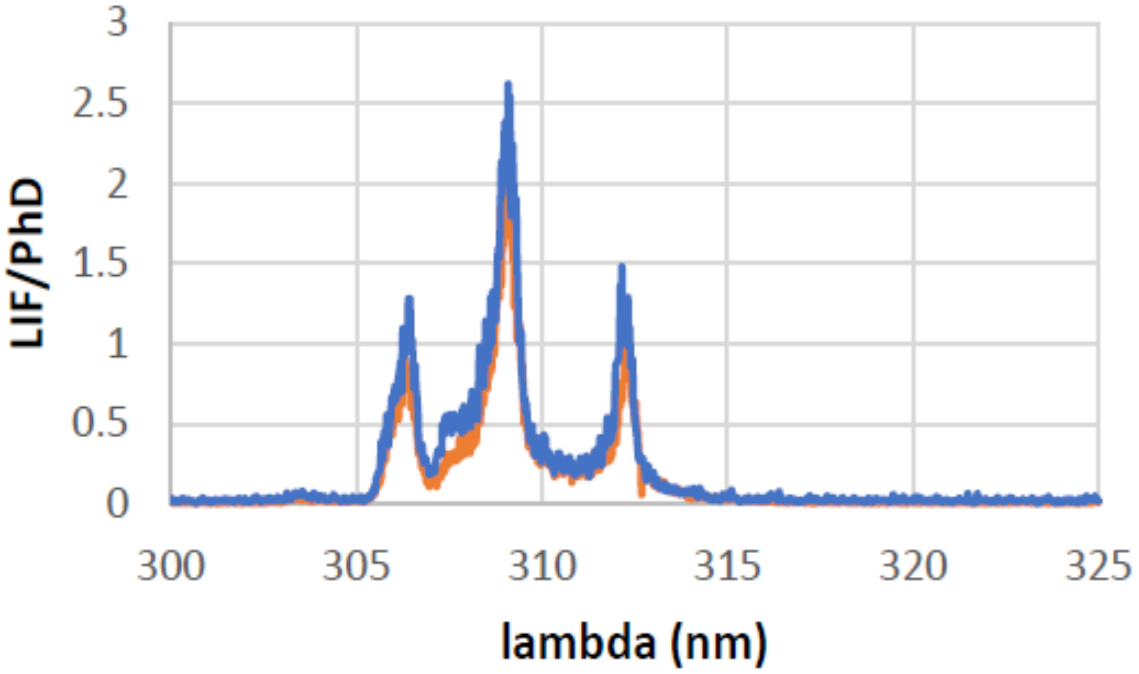

Excitation of the $R_{21}(7)$ of OH $A^2\Sigma^+$-$X^2\Pi(0\text{-}0)$ at p=35 torr

Tirthankar Mitra, PC2A data

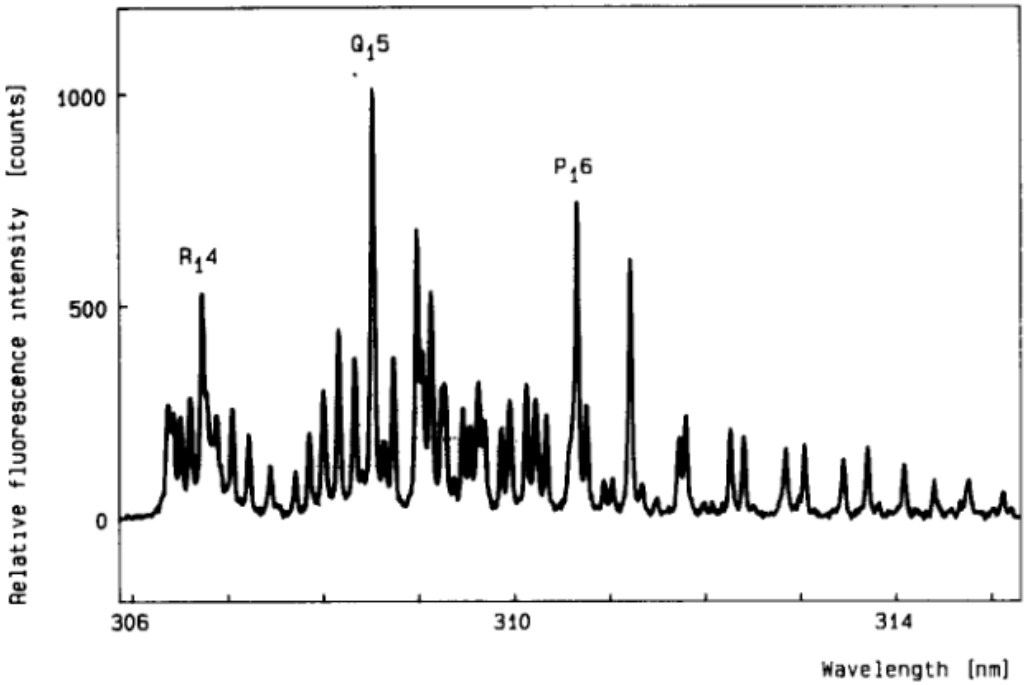

Excitation of the $Q_1(5)$ of OH $A^2\Sigma^+$-$X^2\Pi(0\text{-}0)$ at atmospheric pressure

Cignoli et al. Spectrochimica Acta 46B (1991) 1285

Multi-level scheme, rate equations: occurs at Patmo or high pressure

- Incorporating these interactions (RET r_{2j} here) into the rate equations
  - Level 2, absorption

$$\frac{dN_2}{dt} = N_1 B_{12} U_\nu - N_2 B_{21} U_\nu - N_2 A_{21} - N_2 \left(\sum_j Q_{ej} + \sum_j r_{2j} \right) + \sum_j N_j r_{j2}$$

  - Levels j, RET

$$\frac{dN_j}{dt} = N_2 r_{2j} - N_j r_{2j} - N_j A_{jl} - \sum_{k \neq j} N_j r_{jk} + \sum_j N_{kj} r_{kj}$$

Index 1 : level (J'',v''), generally X state
Index 2 : level (J',v'), generally A state
Index j, k : rotational levels in A,v'
Index l : all levels in X,v'' states to which transfers occurs

cf code LASKIN, Kienle; Brokhinke, Kohse-Hoïnghaus (Appl. Phys.B, 1996) → Fundamental studies on RET

Multilevel scheme

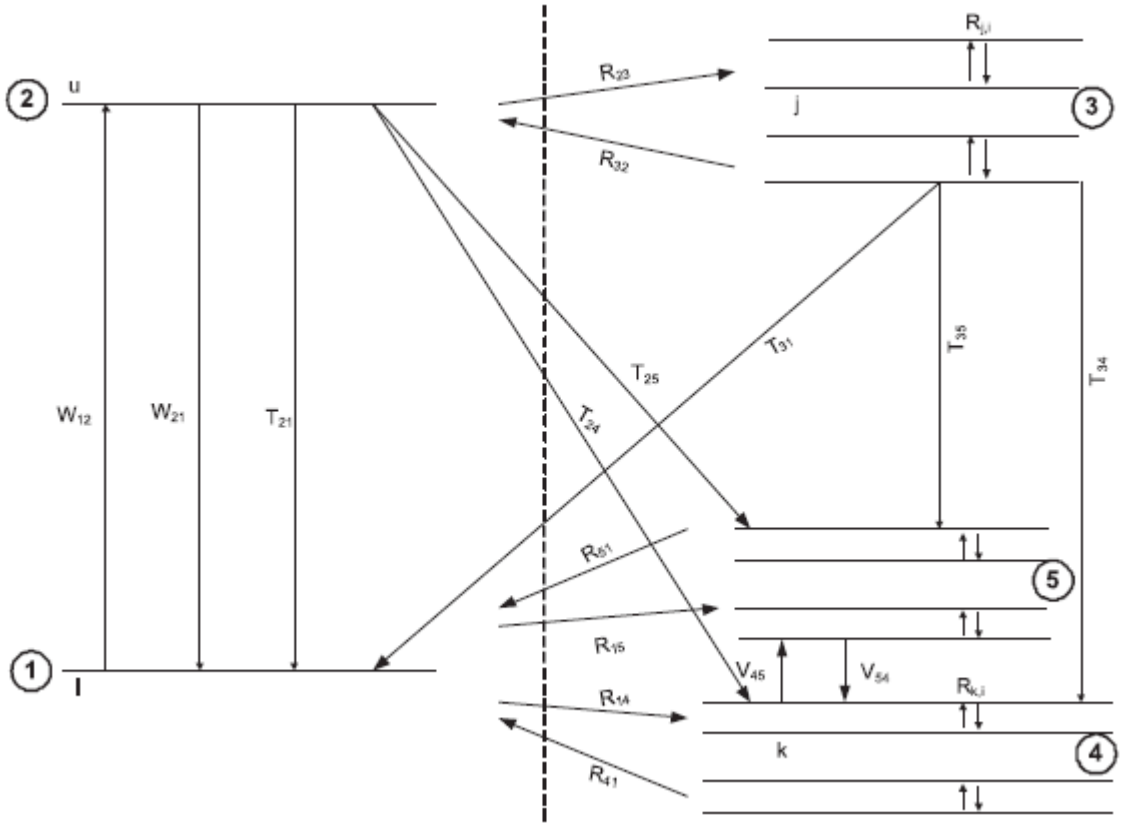

- Levels 1 and 2 are coupled by the laser (U_ν)
- Levels 3, (4 and 5): all rotational levels in the upper state and lower state respectively

notations :
$W_{12} = B_{12}U_\nu$
$W_{21} = B_{21}U_\nu$
$T_{ij} = A_{ij}+Q_{ij}$, Q_{24} and Q_{34} electronic quenching
r_{ij} and v_{ij} collisional transfer rate constant: RET and **VET**

Lucht, Sweeney, Laurendeau, Appl. Opt. 19, 3295 (1980) (Balanced Cross-Rate Model)
Naik&Laurendeau, Appl. Phys. B 79 (2004) 641
A. Cessou Thesis, Rouen
Mulla et al. Comb. Flame 203 (2019) 217

Balanced cross rate model (BCRM) Model (Naik's version, 5 levels)

$$\dot{N}_1 = -N_1(B_{12}U_\nu + r_{14} + r_{15}) + N_2(B_{21}U_\nu + T_{21}) + N_3T_{31} + N_4r_{41} + N_5r_{51}$$

$$\dot{N}_2 = N_1B_{12}U_\nu - N_2(B_{21}U_\nu + T_{21} + T_{24} + T_{25} + r_{23}) + N_3r_{32}$$

$$\dot{N}_3 = N_2r_{23} - N_3(T_{31} + T_{34} + T_{35} + r_{32})$$

$$\dot{N}_4 = N_1r_{14} + N_2T_{24} + N_3T_{34} - N_4(r_{41} + v_{45}) + N_5v_{54}$$

$$\dot{N}_5 = N_1r_{15} + N_2T_{25} + N_3T_{35} - N_5(r_{51} + v_{54}) + N_4v_{45}$$

$$N_T = N_1^0 + N_4^0 + N_5^0 = N_1 + N_2 + N_3 + N_4 + N_5$$

Lucht, Sweeney, Laurendeau, Appl. Opt. 19, 3295 (1980) (Balanced Cross-Rate Model)
Naik&Laurendeau, Appl. Phys. B 79 (2004) 641

BCRM model, Naik's

- The principle of the BCRM is based on the idea that the rate of population transfer between levels 1 and 2 is approximately the same as the rate of transfer from levels (1,2) to levels (3,4).

$$N_3(r_{32} + T_{31}) + N_4 r_{41} + N_5 r_{51} \cong N_2(r_{23} + T_{24} + T_{25}) + N_1(r_{14} + r_{15})$$

- If these cross-rates are balanced, equilibrium between levels 1 and 2 is quickly reached: $N_1 + N_2 = N_1^0$
- Then the equations become simpler :

$$N_2 = N_1^0 \frac{B_{12}}{B_{12}+B_{21}} \frac{1}{1+\frac{U_\nu^S}{U_\nu}} \qquad \text{with } U_\nu^S = (T_{21} + T_{24} + T_{25} + r_{23} - (N_3/N_2) r_{32}) \Big/ (B_{12} + B_{21})$$

- For linear LIF regime :

$$N_2 = N_1^0 \frac{B_{12}}{B_{12}+B_{21}} \frac{U_\nu}{U_\nu^S}$$

Same expression as for the two-level model: RET effects in 5-level model only influences U_ν^S

Message in presence of large RET

For linear LIF regime :

$$N_2 = N_1^0 \frac{B_{12}}{B_{12}+B_{21}} \frac{U_\nu}{U_\nu^S}$$

Same expression as for the two-level model: RET effects in 5-level model only influences U_ν^S

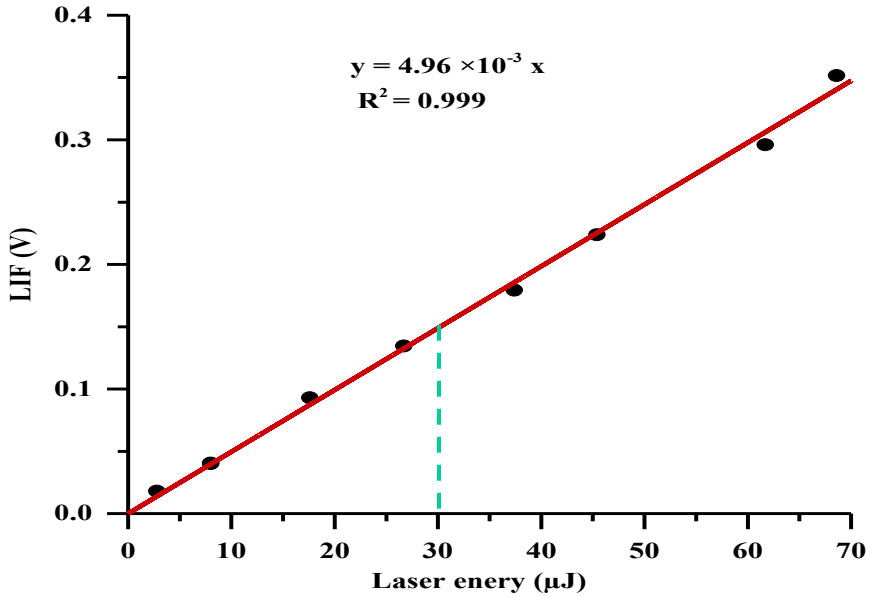

With PMT, much easier and faster than with a ICCD camera

Check the linearity of LIF with E_L, then LIF signal proportional to the ground state rotational population but needs to be corrected for U_ν^S

Few words on VET

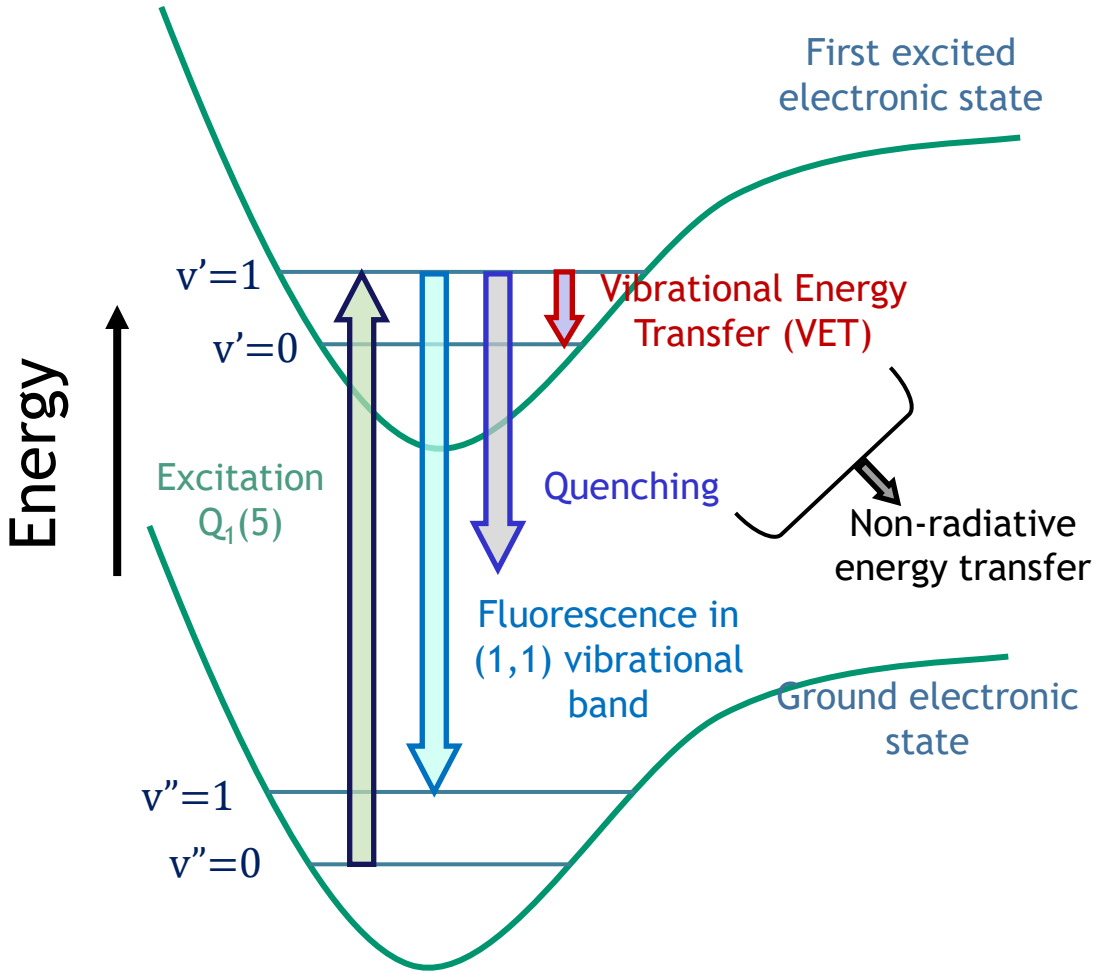

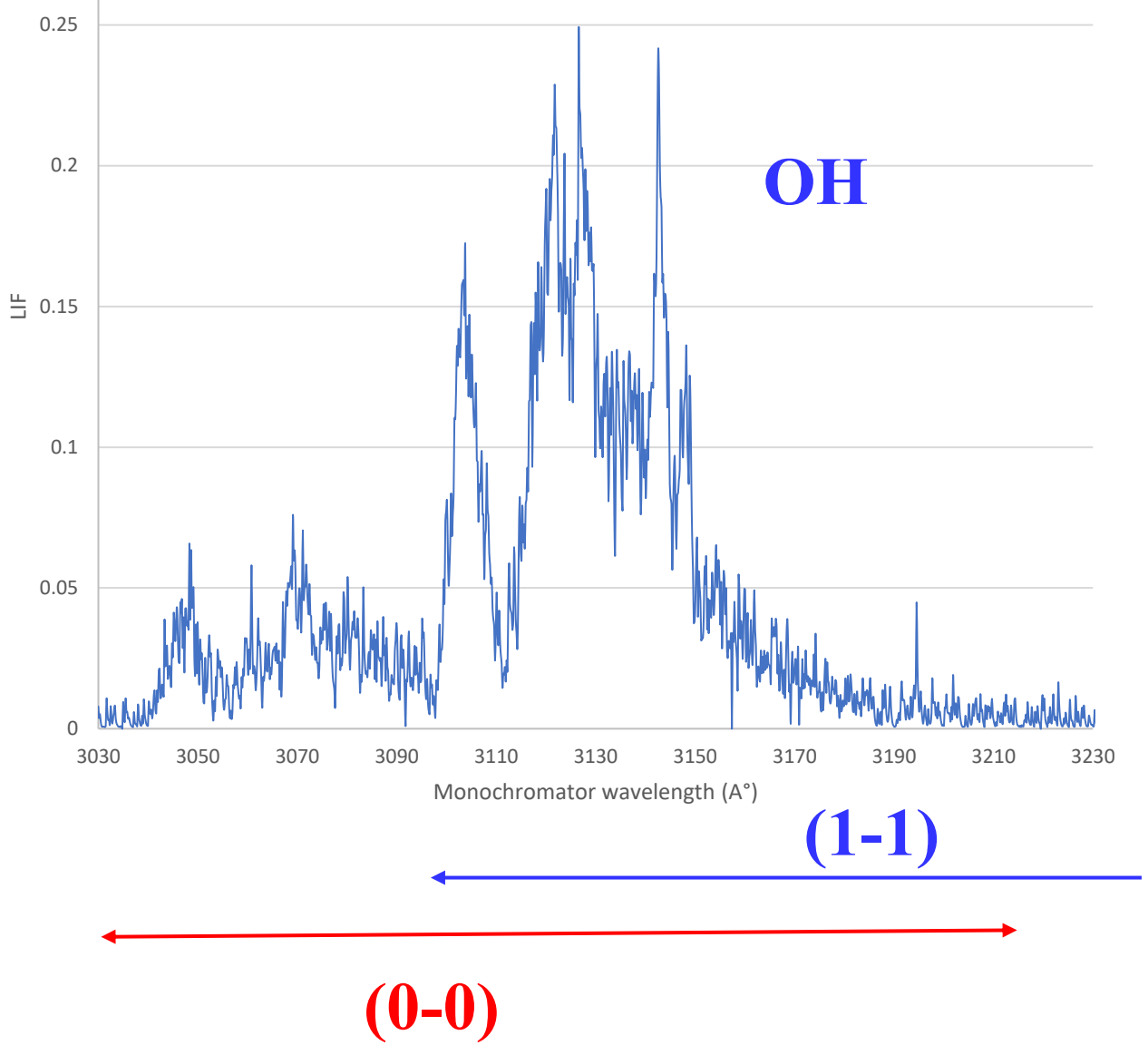

Ankit Sahay, PC2A, 2026

Hartlieb, Markus, Kreutner, and Kohse-Höinghaus, Appl. Phys. B, 65, 81-91, 1997

Copeland, Wise, and Crosley, J. Phys. Chem., 1988, 92, 5710-5715

VII.3 About reaching the saturation: the wings effects

The wings effects

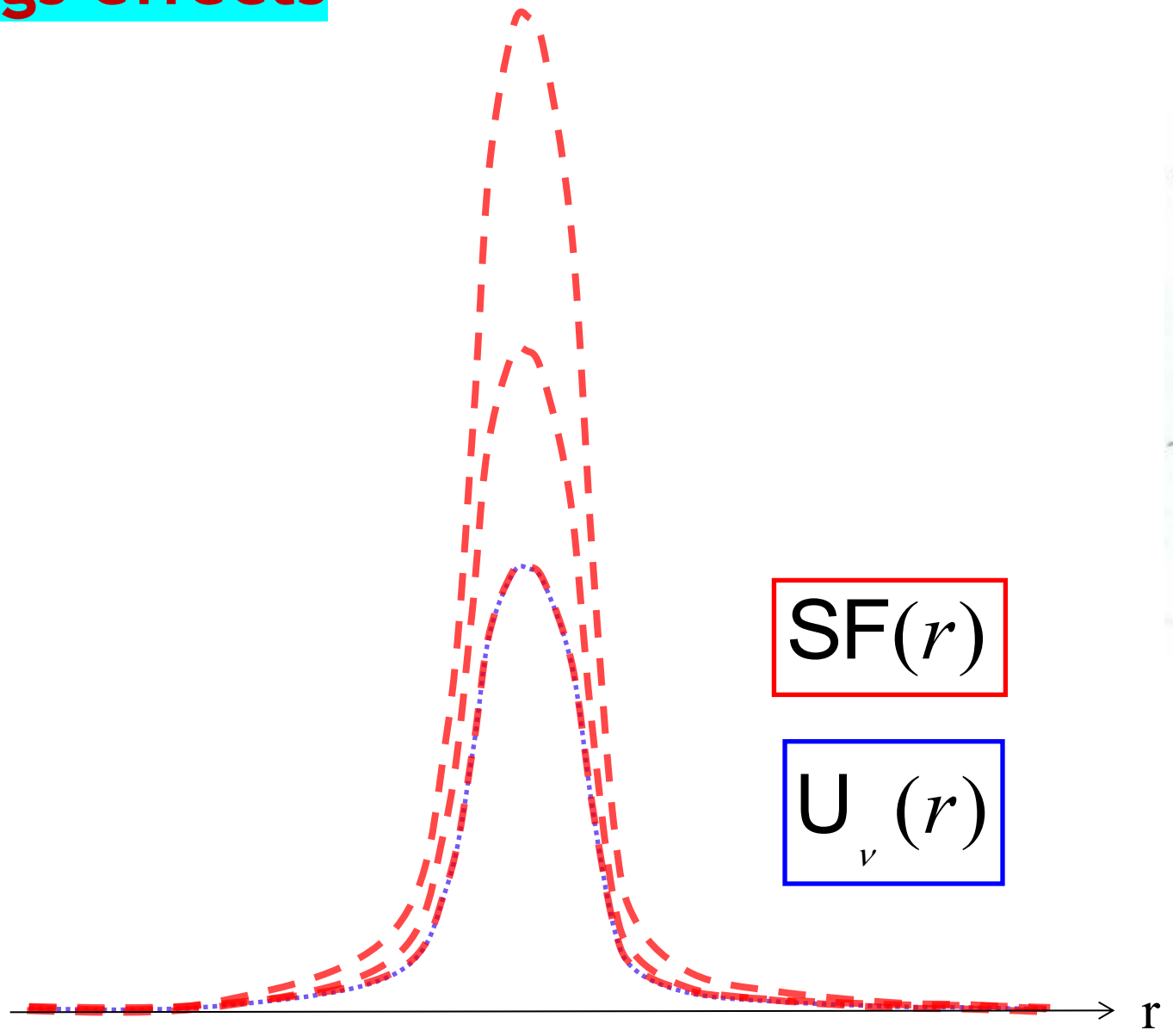

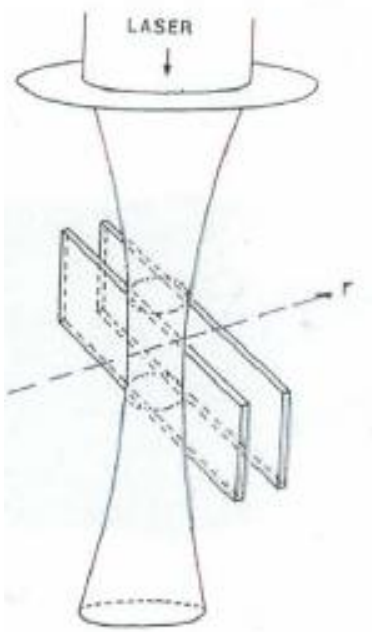

Case of a signal linear in energy

114

The wings effects

$$N_2(r) = N_1^0 . \frac{B_{12}}{B_{12} + B_{21}} \frac{1}{1 + \frac{U_\nu^s}{U_\nu(r)}}$$

$$SF = \iiint N_2(r) A_{21} \frac{\Omega}{4\pi} dV$$

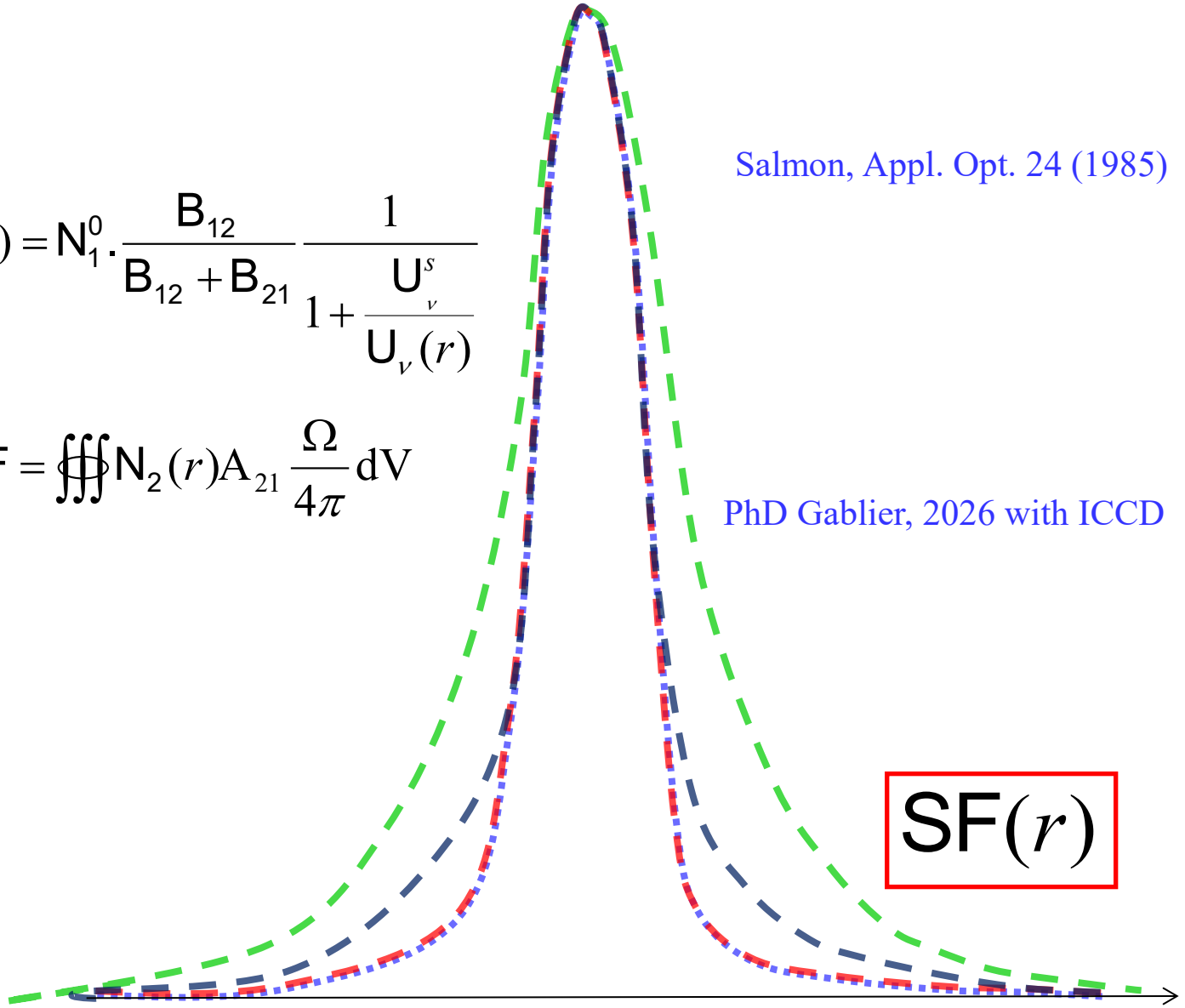

Salmon, Appl. Opt. 24 (1985)

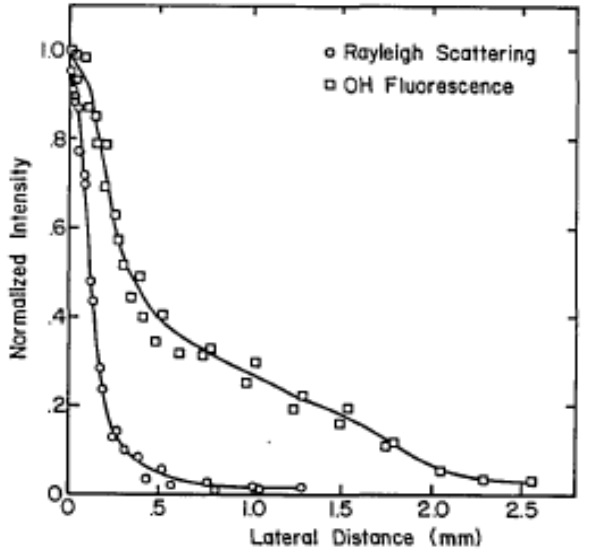

PhD Gablier, 2026 with ICCD

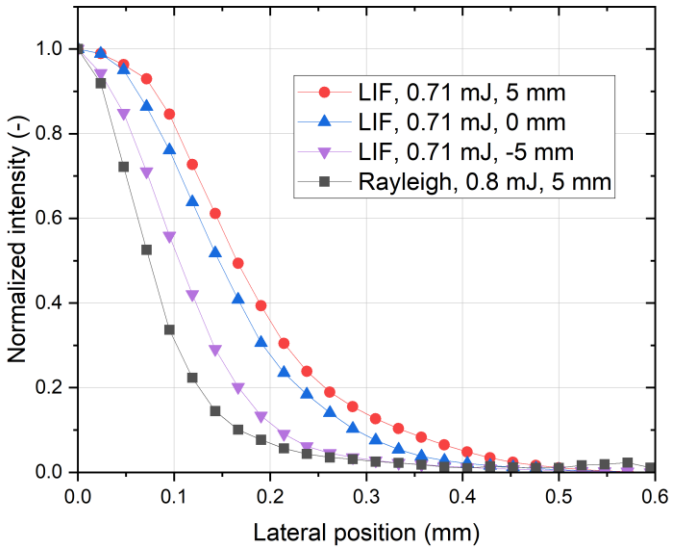

Size of the effective volume depends on level of saturation (Q)

Desgroux P., Cottereau M.J.,, App. Opt., **30**, 90-97 (1991)
Daily J.W., Appl. Opt., **17**, 225 (1978)

The wings effects

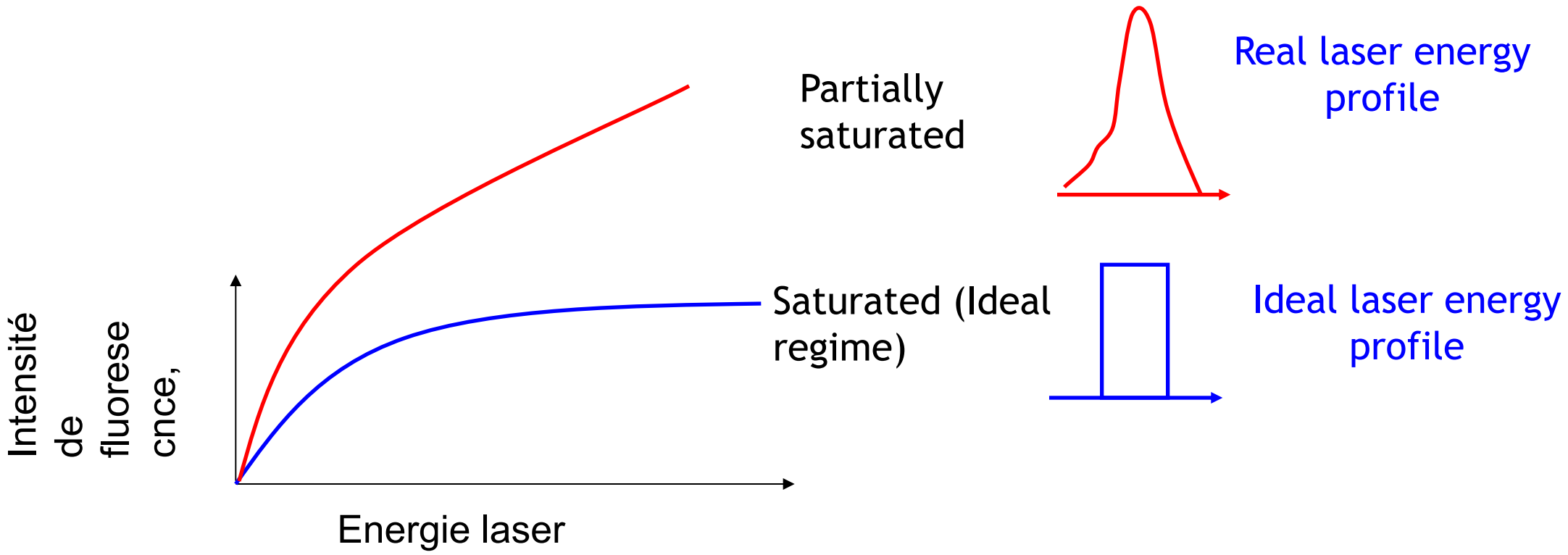

$$SF = \frac{G\Omega V}{4\pi}\frac{B_{12}}{B_{12}+B_{21}}\iiint_V \frac{dV}{1+\frac{U_\nu^S}{U_\nu}}$$

Concept of effective volume : $F\left(\frac{U_\nu^S}{U_\nu}\right) = \iiint \frac{1}{\left(1+\frac{U_\nu^S}{U_\nu}\right)} dV$, in partially saturated : $\mathrm{SF} \propto N_1^0 F\left(\frac{U_\nu^S}{U_\nu}\right)$

Size of effective volume depends on level of saturation (Q): prefer selecting linear regime

Lecture of Mark linne, Tsinghua summer school 2025

“Saturated fluorescence is an idea to escape the Quenching problem. Here we have such high laser intensity that Wnm (the stimulated rate) dominates over the spontaneous and quenching rates, and so they can be eliminated from the equations to get “ a LIF signal independent of quenching.

“In practice it is not possible to saturate fluorescence fully. Saturation requires very high laser irradiance. The edges of a Gaussian cross section beam will never reach saturation irradiance, and the trailing edge of a ns pulse dies away slowly, so the tail of the pulse does not saturate either”.

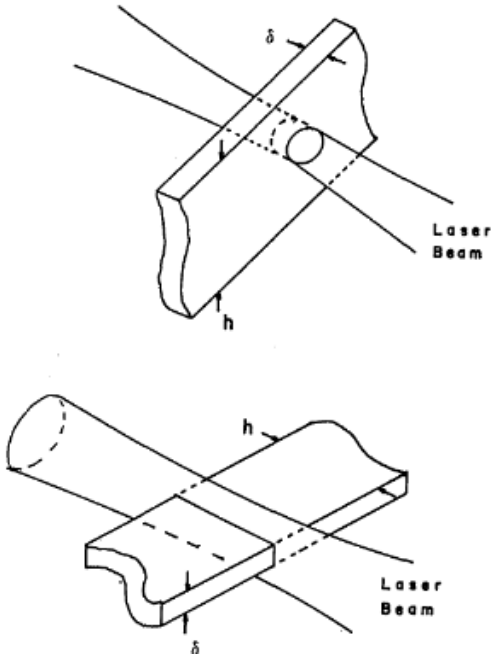

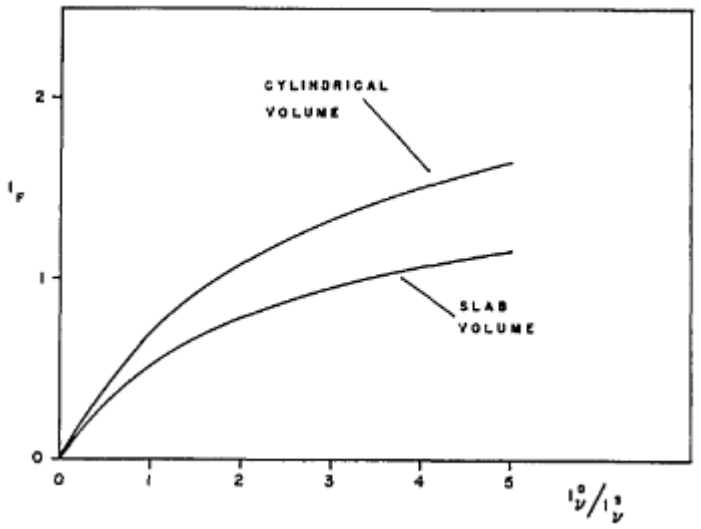

Daily, Appl. Opt. (1978) 225

Examples of LIF= f(E_L) curves

Desgroux&Cottereau,
Appl.Opt 30 (1991) 90

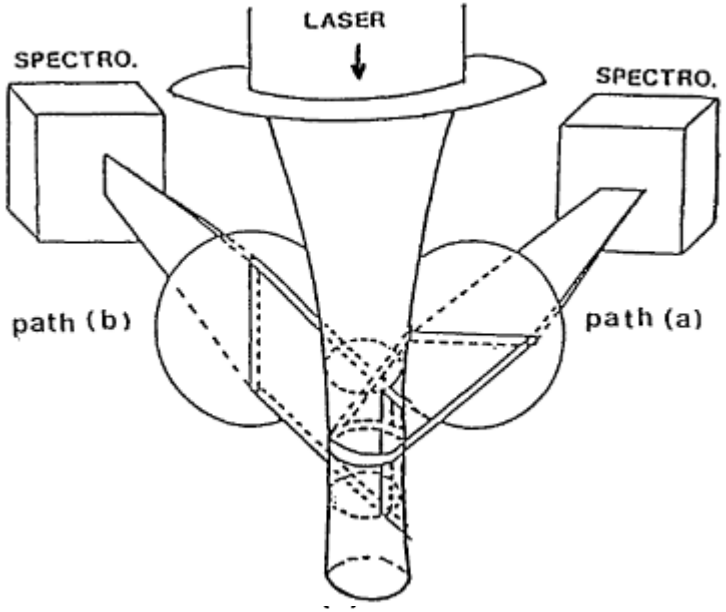

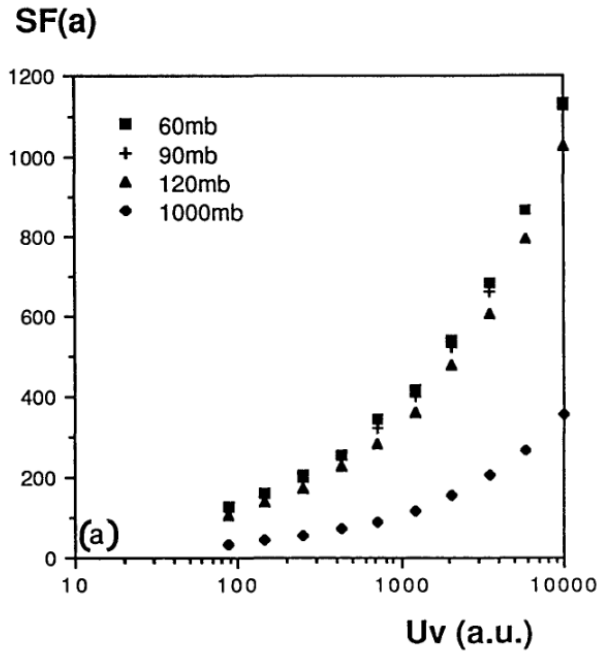

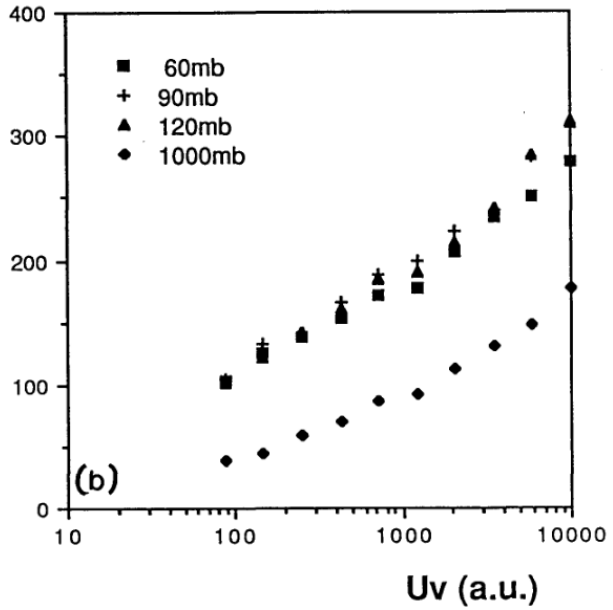

Tang et al. CNF 267 (2024)113556

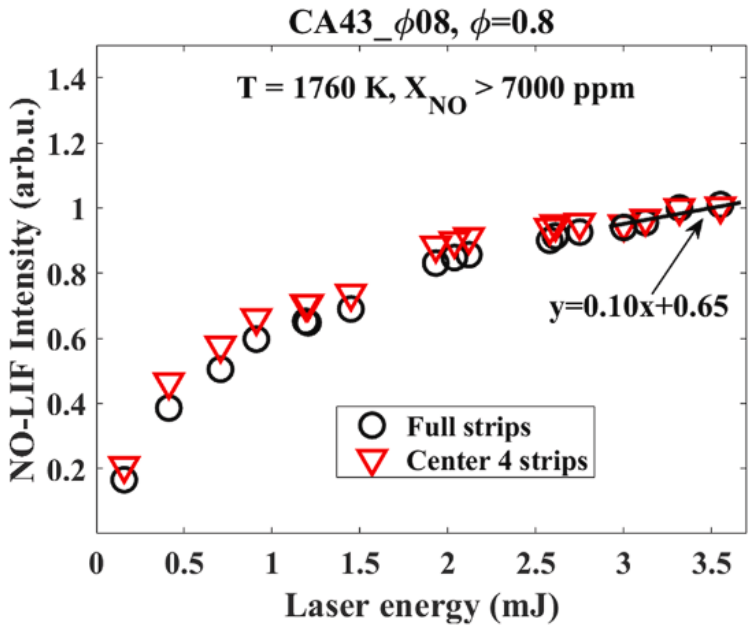

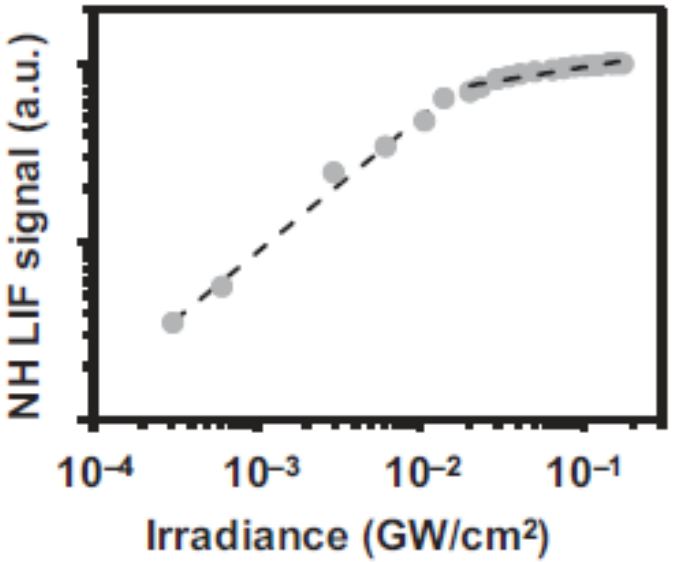

Brackmann et al. CST 188 (2016) 529

Beam profiler: examples of dye laser energy distribution

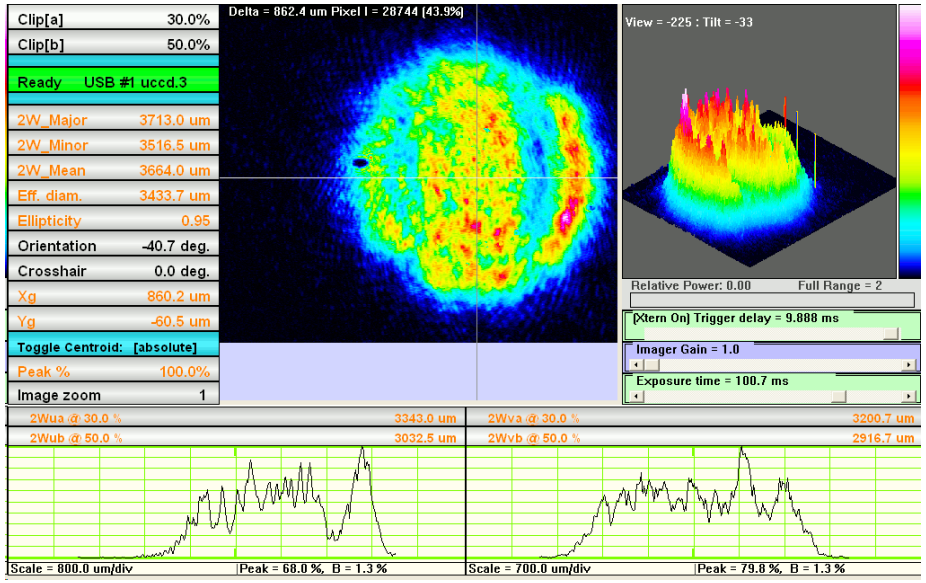

VII.4 Predissociated LIF

LIPF: predissociated LIF: an alternative to quenching dependence

Predissociation ≠ Dissociation

Transition 1-2 resonant

Potential energy curve of OH

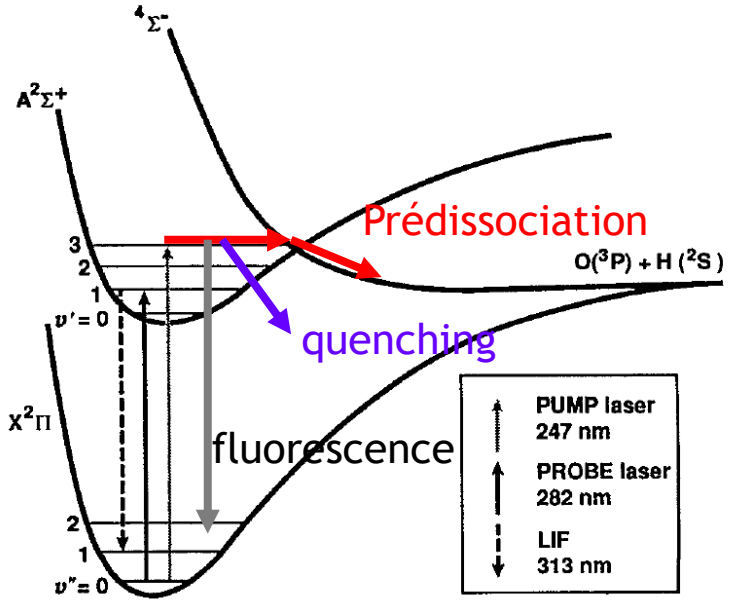

$$\frac{dN_2}{dt} = N_1 B_{12} U_\nu - N_2 \left(B_{21} U_\nu + A_{21} + Q_{21} + p \right)$$

→ **Quantum yield of a predissociated state**

$$\Phi = \frac{A}{A+Q+P}$$

Predissociation rate
P (10^{10} to 10^{12} s^{-1}) >> A (10^5 s^{-1})
P >> Q

Q(1bar) ~ $10^9 s^{-1}$
P(OH, $A^2\Sigma$,v'=3) ~ 10^{10} s^{-1}
P(O_2, $B^3\Sigma_u^-$,v'<10) ~ 10^{12} s^{-1}

→ **Weak dependence on quenching (up to 1 atm)**
but very weak quantum yield

ex : O_2 and OH (abundant species) around 193 nm,

Gray and Farrow, J. Chem. Phys. 95 (1991) 7054

LIPF, exemple du CH C-X

Advantages of $C^2\Sigma^+$ state of CH ?

Same wavelength range as OH $A^2\Sigma^+$-$X^2\Pi$ (0,0)

Weakly predissociated state ($p \sim 10^8\ s^{-1}$) $\Rightarrow$ fluorescence quantum yield not negligible

Much less dependent on quenching variations

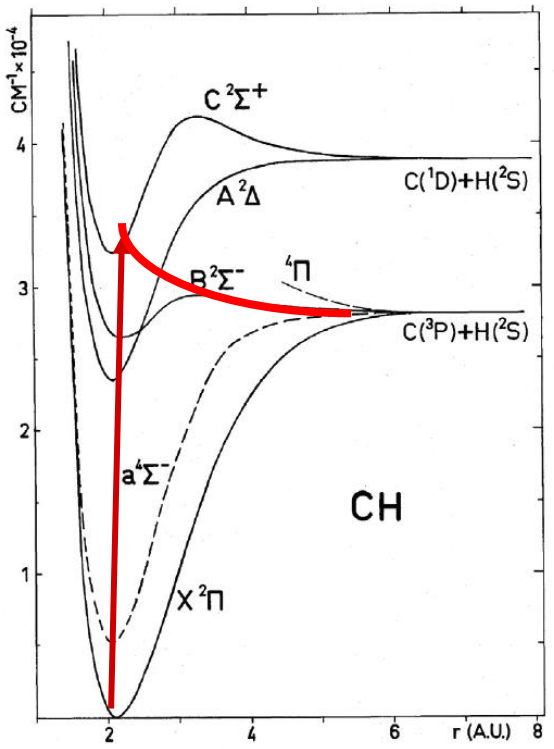

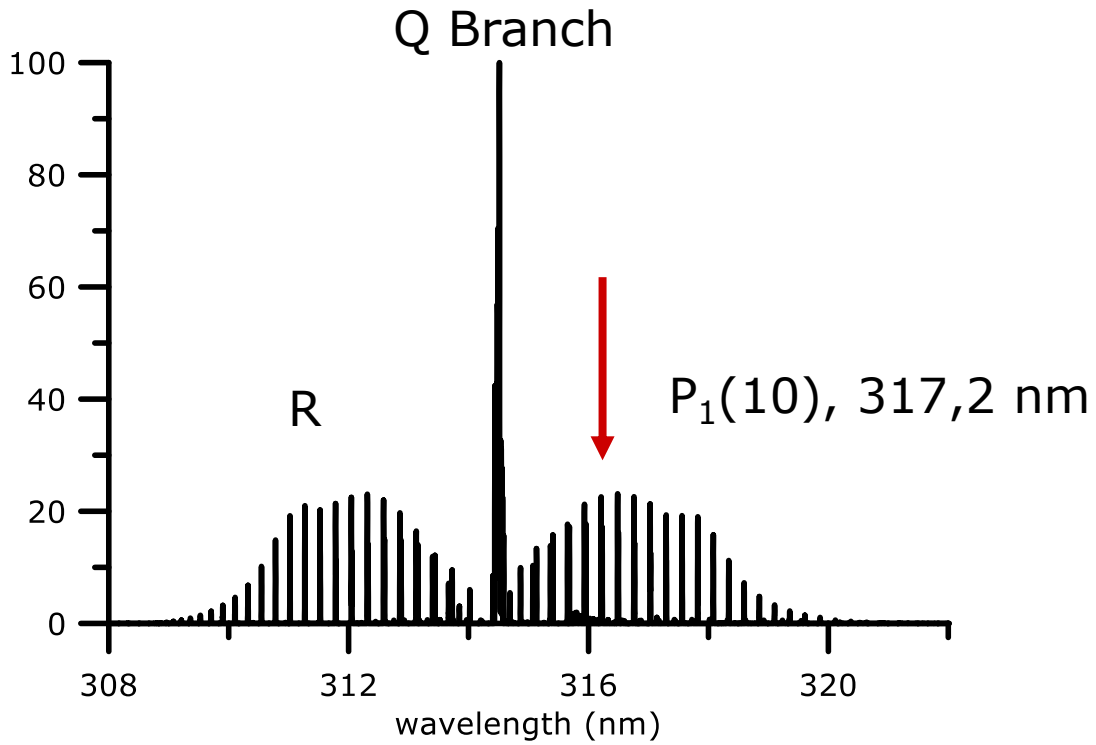

Rq: CH radical involved in prompt-NO formation

CH measurement: single-shot application in a lifted flame

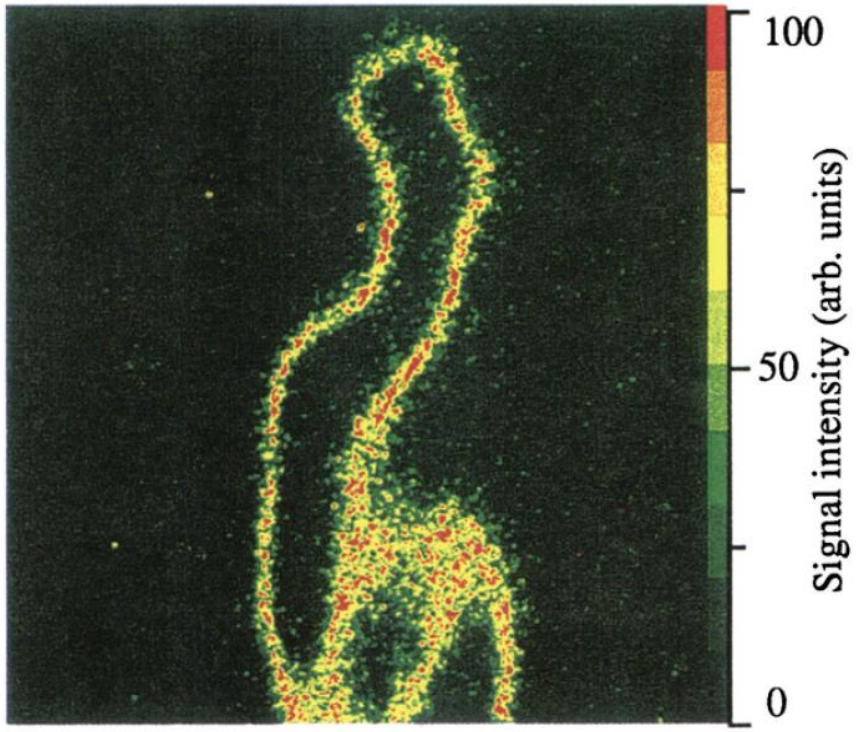

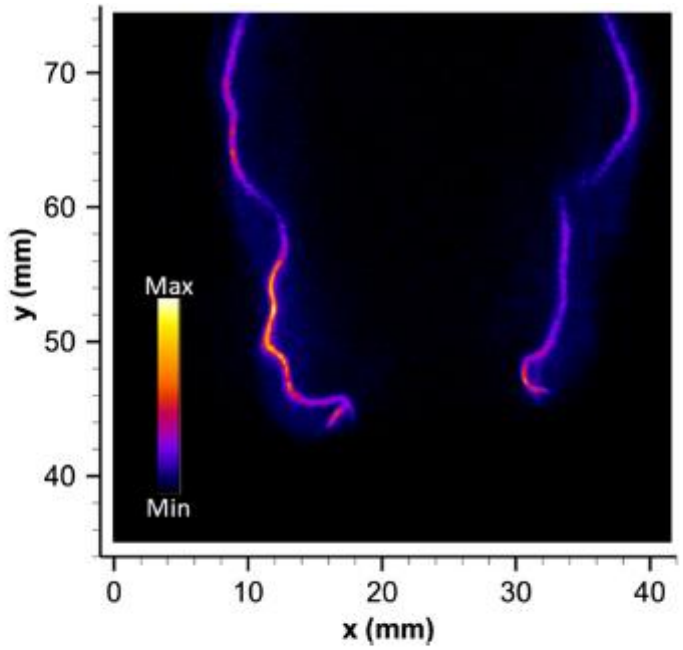

Fig. 4 Single-shot CH PLIF image from a lifted jet flame. *y* is the distance from the fuel tube

Visualisation PLIF CH C-X, Flamme CH4/air, ϕ=1.25
Tsujishita, Jpn J. Pall. Phys. 32 (1993) 5564

Carter et al. Appl. Phys. B (2014) 116:515–519

CH measurements in the C-X band

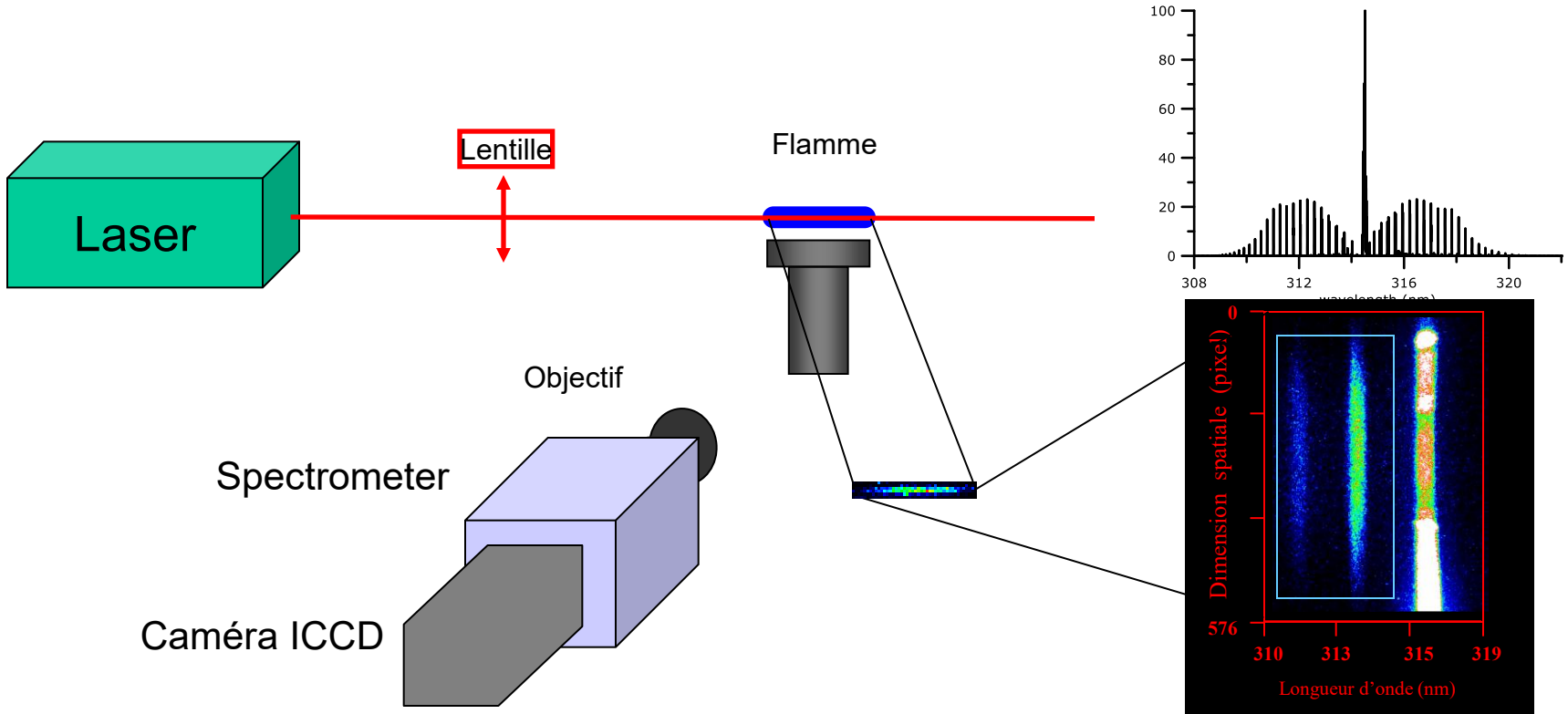

1D spectral LIF imaging

Image 2D de CH reconstituée

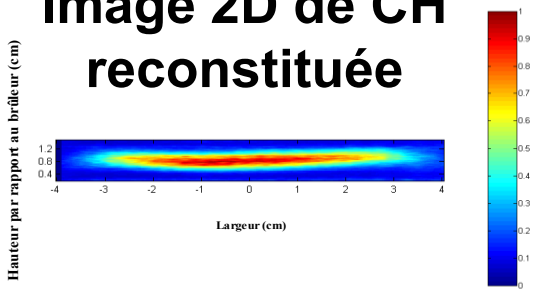

Reconstruction of 2D image

PhD Laure Pillier, Lille 2003

Pillier et al. PROCI 30 (2005) 1183

VIII Two-Photon LIF

TPLIF (Two-Photons LIF), TALIF (Two photons Absorption LIF)

- Principles
- Issues: linearity, stimulated emission, photoionisation, photodissociation…
- Fluorescence quantum yield (quenching rate)
- Calibration
  - Indirect
  - Noble gas (Xenon)

Absolute mole fraction profiles of atoms by MBMS

Peeters&Mahnen, Sympo Comb (1973) 133

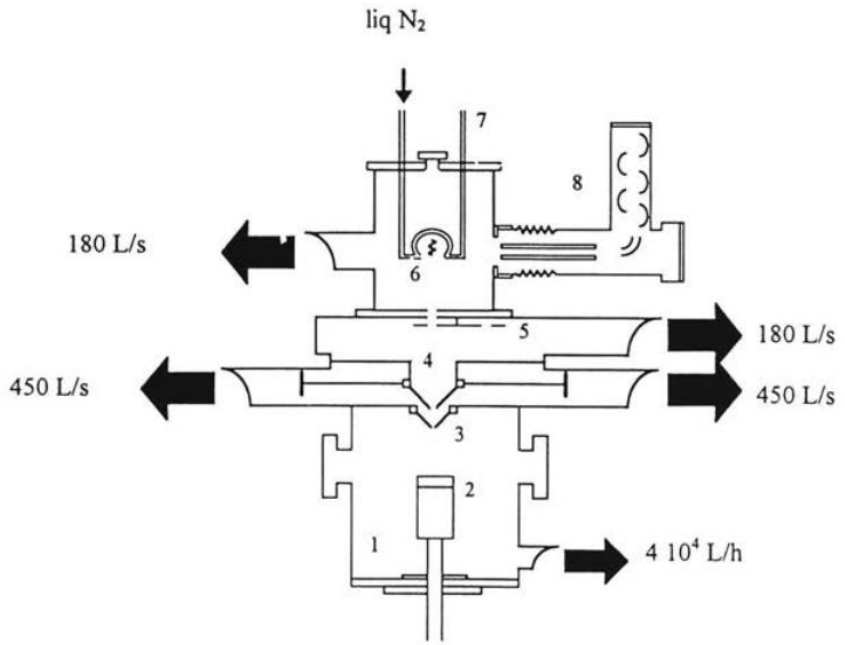

Figure 1: Experimental apparatus: 1 - combustion chamber; 2 - movable burner; 3 - quartz cone; 4 - skimmer; 5 - rotated toothed wheel; 6 - ion source; 7 - cryogenic trap; 8 - quadrupole mass filter and electron multiplier.

Crunelle et al. J. Chim. Phys.94 (1997) 483

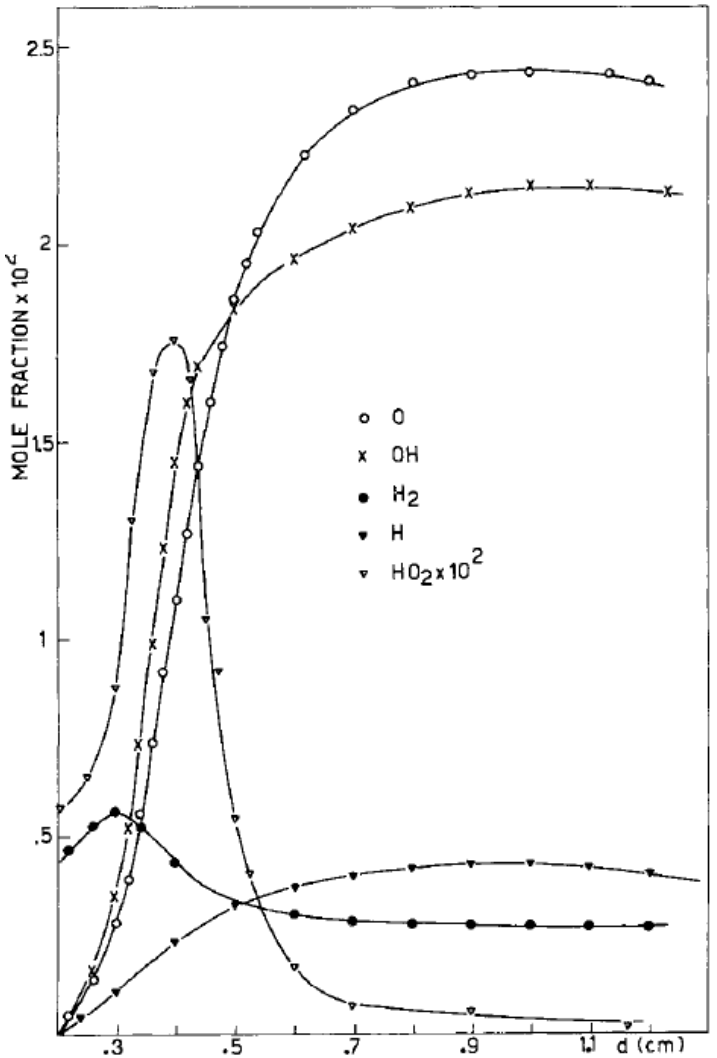

40 Torr CH_4/O_2 lean flame

$$H + O_2 = O + OH \quad (K1)$$

$$OH + H_2 = H + H_2O \quad (K2)$$

$$H_2 + O_2 = OH + OH \quad (K3)$$

$$(i_O \cdot i_{OH})/(i_H \cdot i_{O_2}),$$

$$(i_{OH} \cdot i_H)/(i_O \cdot i_{H_2}),$$

and

$$(i_H \cdot i_{H_2O})/(i_{OH} \cdot i_{H_2}),$$

Quantification of H, O, OH assuming partial equilibrium is reached

Synchrotron VUV beam photoionization mass spectrometry (PIMS)

photons in the 5–21 eV range, with a photon flux of 10^{13} photons s^{-1} at 10 eV

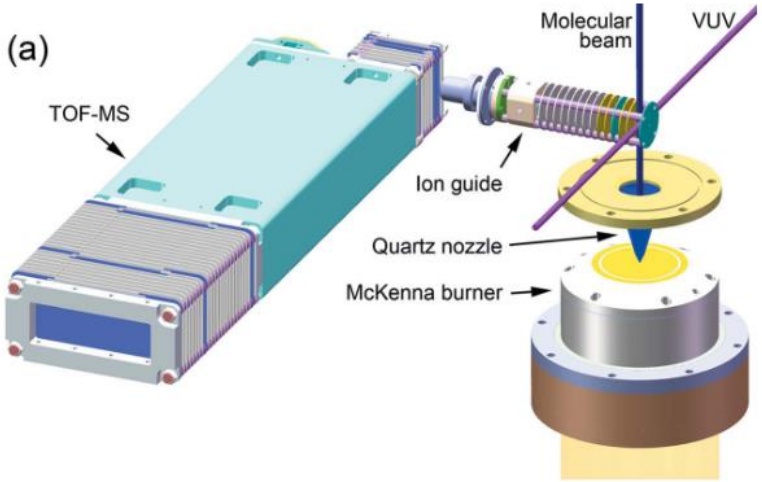

National Synchrotron Radiation Laboratory (NSRL), Hefei

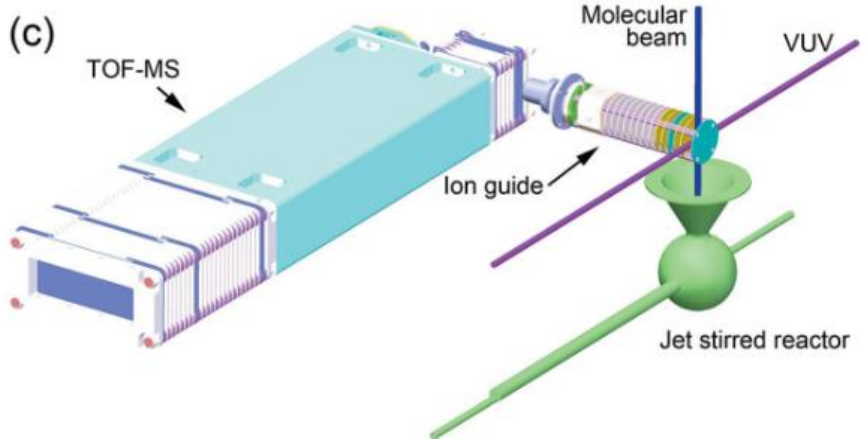

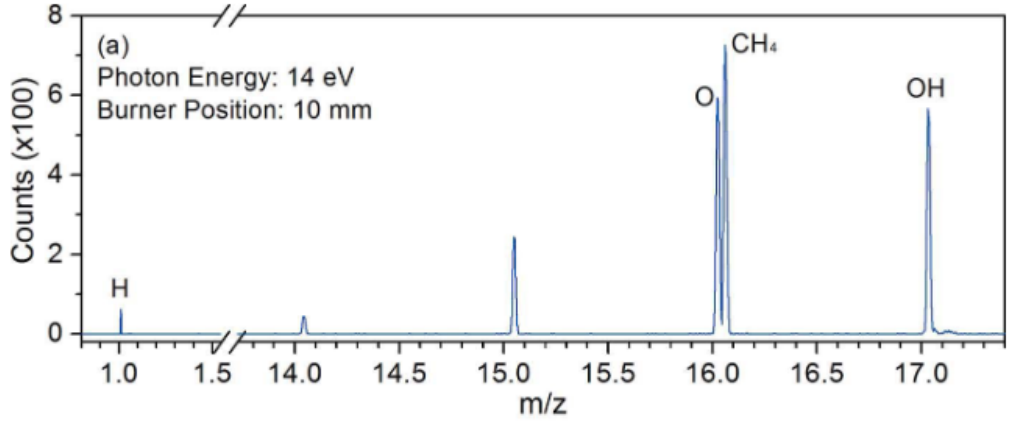

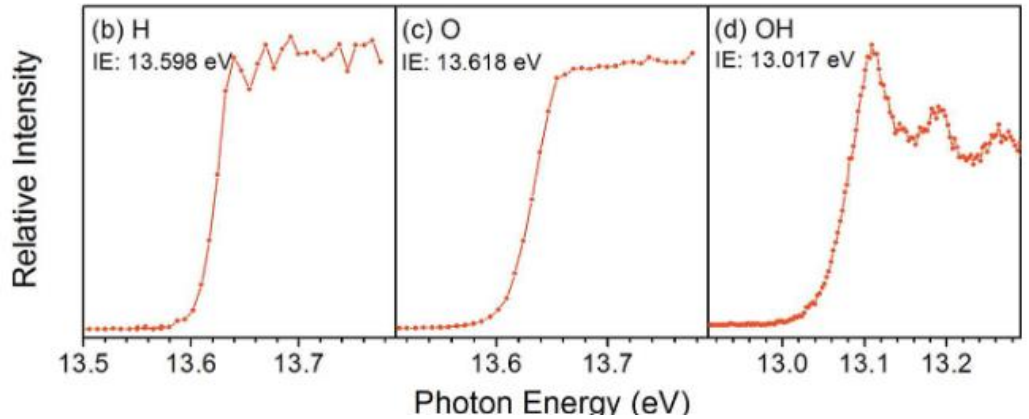

Z. Zhou, X. Du, J. Yang, Y. Wang, C. Li, S. Wei, L. Du, Y. Li, F. Qi and Q. Wang , J. Synchrotron Rad. (2016). 23, 1035

Multiphoton fluorescence

level 3 : at 10-13 eV from the fondamental state (≈ 100 nm)

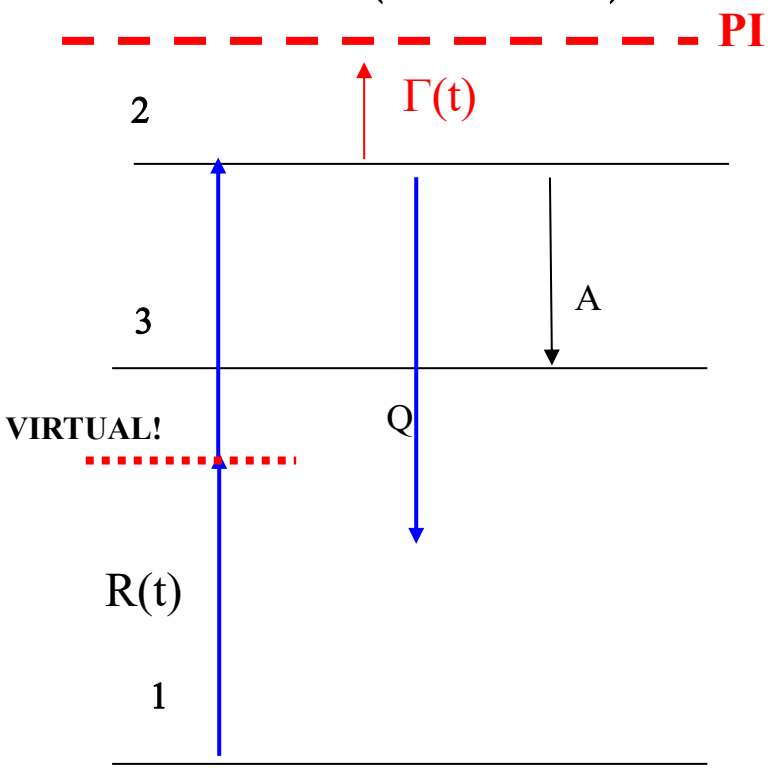

$$\frac{dN_2}{dt} = R(t)N_1(t) - \left(A_{23} + Q + \Gamma(t)\right)N_2(t)$$

with

- $R(t) = G^2\hat{\sigma}^2 g(\Delta\omega)\left(\frac{I_0}{h\nu}\right)^2$ (s^{-1}) : 2 photons absorption probability
- I_0 (W/m^2) Laser irradiance
- $\hat{\sigma}^2$ (m^4/W) : 2 photons absorption cross section
- A fluorescence, Q quenching
- $\Gamma(t)$ Ionisation rate (negligible)

Goehlich et al. J. Chem. Phys 108 (1998) 9362-9370)

Bamford et al., Phys. Rev. A (1986)

TPLIF, A bit of history

- Bischel, Perry and Crosley (1981) demonstrated the feasibility of measuring atoms (O, N) in a flow discharge tube (few mTorr)
- Aldén et al. (1982) reported O-atoms measurements in atmospheric flame, but not quantified
- Goldsmith (1984), reported H, O and OH measurement in lean H_2/O_2 flame
  - O and H atoms quantified from OH and assuming partial equilibrium
- Meier, Kohse-Höinghaus (1986), H and O atoms in flame,
  - Calibrated using discharge flow system at room T
  - Photolytic effects
- Goldsmith (1987) photochemical effect
- Aldén et al. (1989) stimulated emission (SE)

TPLIF expression for atom (i)

$$S_{\mathrm{i}} = C_{\mathrm{i}}\sigma_{\mathrm{i}}^{\langle 2\rangle}G^{\langle 2\rangle}g(\Delta\bar{\nu}_{\mathrm{i}})\frac{A_{23,\mathrm{i}}}{A_{\mathrm{i}}+Q_{\mathrm{i}}}f_{\mathrm{B}}(T)[\mathrm{i}]\left(\frac{I_{\nu_{\mathrm{i}}}}{h\nu_{\mathrm{i}}}\right)^2$$

- S_{i}: **time-integrated TPLIF signal**
- C_{i}: global efficiency of the LIF collection (conversion of signal into nb of photons)
  - Gain, collection volume, lenses and spectrometer transmission, PMT spectral efficiency
- $\sigma_{\mathrm{i}}^{\langle 2\rangle}G^{\langle 2\rangle}$ ($=\hat{\sigma}_i^{\langle 2\rangle}$): lineshape-independent two-photon absorption cross-section × photon statistical factor (known)
- $g(\Delta\bar{\nu}_{\mathrm{i}})$: normalized line profile ($\int g(\Delta\bar{\nu}_{\mathrm{i}})\,d\nu_{\mathrm{i}} = 1$)
- $\frac{A_{23,\mathrm{i}}}{A_{\mathrm{i}}+Q_{\mathrm{i}}}$: fluorescence quantum yield, ($A_{23,\mathrm{i}}$ and A_{i} are known, but ??Q_{i} ??)
- $f_{\mathrm{B}}(T)$: Boltzmann factor (to be calculated, knowing T)
- $[\mathrm{i}]$: species concentration
- $\left(\frac{I_{\nu_{\mathrm{i}}}}{h\nu_{\mathrm{i}}}\right)^2$: nb of photons per time unit at the excitation frequency ν_{i} (controlled and measured)

Goehlich et al. J. Chem. Phys 108 (1998) 9362-9370)
Stancu, Kaddouri, Lacoste, Laux, J. Phys. D 43 (2010)124002
Stancu, PSST 29 (2020) 054001

O-atom

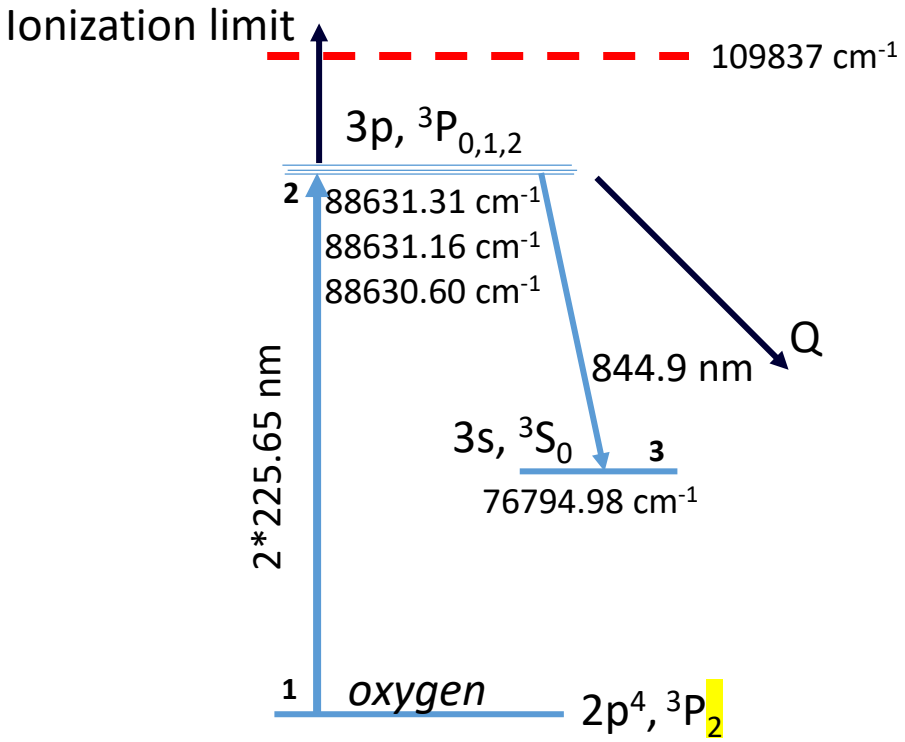

- A_{23} fluorescence rate, ($\sim 2.8 \times 10^7\ s^{-1}$)
- $\Gamma(t)$ photoionisation rate (negligible)

3 Levels J=0,1, 2
J: Total angular momentum quantum number

Goehlich et al. J. Chem. Phys 108 (1998) 9362-9370)

Bamford et al., Phys. Rev. A (1986)

TPLIF experimental setup

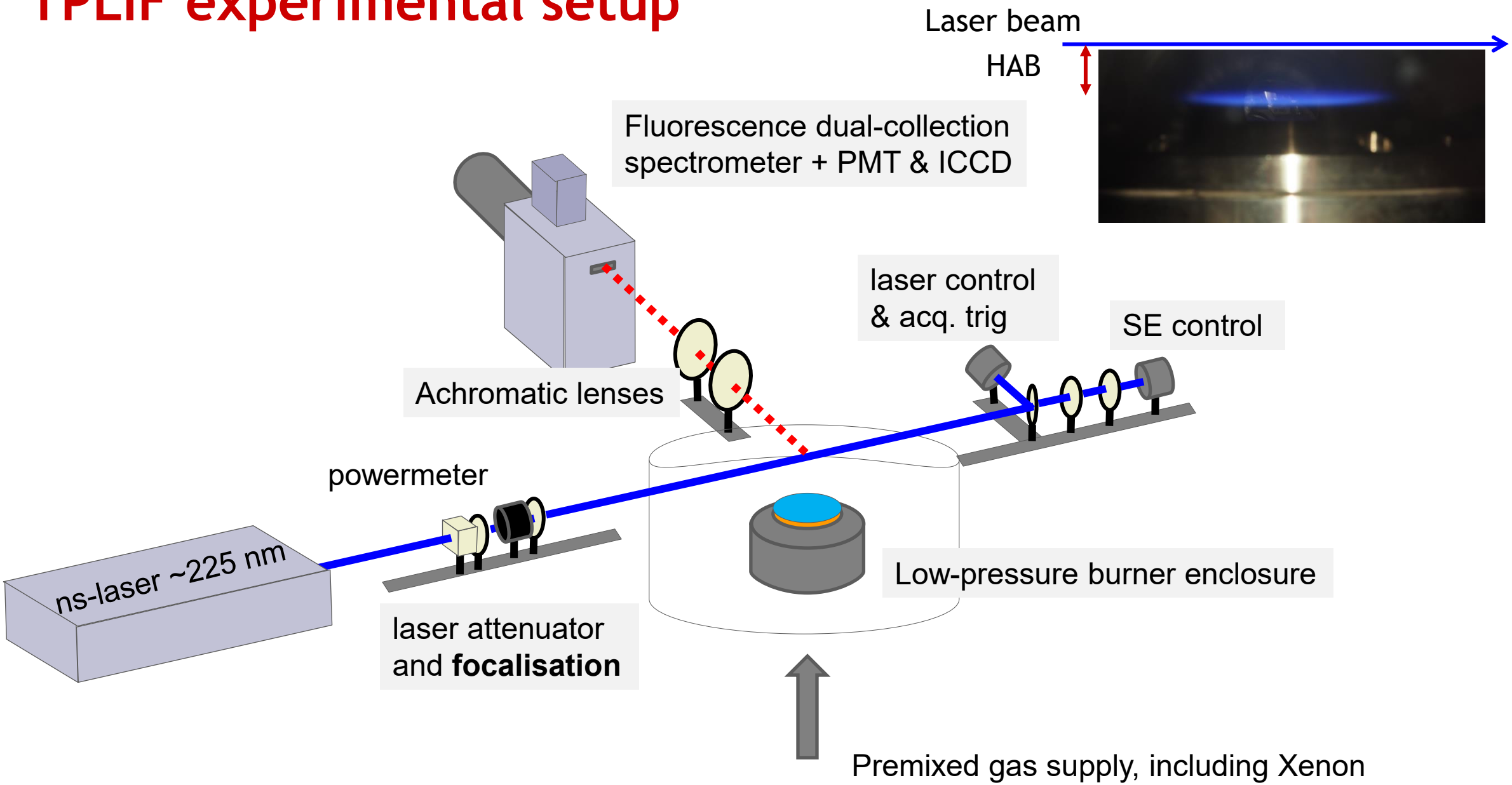

Quenching rate - O atom

$$S_i = C_i \sigma_i^{\langle 2 \rangle} G^{\langle 2 \rangle} g(\Delta \bar{\nu}_i) \frac{A_{2,3,i}}{A_i + Q_i} f_B(T)[i] \left(\frac{I_{\nu_i}}{h\nu_i} \right)^2$$

- $Q_i = \sum_q [q] \sigma_q^i \langle v_{q,i} \rangle$,
  - [q], collider concentration
  - σ_q^i, quenching cross section
  - $\langle v_{q,i} \rangle = \sqrt{8k_B T / \pi \mu_i}$, relative collision velocity, μ_i mass reduced
  - $k_q^i = \sigma_q^i \langle v_{q,i} \rangle$, quenching rate coefficient
- lack of data (few k_n^i measured at room *T*): Bittner et al. Chem. Phys. Lett. (1988)

Quencher, n	H_2O	N_2	O_2	CO_2	CO	CH_4
k_q (10^{-10} $cm^3 s^{-1}$)	49	4.3	6.3	6.6	4.9	5.5
σ_q ($Å^2$)	570	55	82	90	63	62

  - $k_{H2O} < 10 \times 10^{-10}$ $cm^3 s^{-1}$, Quickenden et al. (JCP71(1979), Gasnot et al. Appl. PhysB (1997)

Quenching rate T-dependency?

- T-dependency of the cross section?
  - σ_n^i ~T^0, Q ~ $T^{-1/2}$
  - σ_n^i ~T^{-1}, Q ~ $T^{-3/2}$

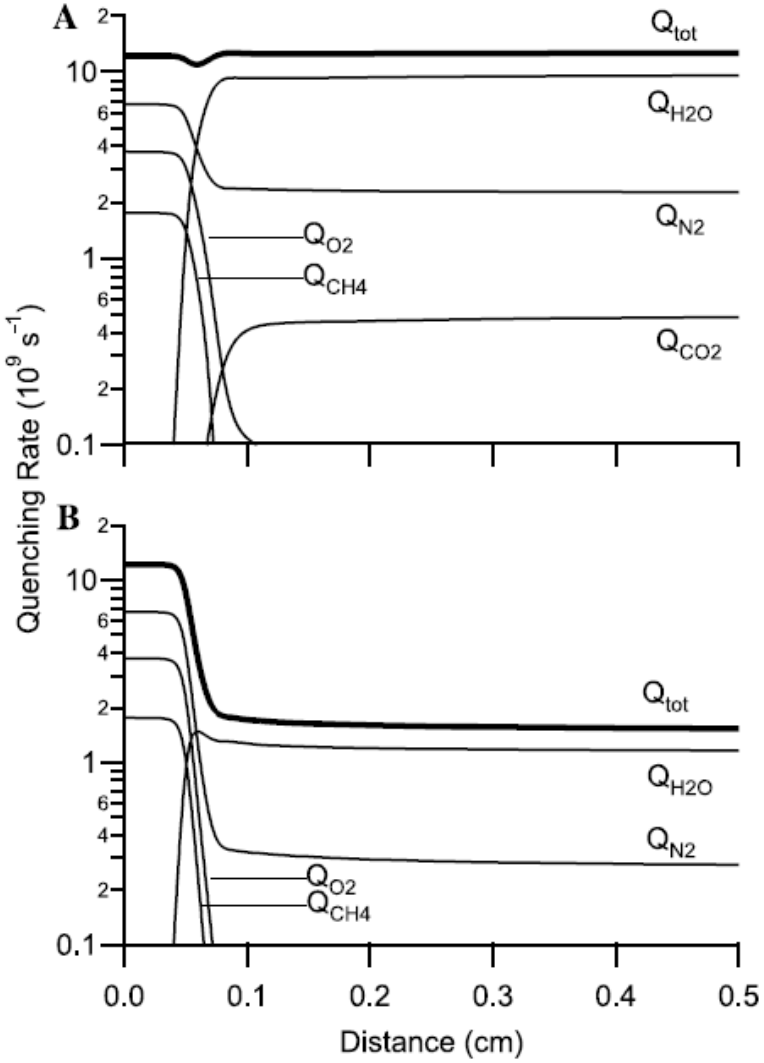

σ ~T^0

σ ~T^{-1}

Frank, Settersten, ProCI30(2005)

Quenching rate measurements: Case of O-atom

Determined from fluorescence decaytime ($\tau = 1/(A+Q)$)

Convolution/deconvolution

- $S = I^2 \otimes \exp(-(A+Q)t)$

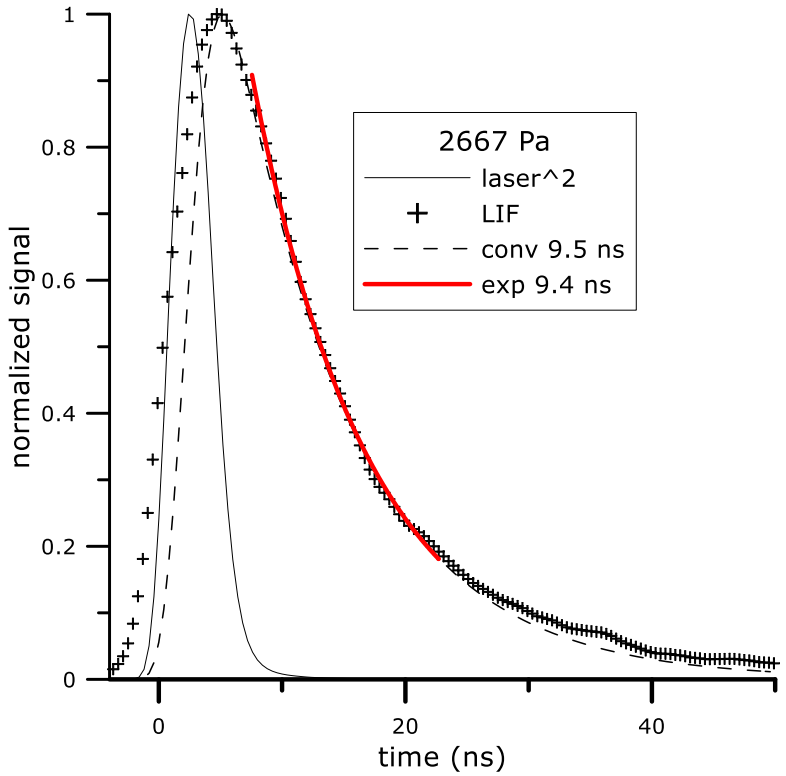

Stern-Volmer plot (O)

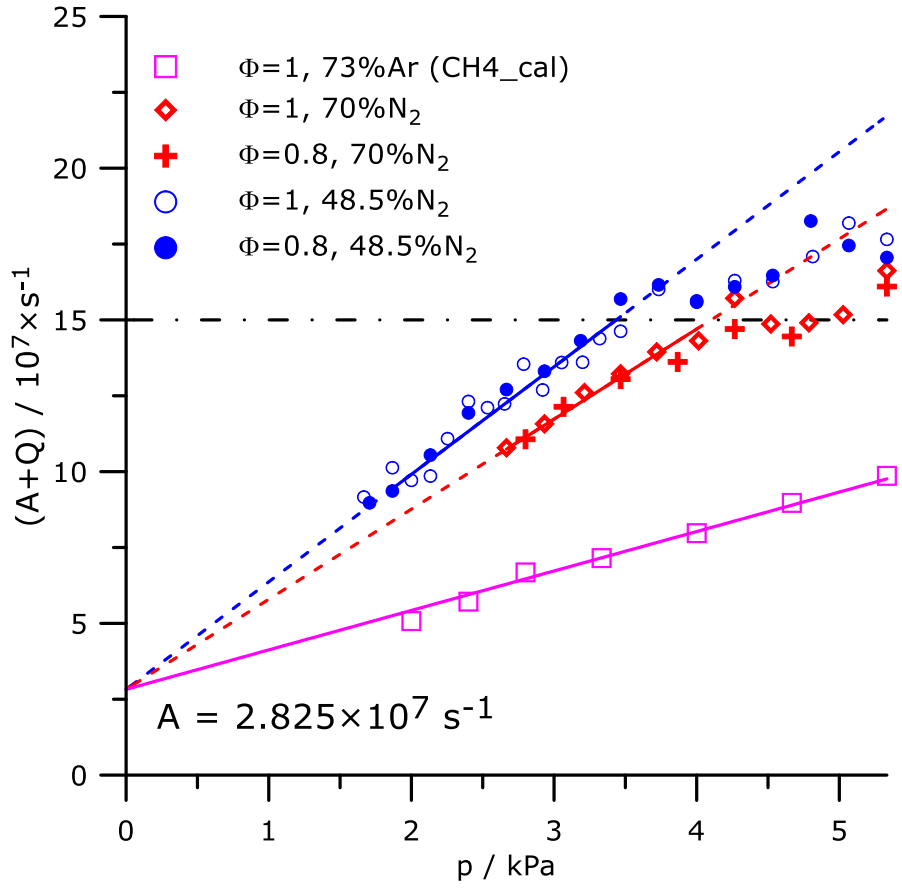

Lamoureux et al., ProCI 38 (2021)1753-1760

Importance of the risetime of the photomultiplier

Stern-Volmer plot (H)

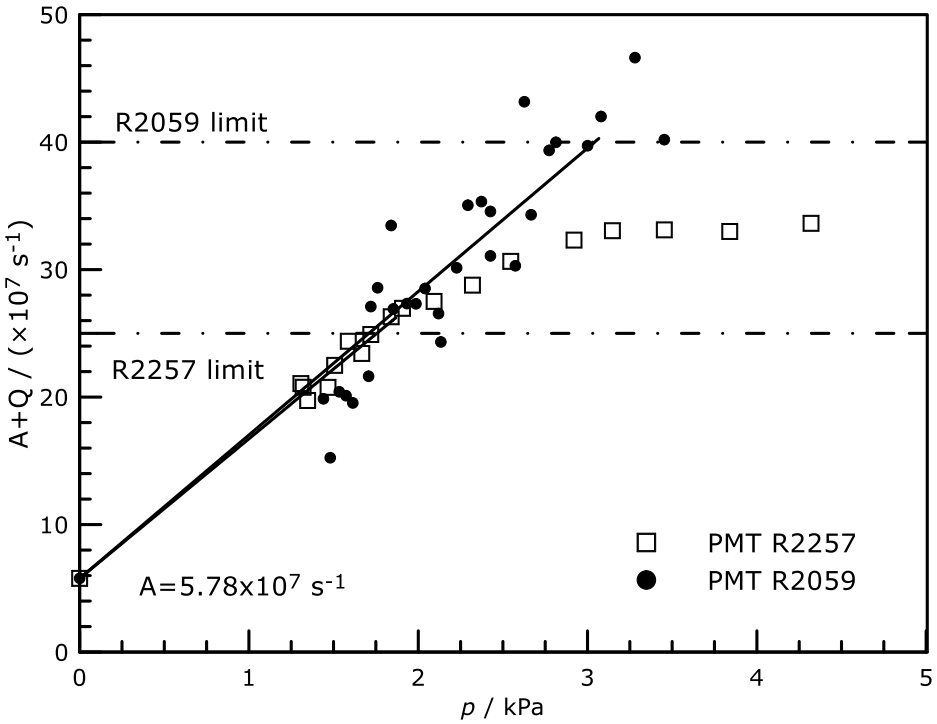

2257, 2.6 ns

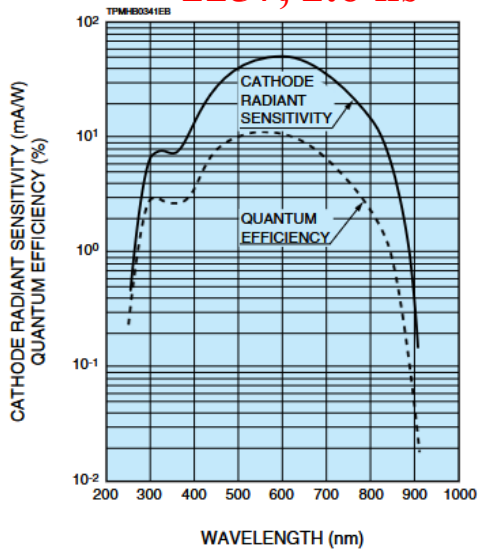

2059, 1.3 ns

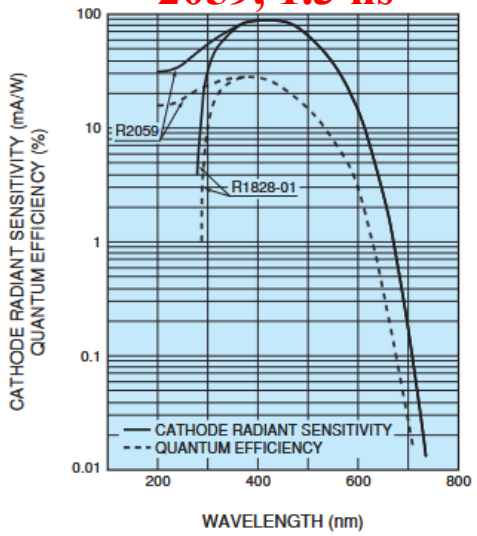

Stern-Volmer plot (O)

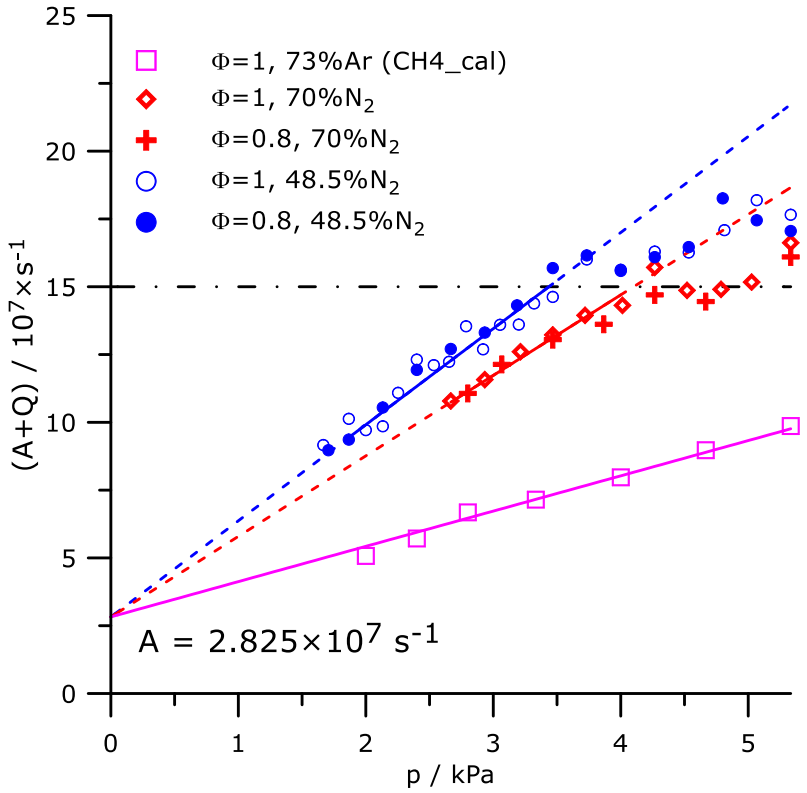

Lamoureux et al., ProCI 38 (2021)1753-1760

The limiting factors: photolytic effects, spectral interferences…

Stimulated emission (Case of O-atom)

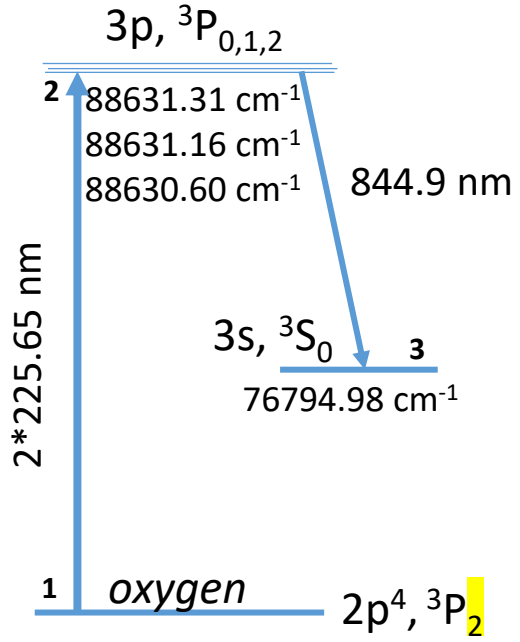

3 Levels J=0,1, 2
J: Total angular momentum quantum number

- Rapid population of the level 2, and short lifetime of the level 3

⇒ **Stimulated Emission at 845 nm**

- SE depends on multiple parameters (laser energy, species density, …)
- Controlled by measuring the 845 nm in the laser axis (forward /backward) burner

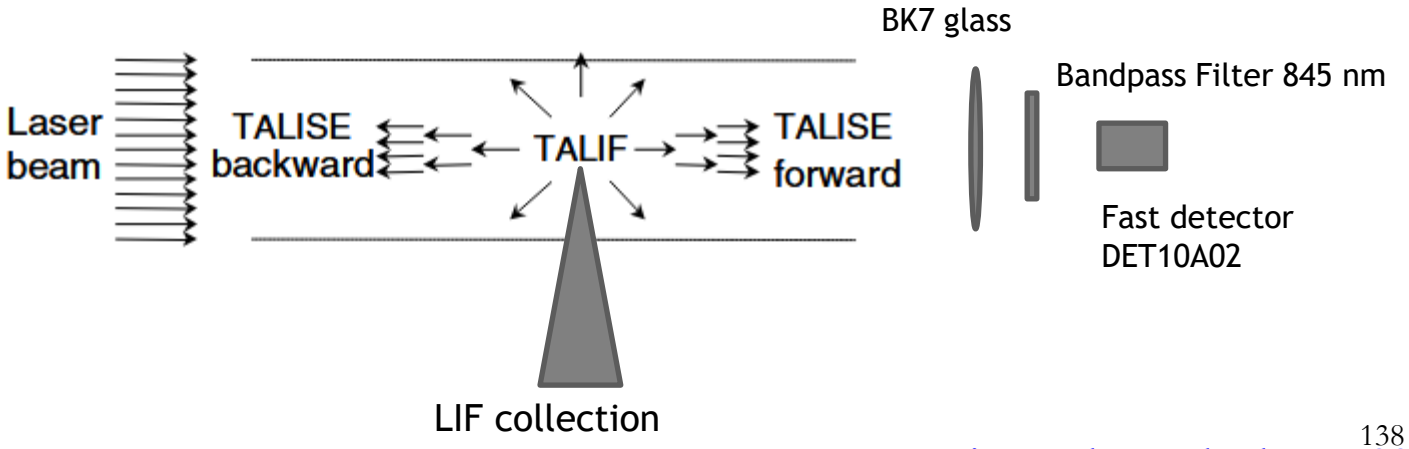

TALIF: Two-photon Absorption LIF
TALISE: Two-photon Absorption SE

Amorim at el., Appl. Phys. D33(2000)

Quadratic LIF regime, and Stimulated Emission

$$S_i = C_i \sigma_i^{\langle 2 \rangle} G^{\langle 2 \rangle} g(\Delta\bar{\nu}_i) \frac{A_{2,3,i}}{A_i + Q_i} f_B(T)[i] \left(\frac{I_{\nu_i}}{h\nu_i} \right)^2$$

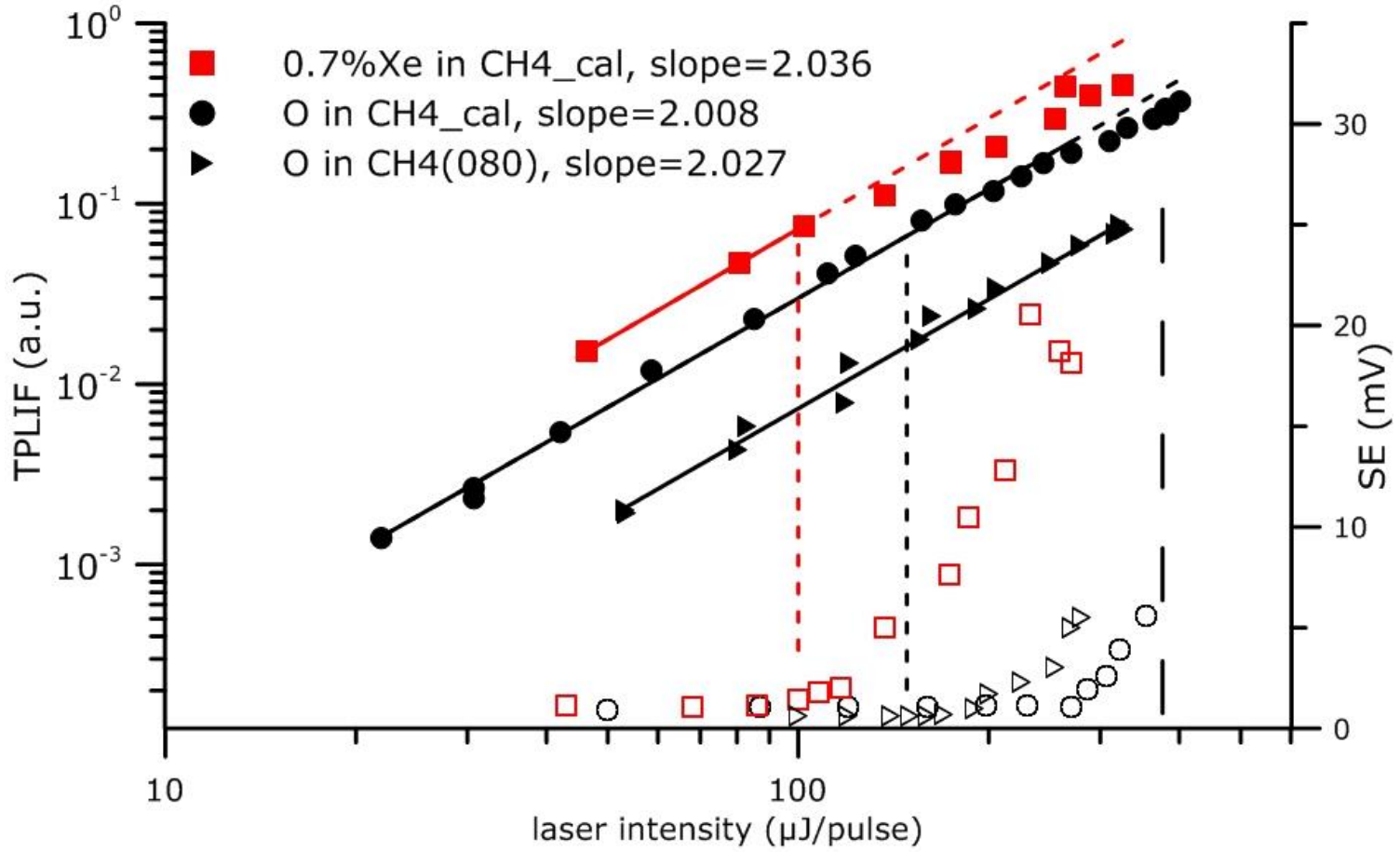

Filled symbols, TPLIF
Open symbols, SE

SE, non linear, depends on density, laser energy, length of medium…

Lamoureux et al., ProCI 38 (2021)1753-1760

See also
Wysong, Jeffries, Crosley, Opt Lett 14 (1989)
Goldsmith, J. Opt. Soc. Am 6 (1989)
Alden, Westblom, Goldsmith, Opt Lett 14 (1989)

Laser impulsion (ps/ns), photolytic effect of O_2 and CO_2

- in lean H_2/O_2 premixed flame
- in lean $CH_4/O_2/N_2$ premixed flame

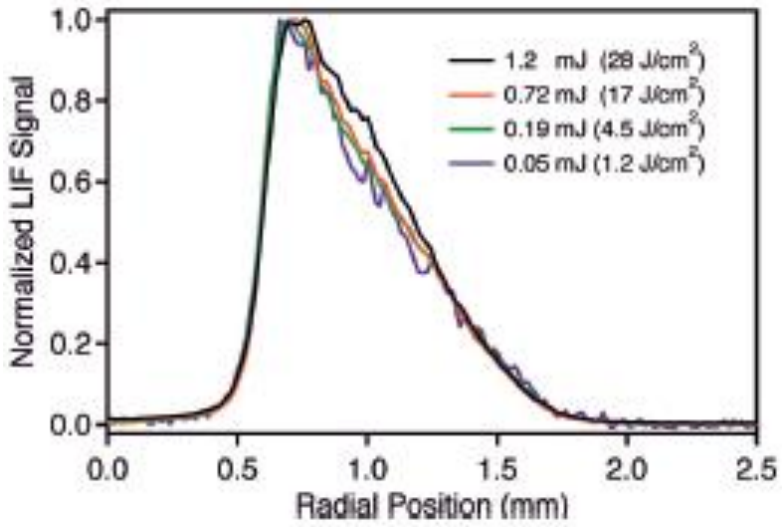

ns-laser

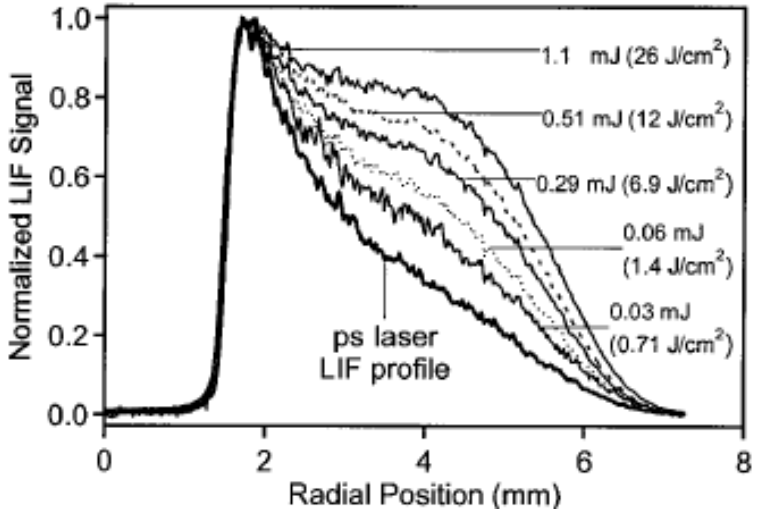

$CO_2 + h\nu_{226\ nm} \rightarrow CO_2^*$

$CO_2^* \rightarrow CO + O$

Combination of SE and photoionisation

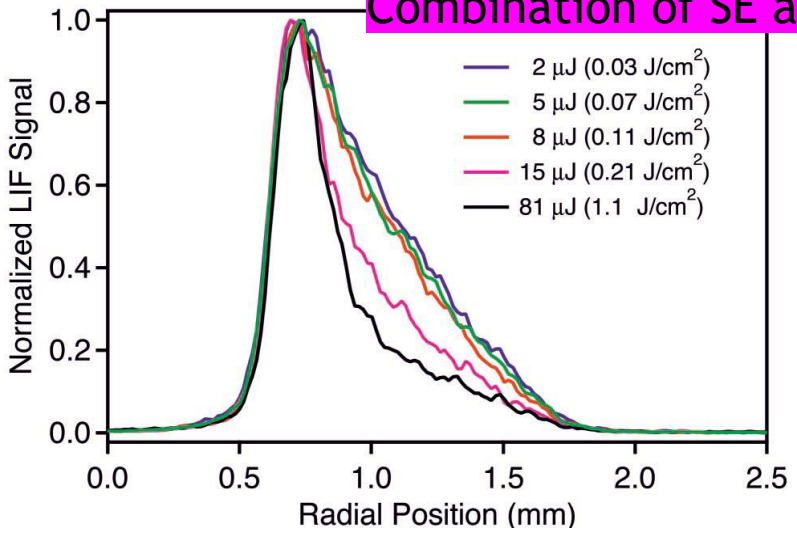

ps-laser

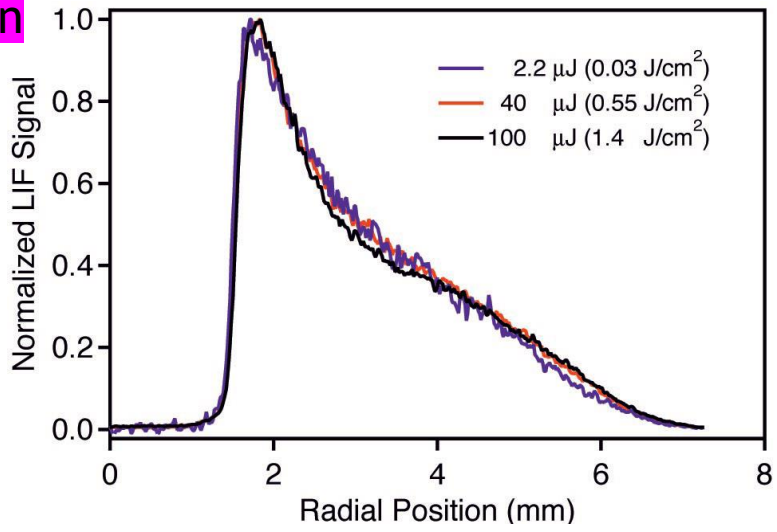

Frank, Chen, Patterson, Settersten. Appl. Opt.43 (2004)

Interferences with O_2 Schumann-Runge and NO

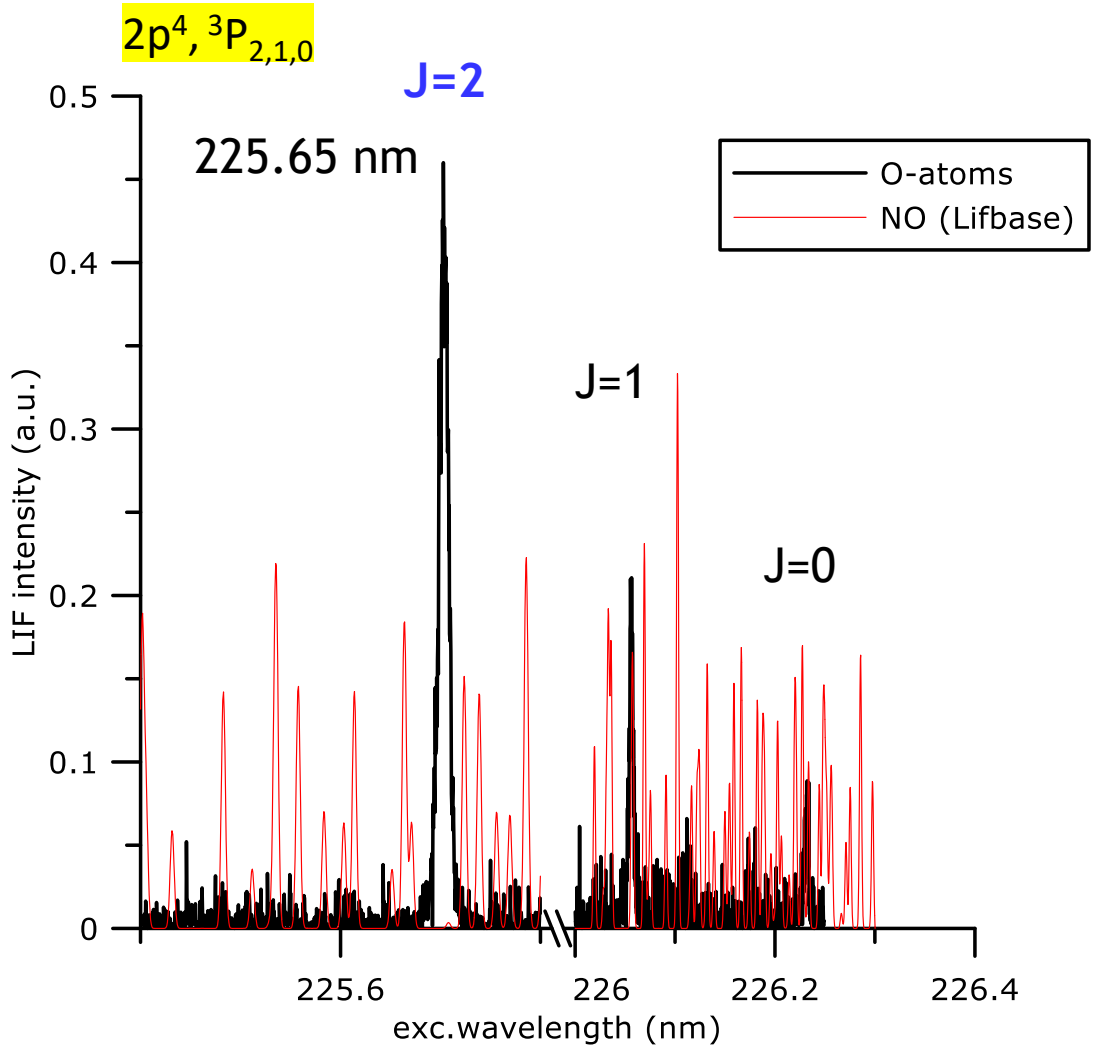

PC2A, in low pressure $CH_4/O_2/N_2$ flame

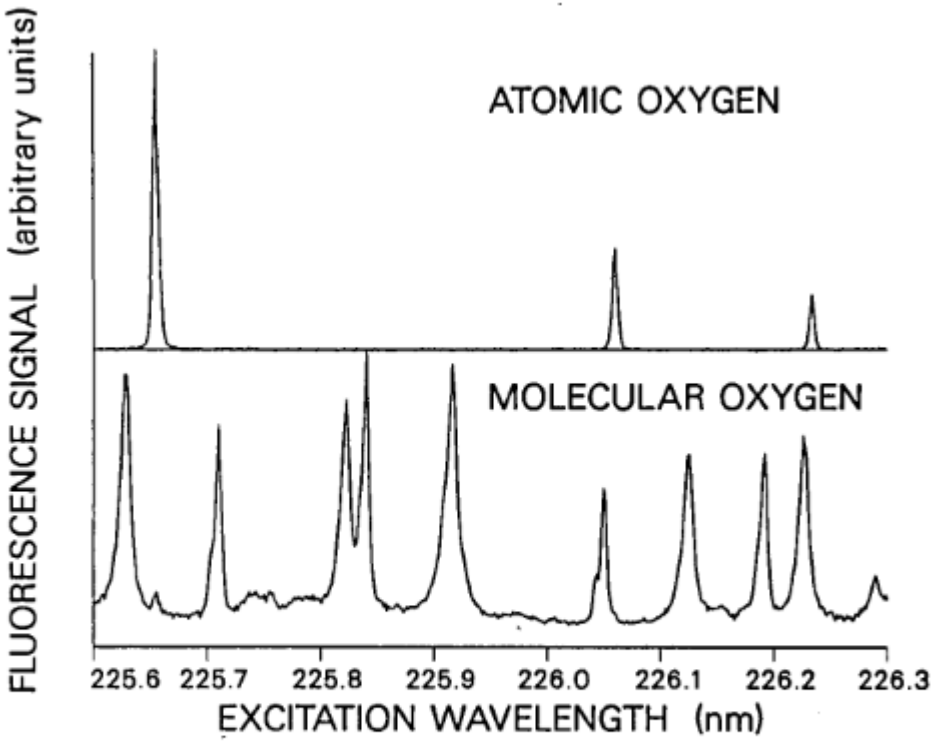

Fig. 5. Simultaneously recorded fluorescence excitation spectra of atomic and molecular oxygen. The three peaks in the atomic spectrum are from fine-structure splitting of the ground 2^3P electronic state. The peaks in the molecular spectrum are from the (0, 3) and (2, 4) rovibronic bands.

Goldsmith, Anderson, Opt. Lett.11(1986)

O_2 predissociation

- in H_2/O_2 flame at Patm

Increase of the laser energy from 0.2 to 60 mJ

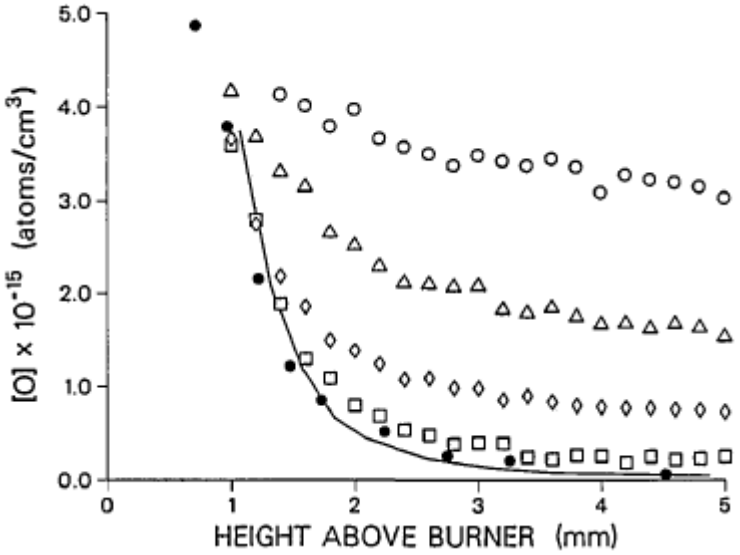

- $O_2 + h\nu_{226\ nm} \rightarrow 2\ O$
- O induced by the laser

Goldsmith, Appl. Opt. 26(1987)

Dispersed fluorescence spectrum (case of O-atom)

- H_2/O_2 flame at Patm
- J=2 of O-atm excitation
- O_2 Schumann-Runge

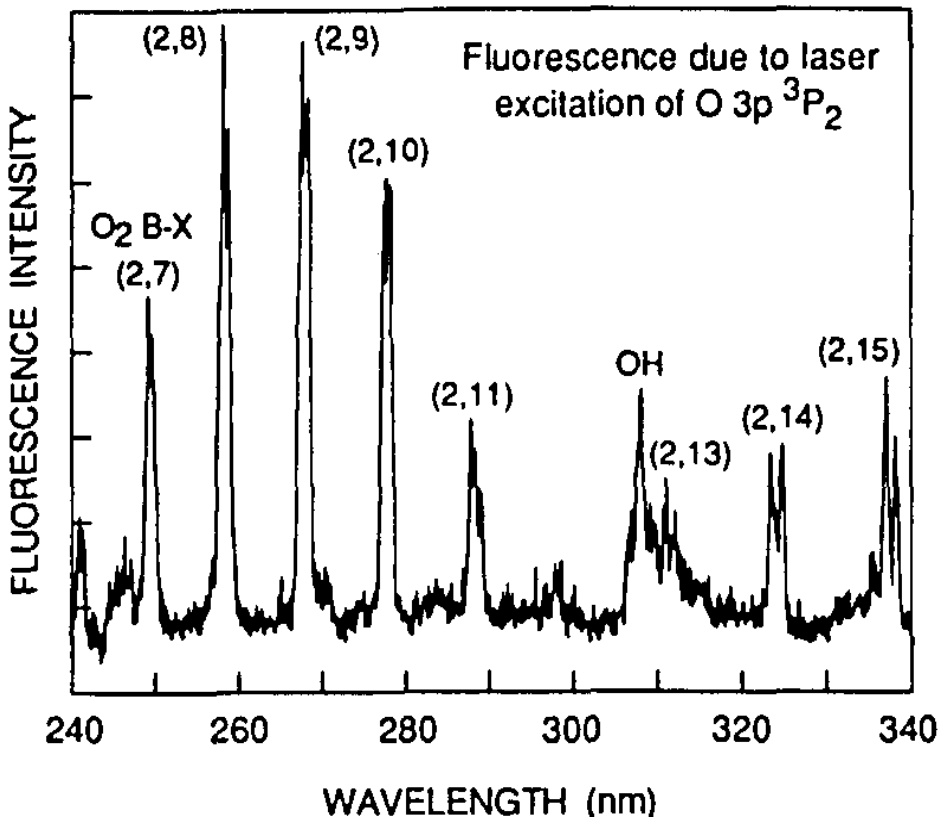

Wysong Jeffries, Crosley, Opt. Lett.14 (1989)

- $CH_4/O_2/N_2$ flame (5 kPa), interaction between O*-N_2
- J=2 of O-atom excitation
- Fluorescence of N_2 absent in Ar diluted flame

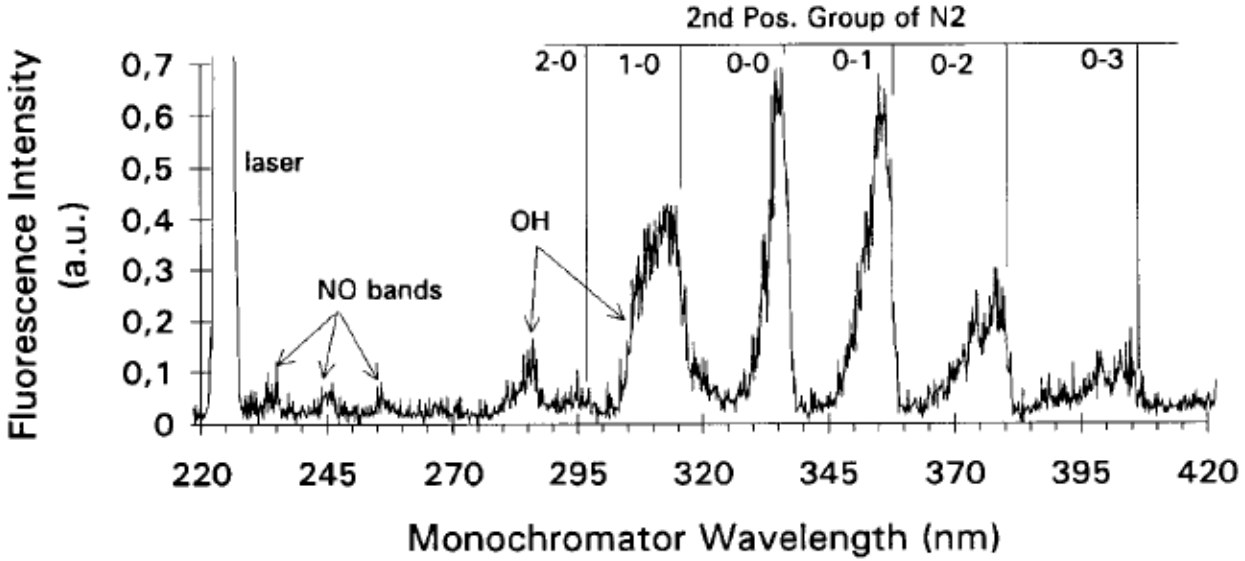

Gasnot, Desgroux, Appl. Phys. B 65 (1997)

Photolytic effects : an opportunity to study fascinating matter-laser interaction

Multiphoton excitation of H-atom at 205 nm, collection at 656 nm: photolytic effects!

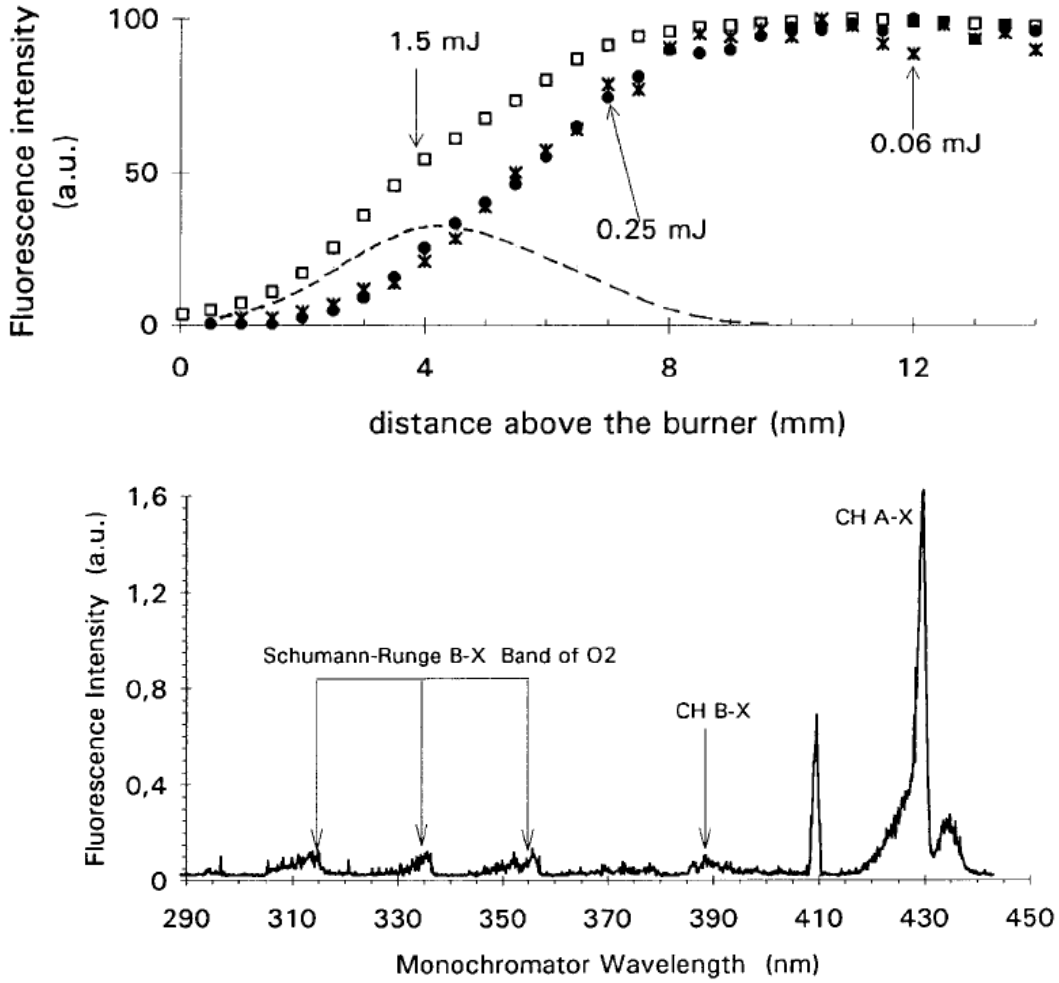

H-atom profiles at different laser energy

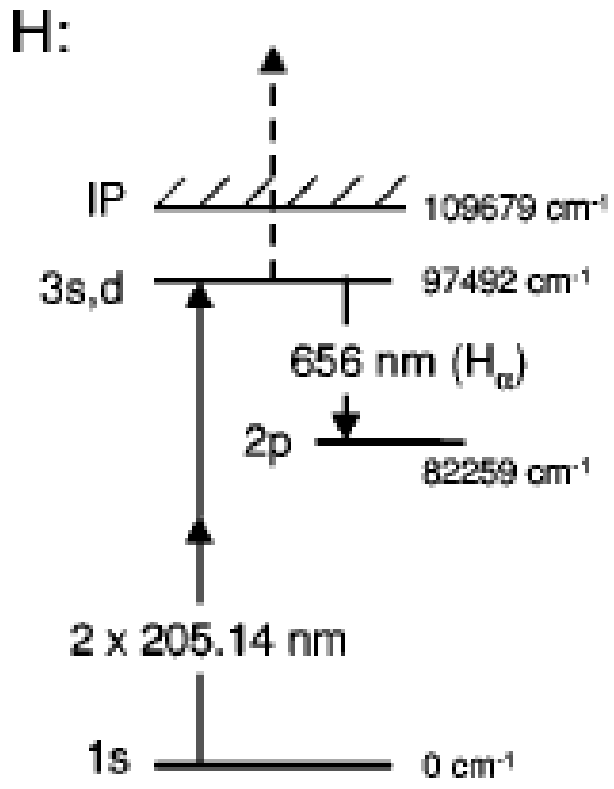

Gasnot et al., Appl. Phys. B 65 (1997) 639-646
Desgroux et al., ProCI 26 (1996) 967-974

Photolytic effects associated with multiphoton LIF: case of H-atom

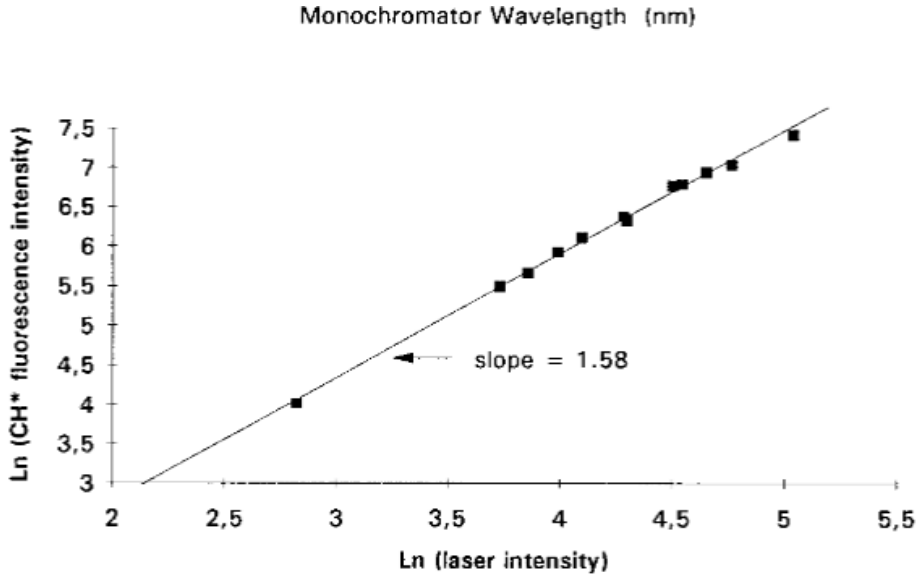

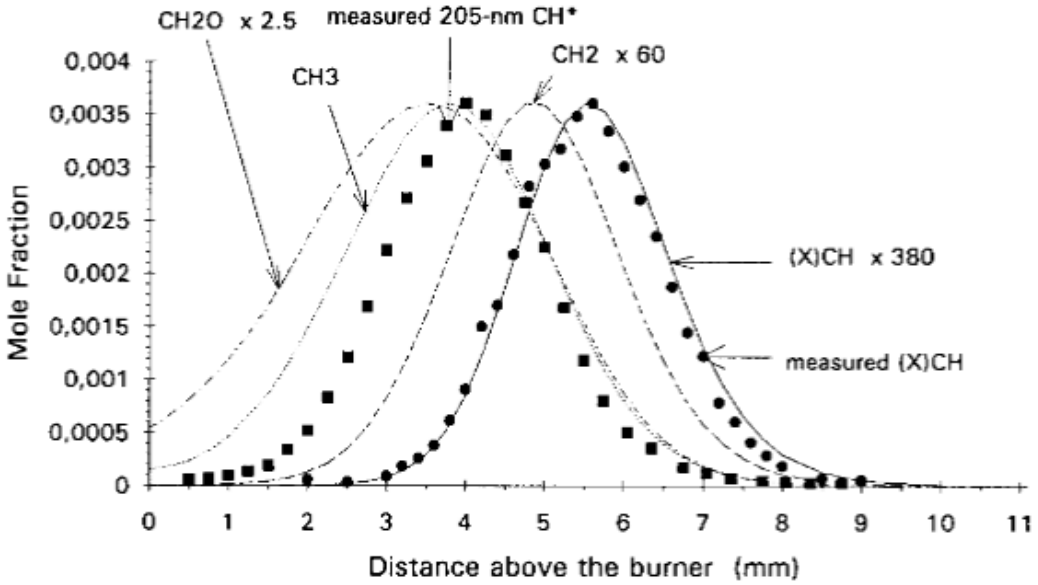

Confirmation by MBMS of CH3

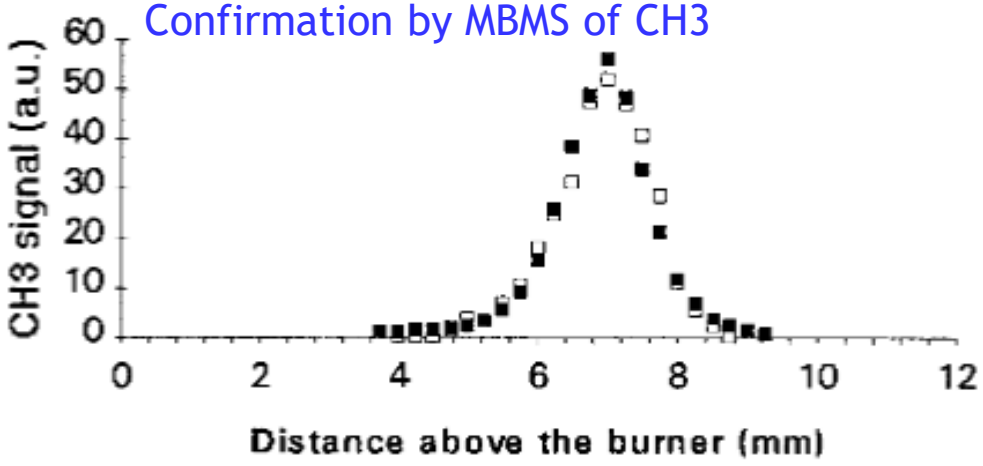

$\Phi = 1.2$

Gasnot et al., Appl. Phys. B 65 (1997) 639-646
Desgroux et al., ProCI 26 (1996) 967-974

Photochemical effects

$O_2+h\nu_{(205nm)} \rightarrow O$, et $O+H_2=OH+H$
(X) $CH_3 + h\nu_{(205nm)} \rightarrow$ (B) CH_3
(B) $CH_3 \rightarrow (1^3B,1^1A)CH_2 + H$, $CH+H_2$
$(1^3B)\ CH_2 + h\nu_{(205nm)} \rightarrow (2^3B)CH_2 \rightarrow$ (A) $CH+H$

Revised mechanism involving rapid collision-induced intersystem crossing (CIISC)

$$CH_2(\tilde{a}\,^1A_1) + M \rightarrow CH_2(\tilde{X}\,^3B_1),$$

$$CH_2(\tilde{X}\,^3B_1) + h\nu \rightarrow CH(X\,^2\Pi) + H(1s\,^2S)$$

Kulatilaka et al. Appl. PhysB 97 (2009) 227

Message: the control of the dispersed LIF is indispensable to check the absence of photolytic effects

Quantification of TPLIF

- Titration
  Calculation
  Rayleigh Scattering
  Absorption
  Noble gas

Titration in discharge flow tube (NO, NO_2)

- Meier et al. ProCI22(1988): discharge flow reactor (N-atom produced by a microwave discharge in N_2/He)

O-atoms produced by N+NO = O + N_2

100 % conversion of NO into O

From calculation (not really a calibration)

- Comparison of the TPLIF signal with a reference flame
  - Bunsen flame, premixed flame calculation
  - Partial equilibrium calculated in the burned gases

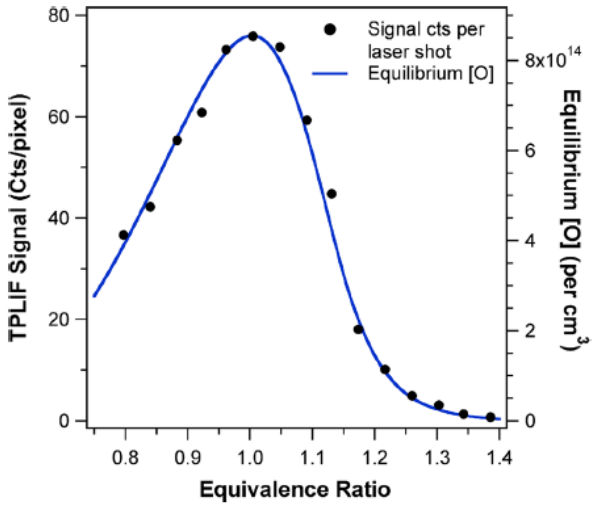

Fig. 5 Atomic oxygen fs-TPLIF signal of O as a function of flame equivalence ratio in a premixed CH_4/air flame stabilized over a Hencken calibration burner. *Solid line* represents the calculated equilibrium O-atom mole fraction

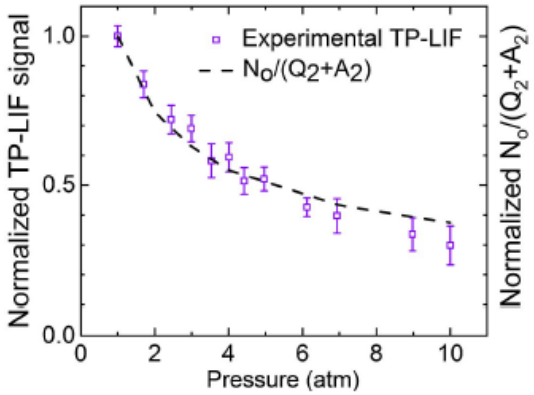

Fig. 8. Fs TP-LIF signal of atomic oxygen and normalized $N_o/Q_2 + A_2$ at different pressures in a $\phi = 0.85$ H_2/air Hencken burner flame. Both curves are normalized to the corresponding atmospheric pressure value. Laser energy of 5 μJ/pulse. Error bar represents $\pm 2\sigma$.

1 < p(atm) < 5

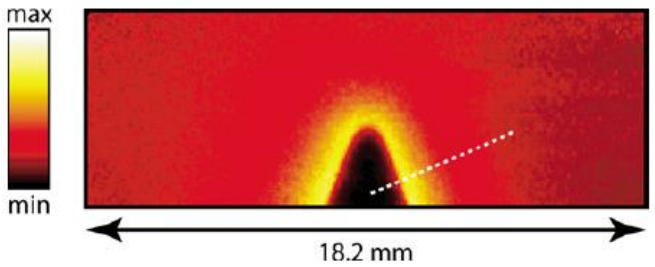

Kulatilaka et al. Apl. Phys B122 (2016)

Rahman et al., Appl. Opt. 58 (2019)

Frank, Settersten, ProCI30(2005)

VUV absorption (plasma), absorption 1 photon

- VUV absorption (plasma), absorption 1 photon
  - Gousset, Panafieu, Touzeau, Vialle, Plasma Chem. Plasma Process (1987)
    - Microwave discharge lamp, 130.22 nm
  - N(^{4}S); Dumitrache, Laux, Stancu, PSST31(2022)
    - Ligne DESIR synchrotron SOLEIL, 120 nm

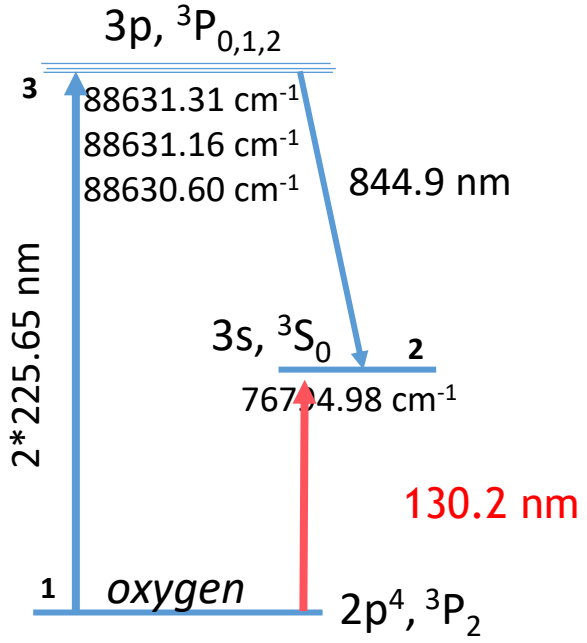

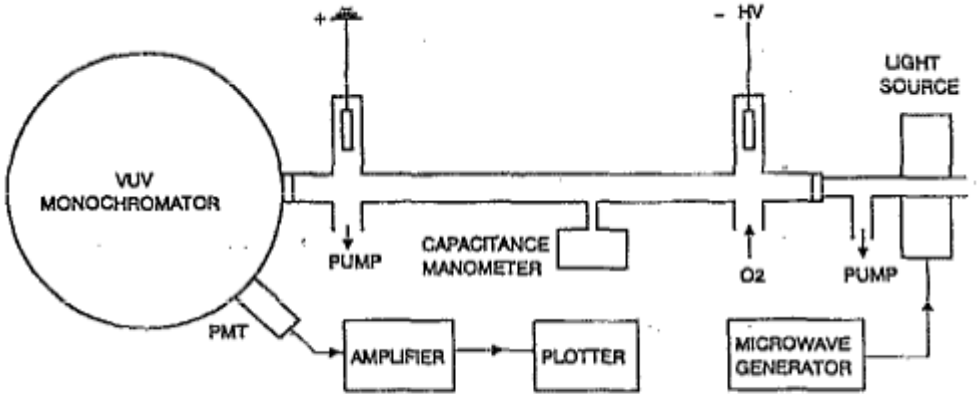

FIG. 3. VUV absorption experiment for calibration.

Calibration using noble gas (similar excitation schemes between atoms)

H and Krypton atoms

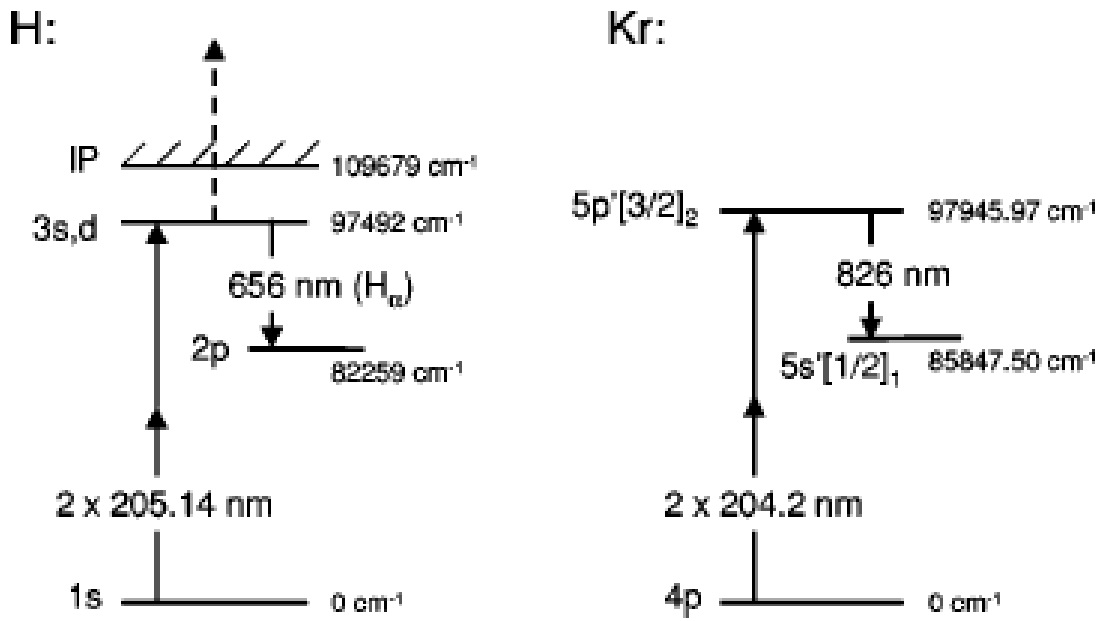

FIG. 2. Energy level schemes for the two-photon excitation laser-induced fluorescence measurements of ground-state hydrogen atoms (left) and ground-state krypton atoms (right).

O and Xenon atoms

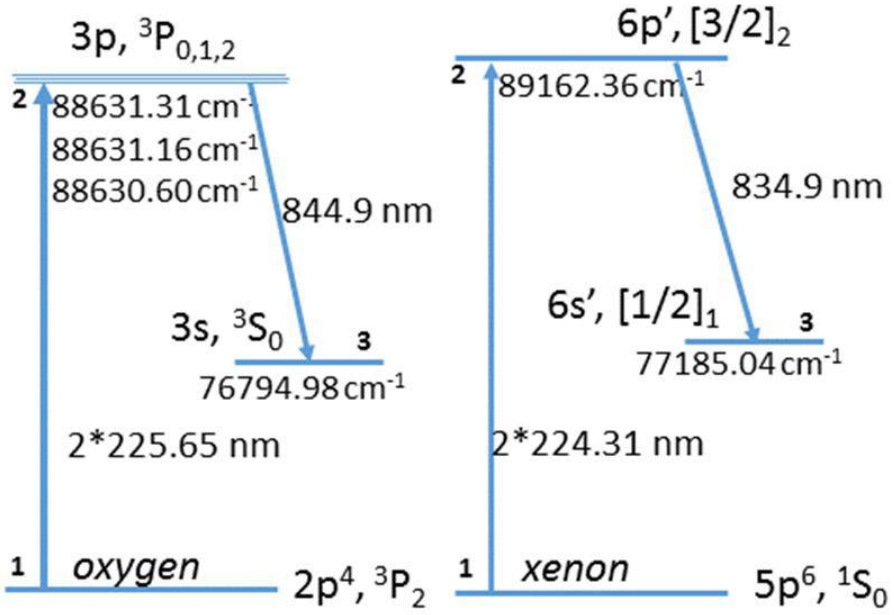

The idea (plasma): ratio of the LIF signals (H and Kr) corrected for variation of absorption lineshape (important) , spectroscopic parameters, Boltzmann, quenching allows to determine the absolute H-atom concentration

Boogaarts et al., Rev. Sci Instr. 73 2002

NIST Atomic Spectra Database

Line profile @ 2.8 kPa, flame diluted in Ar

$$S_i = C_i \sigma_i^{\langle 2 \rangle} G^{\langle 2 \rangle} g(\Delta\bar{\nu}_i) \frac{A_{32,i}}{A_i + Q_i} f_B(T)[i] \left(\frac{I_{\nu_i}}{h\nu_i}\right)^2$$

$$\int g(\Delta\bar{\nu}_i) d\bar{\nu} = 1$$

$$\int S_i d\nu = C_i \sigma_i^{\langle 2 \rangle} G^{\langle 2 \rangle} \frac{A_{32,i}}{A_i + Q_i} f_B(T)[i] \left(\frac{I_{\nu_i}}{h\nu_i}\right)^2$$

Goehlich et al. J. Chem. Phys 108 (1998) 9362

Spectrally and temporally -integrated measurements

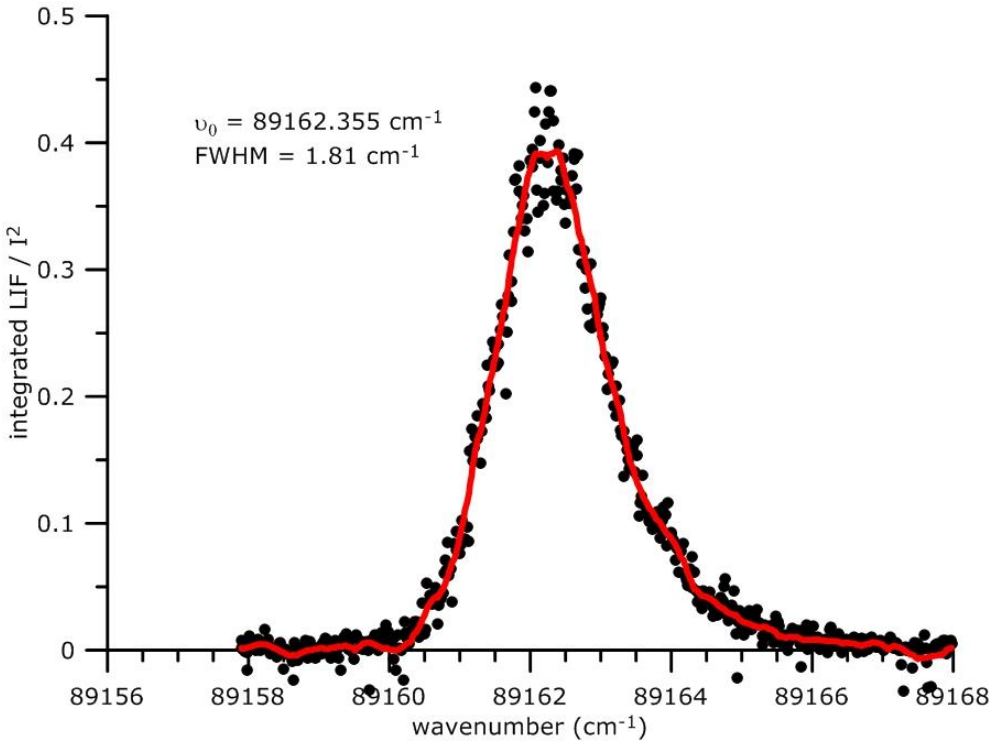

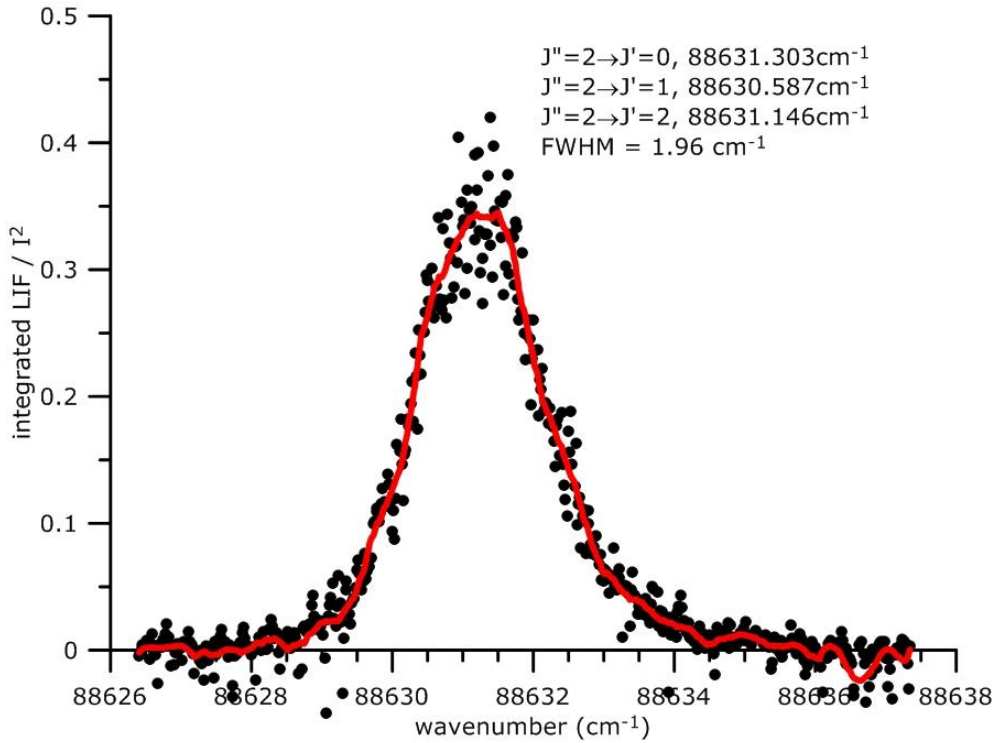

Xenon: $\Delta\bar{\nu}_D = 0.24 cm^{-1}$

Oxygen: $\Delta\bar{\nu}_D = 0.66 cm^{-1}$

Calibration using noble gas: O/Xe

Goehlich et al. J. Chem. Phys 108 (1998) 9362-9370

$$\int S_i dv = C_{\mathrm{i}} \sigma_{\mathrm{i}}^{\langle 2\rangle} G^{\langle 2\rangle} \frac{A_{32,\mathrm{i}}}{A_{\mathrm{i}}+Q_{\mathrm{i}}} f_{\mathrm{B}}(T)[\mathrm{i}] \left(\frac{I_{\nu_{\mathrm{i}}}}{h\nu_{\mathrm{i}}}\right)^2$$

$$[\mathrm{O}] = [\mathrm{Xe}] \frac{C_{\mathrm{Xe}}}{C_{\mathrm{O}}} \frac{\sigma_{\mathrm{Xe}}^{<2>}}{\sigma_{\mathrm{O}}^{<2>}} \frac{A_{32,\mathrm{Xe}}}{A_{32,\mathrm{O}}} \frac{A_{\mathrm{O}}+Q_{\mathrm{O}}}{A_{\mathrm{Xe}}+Q_{\mathrm{Xe}}} \frac{1}{f_{\mathrm{B}}(\mathrm{O}_{J''=2}, T)} \frac{\int S_{\mathrm{O}} dv}{\int S_{\mathrm{Xe}} dv} \frac{I_{\nu_{\mathrm{Xe}}}^2}{I_{\nu_{\mathrm{O}}}^2} \left(\frac{\nu_{\mathrm{O}}}{\nu_{\mathrm{Xe}}}\right)^2$$

	O 3p	Xe 6p'^{2}[3/2]
$\lambda_{(2\ \mathrm{photons})}$ (nm)	225.65	224.31
$\lambda_{\mathrm{collect}}$ (nm)	844.9	834.9
$\sigma_{Xe}^{\langle 2\rangle}/\sigma_{O}^{\langle 2\rangle}$	1.9 ±20%	
A_3 (10^7 s^{-1})	2.9	2.5
A_{32} (10^7 s^{-1})	2.9	1.8

LPP, Saclay

1.9 ±20%, Niemi et al. PSST 14 (2005) 375-386
1.8 ±0.2, Shu et al. PSST33 (2024)02519

Xe and O quenching rate in flame

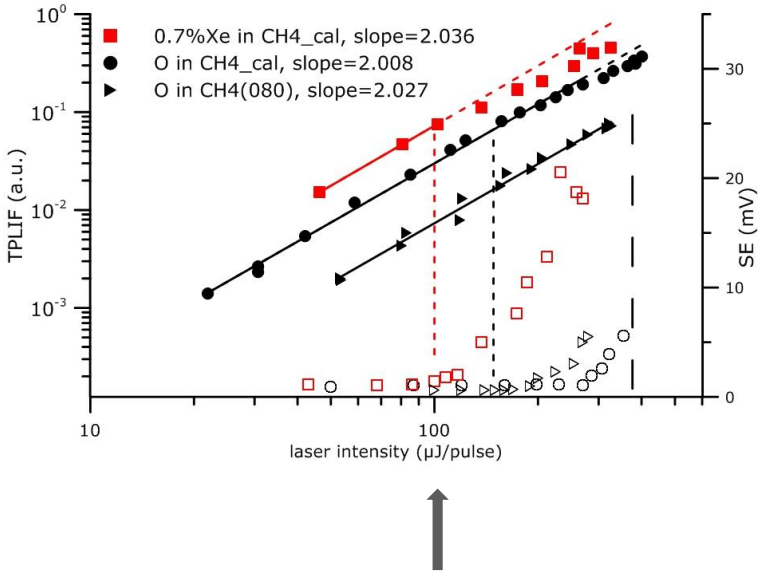

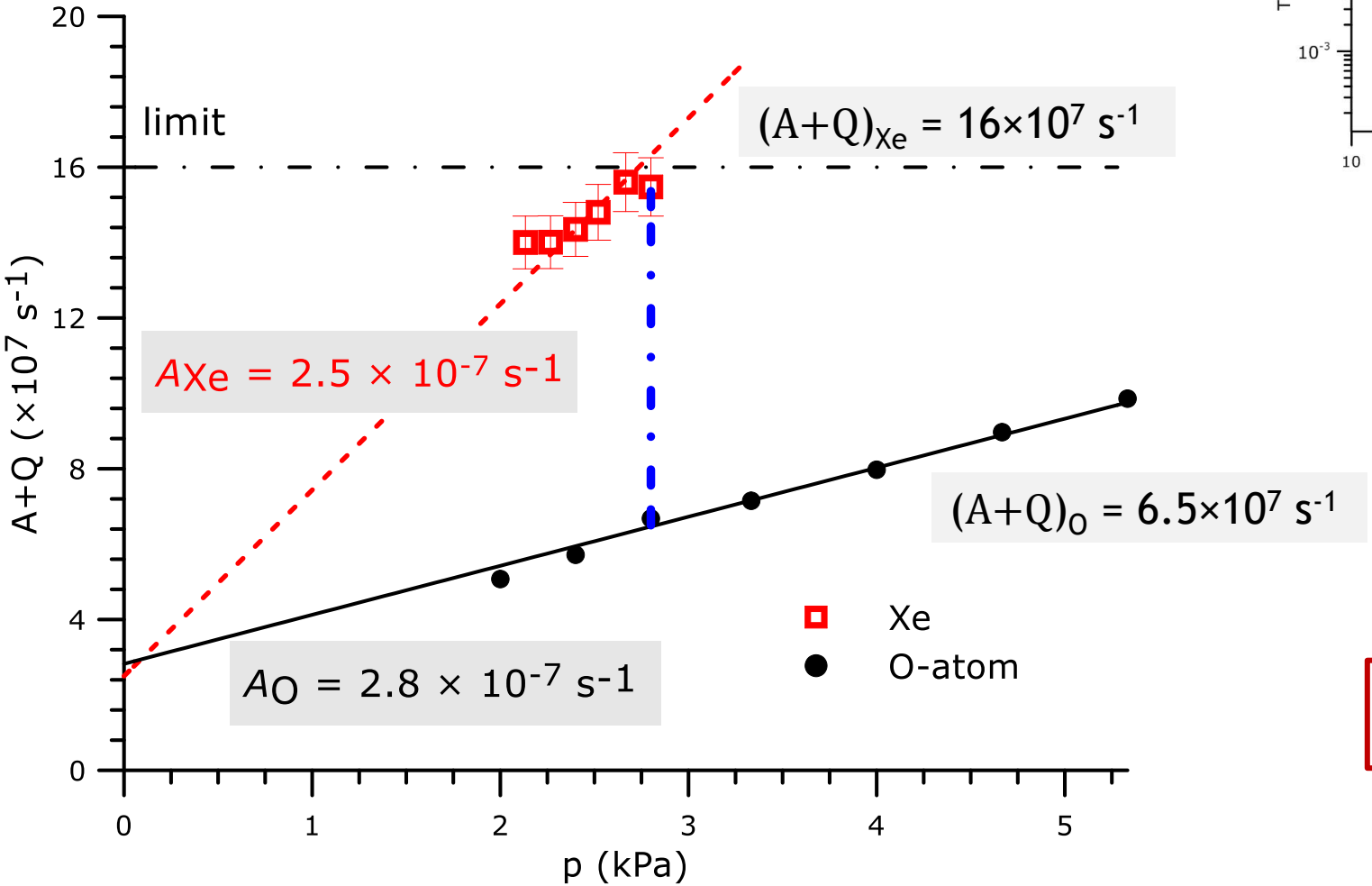

$$\frac{A_O+Q_O}{A_{Xe}+Q_{Xe}} = 0.406$$

O calibration in an unique flame (CH4_cal)

- $[\mathrm{O}] = [\mathrm{Xe}] \frac{C_{\mathrm{Xe}}}{C_{\mathrm{O}}} \frac{\sigma_{\mathrm{Xe}}^{<2>}}{\sigma_{\mathrm{O}}^{<2>}} \frac{A_{32,\mathrm{Xe}}}{A_{32,\mathrm{O}}} \frac{A_{\mathrm{O}}+Q_{\mathrm{O}}}{A_{\mathrm{Xe}}+Q_{\mathrm{Xe}}} \frac{1}{f_{\mathrm{B}}(\mathrm{O}_{J"=2},T)} \frac{\int S_{\mathrm{O}} d\nu}{\int S_{\mathrm{Xe}} d\nu} \frac{I_{\nu_{\mathrm{Xe}}}^2}{I_{\nu_{\mathrm{O}}}^2} \left(\frac{\nu_{\mathrm{O}}}{\nu_{\mathrm{Xe}}}\right)^2$

  - χ_{Xe} = 0.8% substituted to Ar
  - $\frac{C_{\mathrm{Xe}}}{C_{\mathrm{O}}}$ = 1.6 from 834 to 845 nm (calibrated light source)
  - Boltzmann factors (1 for Xe)
    - At HAB = 25 mm, T = 1983 K, $f_{\mathrm{B}}(\mathrm{O}_{J"=2},T) \approx 0.587$
  - $I_{\nu_{\mathrm{Xe}}} = I_{\nu_{\mathrm{O}}}$ = 100 μJ/pulse
  - [O]= 2.2×10^{-9} mol cm^{-3}, χ_{O} = 0.013 ± 40%

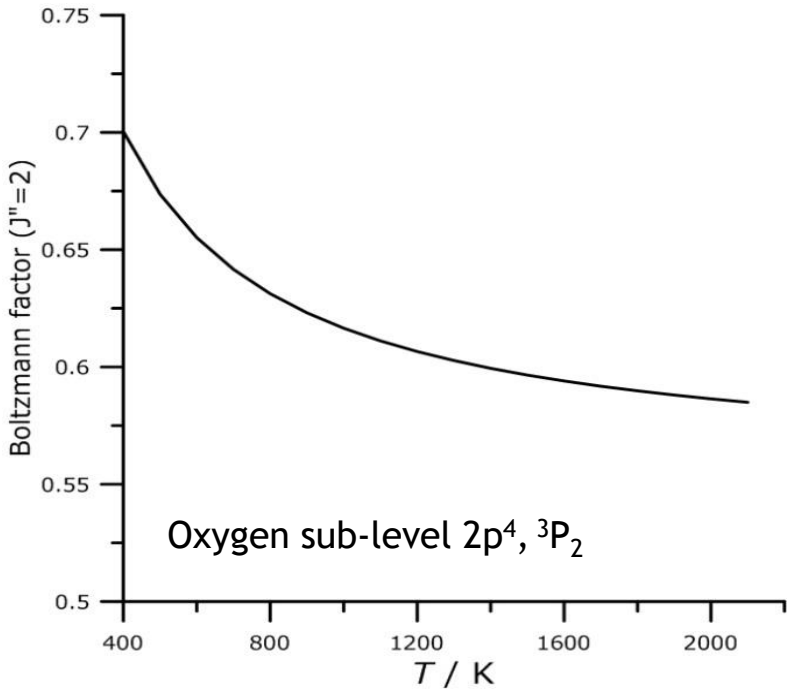

Absolute O-atoms mole fraction profiles

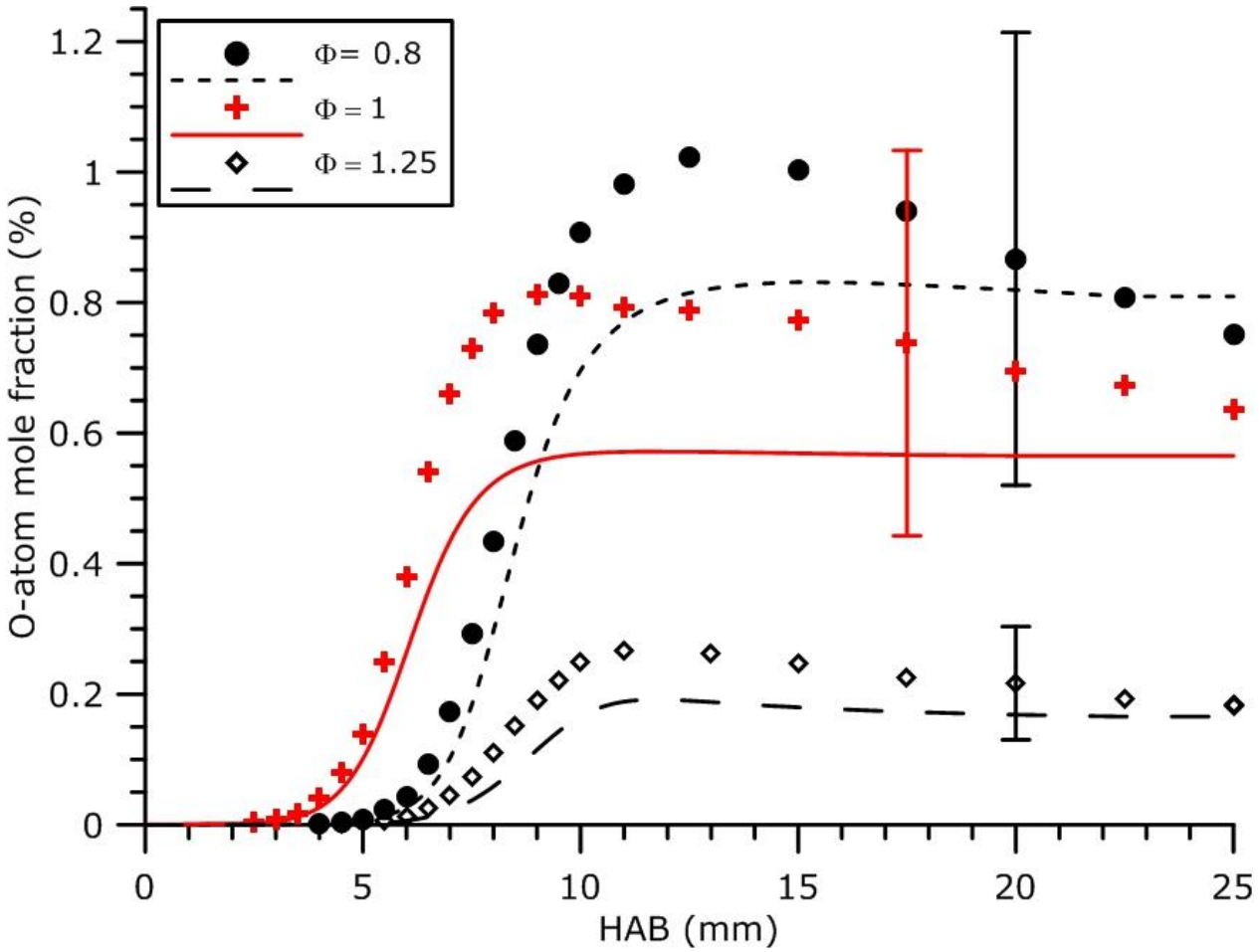

At HAB = 25 mm

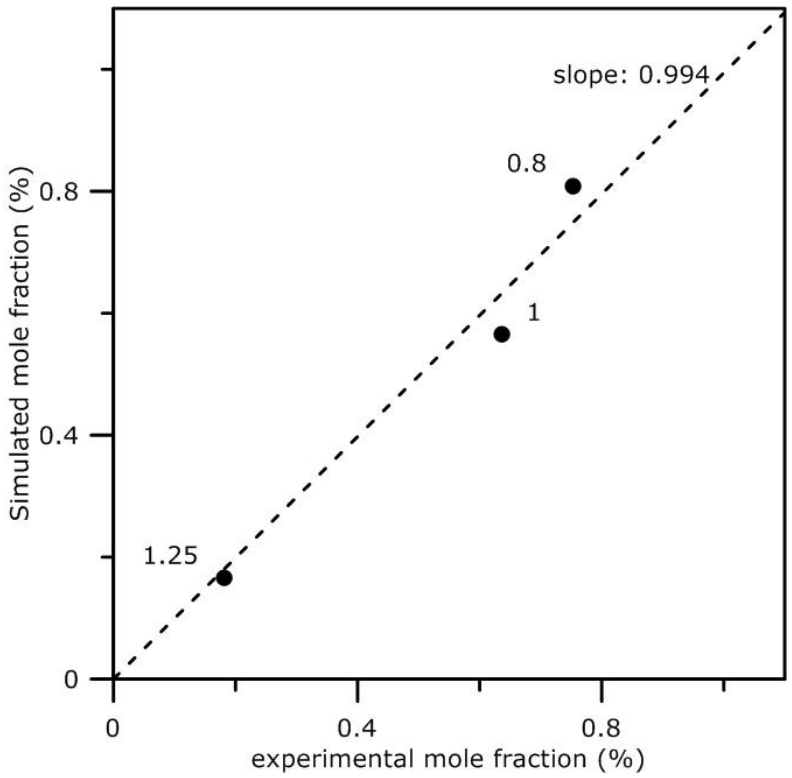

Lamoureux et al., ProCI 38 (2021)1753-1760

O-atoms measurements

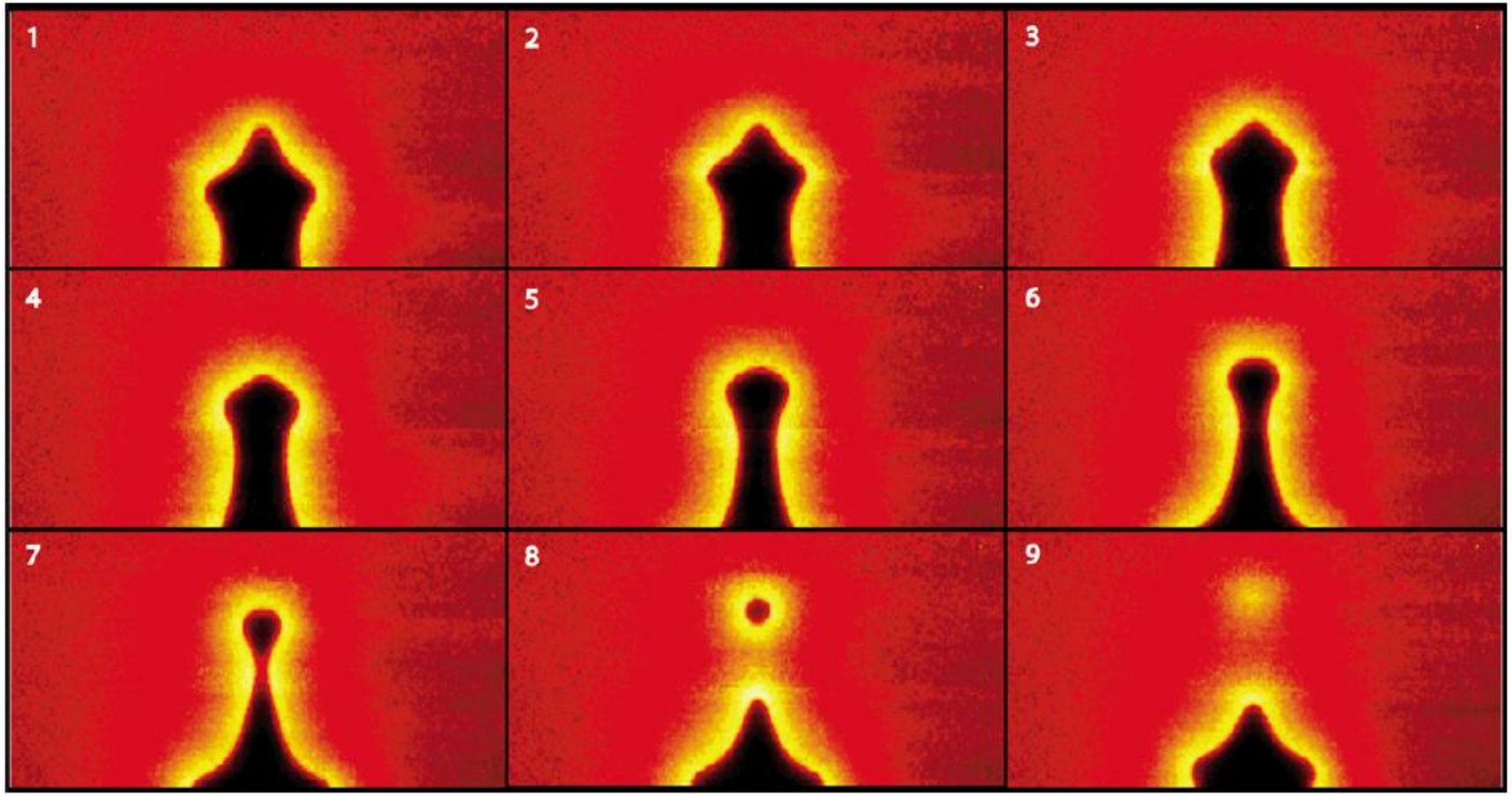

Fig. 6. Temporal evolution of atomic oxygen in an acoustically forced axisymmetric premixed $CH_4/O_2/N_2$ flame. The color table indicates O-atom LIF signal levels, and the black region corresponds to the unburned reactants. Numbering in the upper left corner of each frame indicates the time ordering of the images.

Δt + 200 μs

20-shot average

Frank, Settersten, ProCI30(2005)

Take-away

- Check that
  - Quadratic LIF regime
  - No parasite signal (stimulated emission, photocatalytic, …)
- Quenching
  - Quenching calculation using Bittner's data (at room T)
  - Colliders density ?
- Absolute quantification
  - Indirect from calibrated flame + kinetic calculations
  - Noble gas (Xe/O, Kr/H…)

IX. LIF Thermometry

(if Raman or CARS not available!)

LIF Thermometry, distribution of Boltzmann

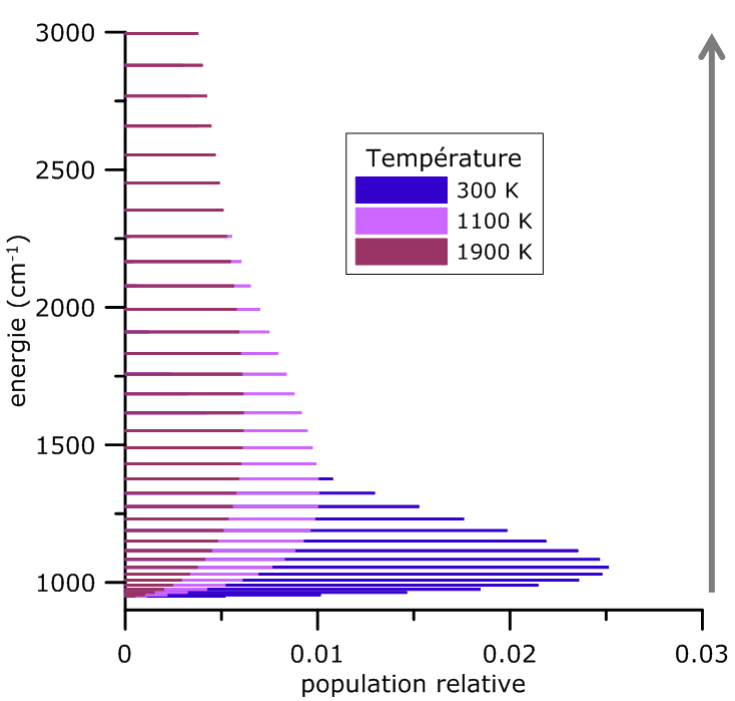

$$N_{J''}^{0} = f_b(T, J'')N_{tot}$$

$$f_b(T, J'') = \frac{g_{J''}}{Q_e Q_v Q_r} \exp\left(-\frac{E_{elec} + E_{v''} + E_{J''}}{kT}\right)$$

Thermodynamic equilibrium (rotational temperature= vibrational temperature= gaz temperature)

By exciting different rotational levels, and measuring their LIF (or absorption) signal, we obtain information about the relative variation in the population of the excited levels, from which we can determine the temperature.

Dispersed fluorescence spectrum

Selection rules

$\Delta N = N' - N'' = 0, \pm 1$

$\Delta J = J' - J'' = 0, \pm 1$

3 main fluorescence lines

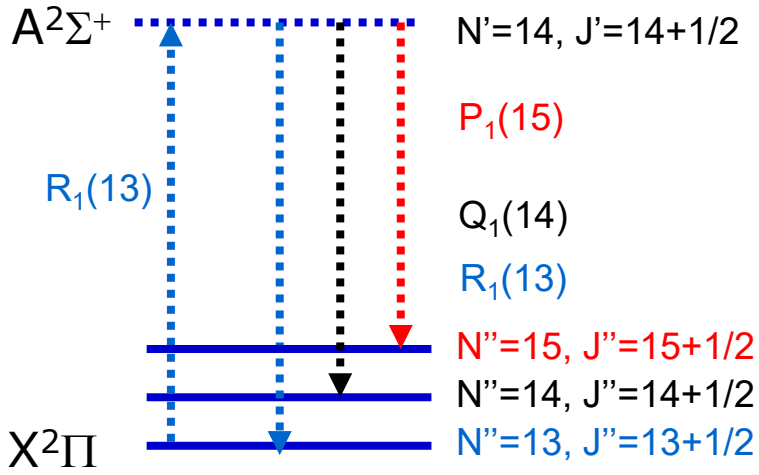

$R_1(13)$, 306.721 nm

$Q_1(14)$, 311.568 nm

$P_1(15)$, 316.725 nm

Dispersed fluorescence spectra of OH $A^2\Sigma^+$-$X^2\Pi$ (0-0)
Narrowband collection (~1nm) + prompt-LIF

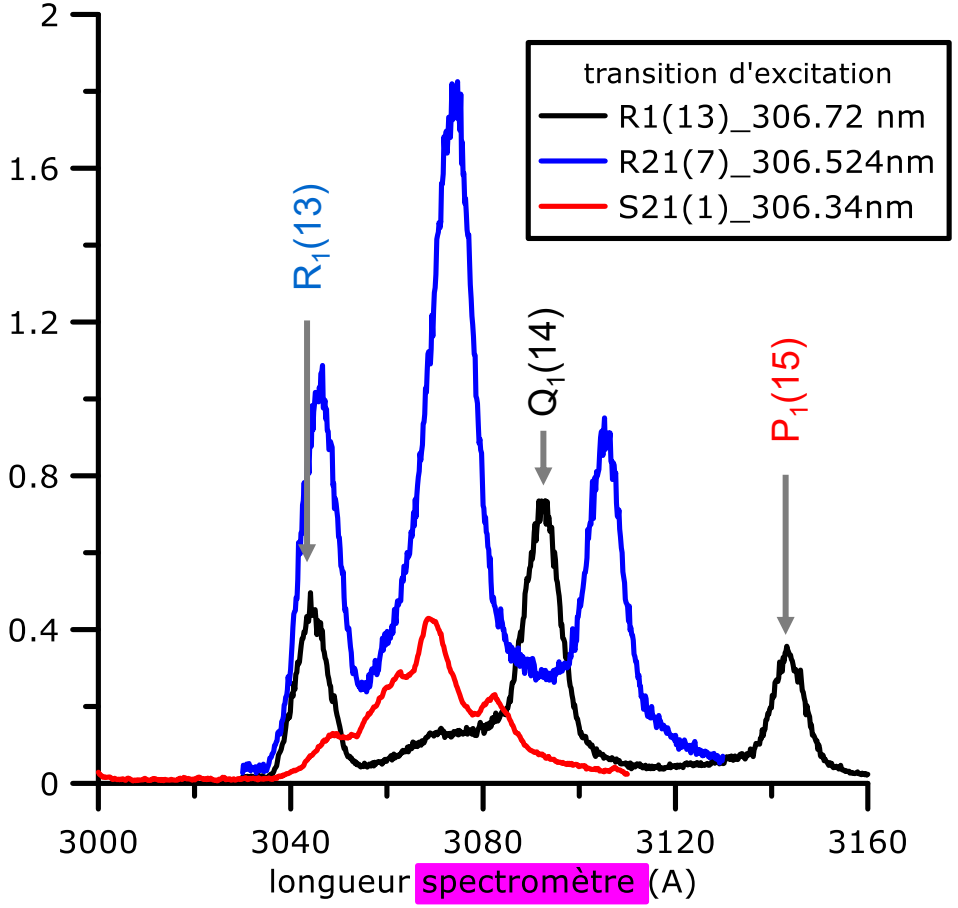

Expression of LIF signal, multi-level

$$SF(J") = \frac{GV\Omega}{4\pi} f_b(T, J") N_{tot} B_{J"J'} U_\nu \Phi$$

$$\Phi = \frac{\sum_{coll} A^{v'J'}_{v"J"}}{\sum_{tot} Q^{v'J'}_{v"J"} + \sum_{tot} A^{v'J'}_{v"J"}}$$

The temperature measurement requires to excite several rotational levels. They are linked by their Boltzmann factor, which is a function of J'' and T. Since all populations are sampled at a given HAB (a given temperature T), the rotational partition function (which depends on T) is therefore constant.

$$SF(J") \propto g_{J"} \exp\left(-\frac{E_{v",J"}}{kT}\right) B_{J"J'} \Phi$$

- Linear regime en fluorescence
- Suitable bandpass
- Correct for fluorescence quantum yield

Absorption/trapping (OH)

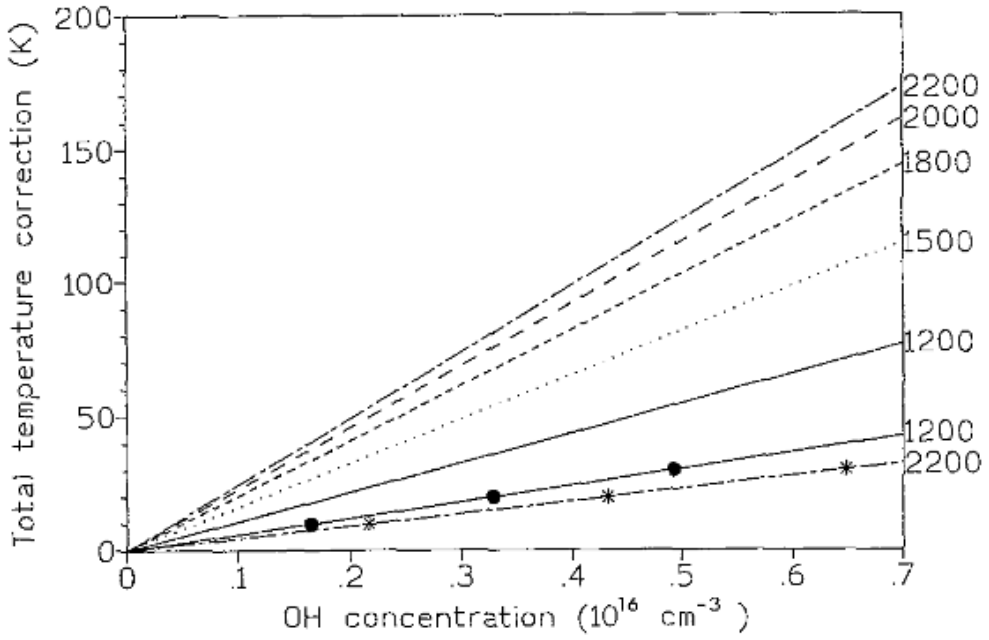

$$U(x) = U(0)\exp(-k_{ij}\,x)$$

$$\mathrm{SF}_{\mathrm{broad}_{ij}} = \sum_l \mathrm{SF}_{lj}\exp(-k_{lj}L)$$

$$= G\frac{\sum_l A_{lj}\exp(-k_{lj}L)}{\sum_l A_{lj} + Q} B_{ij} N_i U(x)$$

Desgroux et al. Appl. Phys. B 61 (1995)

Choice of the diatomic species

OH

- Absence in the fresh gases
- Dependance of Φ with J”

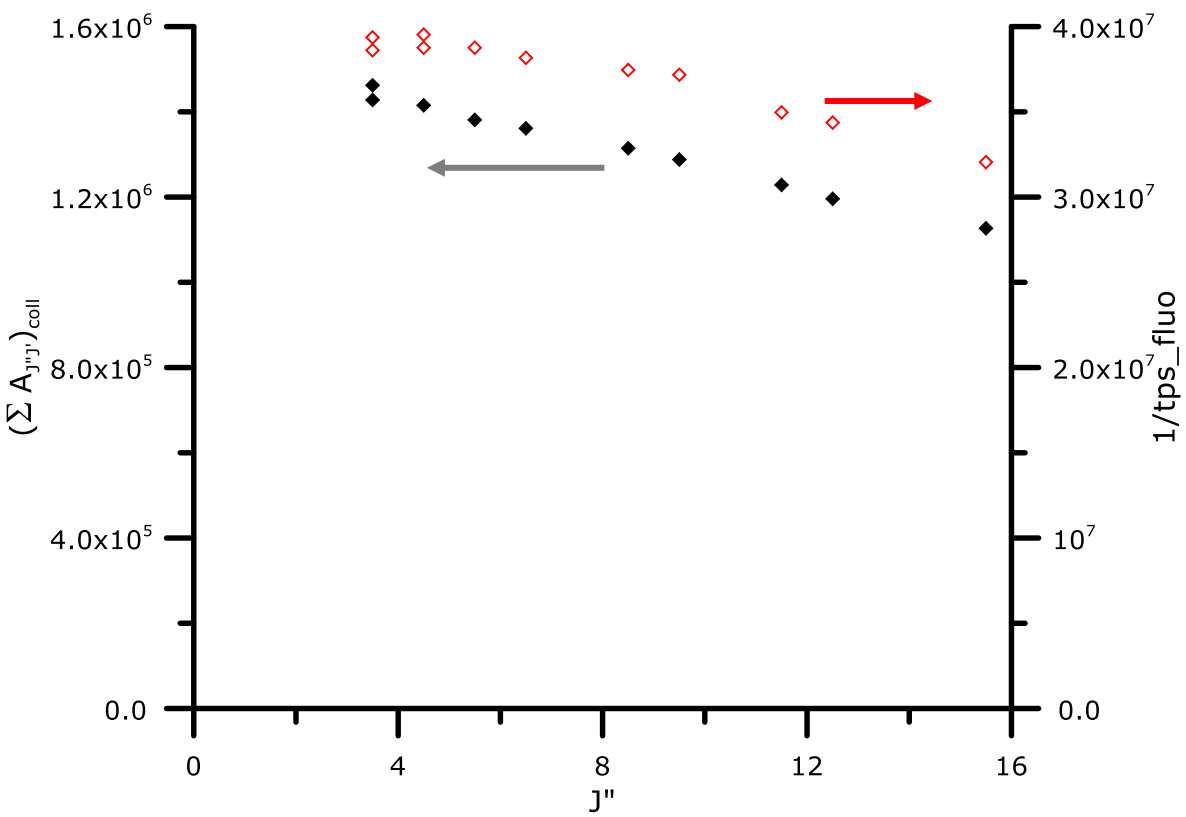

NO

- Seeded in low quantity (50 ppm – 1%)
- Very weak variation of Φ with J”

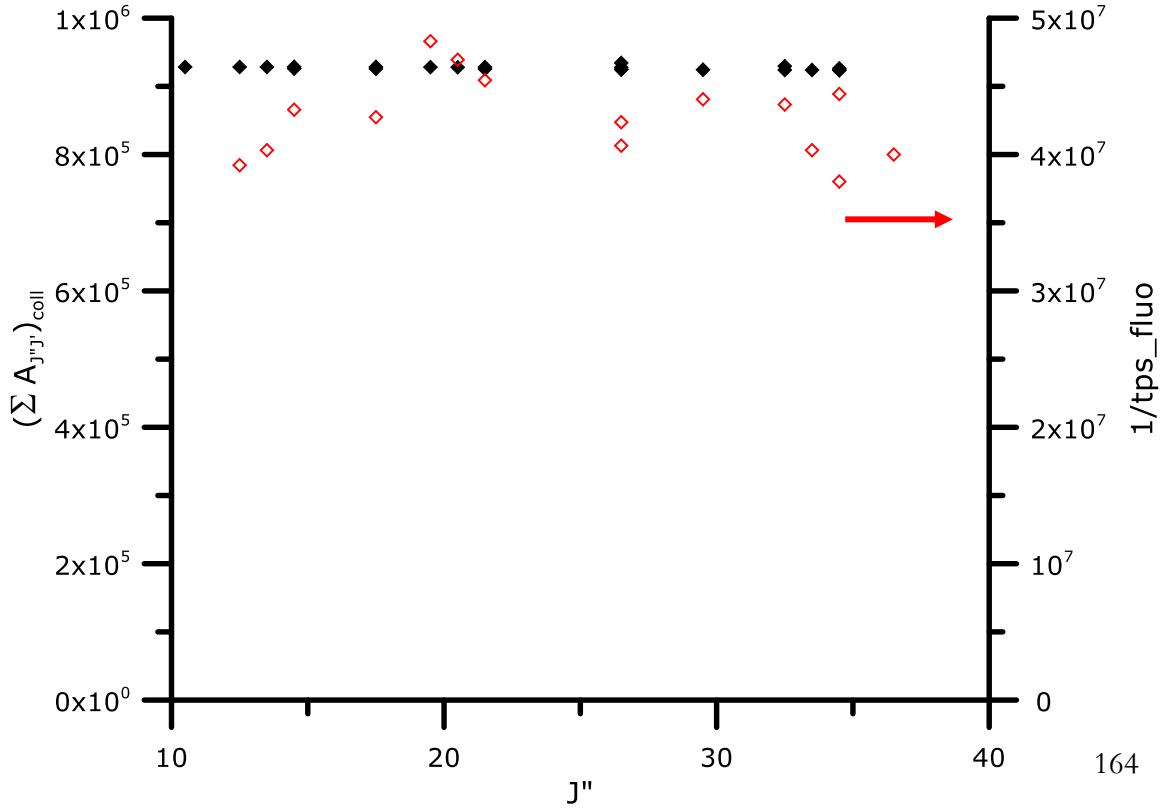

Spectroscopy of NO, Factor of Franck-Condon, $q_{v'',v'}$

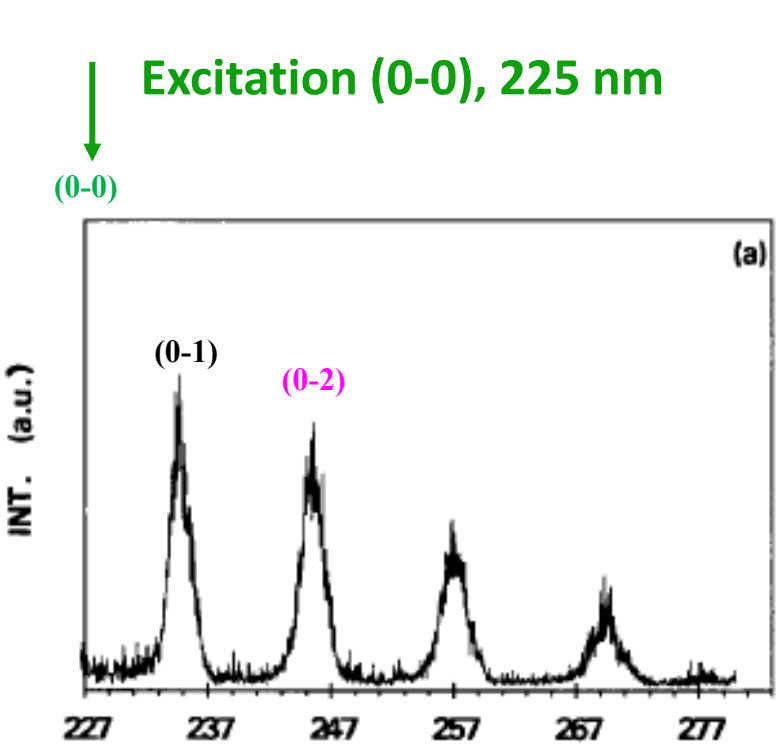

Dispersed LIF spectrum

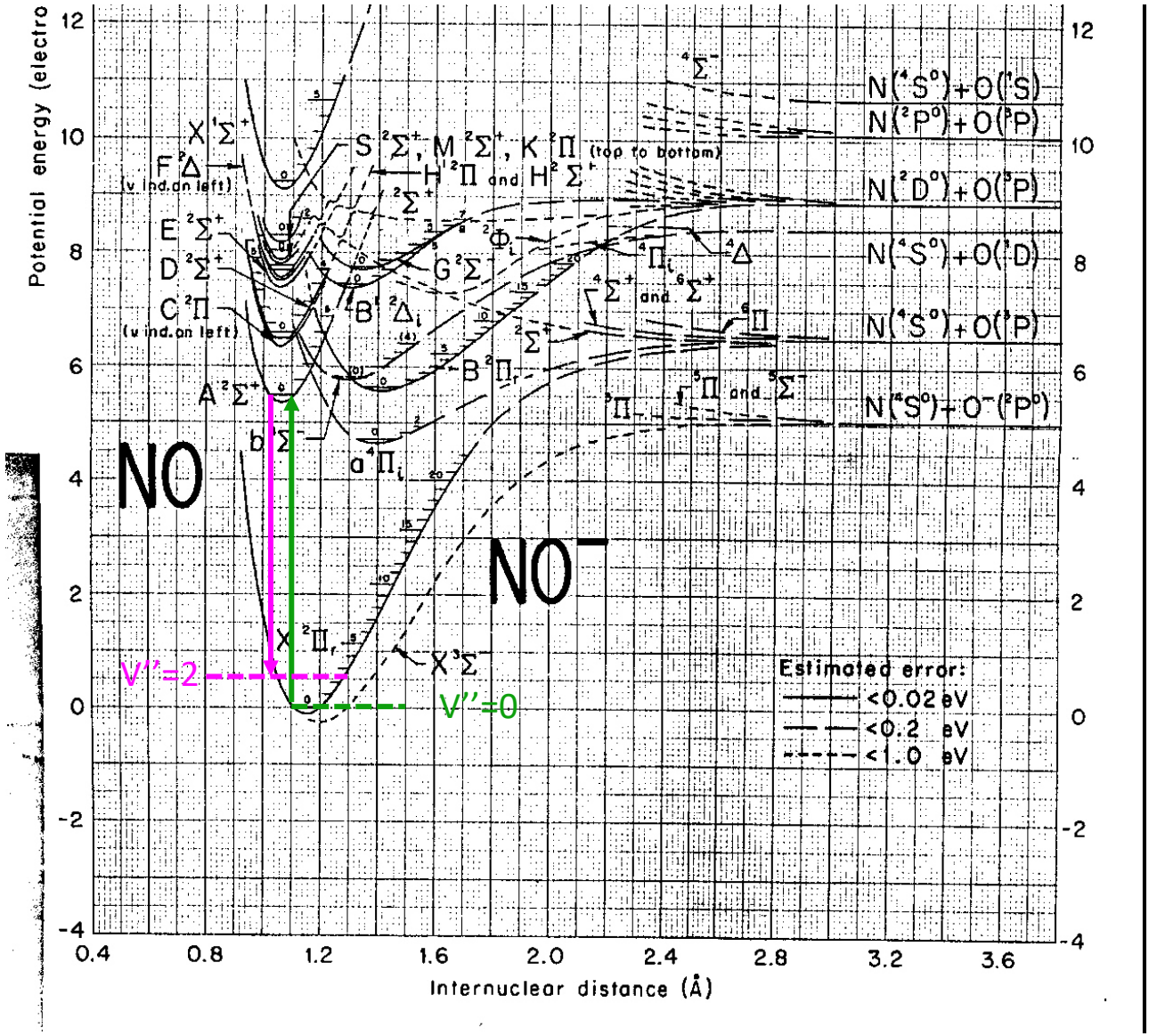

Desgroux et al., Appl.Opt.37 (1998)

Farmer et al. JQSRT 12 (1972) 627-633

Gilmore JQSRT 5 (1965)

Boltzmann plot

Φ indpt de J”

$$\frac{SF}{U_v} \propto g_{J''} \exp\left(-\frac{E_{v'',J''}}{kT}\right) N_{tot} B_{J''J'} \Phi$$

$$\ln\left(\frac{SF_{pk}}{g_{J''} B_{J''J'} U_v}\right) = cst + \left(-\frac{E_{v'',J''}}{kT}\right)$$

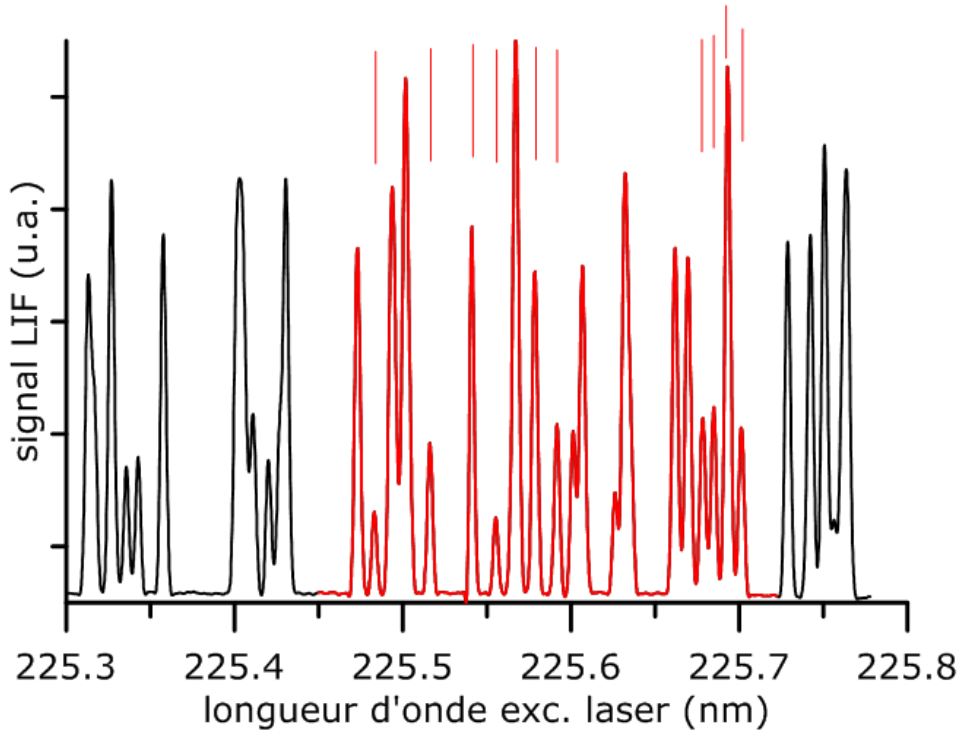

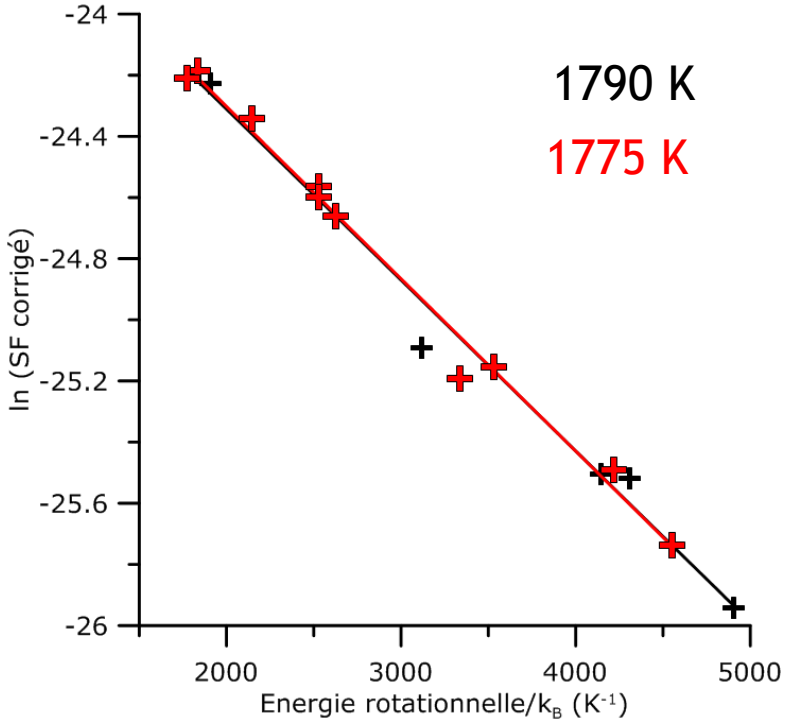

Spectrum obtained using a laser with a spectral width of 0.7 cm^{-1} 10 selected lines

Scan de 20 min

Impact of the laser bandwidth and of P: simulation using Thermo NO-LIF software

5.3 kPa

100 kPa

0.12 cm^{-1}

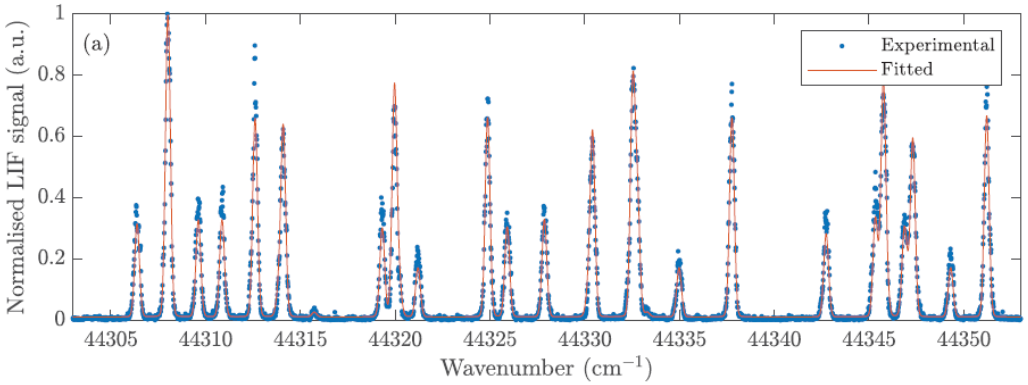

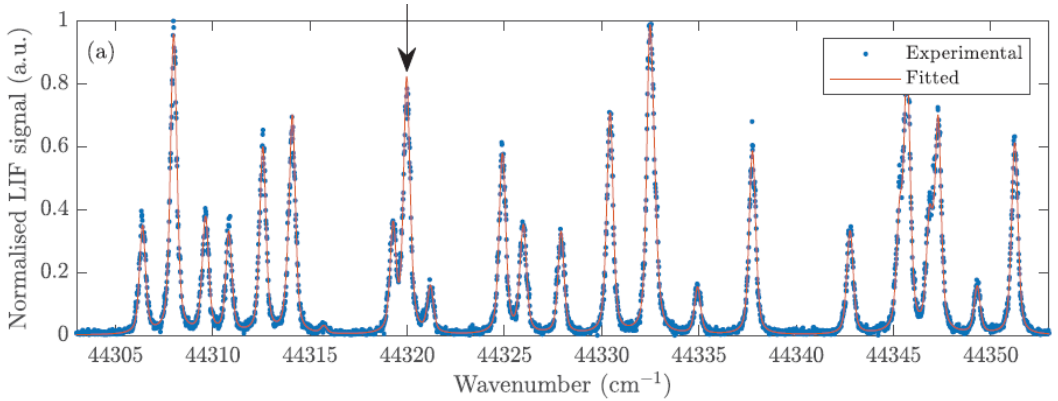

0.7 cm^{-1}

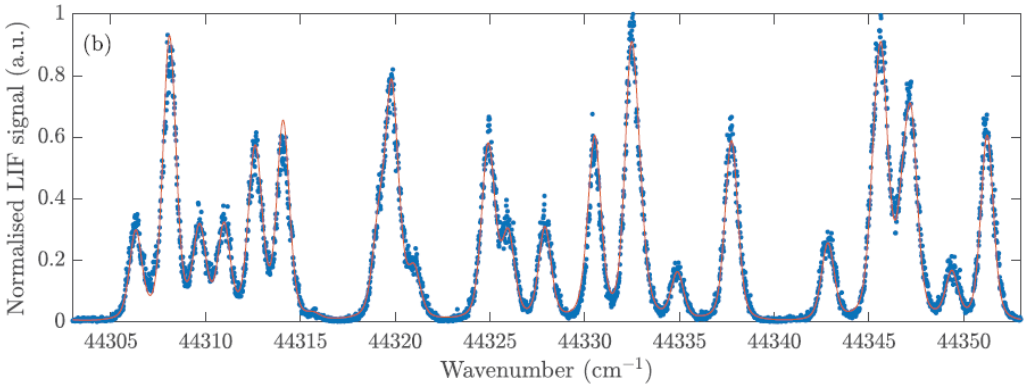

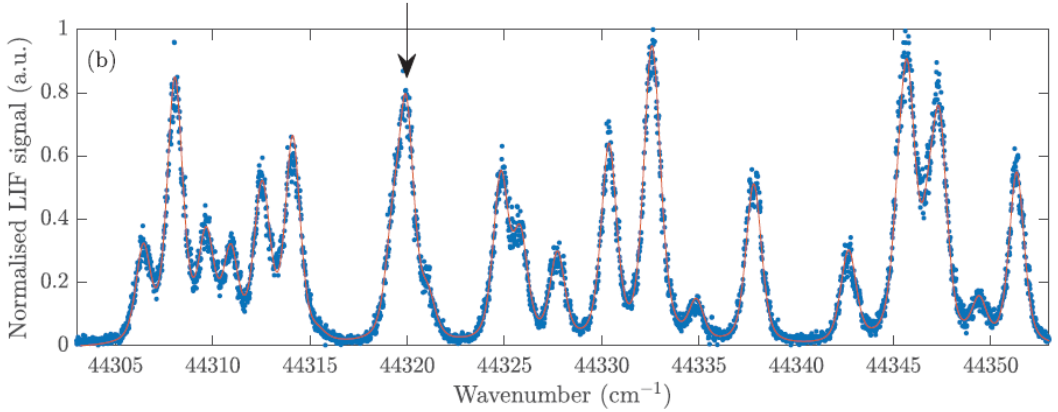

K.K. Foo, JQSRT 255(2020)107257
https://pc2a.univ-lille.fr/thermo-no-lif

See also LIFSIM El Moussawi et al. Appl. Phys. B 131, p-72, (2025).

Two-Line Atomic Fluorescence (TLAF)

- Atomic species → high oscillator strength
  → strong LIF signal

Indium:

Suitable 3-level electronic structure

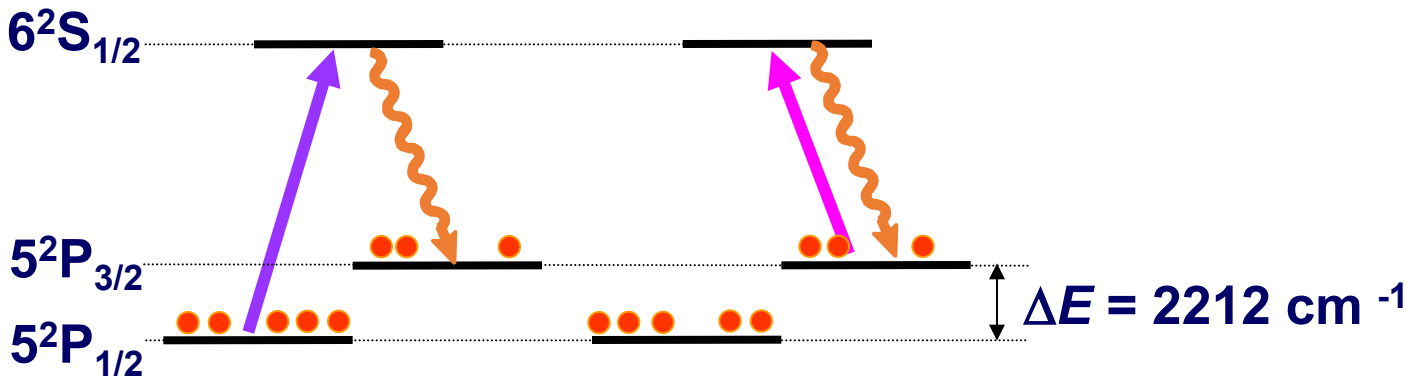

Hult et al., PROCI 30 (2005) 1535

Two-Line Atomic Fluorescence (TLAF)

TLAF:

ECDL scanning at 20 Hz

$5^2P_{1/2} \rightarrow 6^2S_{1/2}$ excitation at 410 nm

$5^2P_{3/2} \rightarrow 6^2S_{1/2}$ excitation at 451 nm

Detect $6^2S_{1/2} \rightarrow 5^2P_{3/2}$

fluorescence at 451 nm

Spatial resolution: ~100 μm

Low-pressure Flame:

Premixed laminar $CH_4/O_2/N_2$

Indium seeding: <100 ppbv

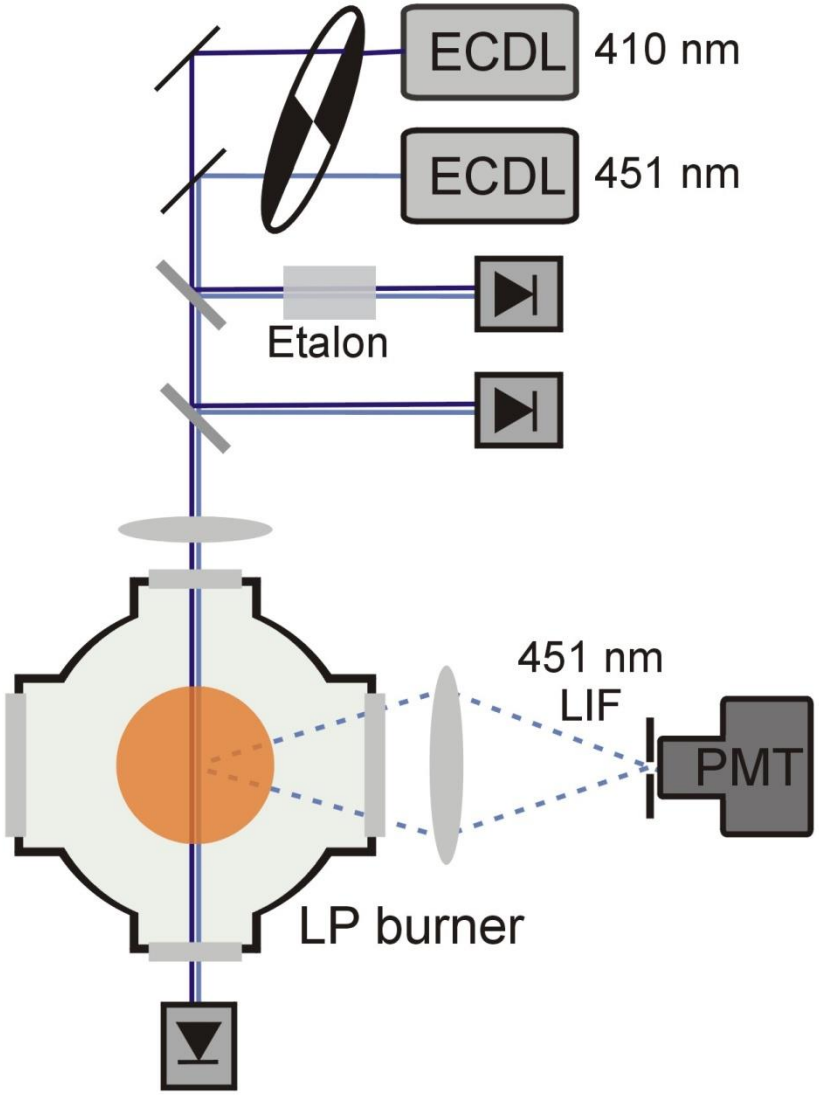

Burns et al., App.Phys.B 93 (2008) 907

Two-Line Atomic Fluorescence (TLAF)

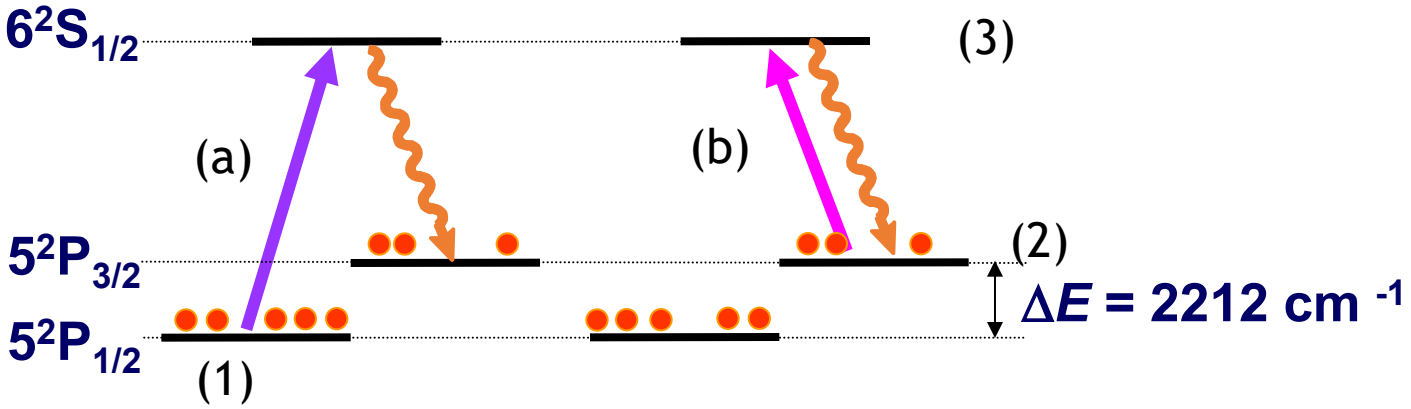

$$F(a) = G\frac{\Omega V}{4\pi}\boldsymbol{N_a^0}\frac{\boldsymbol{B_{13}}}{\boldsymbol{A_{32}+Q_{32}}}A_{21}\mathrm{I}_{13} \qquad F(a)\,/F(b) = N_a^0/N_b^0\,\frac{B_{13}}{B_{23}}\mathrm{I}_{13}/\ \mathrm{I}_{23} \qquad f_b \propto e^{-E/kT}$$

$$F(b) = G\frac{\Omega V}{4\pi}\boldsymbol{N_b^0}\frac{\boldsymbol{B_{23}}}{\boldsymbol{A_{32}+Q_{32}}}A_{21}\ \mathrm{I}_{23} \qquad \mathrm{B}_{21} = \frac{\mathrm{g}_1}{\mathrm{g}_2}\mathrm{B}_{12} = \mathrm{A}_{21}\frac{\mathrm{c}^3}{8\pi\mathrm{h}\nu^3} = \mathrm{A}_{21}\frac{1}{8\pi\mathrm{h}\bar{\nu}^3}$$

$$T = \frac{\Delta E/k}{\ln\left(\frac{F_a/I_{13}}{F_b/I_{23}}\right) + 3\ln\left(\frac{\lambda_{32}}{\lambda_{31}}\right) + \ln\left(\frac{A_{32}}{A_{31}}\right)}$$

Only one detector needed

No need to correct for spectral dependence of the detectors

Hult et al., PROCI 30 (2005) 1535

Comparison thermometry LIF OH/LIF NO/ Indium TLAF

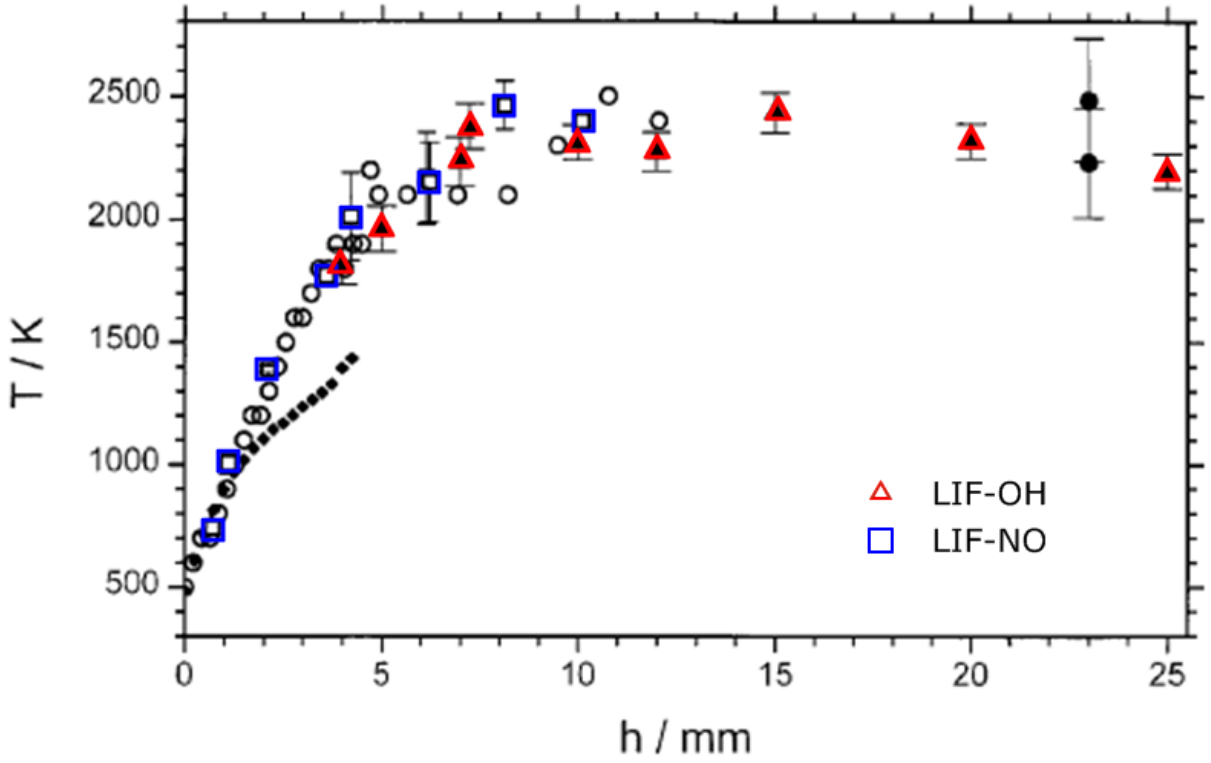

Hartlieb et al. Appl. Phys. B70 (2000) 435-445
50 mbar

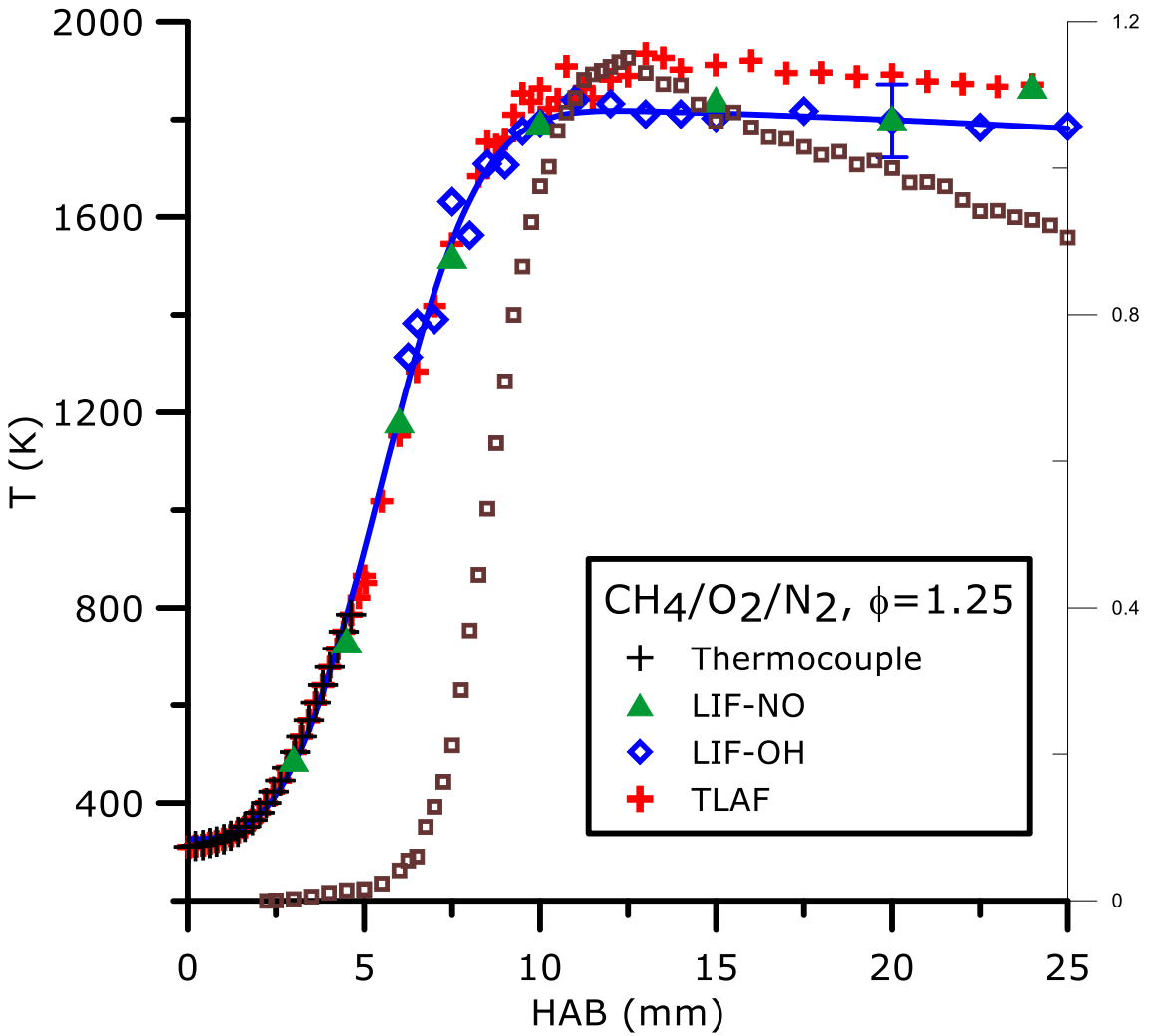

Lamoureux et al., CF 157 (2010) 1929-1941
53 mbar

Other LIF alternatives

- **Two-line thermometry (in turbulent flames)**

  - Faster

  - Same excited level with the 2 transitions: insensitive to quenching+RET

  - Attention: Only 2 points for the Boltzmann plot!

-Use of other tracers :

- **Acetone: at low temperature ».** *PhD Bresson (Univ. Rouen, 2000), Thurber et al. Appl. Opt. 37,4963 (1998)*

-Chlorure d'indium: Two-line atomic fluorescence (TLAF) (pas de RET, indépendant de Q) *Hult et al. Proc. Combust. Inst. 30, 1535 (2005), Burns et al Proc. Combust. Inst. 33 (2011)*

-Toluene :*Schulz, Peterson*

LIF Thermometry of toluene: engine application

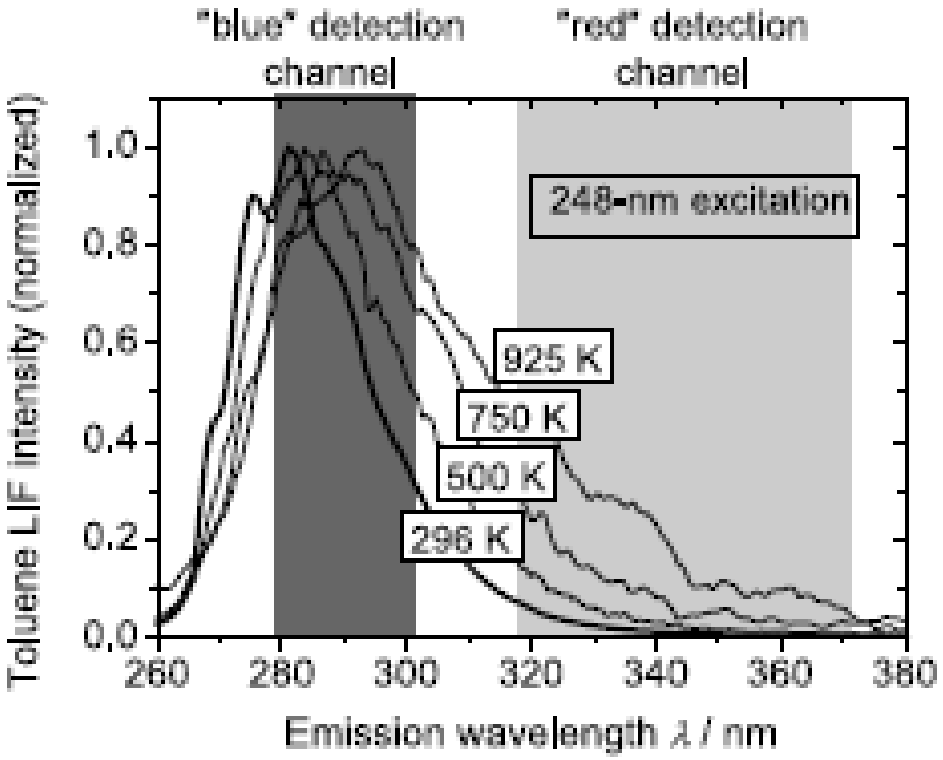

FIGURE 1 Red shift of the emissions spectrum with increasing temperature (adapted from [4])

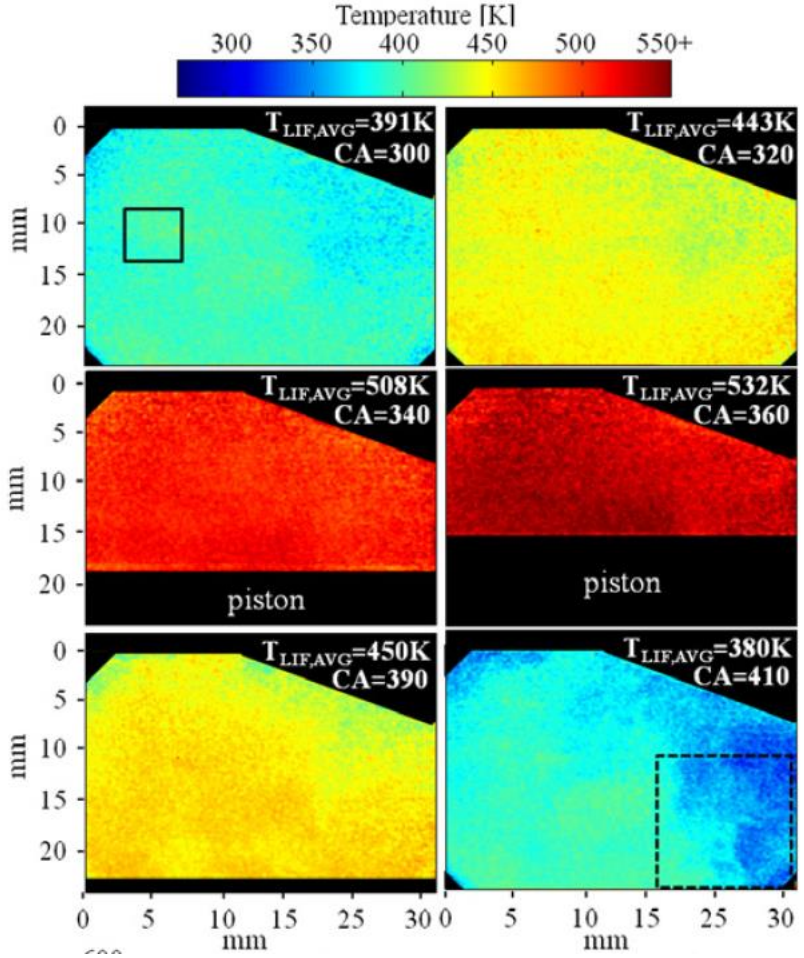

Peterson and Dreizler, Appl. Phys. B 117 (2014), Luong and Schulz, Appl. Phys. B91 (2008) 669-675

X. Case study : NO

Effect of pressure
Interferences

X. 1 Effect of pressure

Effect of pressure, shift and widening of the transitions with P

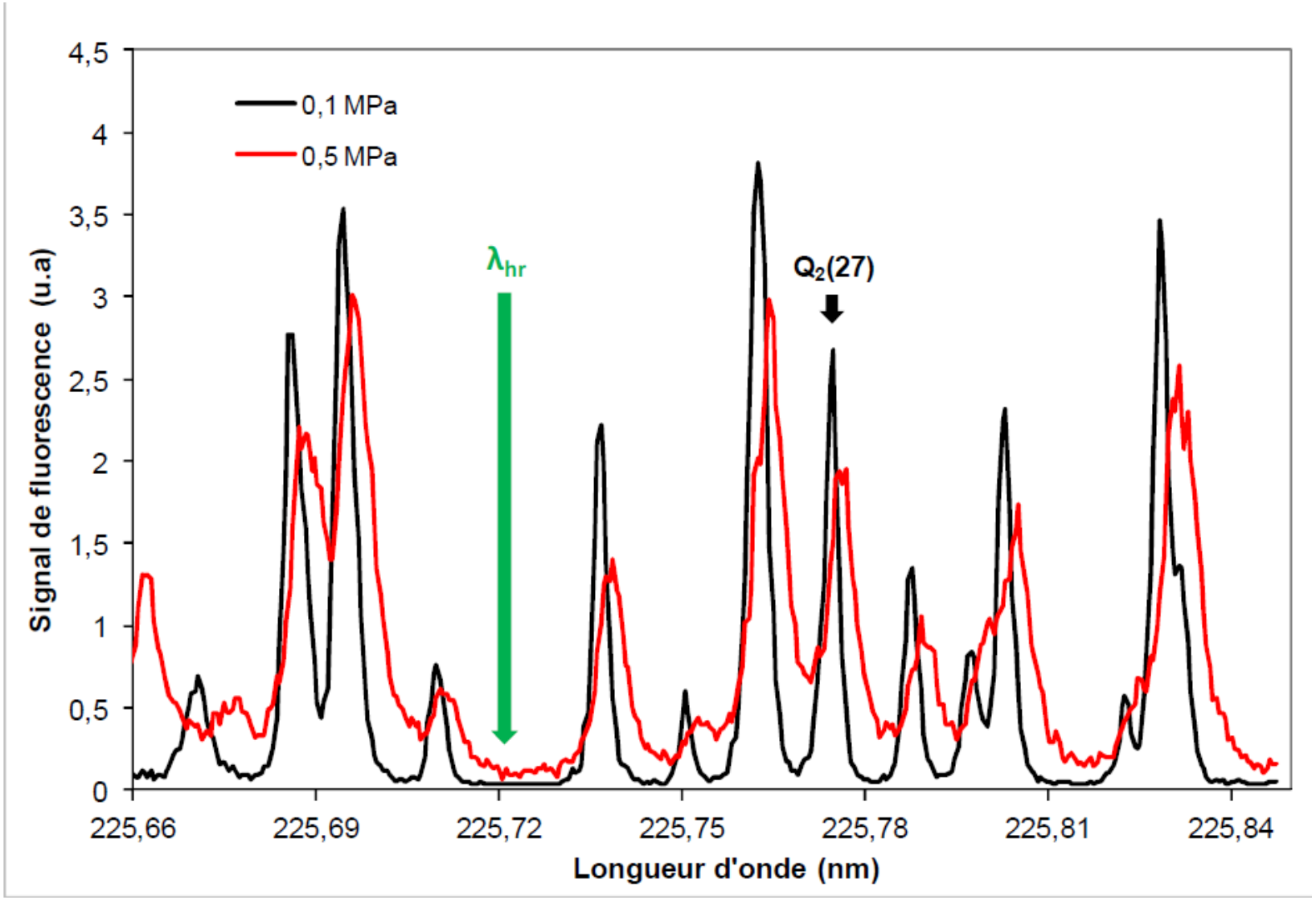

J. Molet, PhD Univ. Orléans, ICARE 2014

Spectral line shape

Factors Contributing to the line broadening :

Doppler broadening (temperature) $G_D(\bar{\nu}) = 2.\sqrt{\frac{\ln 2}{\pi}}.\frac{1}{\Delta\bar{\nu}_D}.\exp\left(-4.\ln 2.\left(\frac{\bar{\nu}-\bar{\nu}_0}{\Delta\bar{\nu}_D}\right)^2\right)$

Gaussien profile

FWHM (full width at half maximum) : $\Delta\bar{\nu}_D = \bar{\nu}_0.\sqrt{\frac{8.k_b.T.N_A.\ln 2}{M.c^2}} = 7.1623\times10^{-7}.\bar{\nu}_0.\sqrt{\frac{T}{M}}$

Collisional broadening (pressure) : $L_C(\bar{\nu}) = \frac{\Delta\bar{\nu}_C}{2\pi}.\frac{1}{(\bar{\nu}-\bar{\nu}_0)+\left(\frac{\Delta\bar{\nu}_C}{2}\right)^2}$

Lorentzian profile :

FWHM : $\Delta\bar{\nu}_C = 2.\sum_i P_i.\gamma_i(T)$ $\gamma_i(T) = \gamma_i^0\left(\frac{T_0}{T}\right)^{\beta_i}$

γ_i : broadening coefficients of the different species

Spectral line shape

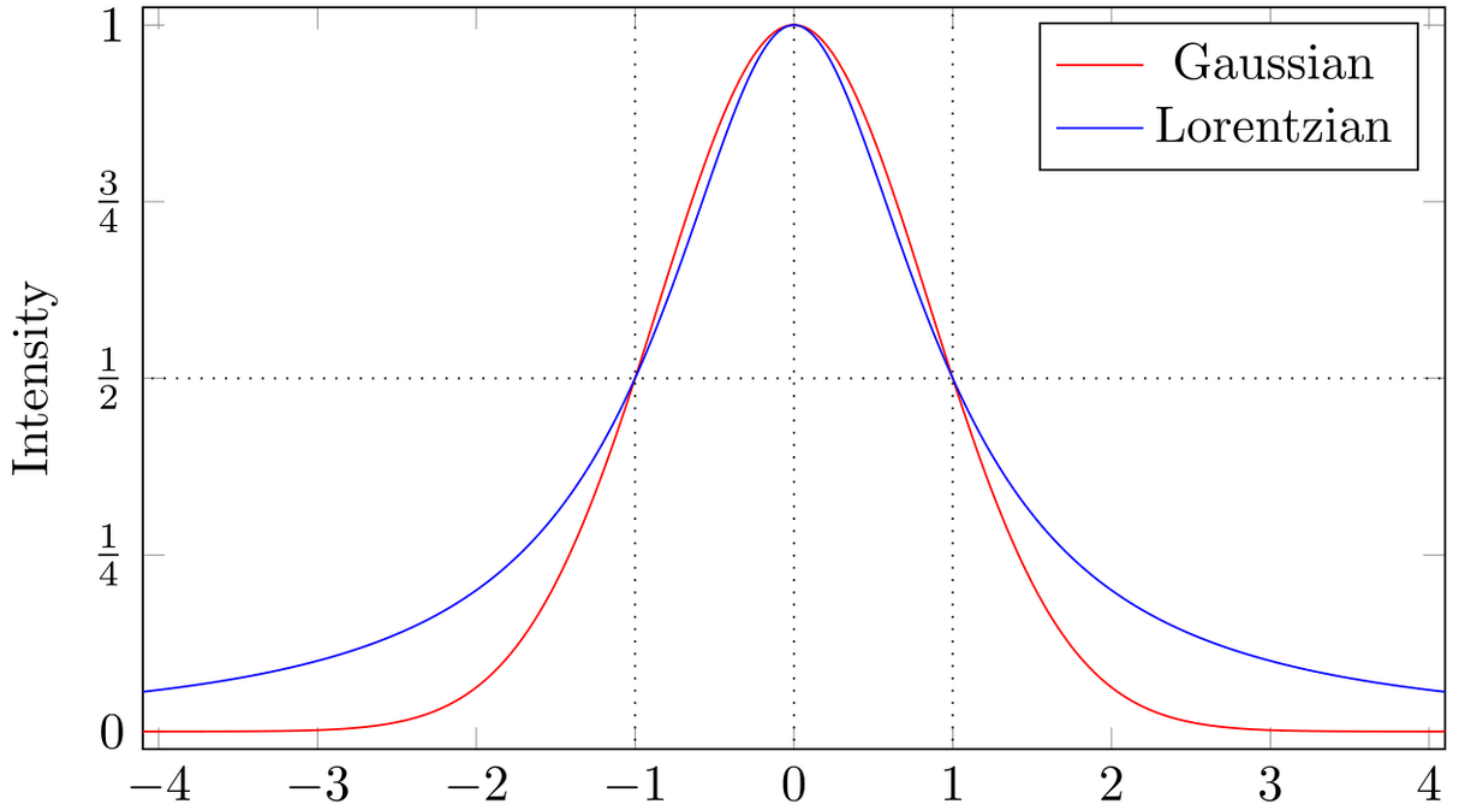

In practice : convolution of the Gaussian and Lorentzian Profiles: **Voigt profile**

$$V(x;\sigma,\gamma) \equiv \int_{-\infty}^{\infty} G(x';\sigma)L(x-x';\gamma)\,dx',$$

Jet-wall stagnation premixed H_2-air flames diluted (Ar, He)

- McGill (Bergthorson's group)
  - *T* and NO by in situ LIF
  - Effect of ϕ @ 1 atm, T ~1800K, Durocher et al. ProCI38(2021)
  - Effect of *T* at p = 1 atm, and ϕ =1, Meulemans et al. CnF261(2024)
  - Effect of *p* at ϕ ~ 1, Durocher et al. ProCI39(2023)

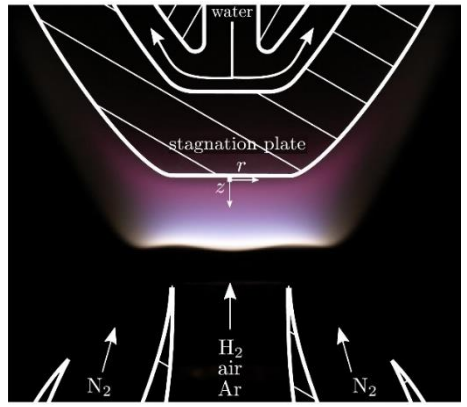

- Broadening of the spectral lineshape
- LIF collected through an ICCD camera (temporally integrated LIF)
- **LIF signal has to be corrected for the quenching Q**

$$S_{LIF} = \frac{\mathrm{GV}\Omega}{4\pi} N^0_{J"} B_{J"J'} U_\nu \frac{A}{A+Q}$$

$$\frac{S_{NO}}{C_{opt} E_L} = \frac{\Gamma}{\Delta\nu_L} n^0_{NO} f_B B_{12} \frac{A}{A+Q}$$

LIF corrections and calibration

- NO profiles are not directly reported in mole fraction but exp LIF signal are compared to synthetic LIF signal
  - Limit sources of error (Connelly et al. ProCI32(2009), paradigm shift)
- LIF synthetic signal calculated based on kinetic modeling and **LIFSim**
  - (1) Integrates instrumental resolution, spectral overlap, pressure broadening, …
  - (2) Calibration using NO standard addition method
  - (3) Quenching rate (N_q)
    - $Q_{A/q} = \sum N_q \, \sigma_{A/q}(T) \, v_{A/q}(T)$
      - Collisional cross section from literature (Tamura et al, Paul et al.)
      - N_q, kinetic simulation
  - (4) C_{opt}, by comparing experimental and synthetic LIF signal

$$④ \frac{F_{NO}}{C_{opt}} = \frac{\Gamma}{\Delta\nu_L} n_{NO}^0 f_B B_{12} \frac{A}{A+Q}$$

(① ② ③)

LIFSim 4.0: A. El Moussawi, S. Karaminejad, J. Menser, W. G. Bessler, T. Dreier, T. Endres, C. Schulz, LIFSim, a modular laser-induced fluorescence code for concentration and temperature analysis of diatomic molecules, Appl. Phys. B 131, p-72, (2025).

Durocher et al.
ProCI39(2023)

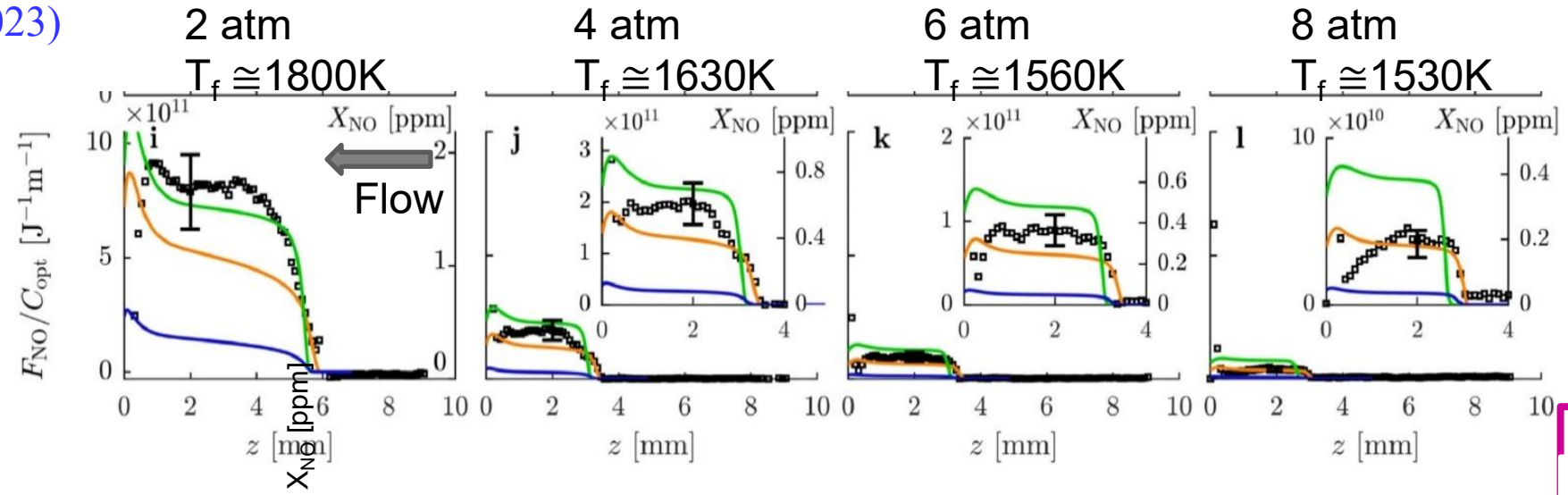

Patmo

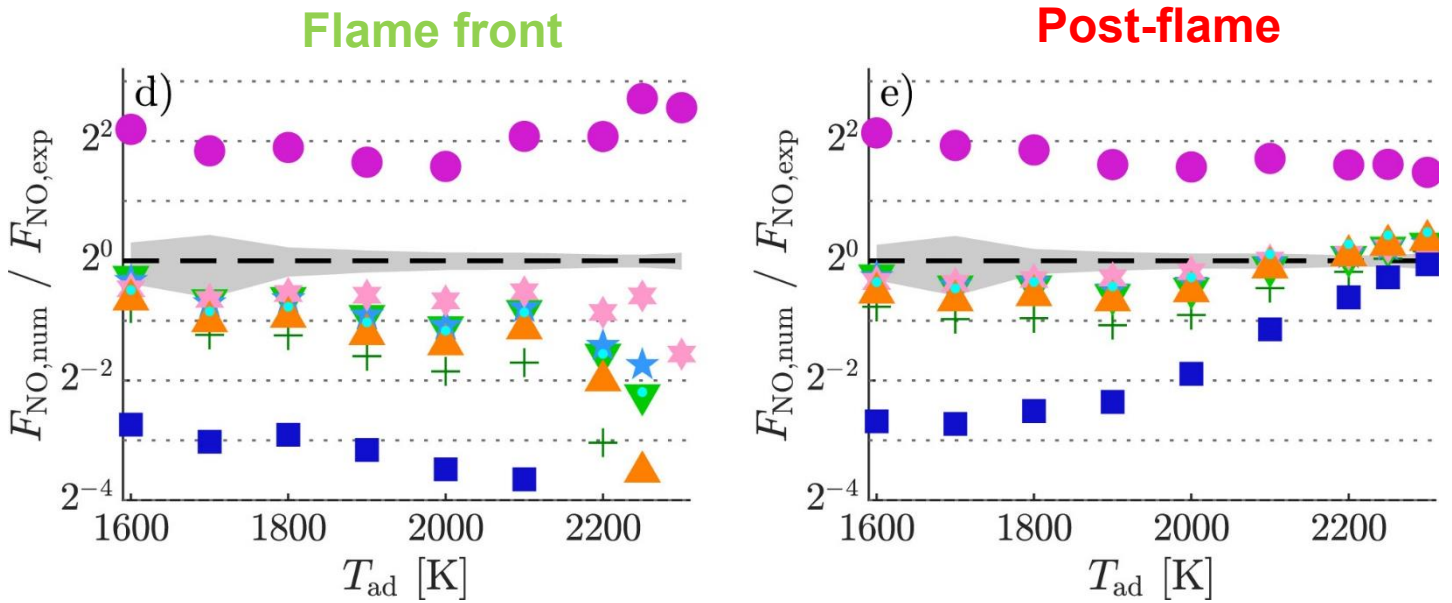

Meulemans et al. CnF261(2024)

OH - PLIF (Application): two-phase flow propulsion studies

HERON test facility
kerosene + 1.8 Mpa

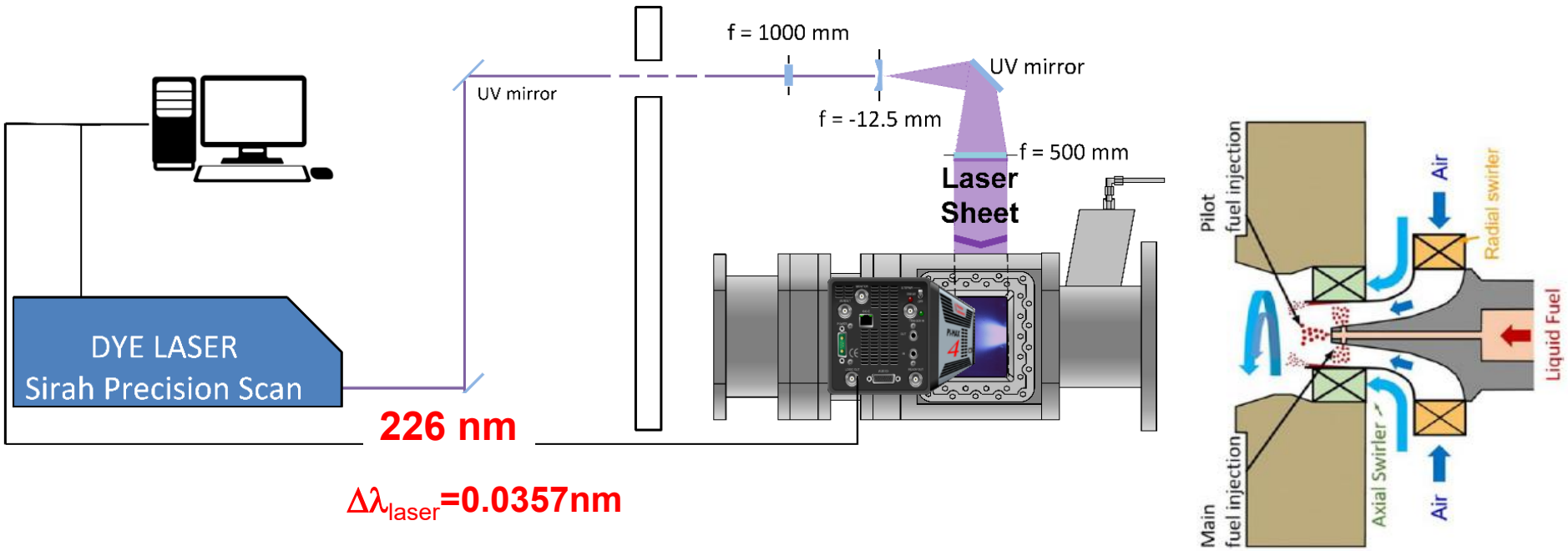

Image processing

- Instantaneous images with laser tuned on transition line and flame → Fluorescence signal
- Instantaneous images without laser (or detuned laser) and flame → Background image
- Instantaneous images with laser (tuned or detuned) with homogeneous concentration of molecules enabling fluorescence signal (for instance Acetone/air) → Laser energy profile and flat field correction

NO-PLIF (1)

Strategy for data processing interferences arising from kerosene fluorescence

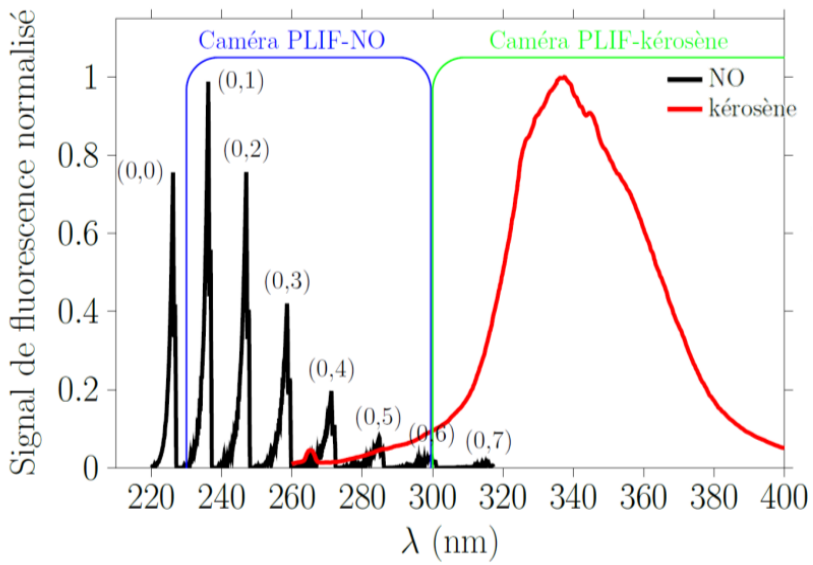

Two detection cameras:

- **Camera 1 :** NO and kerosene (mono-aromatics) fluorescence in the spectral range 235-300nm
- **Camera 2 :** fluorescence of kerosene (di-aromatics) in the spectral range 300-400nm

➔ **Discrimination of kerosene fluorescence from NO fluorescence on the images recorded on camera 1**

➔ **Excitation of the $Q_1(29.5)$ line to minimize dependence of SF on T and Q. Use of a five-level model.**

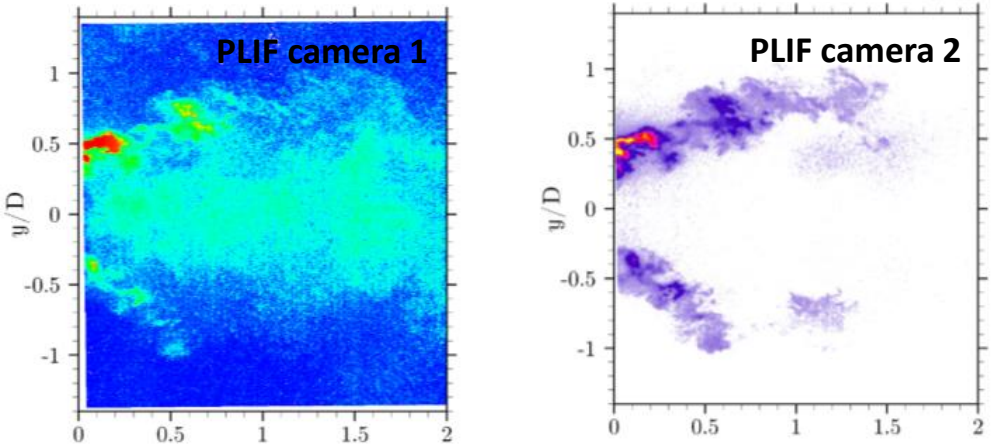

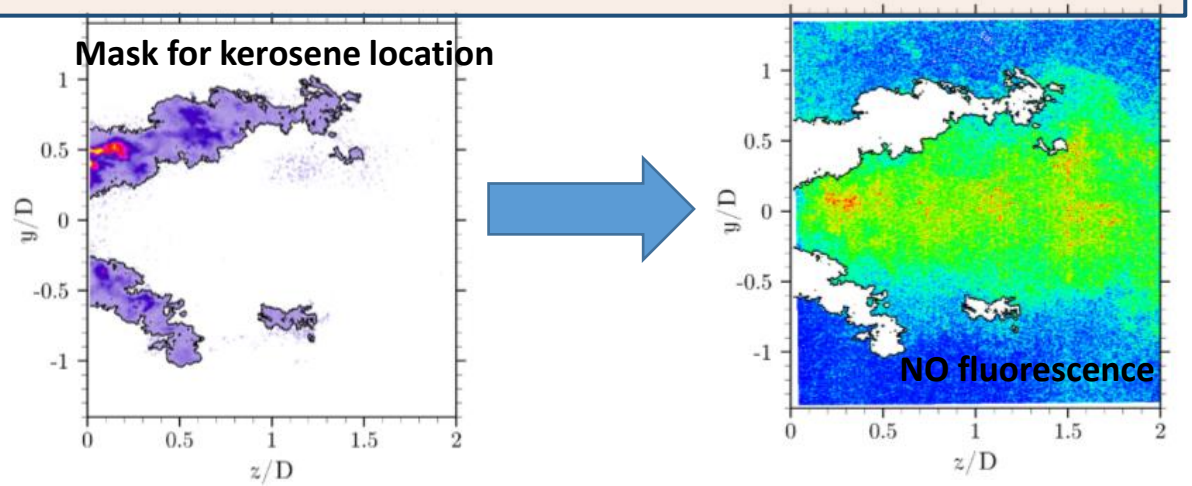

Salaün, Renou, Grisch et al. GT2020-14985 (2020)

Mulla et al. CF 203 (2019) 217

NO-PLIF (2)

Mean NO concentration
P=0.8 MPa, FAR 42‰

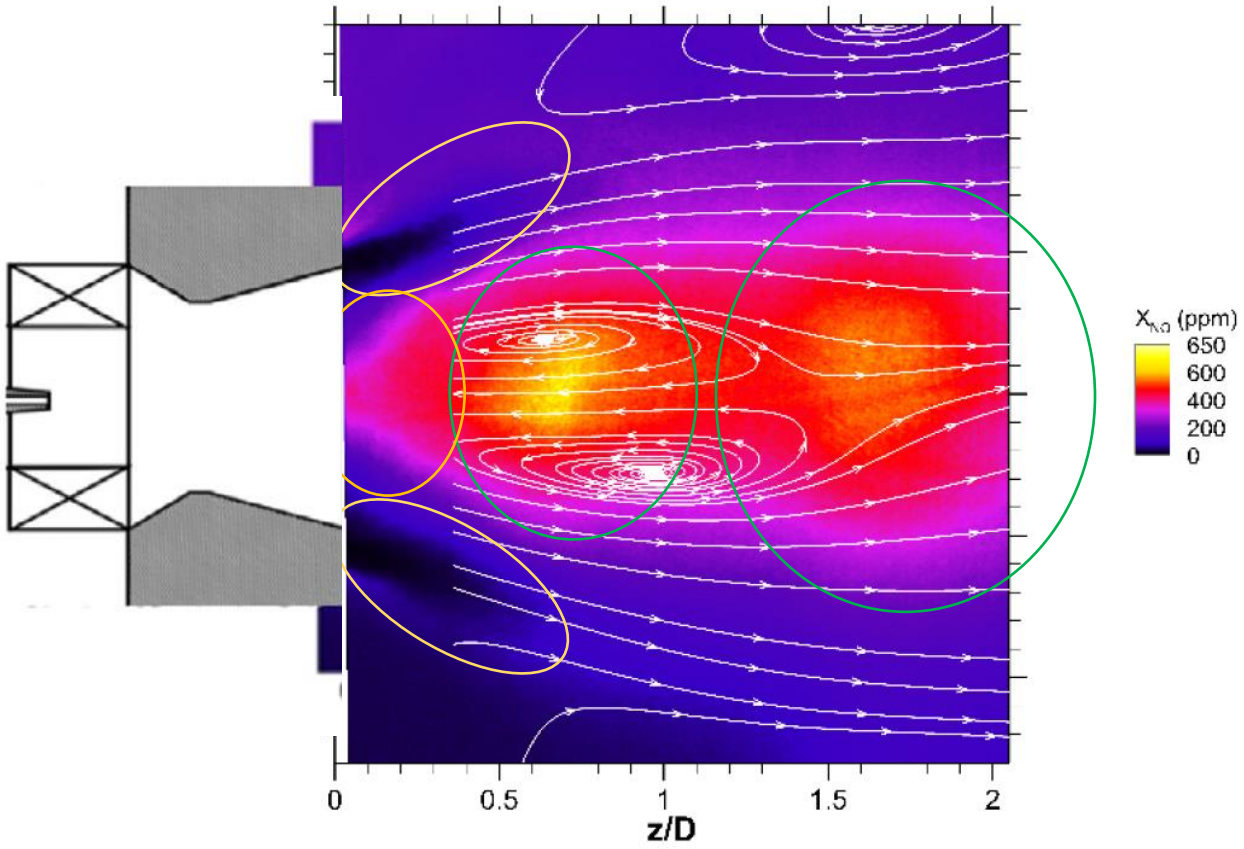

1/ No possible NO detection downstream from the injector in the jet zone

2/ laser absorption from kerosene downstream from the injector → reduction of NO fluorescence

3/ Two detection zones with large [NO]:

IRZ (Inner recirculation zone): Burnt gases at elevated temperature and low velocity → large residence time and high temperature ➔ **Favorable conditions for NO production via thermal mechanism (Zeldovich)**

Second pocket: possible explanation…
Chemical conversion of N_2O in NO in a high temperature zone. N_2O produced in a zone of medium temperature (~ 800 – 1000 K) close to the flame front then convected downstream from IRZ along the center of the flowfield.

Salaün, Renou, Grisch et al. GT2020-14985 (2020)

Legros, Renou, Grisch et al. CF 224 (2021) 273

NO-PLIF (3)

Legros, S., C. Brunet, P. Domingo-Alvarez, P. Malbois, E. Salaun, G. Godard, M. Caceres, B. Barviau, G. Cabot, B. Renou, G. Lartigue, V. Moureau, S. Puggelli, S. Richard, M.A. Boukhalfa, and F. Grisch, Combustion and Flame, 2021. **224**: p. 273-294.

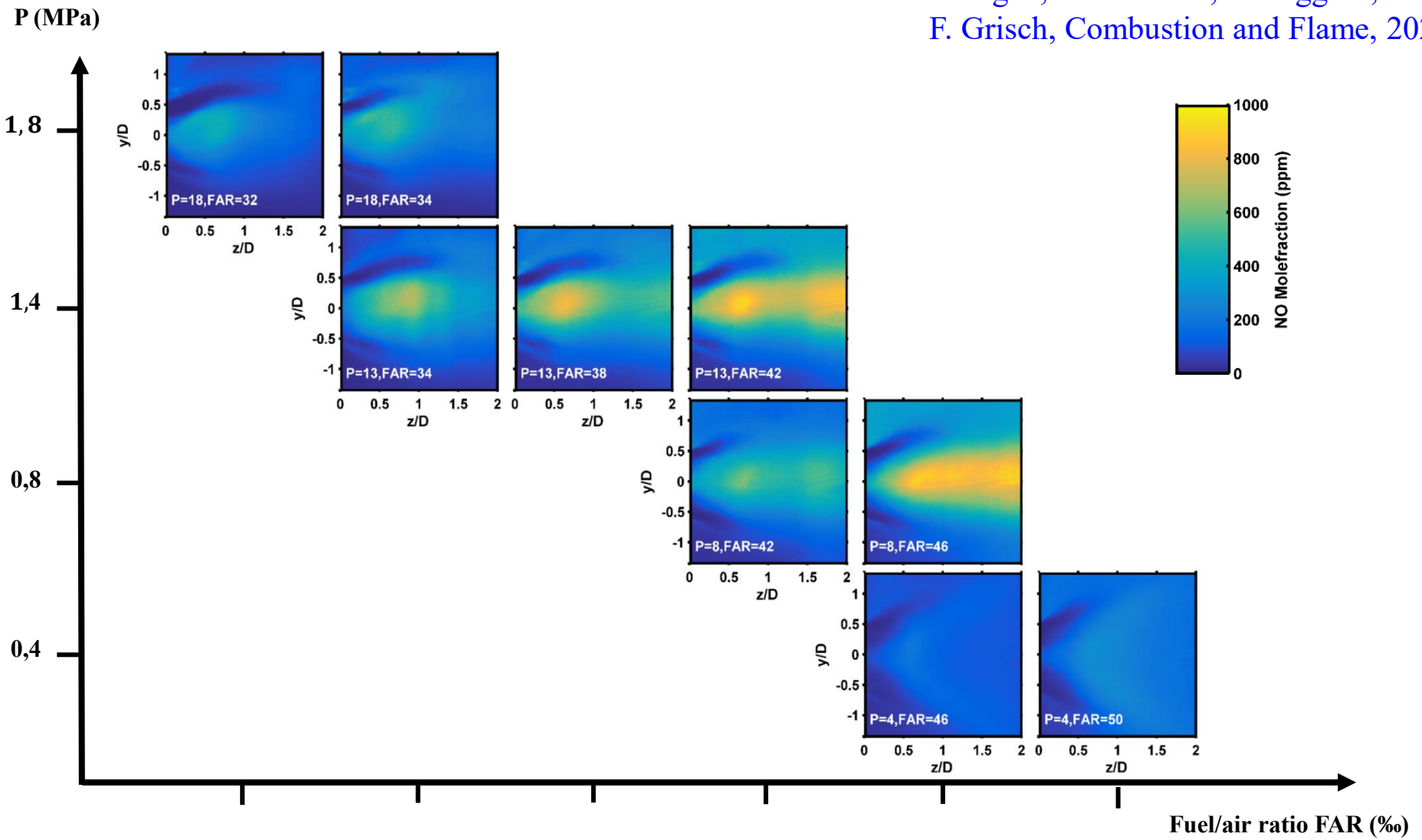

X.2 Spectral interferences

Interferences due to O_2 and Raman at low pressure

Dispersed LIF spectrum: ON resonance with NO. Stoechio flame

(zone without O2)

Dispersed LIF spectrum : ON resonance with NO: Lean flame

(zone with O2)

Dispersed LIF spectrum : OFF resonance lean flame

(zone with O2, Argon instead of N2)

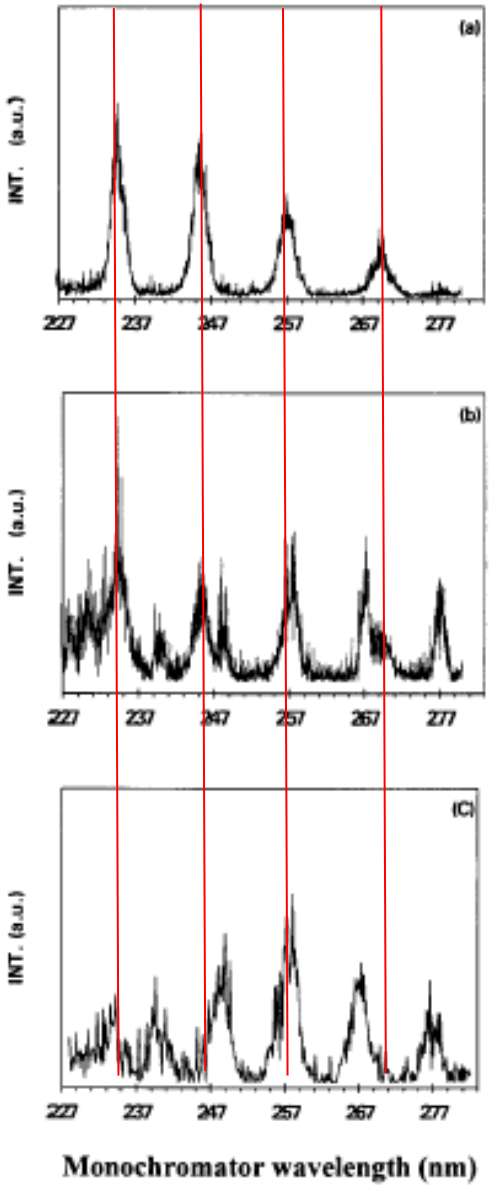

Desgroux et al., Appl. Opt, 37 (1998)

Interference with Schumann-Runge band of O_2 + Raman lines

2-photon of HCl + HCl* and CCl* emission induced by laser photodissociation of vinylchloride

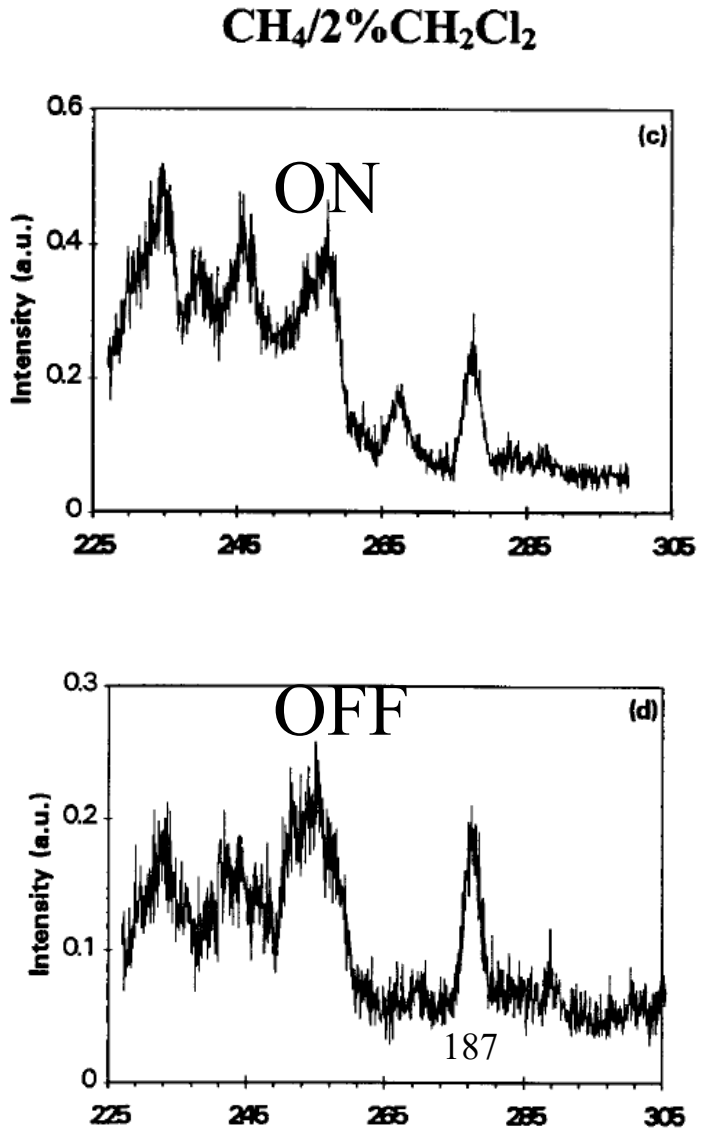

Interferences due to O_2 at high pressure

0.1 MPa

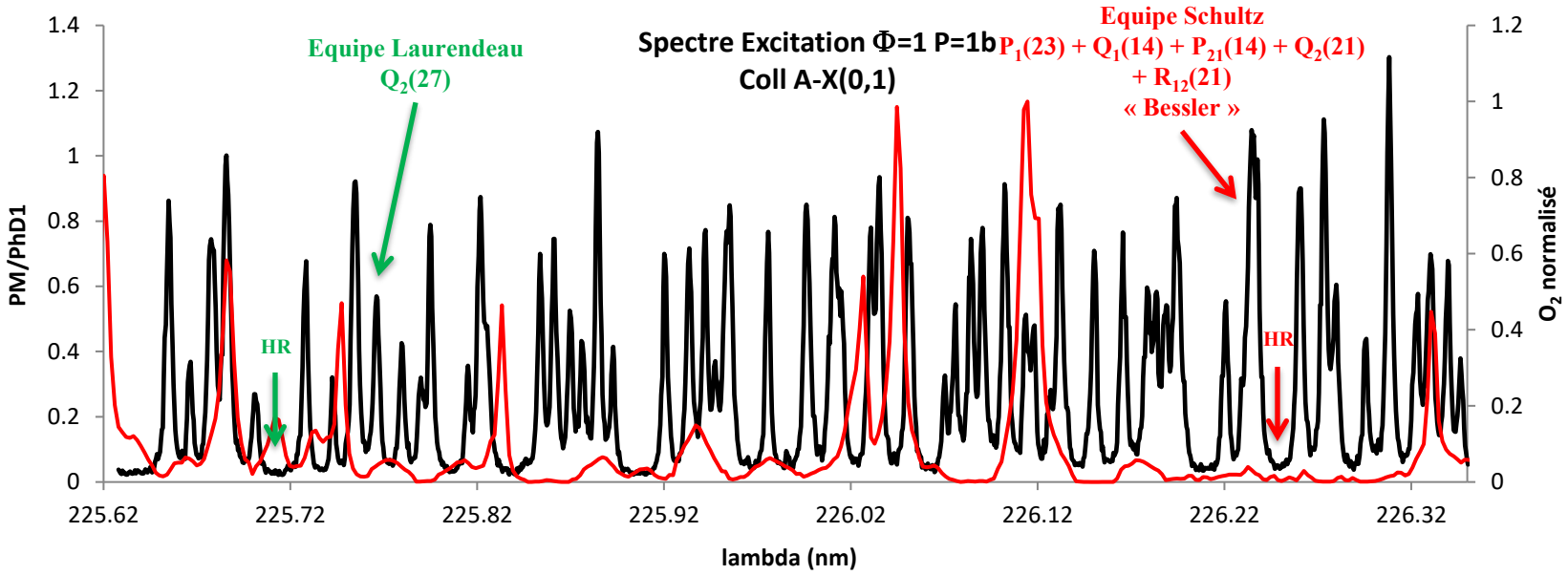

Interferences due to O_2 at high pressure

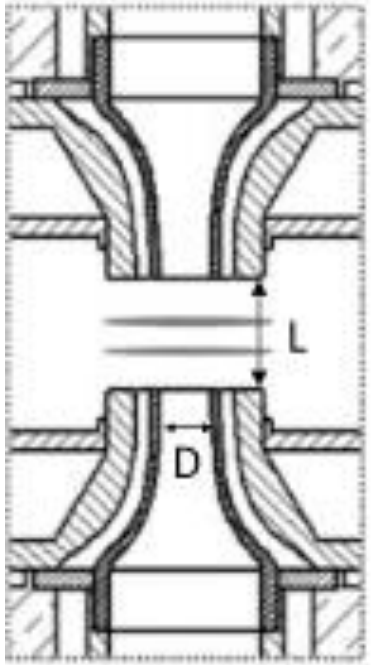

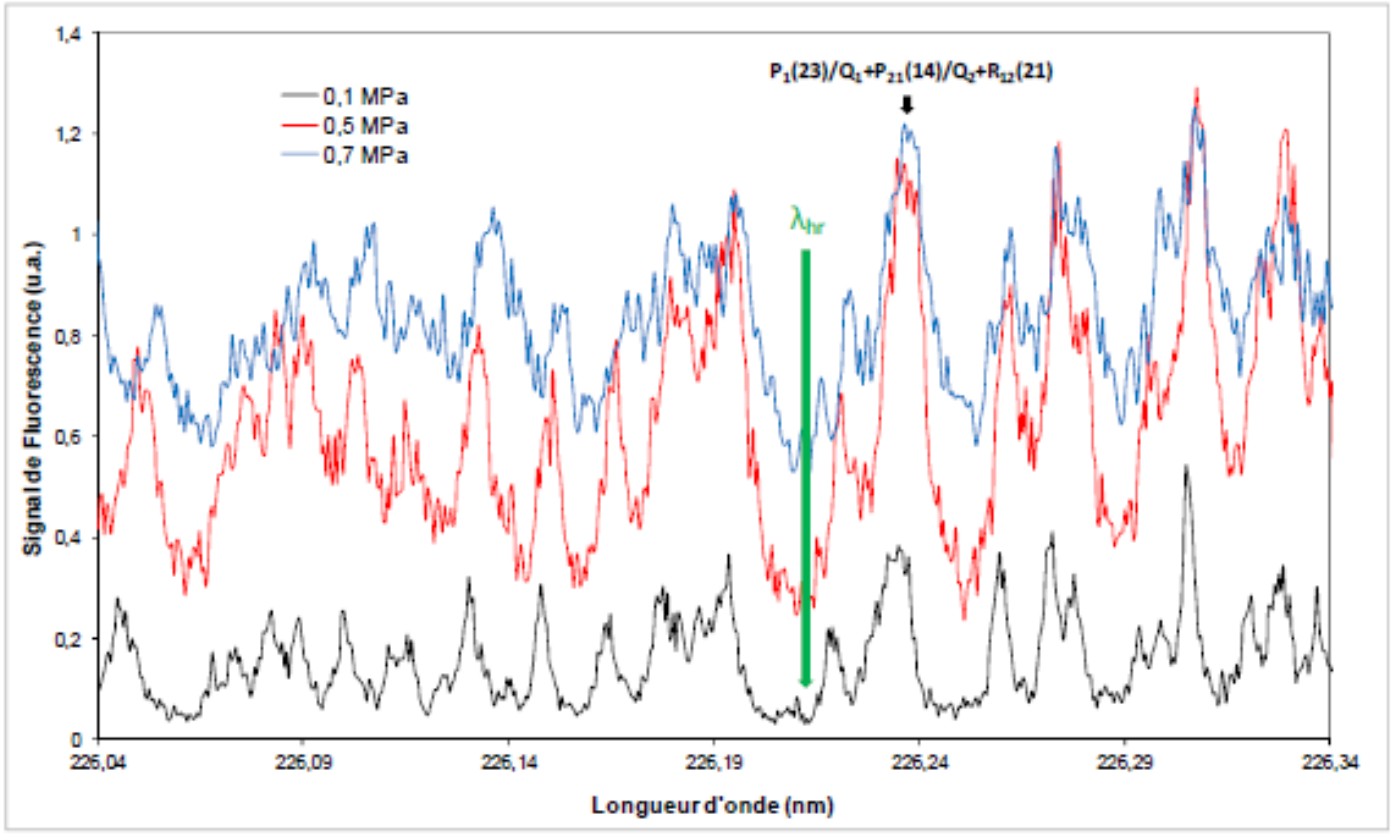

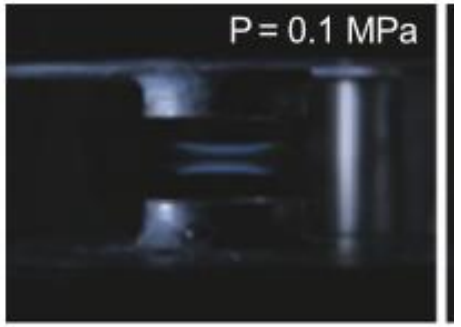

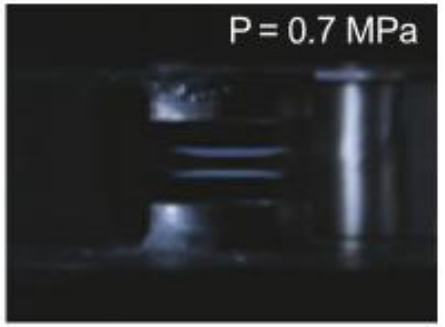

Excitation spectra NO A-X (0-0) in the burnt gases of a premixed counterflow CH_4/air flames
Collection in A-X (0-1)

PhD Julien Mollet, ICARE, Orléans (2014)

Interferences due to O_2 and Raman at high pressure

Excitation
$Q_2(26.5)$)

0.1 MPa

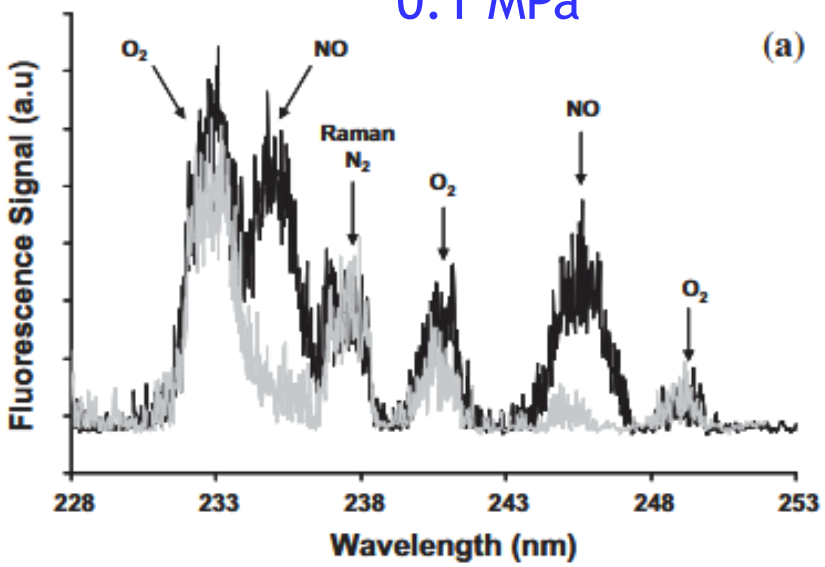

0.1 MPa

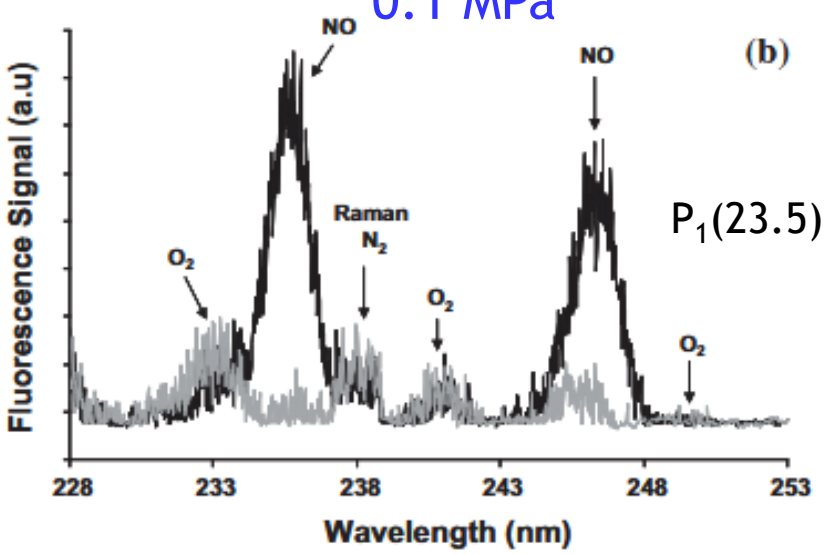

Excitation
$P_1(23.5)/Q_1(14.5)/Q_2(20.5)$

Raman of O_2 (234 nm), N_2 (238 nm), CO_2 (233 nm)
+ O_2 Schumann Runge

ON resonance
OFF resonance
Lean Flame $CH_4/O_2/Ar$

0.7 MPa

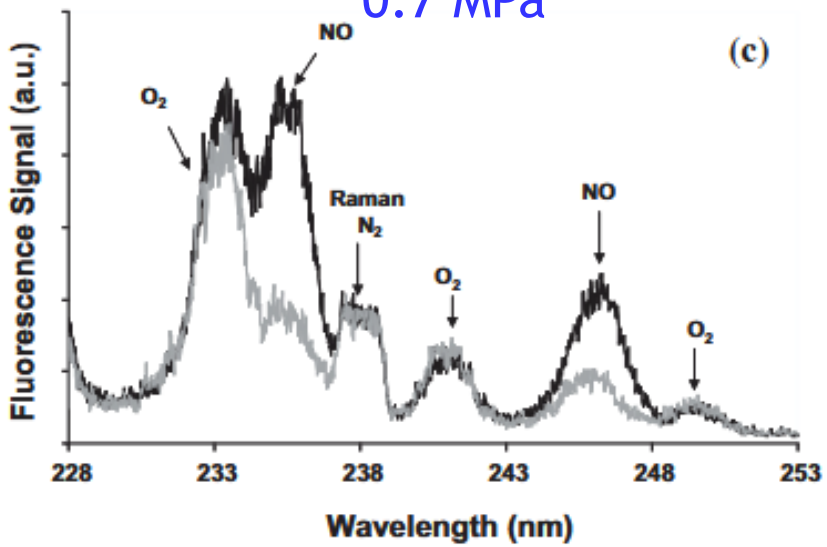

Pillier et al. Fuel 150 (2015) 394

X.3 NO in engines

Effect of pressure on NO spectroscopy (engine or high-pressure turbine applications)

$$\Delta\nu_D = 7.16 \cdot 10^{-7} \cdot \nu \cdot \sqrt{\frac{T}{M}} \qquad \text{in cm}^{-1} \qquad \Delta\nu_c = a \cdot \left(\frac{P}{760}\right)\left(\frac{300}{T}\right)^b$$

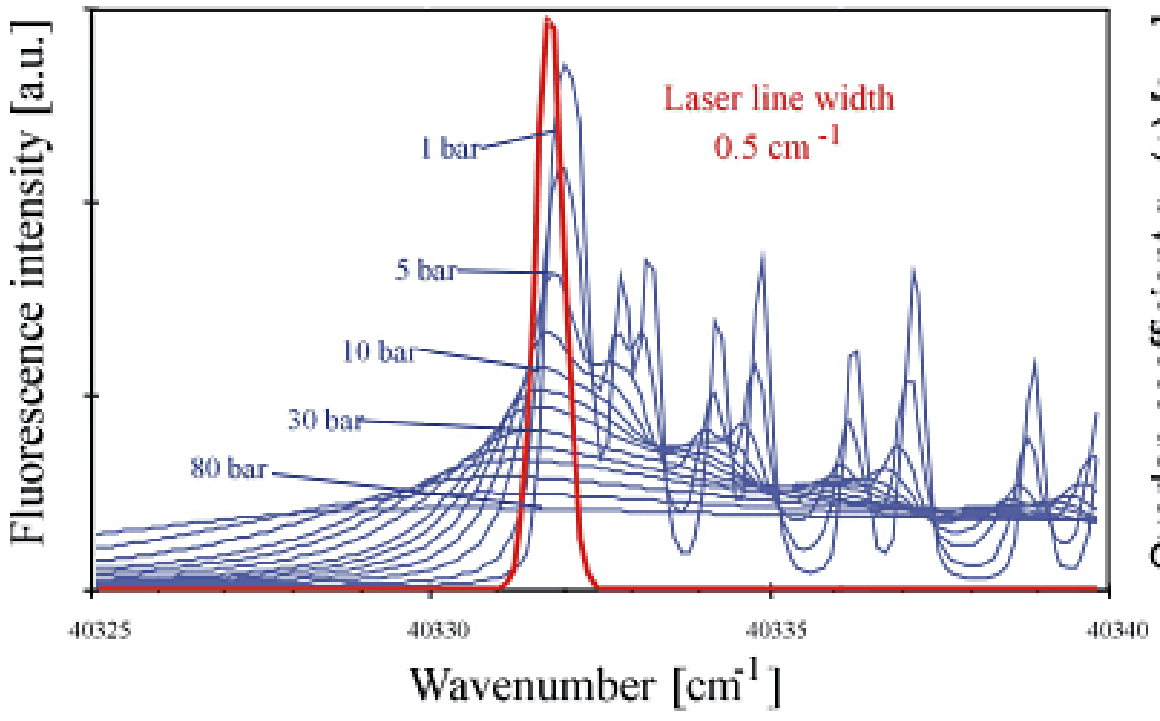

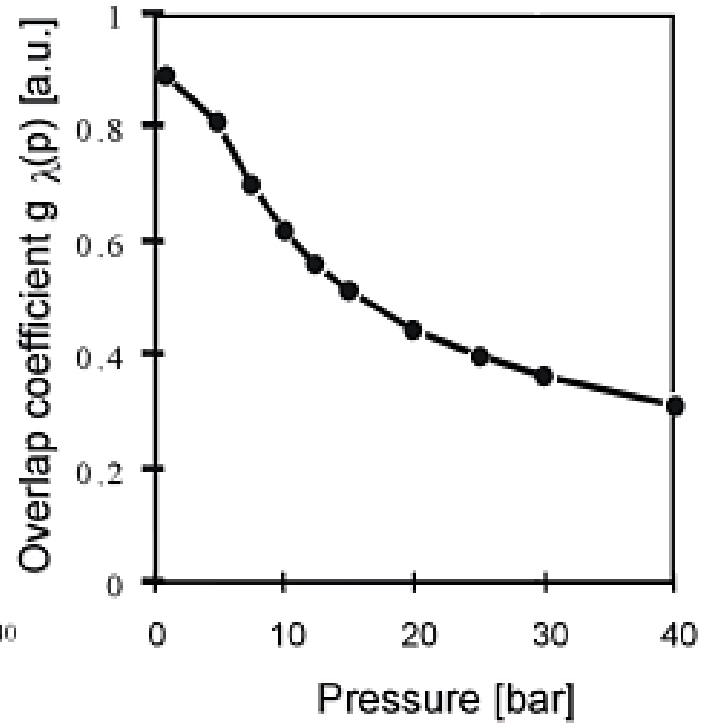

NO A-X(0-2) O_{12} bandhead

Transparent engine

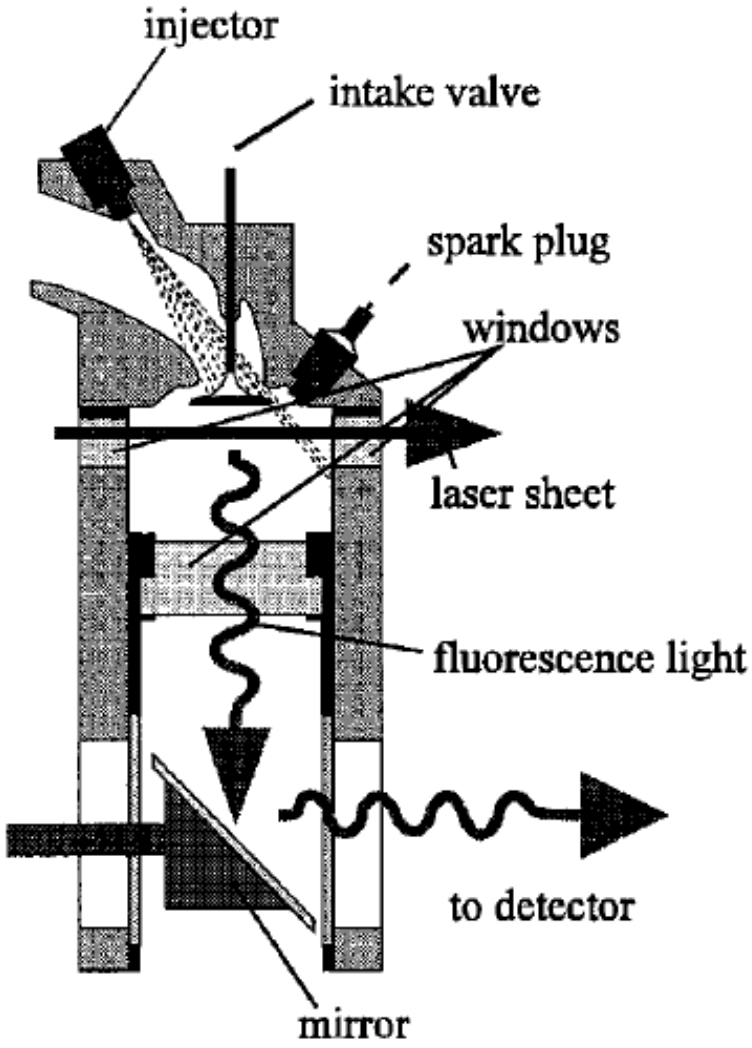

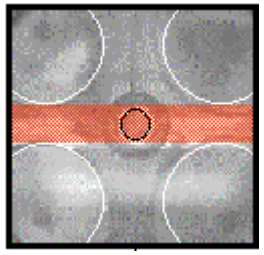

Jamette et al. SAE paper 2001-01-1926

1st difficulty: the collisional broadening of the absorption lines

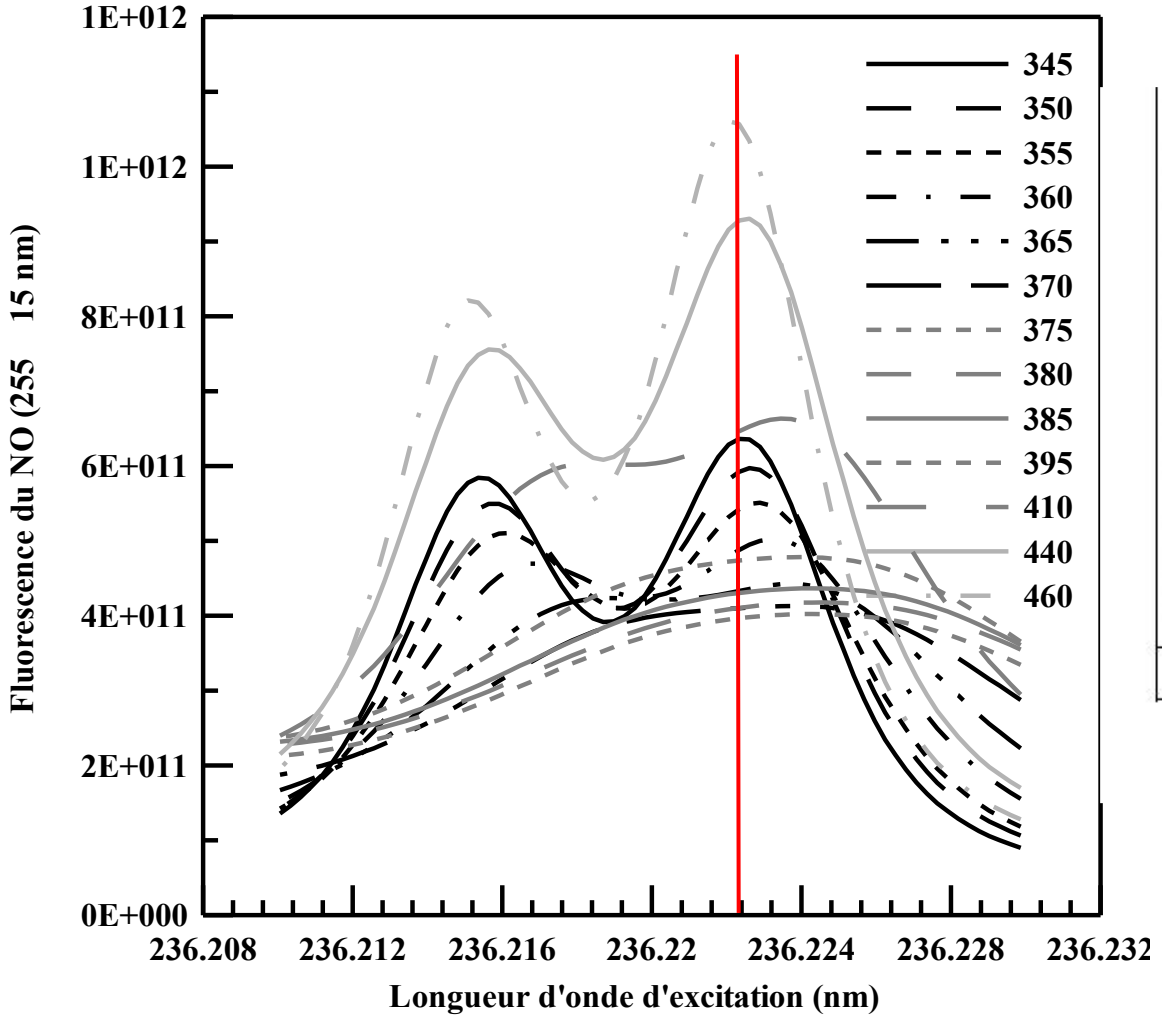

Evolution de la raie 236.221 en fonction de l'angle vilebrequin. La ligne rouge représente la longueur d'onde d'excitation expérimentale (236,223 nm)

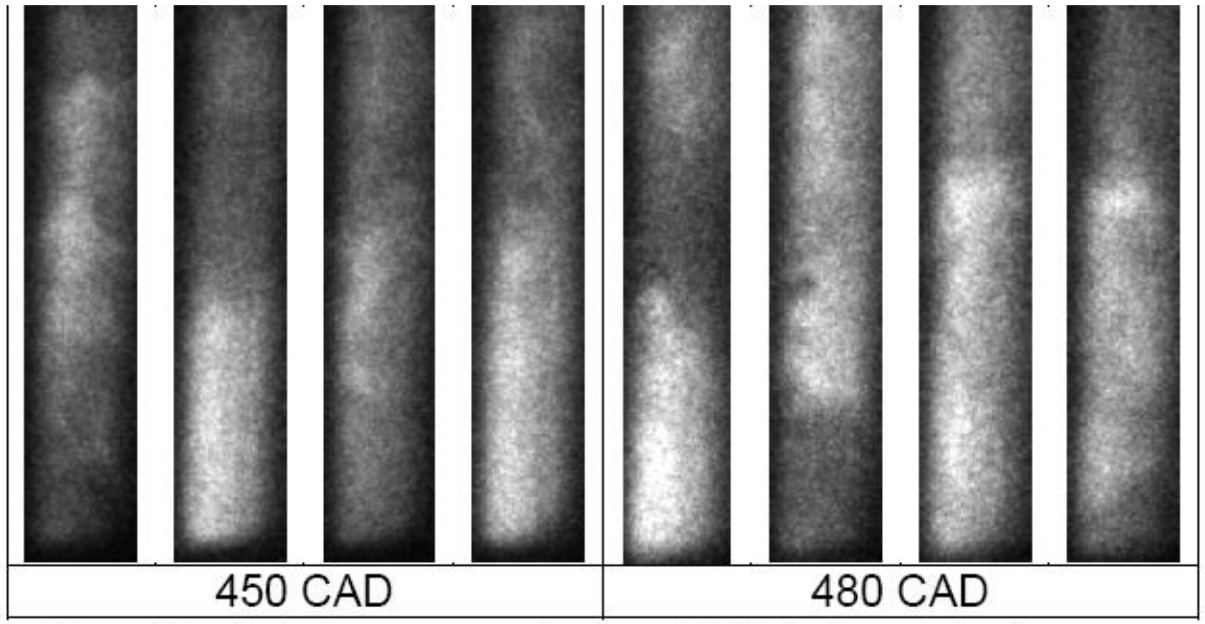

Figure 18 : Instantaneous visualisation of NO into the combustion chamber : raw fluorescence images –

Very difficult measurements in pressure-varying environments

Jamette et al. SAE 2001-01-1926

2nd difficulty : the spectral interferences

Interférences NO/CO_2 à hte température

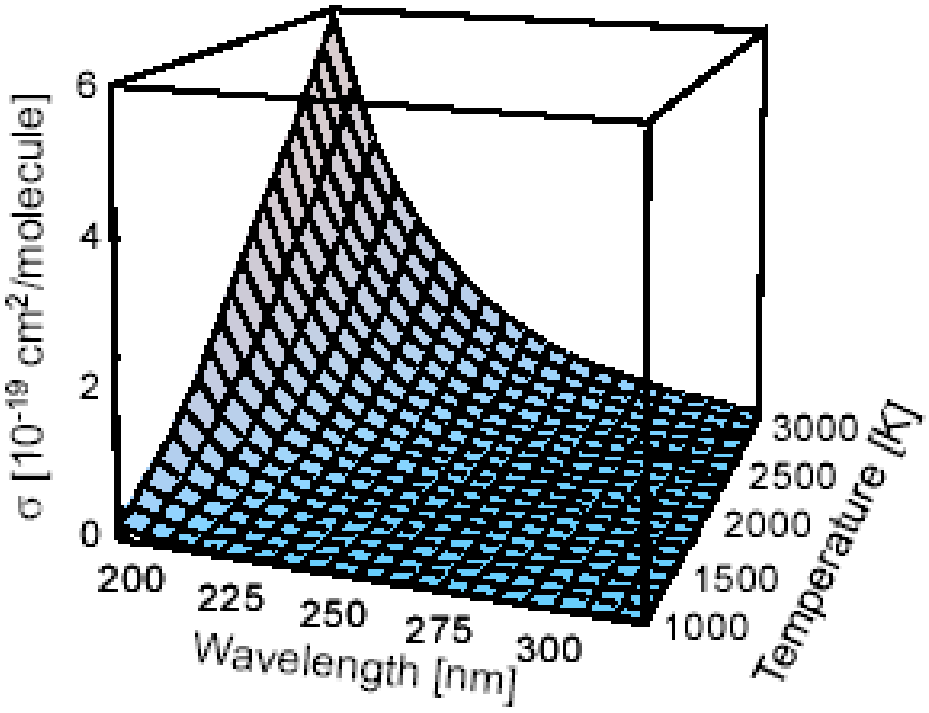

Fig. 2. Variation of CO_2 absorption cross-sections with temperature and wavelength. Calculated from the interpolated parameters shown in table 1.

Hildenbrand and Schulz, PROCI 29 (2002) 2735

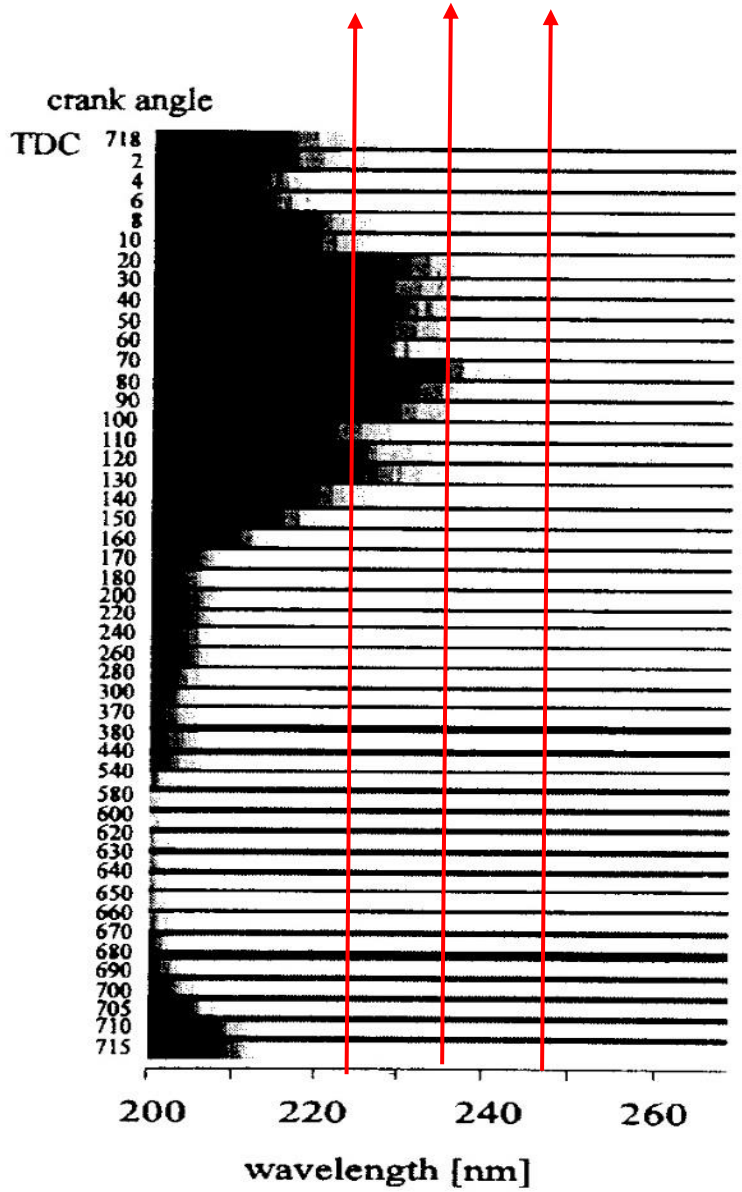

Light transmission

Knapp, Andresen et al, Appl. Opt. 35 (1996) 4009

2D Imaging(spectral-spectral)

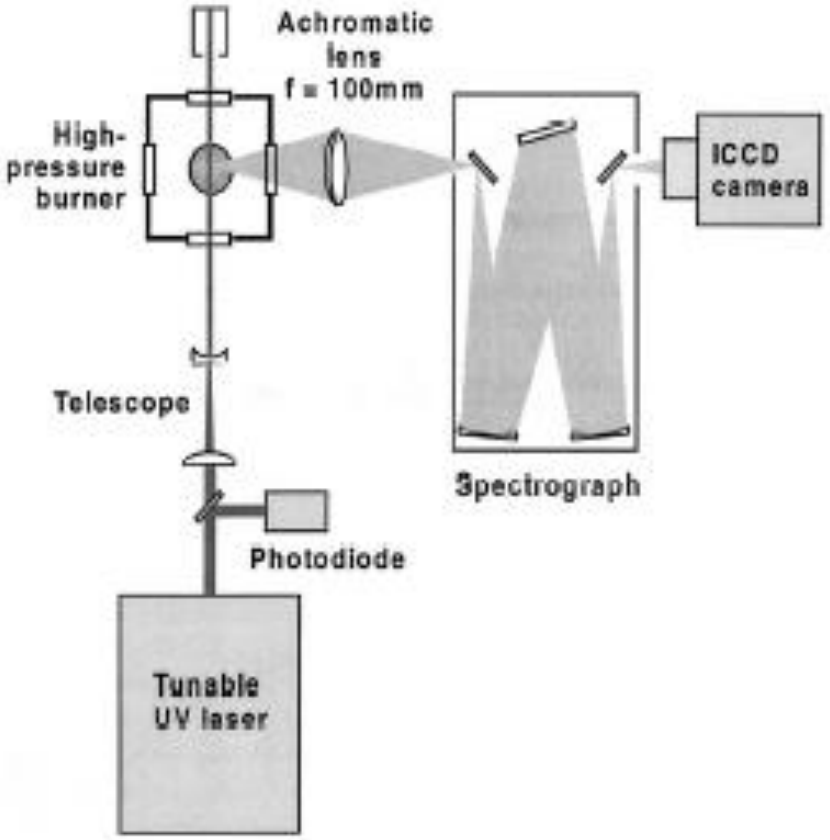

Fig. 1. Experimental arrangement. ICCD, Intensified Charge-coupled device.

Wolfgang G. Bessler, Christof Schulz, Tonghun Lee, Jay B. Jeffries, and Ronald K. Hanson Appl. Opt. 41 (2002) 3547

2D Imaging(spectral-spectral)

Excitation fluorescence chart

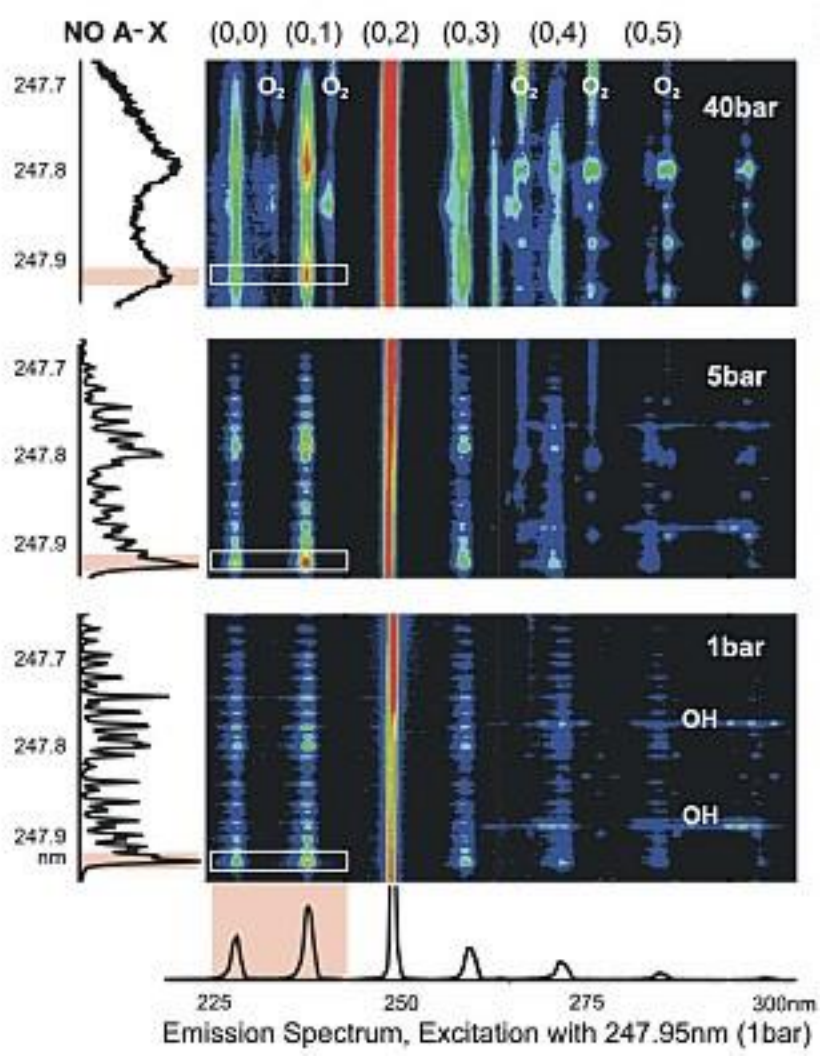

Bessler et al, Appl. Opt, 2002

Merci de votre attention!

Merci à Nathalie Lamoureux

清华大学燃烧能源中心

Center for Combustion Energy